

Aerojet TechSystems

DTIC FILE COPY

①

## Hydrocarbon Fuel/Combustion- Chamber-Liner Materials Compatibility

Contract NAS 3-25071  
Interim Final Report  
NASA CR-185203  
April 1990

**AD-A227 392**

Prepared For:  
National Aeronautics and Space Administration  
Lewis Research Center  
Cleveland, Ohio 44135

DTIC  
ELECTE  
OCT 09 1990  
S B D  
lb

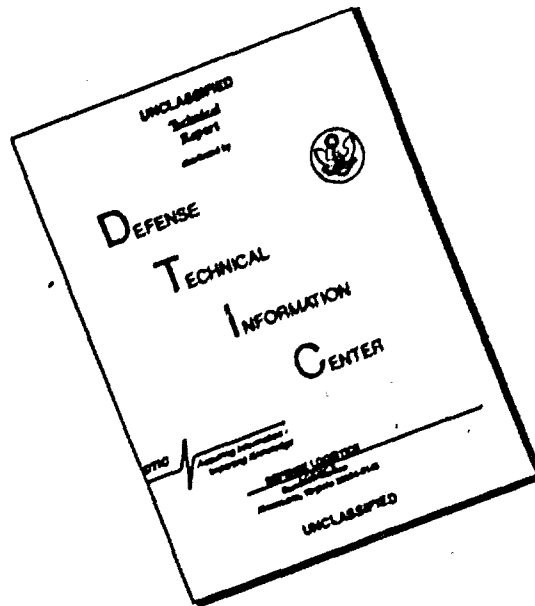
DISTRIBUTION STATEMENT A  
Approved for public release  
Distribution Unlimited

GENCORP  
AEROJET

90 10 08 159

~~90 08 08 283~~

# DISCLAIMER NOTICE



THIS DOCUMENT IS BEST QUALITY AVAILABLE. THE COPY FURNISHED TO DTIC CONTAINED A SIGNIFICANT NUMBER OF PAGES WHICH DO NOT REPRODUCE LEGIBLY.

Report No. KBQ-FR-1  
NASA CR-185203

April 1990

HYDROCARBON-FUEL/COMBUSTION-CHAMBER-LINER  
MATERIALS COMPATIBILITY

Contract NAS 3-25070


Interim Final Report

7 November 1986 - 31 October 1989

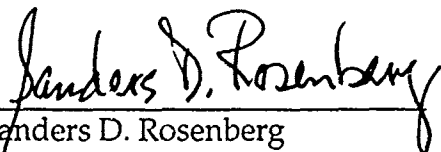
Prepared For

National Aeronautics and Space Administration  
Lewis Research Center  
21000 Brookpark Road  
Cleveland, Ohio 44135

Prepared By:

  
Mark L. Gage  
Project Engineer

Approved By:

  
Sanders D. Rosenberg  
Program Manager

Aerojet TechSystems  
P.O. Box 13222  
Sacramento, California

1. Report No. CR- 185203		2. Government Accession No.		3. Recipient's Catalog No.	
4. Title and Subtitle Hydrocarbon Fuel/Combustion-Chamber Liner Materials Compatibility Interim Final Report				5. Report Date April 1990	
				6. Performing Organization Code	
7. Author(s) Mark L. Gage Dr. Sanders D. Rosenberg				8. Performing Organization Report No.	
				10. Work Unit No.	
9. Performing Organization Name and Address Aerojet TechSystems P.O. Box 13222 Sacramento, CA 95813				11. Contract or Grant No. NAS 3-25070	
				13. Type of Report and Period Covered Interim Final Report 11/7/86 - 10/31/89	
12. Sponsoring Agency Name and Address NASA/Lewis Research Center Cleveland, Ohio 44135				14. Sponsoring Agency Code	
15. Supplementary Notes Project Manager, Richard Quentmeyer NASA/LeRC, Cleveland, Ohio					
16. Abstract Results of material compatibility experiments using hydrocarbon fuels in contact with copper-based combustion chamber liner materials are presented. Mil-Spec RP-1, n-dodecane, propane, and methane fuels were tested in contact with OFHC, NASA-Z, and ZrCu coppers. Two distinct test methods were employed. Static tests, in which copper coupons were exposed to fuel for long durations at constant temperature and pressure, provided compatibility data in a precisely controlled environment. Dynamic tests, using the Aerojet Carbothermal Test Facility, provided fuel and copper compatibility data under realistic booster engine service conditions. Tests were conducted using (1) very pure grades of each fuel and (2) fuels to which a contaminant, e.g. ethylene or methyl mercaptan, was added to define the role played by fuel impurities. Conclusions are reached as to degradation mechanisms and effects, methods for the elimination of these mechanisms, selection of copper alloy combustion chamber liners, and hydrocarbon fuel purchase specifications. <div style="text-align: center; margin-top: 20px;">RH 4</div>					
17. Key Words (Suggested by Author(s)) Methane, Propane, RP-1, NASA-Z, OFHC, ZrCu, Material Compatibility, Corrosion, Carbon Deposition, Protective Coatings, Regenerative Cooling, Booster Engines				18. Distribution Statement Unlimited	
19. Security Classif. (of this report) Unclassified		20. Security Classif. (of this page) Unclassified		21. No. of pages 241	
				22. Price*	

## TABLE OF CONTENTS

	<u>Page</u>
1.0 Introduction	1
2.0 Summary	2
3.0 Task 1 - Corrosive Interaction & Corrosion Rate Determination	12
3.1 Test Methods	12
3.1.1 Static Tests	12
3.1.2 Dynamic Tests	20
3.1.3 Fuel Analysis	26
3.2 RP-1 Test Results	30
3.2.1 Static Tests	30
3.2.2 Dynamic Tests	44
3.3 Methane Test Results	70
3.3.1 Static Tests	70
3.3.2 Dynamic Tests	78
3.4 Propane Test Results	99
3.4.1 Static Tests	99
3.4.2 Dynamic Tests	108
4.0 Task 2 - Protective Measures Development & Evaluation	123
4.1 Task 2.1 - Candidate Material Selection	123
4.2 Task 2.2 - Chemistry Laboratory Tests	127
4.3 Task 2.3 - Thermal Sciences Laboratory Tests	150
5.0 Task 3 - Protective Measures Verification Program	198
5.1 Task 3.1 - Program Plan Preparation	198
6.0 References	208
7.0 Appendices	
Appendix A - Static Test Laboratory Procedures	A-1
Appendix B - Dynamic Test Laboratory procedures	B-1
Appendix C - Dynamic Test Data Reduction Program Listing and Sample Output	C-1

## LIST OF TABLES

<u>Table No.</u>		<u>Page</u>
1	A Summary of Experimental Results	3
2	Fuels and Materials Tested in Program	13
3	General Guidelines of Program	14
4	Dynamic Tests Produced Realistic Simulation of Cooling Channel Conditions	24
5	Vendor Supplied Analysis of Propellants and Additives	27
6	Contents of RP-1 Ampul Tests	31
7	Internal Pressure of Glass Ampules	33
8	Material Balances for Sulfur in Ampul Tests	37
9	Ampul Test Results	43
10	RP-1 Dynamic Test Conditions	45
11	Summary of RP-1 Dynamic Tests	46
12	Summary of ESCA Analysis on Surface Deposits From RP-1 Dynamic Tests	55
13	Summary of Aminco Bomb Tests	71
14	Summary of Methane Dynamic Tests in Task 1	79
15	Propane Static Test Conditions	100
16	Summary of Propane Dynamic Tests	109
17	Physical Properties of Candidate Metals	124
18	Summary of Coupon Weights	139
19	Summary of Methane Dynamic Tests in Task 2	153
20	Proposed Carbothermal Test Matrix	204



Accession For	
NTIS GRA&I	<input checked="" type="checkbox"/>
DTIC TAB	<input type="checkbox"/>
Unannounced	<input type="checkbox"/>
Justification	
By _____	
Distribution/	
Availability Codes	
Dist	Avail and/or Special
A-1	

## LIST OF FIGURES

<u>Figure No.</u>		<u>Page</u>
1	Carbonaceous Tar Covered Channel Surfaces After RP-1 Dynamic Tests	5
2	500 ppm Sulfur Added to RP-1 Roughened Channel Walls	6
3	Pure Methane Did Not React With the Copper Materials	7
4	1 ppm Sulfur in Methane Corroded Channel	8
5	Propane Tests Left Copper Sulfide Deposits	9
6	Electrodeposited Coatings Protected Copper Channels From Corrosion	11
7	Ampul Tests Were Conducted With RP-1	15
8	Oven Temperature For Ampul Tests	16
9	Filling System For Aminco Bomb Tests	18
10	Temperature and Pressure Traces For a Typical Bomb Test	19
11	Schematic of Dynamic Test Facility	21
12	Conceptual Diagram of Aerojet Carbothermal Materials Tester	22
13	Typical Dynamic Test Specimen	23
14	Gas Chromatograph of RP-1 Before Ampul Tests	34
15	Gas Chromatograph of RP-1 After Ampul Tests	35
16	Specimen Before and After Ampul Test With Air Saturated RP-1	38
17	Specimen Before and After Ampul Test With <u>n</u> -Dodecane Plus 525 ppm <u>n</u> -Dodecanethiol	39
18	SEM of Copper Surface Before and After Ampul Test With Air Saturated RP-1	41
19	SEM of Copper Surface Before and After Ampul Test With <u>n</u> -Dodecane Plus 525 ppm <u>n</u> -Dodecanethiol	42
20	Heat Transfer Performance During RP-1 Dynamic Test R103	48
21	NASA-Z Channel Before and After RP-1 Dynamic Test R104	49
22	Heat Transfer Performance During RP-1 Dynamic Test R105	51
23	SEM Photos of Channel Surface Before and After RP-1 Dynamic Test R107	53
24	Heat Transfer Performance During RP-1 Dynamic Test R109	56
25	Pressure Drop Through Channel During RP-1 Dynamic Test R111	58

## LIST OF FIGURES

<u>Figure No.</u>		<u>Page</u>
26	Heat Transfer Performance During RP-1 Dynamic Test R112	60
27	Apparent Channel Roughness During RP-1 Dynamic Test R112	61
28	Heat Transfer Performance During RP-1 Dynamic Test R113	63
29	Apparent Channel Roughness During RP-1 Dynamic Test R113	64
30	SEM Photos of Channel Surface After RP-1 Dynamic Test R113	65
31	SEM Photos of Channel Surface After RP-1 Dynamic Test R113	66
32	Thermal Resistance Buildup Rate Is a Strong Function of Wall Temperature	68
33	SEM of NASA-Z After Static Exposure to UHP Methane	72
34	SEM of NASA-Z After Static Exposure to UHP Methane Plus 1% Air	74
35	SEM of NASA-Z After Static Exposure to UHP Methane Plus 272 ppm Methyl Mercaptan	76
36	Analysis of Surface Composition After Static Exposure to UHT Methane Plus 272 ppm Methyl Mercaptan	77
37	Heat Transfer Performance During Methane Dynamic Test M10383	80
38	Cooling Channel Before and After Methane Dynamic Test M103	82
39	SEM Photos of Channel Surface After Methane Dynamic Test M103	83
40	Cooling Channel After Methane Dynamic Test M109	87
41	Mass Flowrate Through the Channel Was Affected by Sulfur Added to the Methane	89
42	SEM Photos of Channel After Methane Dynamic Test M111	92
43	Cooling Channel After Methane Dynamic Test M112	93
44	Heat Transfer Performance During Methane Dynamic Test M113	94
45	Cooling Channel After Methane Dynamic Test M113	96
46	SEM Photos of Channel After Methane Dynamic Test M113	97
47	NASA-Z After Static Exposure to IG Propane	101
48	NASA-Z After Static Exposure to RG Propane	103
49	NASA-Z Before and After Exposure to IG Propane Plus 2000 ppm Water	105

## LIST OF FIGURES

<u>Figure No.</u>		<u>Page</u>
50	SEM Photos of NASA-Z After Static Exposure to IG Propane Plus 2000 ppm Water	106
51	NASA-Z After Static Exposure to IG Propane Plus 94 ppm Methyl Mercaptan	107
52	Cooling Channel After Propane Dynamic Test P101	110
53	SEM Photos of NASA-Z After Propane Dynamic Test P101	112
54	Downstream Filters Trapped Many Powdery Black Deposits During Dynamic Tests With Propane	113
55	Cooling Channel Before and After Propane Dynamic Test P104	115
56	Heat Transfer Performance During Propane Dynamic Test P105	117
57	Apparent Channel Roughness During Propane Dynamic Test P105	118
58	SEM Photos of Channel After Propane Dynamic Test P105	119
59	SEM Photos of Channel After Propane Dynamic Test P106	120
60	SEM Photos of Channel After Propane Dynamic Test P106	121
61	Temperature and Pressure Traces From Static Test M201	129
62	Gold Foil Before and After Static Exposure to UHP Methane Plus 500 ppm Methyl Mercaptan (Test M201)	131
63	SEM Photos of Gold Foil Before and After Static Test M201	132
64	Zirconium Foil Before and After Static Test M201	133
65	SEM Photos of Zirconium Foil Before and After Static Test M201	134
66	Iridium Foil Before and After Static Test M201	135
67	SEM Photos of Iridium Foil Before and After Static Test M201	136
68	NASA-Z Before and After Static Test M201	137
69	SEM Photos of NASA-Z Before and After Static Test M201	138
70	Temperature and Pressure Traces From Static Test M202	141
71	Platinum Foil Before and After Static Exposure to UHP Methane Plus 500 ppm Hydrogen Sulfide (Test M202)	142
72	SEM Photos of Platinum Before and After Static Test M202	143
73	SEM Photos of Platinum Before and After Static Test M202	144
74	Rhenium Foil Before and After Static Test M202	145

## LIST OF FIGURES

<u>Figure No.</u>		<u>Page</u>
75	SEM Photos of Rhenium Before and After Static Test M202	146
76	Niobium Before and After Static Test M202	147
77	SEM Photos of Niobium Before and After Static Test M202	148
78	NASA-Z Before and After Static Test M202	149
79	SEM Photos of NASA-Z Before and After Static Test M202	151
80	Dynamic Test Specimen After Gold Coating	154
81	SEM Photos of Gold Coating Before Dynamic Tests	155
82	Cross Section of Gold Plated Channel Before Dynamic Tests	157
83	Design of Specimen Used in Dynamic Tests M207 and M208	158
84	Cross Section of Alkaline Nickel Strike Followed by Gold	160
85	Cross Section of Acidic Nickel Strike Followed by Gold	161
86	Cross Section of Acidic Nickel, Followed by Alkaline Nickel and Gold	162
87	Pressure Drop and Heat Transfer Performance During Methane Dynamic Test M201	163
88	SEM Photos of Channel After Methane Dynamic Test M201	164
89	EDS of Scale Formed During Methane Dynamic Test M201	165
90	Flowrate Through Channel During Methane Dynamic Tests M201-M203	167
91	Heat Transfer Performance During Methane Dynamic Tests M201-M203	168
92	SEM Photos of Gold Coated Channel After Test M202	169
93	SEM Examination Revealed Ruptures in Gold Coating After Test M202	170
94	Coating Disbond Occurred During Test M202	171
95	SEM Photos of Platinum Coated Channel Before and After Test M203	173
96	SEM Examination Showed Isolated Deposits on Channel Surface After Test M203	174
97	Flowrate Through Channel During Methane Dynamic Tests With 5 ppm H <sub>2</sub> S (Tests M204-M206)	176
98	Heat Transfer Performance During Methane Dynamic Tests With 5 ppm H <sub>2</sub> S (Tests M204-M206)	177
99	SEM Photos of Uncoated Amzirc After Dynamic Test M204	178

## LIST OF FIGURES

<u>Figure No.</u>		<u>Page</u>
100	SEM Photos of Gold Coating Before and After Methane Dynamic Test M205	180
101	Cross Section of Channel After Test M205	181
102	SEM Photos of Platinum Coating Before and After Methane Dynamic Test M206	182
103	Cross Section of Channel After Test M205	184
104	Cross Section of Channel After Test M205	185
105	Disassembled Specimens Before and After Methane Dynamic Tests M207 and M208	187
106	Gold Coating Before Test M207	188
107	Cross Sections of Untested Channel	190
108	SEM Photos of Gold Coating After Test M207	192
109	Cross Sections of Channel After Test M207	193
110	SEM Photos of Gold Coating After Test M208	194
111	Cross Sections of Channel After Test M208	195
112	Cross Sections of Channels After Tests With 5 ppm H <sub>2</sub> S in Methane	196
113	Protective Measures Verification Program Logic	199
114	Protective Measures Verification Program Schedule	200
115	Protective Measures Verification Program Coatings Development	202
116	Closeout Test Methods	203
117	Existing Hardware Will Be Utilized in the Protective Measures Verification Program	206
118	The Protective Measures Verification Program Will Build a 40,000 lbF Coated Chamber	207

## ACKNOWLEDGEMENTS

The Hydrocarbon-Fuel/Combustion-Chamber-Liner Materials Compatibility Program is an ongoing program which is being performed by Aerojet TechSystems, Sacramento, California for NASA Lewis Research Center, Cleveland, Ohio. The Aerojet Program Manager and Project Engineer are Dr. Sanders D. Rosenberg and Mr. Mark L. Gage, respectively. The NASA-LeRC Program Manager is Mr. Richard Quentmeyer. The following individuals have also contributed to the success of this program.

A. Ballunguy  
F. Chen  
G. Farlee  
G. Fazzio  
J. Franklin  
D. Homer  
R. LaBotz  
D. Makel

T. Peterson  
R. Pruett  
K. Schaplowsky  
L. Schoenman  
G. Sheble  
W. Sobalralski  
E. VanderWall  
J. Wooten

## 1.0 INTRODUCTION

The Hydrocarbon-Fuel/Combustion-Chamber-Liner Materials Compatibility Program has three major technical objectives. They are (1) to define the corrosive interaction process that occurs between hydrocarbon fuels and candidate combustion chamber liner materials, (2) to develop and evaluate protective measures to remedy the defined corrosive interaction process, and (3) to recommend a test program which will verify the validity of the measures under actual service conditions. A four-task program is being conducted to achieve these program objectives, i.e., Task 1 — Corrosive Interaction and Rates Determination, Task 2 — Protective Measures Development and Evaluation, Task 3 — Protective Measures Verification Program, and Task 4 — Reporting Requirements.

This interim final report covers the period from 7 November 1986 through 31 October 1989. The original scope of work of the program was completed during this period. A contract modification to perform additional research was finalized on 7 August 1989. It extended the period of performance on the contract to 7 April 1991. A final report covering the entire period of performance on the contract will be issued upon completion of this work.

## 2.0 SUMMARY

Material compatibility studies were conducted between hydrocarbon fuels and copper chamber liner materials. The hydrocarbon fuels tested were MIL-Spec RP-1, n-dodecane, propane, and methane. The copper chamber liner materials tested were OFHC, NASA-Z, and Zirconium Copper. Two distinct methods were employed. Static tests, in which copper coupons were exposed to fuel for long durations at constant temperature and pressure, were used to provide compatibility data in precisely controlled environments. Dynamic tests, using the Aerojet Carbothermal Test Facility, were conducted to provide fuel and copper compatibility data under realistic booster engine service conditions. Dynamic test conditions simulated the heat flux, coolant channel wall temperature, fuel velocity, temperature, and pressure expected in the cooling channels of a regeneratively cooled LOX/hydrocarbon booster engine operating at chamber pressures up to 3000 psia. Tests were conducted using (1) very pure grades of each fuel and (2) fuels to which a contaminant, e.g., ethylene, methyl mercaptan, hydrogen sulfide, etc., was added to define the role played by fuel impurities.

This material compatibility research was motivated, in part, by prior work conducted by United Technologies Research Center and Rockwell International Rocketdyne Division (Ref. 1, 2, 3). In these programs, severe copper corrosion and carbon deposition were encountered during this conduct of electrically heated tube tests. These results had very important implications for the development of long-life oxygen/hydrocarbon booster engines. Thus, the first two objectives of the current program are (1) to define the corrosive interaction process that occurs between hydrocarbon fuels and copper combustion chamber liner materials, and (2) to develop and demonstrate protective measures against this corrosive process.

In Task 1 of this program, compatibility tests were conducted between hydrocarbon fuels and copper chamber liner materials. It was found that each of the copper materials exhibited similar compatibility behavior. However, there were significant differences among the various hydrocarbon fuels tested. Table 1 summarizes the test results obtained in Task 1 of this program.

TABLE 1

A SUMMARY OF EXPERIMENTAL RESULTS

	<u>RP-1</u>	<u>Methane</u>	<u>Propane</u>
Carbon Containing Deposits	Yes Above T <sub>Wall</sub> 580 F	No Up to T <sub>Wall</sub> 934 F	No Up to T <sub>Wall</sub> 865 F
Copper Corrosion	Yes* With 50 ppm S	Yes* Down to 1 ppm S	Yes* In All Tests

---

\*Copper corrosion occurs only when sulfur is present in these fuels.  
Cuprous sulfide is the corrosion product.

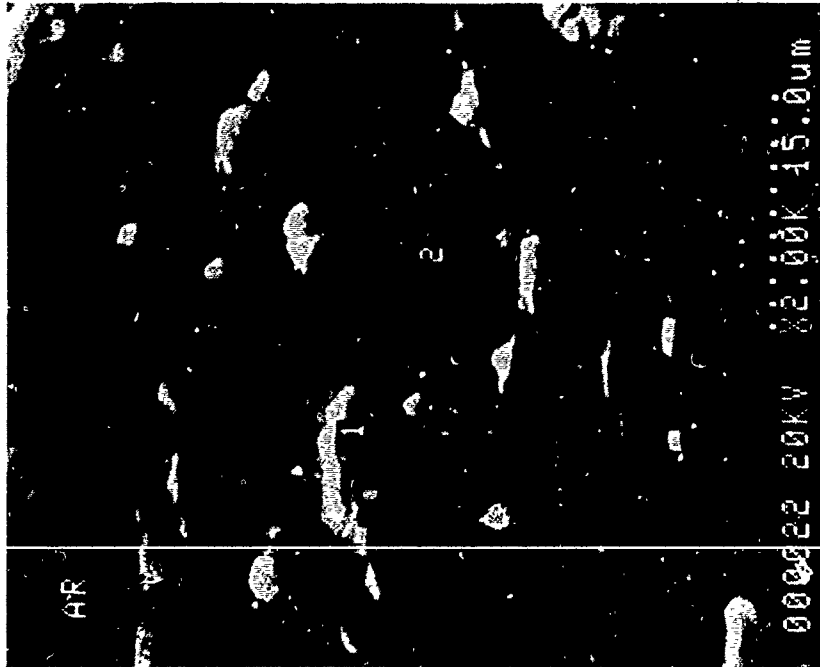
## 2.0, Summary (cont.)

Task 1 tests with RP-1 and n-dodecane demonstrated a deposition reaction occurs when the surface temperature of the copper exceeded 580 F. The result of this deposition process was the formation of a chemically complex, thin, but very tenacious, tar on all exposed copper surfaces, as seen in the photomicrographs shown in Figure 1. This tar inhibited heat transfer, but had little effect on the flowrate or pressure drop through the channel during the dynamic tests. A corrosive reaction between the fuel and the copper was also demonstrated with RP-1 when 50 ppm (by weight) sulfur was added to the fuel in the form of n-dodecanethiol. The copper cooling channels reacted with the sulfur impurity to form cuprous sulfide ( $\text{Cu}_2\text{S}$ ). This corrosive process roughened the copper surfaces, as seen in Figure 2, and substantially increased the pressure drop through the cooling channel. It did not have a major impact on the heat transfer characteristics of the channel.

In contrast, Task 1 tests with methane did not show any deposition reactions, even at copper surface temperatures up to 934 F. Figure 3 documents that, even at high magnification, no changes were observed on the surface of the dynamic test specimen. However, severe corrosion of copper was observed when very small amounts of sulfur impurities (e.g., 1 ppm of methyl mercaptan) were added to the methane. Figure 4 shows the subsurface gouges formed in the channel surface during a dynamic test with methane plus 1 ppm methyl mercaptan. In two tests conducted with a relatively high concentration of methyl mercaptan in the methane (200 and 10 ppm, respectively) the formation of corrosion product ( $\text{Cu}_2\text{S}$ ) became so massive as to block entirely the flow of fuel through the channel.

Task 1 tests with propane did not show any carbon deposition, even at copper surface temperatures up to 865 F. However, corrosion of copper by sulfur compounds was observed in every test with propane, and resulted in the formation of powdery black deposits of  $\text{Cu}_2\text{S}$  on the channel surfaces, such as shown in Figure 5. Samples of the propane used in the testing were analyzed by industrial and university laboratories in an attempt to characterize the impurities causing the corrosion. No sulfur compounds could be detected in the gas phase of the propane, even when using very sensitive analytical methods reportedly accurate to levels as low as 50 parts per billion. The inability of the analytical method to identify the source of contamination observed in

As  
Received



Post Test  
R107

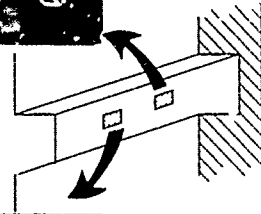
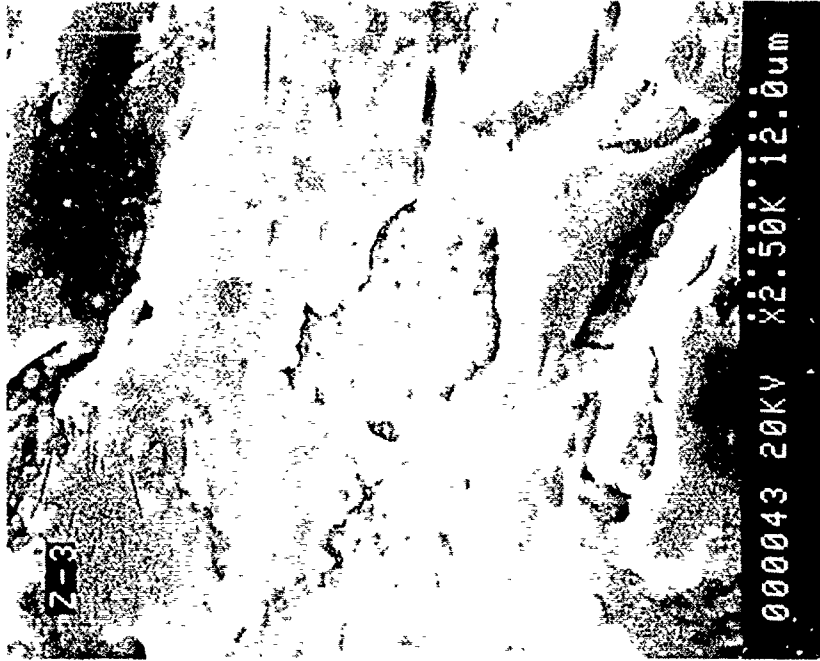
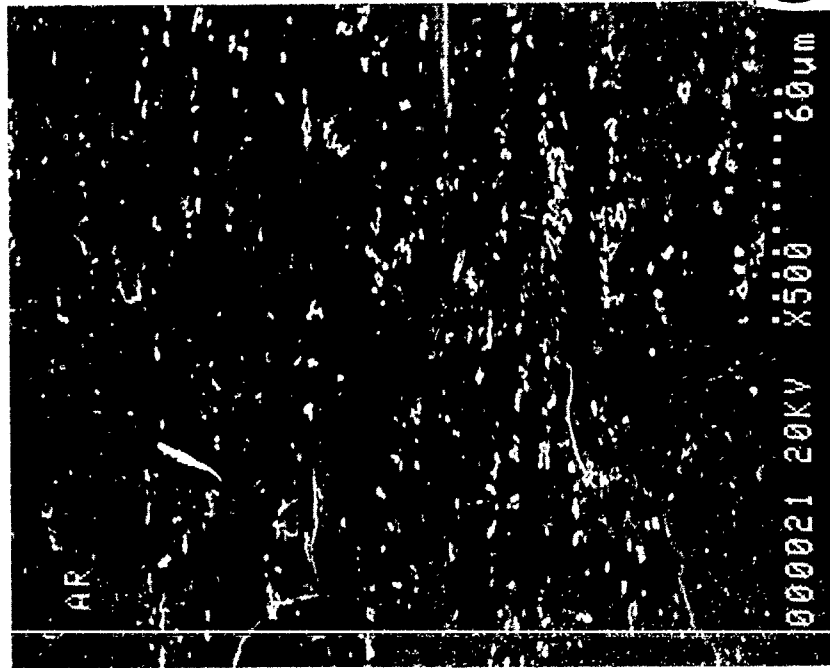


Figure 1. Carbonaceous Tar Covered Channel Surfaces After RP-1 Dynamic Tests



Figure 2. Addition of 50 ppm Sulfur to RP-1 Resulted in Corrosion of NASA-Z Channel, Even at Low Wall Temperature (586°F)

Before  
Test M108



After  
Test M108

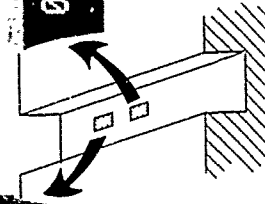
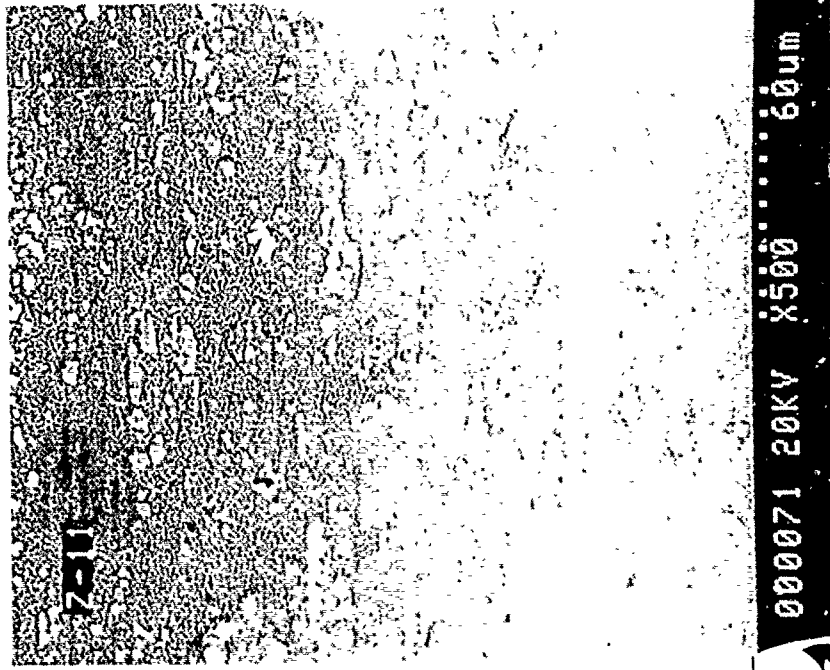


Figure 3. The Surface of a NASA-Z Cooling Channel Was Unaffected After Testing for 819 sec at a  $T_{wall}$  of 934°F With Technical Grade Methane

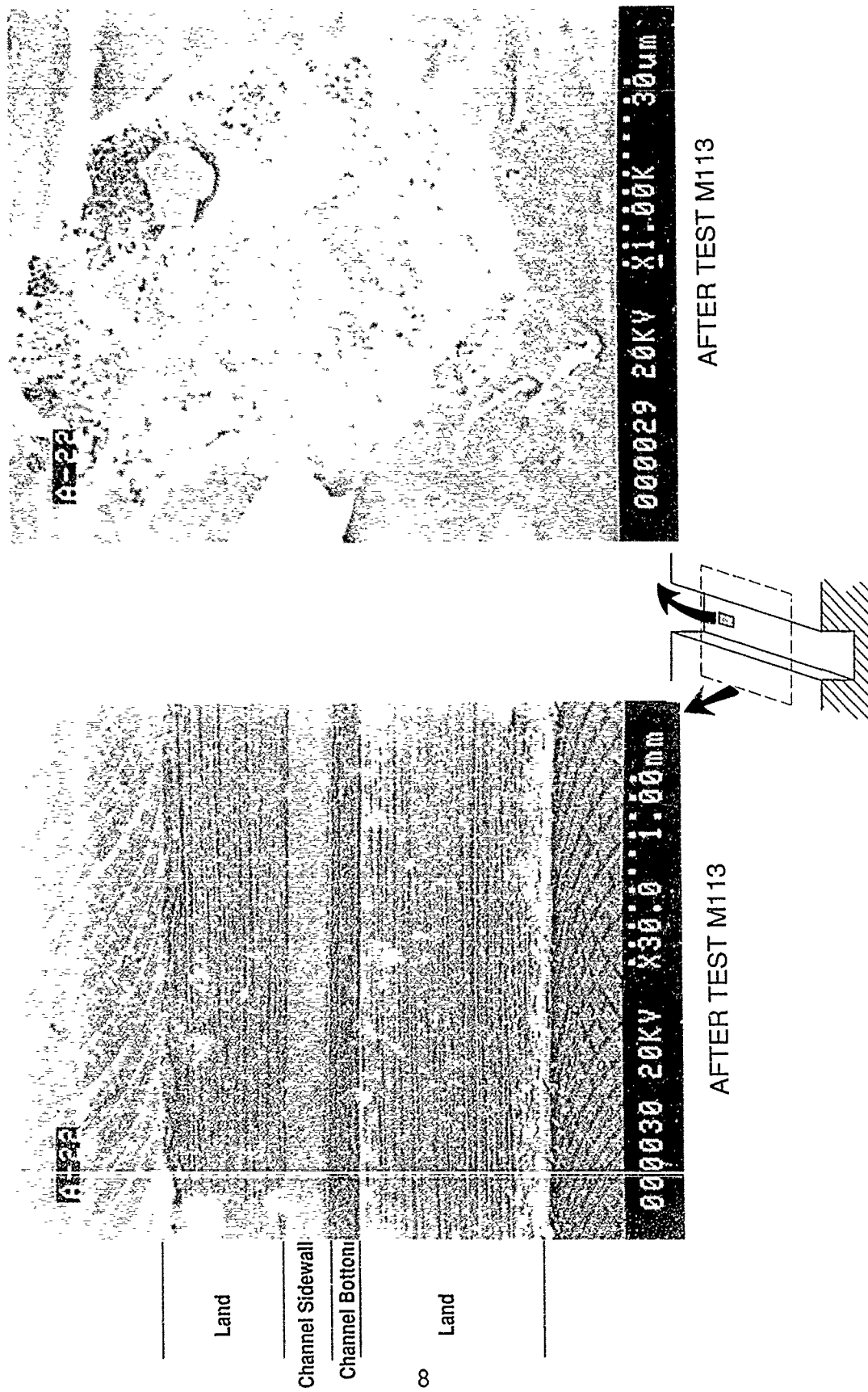
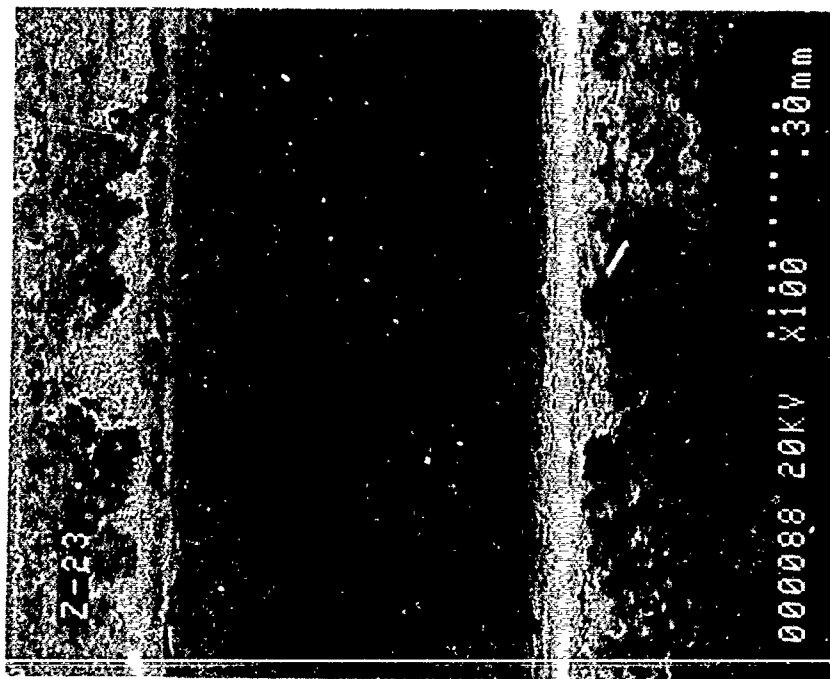
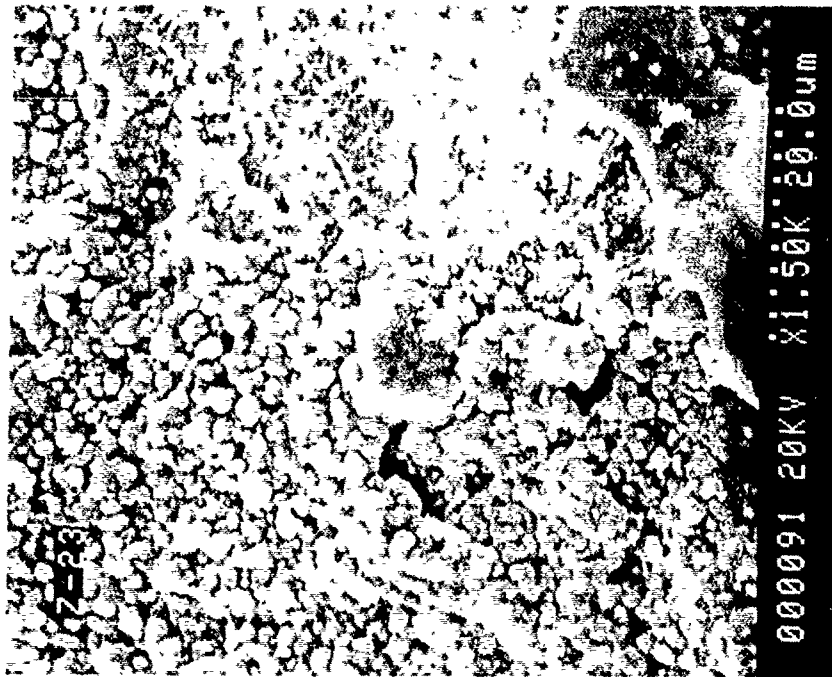


Figure 4. Just 1 ppm of Sulfur in Methane Produced Corrosion of the Amzirc Cooling Channel



After Test P101



After Test P101

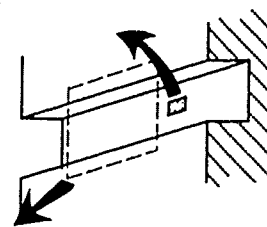


Figure 5. Dynamic Tests with Propane Resulted in the Formation of Cuprous Sulfide Scale on Channel Surfaces

## 2.0, Summary (cont.)

the propane tests indicates representative samples of the propane could not be delivered to the analytical device. Parametric testing with the propane confirmed earlier results reported by UTRC, i.e., the velocity and inlet temperature of the propane were significant factors in the amount of corrosion product formed in the channel.

Task 2 tests demonstrated the efficacy of metallic coatings as a means of corrosion protection for the cooling channels. Static tests established the nobility of six metals in a high pressure, high temperature environment of methane plus relatively high concentrations of sulfur compounds. Two of the six metals, i.e., gold and platinum, were selected for further study. Dynamic test specimen were fabricated and the test channels were protected by a thin layer of electrodeposited gold or platinum. The specimen were subjected to dynamic tests at realistic booster engine conditions while operating with methane coolant containing 5 ppm (by vol) methyl mercaptan. Additional tests were conducted with 5 ppm (by vol) hydrogen sulfide. Corrosion of the cooling channels was effectively reduced by the gold and platinum coatings. Figure 6 compares the condition of the copper cooling channel surface in similar tests conducted with and without the protective coating.

In Task 3, a program plan was developed which called for the fabrication and testing of a 40,000 lbF thrust chamber with copper cooling channels protected from corrosion with a metallic coating, e.g., gold. Tests were described in which the chamber is to be cooled with (1) sulfur-free methane and (2) methane containing a measured amount of sulfur contaminant to demonstrate the effectiveness of the coatings in extending the useable chamber life in booster engines to be used in recoverable, reusable vehicles.

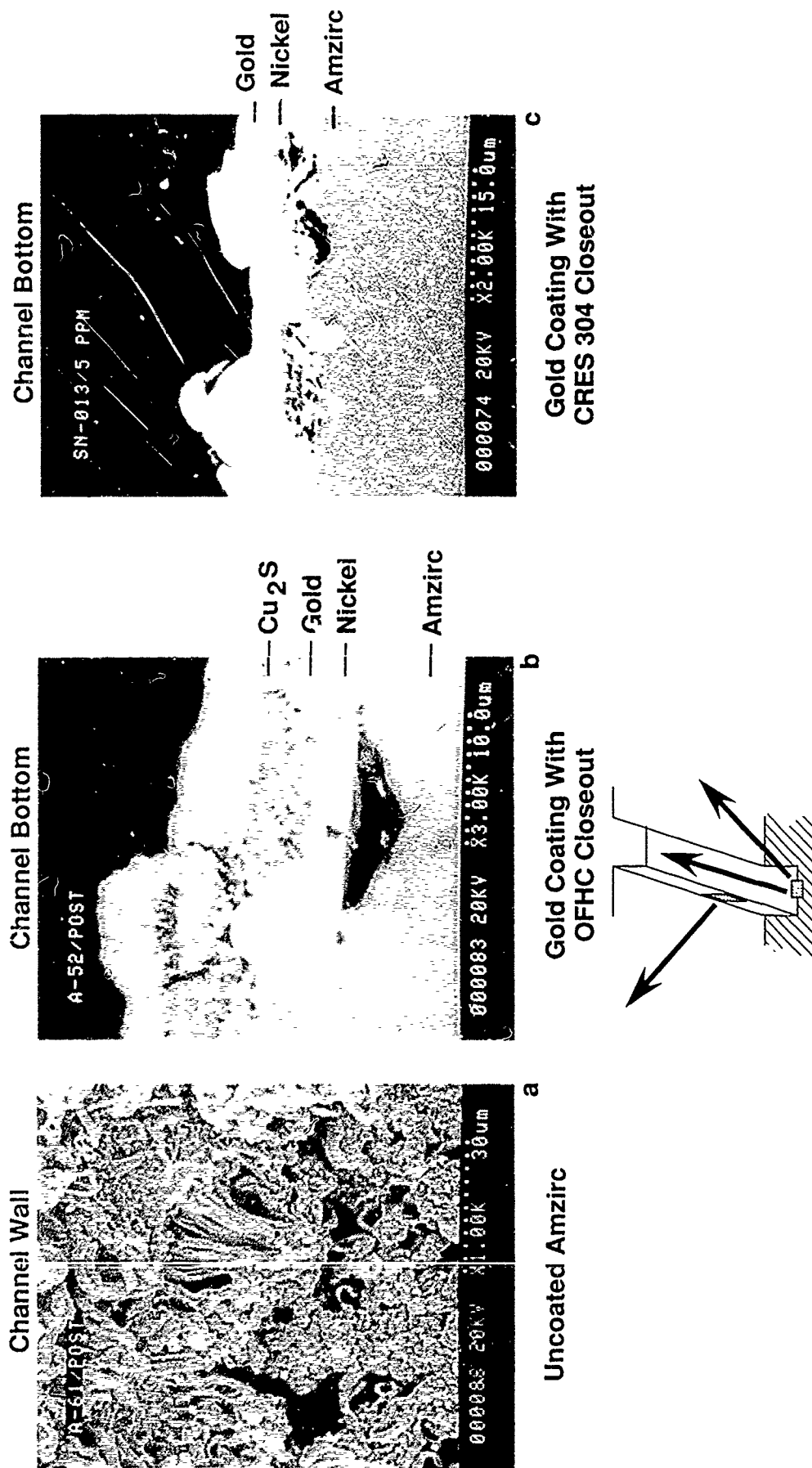


Figure 6. Post Test SEM Photos of Dynamic Test Specimen After Tests With Methane Plus 5 ppm H<sub>2</sub>S

### 3.0 TASK 1 — CORROSIVE INTERACTION AND CORROSION RATE DETERMINATION

The objective of Task 1 was to conduct an investigation which would result in a definition of the corrosive interaction process and a determination of the corrosion rates that occur in the reactions between hydrocarbon fuels and copper, alloyed and unalloyed. The specific fuels and materials which were investigated in Task 1 are listed in Table 2. General guidelines for the performance of Task 1 are listed in Table 3. This section of the report discusses the results of Task 1: a discussion of the test methods and procedures used in the conduct of this investigation is followed by a presentation of the results of experiments with RP-1, n-dodecane, methane, and propane, respectively.

#### 3.1 TEST METHODS

This section describes the test apparatus, test procedures, and analytical methods which were used in the static and dynamic tests of this program. The static test methods are described first, followed by a review of the dynamic test facility and procedures. A third section is devoted to a description of the chemical analyses of the fuels used in this program.

##### 3.1.1 Static Test Methods

Two static test methods were used to study the compatibility of hydrocarbon fuels with copper in a carefully controlled environment. Sealed Glass Ampul Tests were conducted with RP-1 and n-dodecane. Aminco Bomb Tests were conducted with methane and propane. The Sealed Glass Ampul Test offers the advantage of visual observation of the fuel/specimen sample throughout the course of the test, but its applicability is limited to low pressure tests with comparatively nonvolatile fuels. The Aminco Bomb Test offers the advantage of testing at high pressure, but it is best suited to the evaluation of comparatively volatile fuels.

In the Sealed Glass Ampul Test, the fuel and metallic coupons were loaded in an ampul as depicted in Figure 7. The sealed ampul was then heated to 400 F in a constant temperature oven for 14 days. Figure 8 shows a trace of the temperature in the oven during the test period. After removal from the oven, the ampules were opened into a measured volume, so that any pressure rise attributable to the formation of volatile reaction products, such as light hydrocarbons or hydrogen, could be measured.

TABLE 2  
HYDROCARBON-FUEL/COMBUSTION-CHAMBER-LINER  
MATERIALS COMPATIBILITY PROGRAM FUELS AND MATERIALS

<u>Fuels</u>	<u>Temperature Range of Interest</u>
RP-1 <sup>a</sup>	273.16 to 616.49 K (32 to 650 F)
Propane	90.39 to 616.49 K (-297 to 650 F)
Methane	111.66 to 616.49 K (-258.7 to 650 F)

<sup>a</sup>n-Dodecane was used for comparative purposes.

Copper Base Materials<sup>b</sup>

OFHC Copper

Amzirc (copper, 0.15 wt % zirconium)

NASA-Z (copper, 3 wt % silver, 0.5 wt % zirconium)

<sup>b</sup>All of the material noted was provided by the Government in the forged and annealed condition.

TABLE 3  
HYDROCARBON-FUEL/COMBUSTION-CHAMBER-LINER  
MATERIALS COMPATIBILITY PROGRAM GENERAL GUIDELINES

Engine Definition

Thrust Level	3,336 kN	(750,000 lbF)
Chamber Pressure	20,684 kPa	(3,000 psia)
Cycle	Gas Generator	
Number of Flights	50	

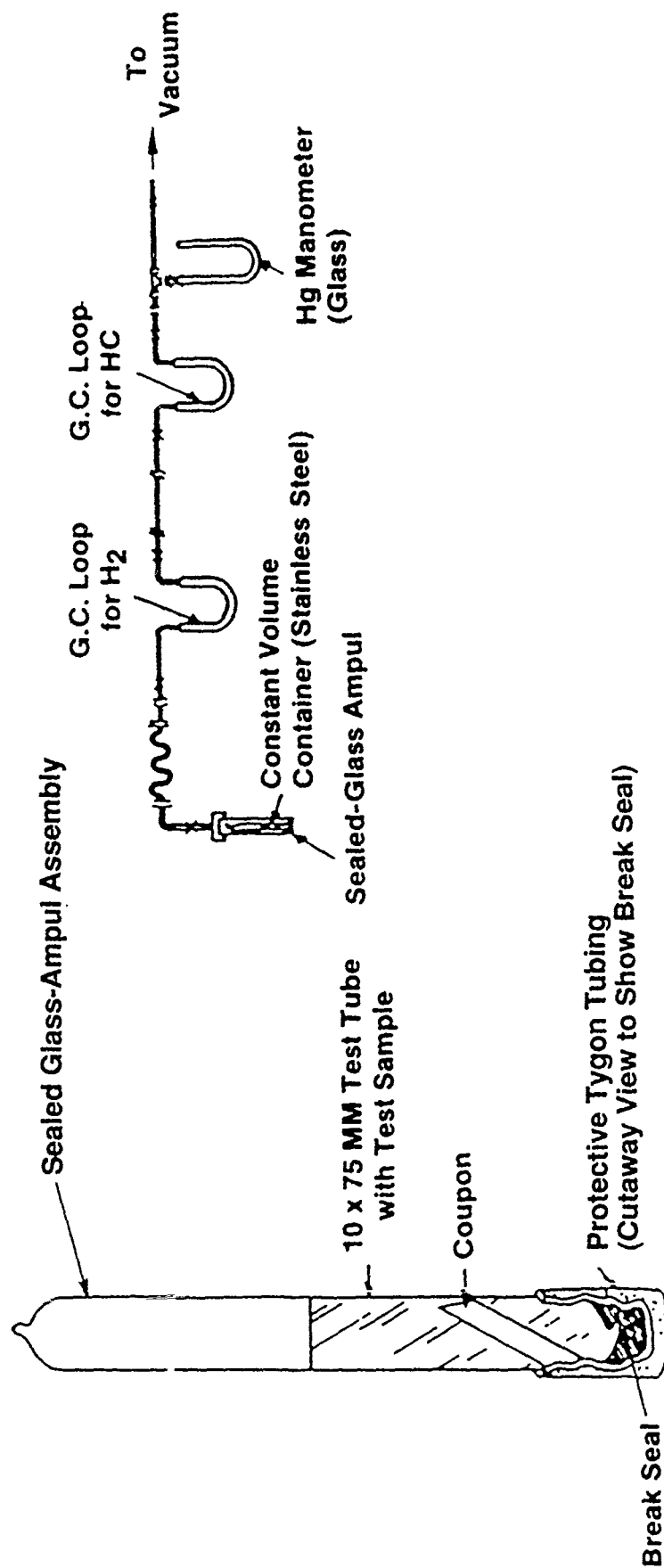
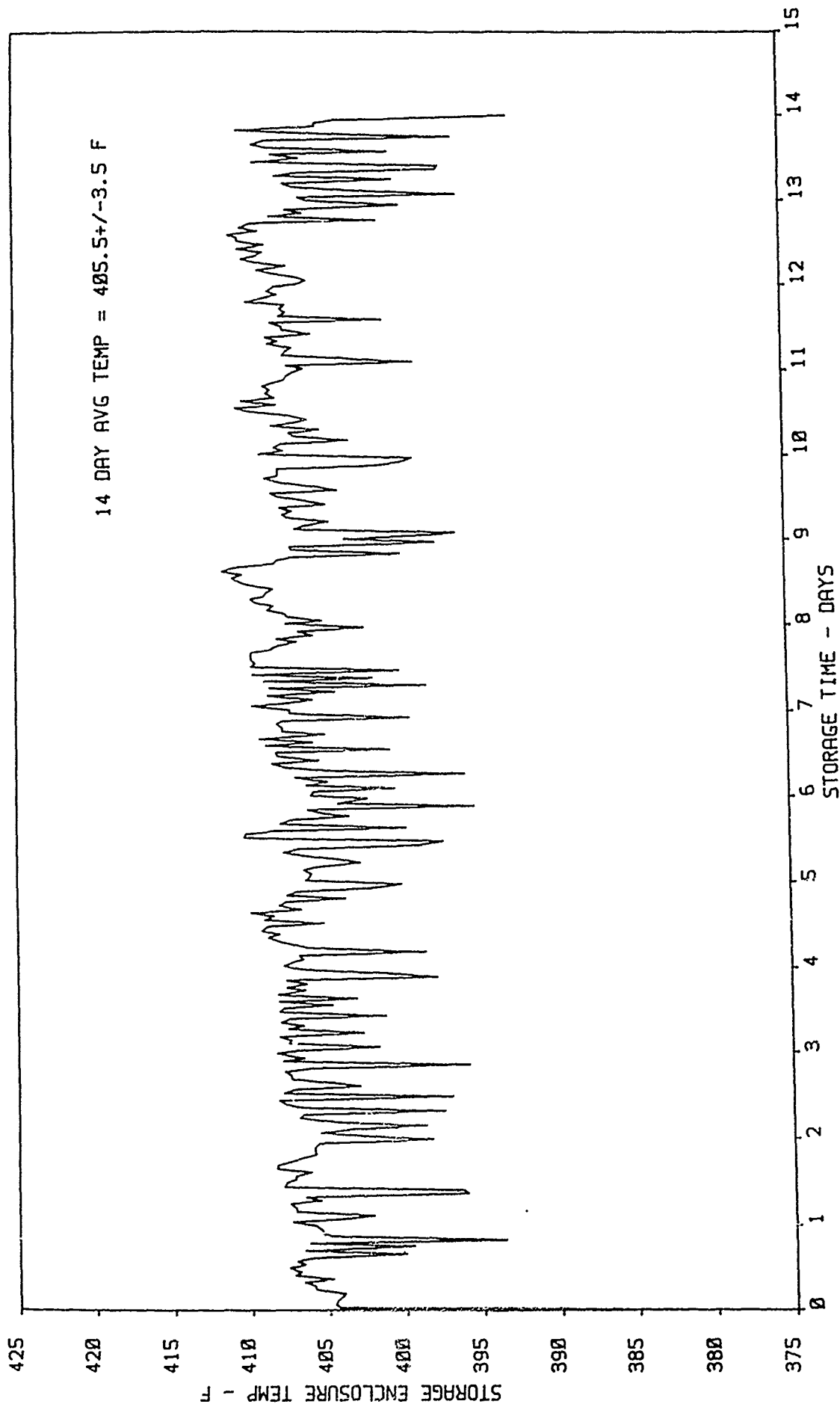


Figure 7. Sealed Glass Ampul Test Schematic



START DATE - 3/11/87●1400

Figure 8. Ampul Test Temperature

### 3.1, Test Methods (cont.)

The gas and liquid phases of the ampul were analyzed for hydrogen and hydrocarbons by gas chromatography. The metallic coupons were weighed and examined with optical and scanning electron microscopes.

The coupons used in the Sealed Glass Ampul Test were cut by EDM from 0.020-in. thick sheet. The material was made by cold rolling pieces cut from billets of OFHC, Amzirc, and NASA-Z supplied by NASA-LeRC. The coupons were cut into 0.25 x 1.0-in. rectangles which were cleaned, weighed, and photographed before they were placed in the ampules. The surface of each specimen was also examined under a scanning electron microscope (SEM) and micrographs were taken of a point on the middle of the surface of each coupon at 200, 400, and 2000x prior to the tests. When the coupons were removed from the ampules, they were immediately weighed and photographed, and posttest micrographs were taken of the same spot on the surface, again at 200, 400, and 2000x.

In the Aminco Bomb Tests, the fuel and metallic coupons were sealed in a high pressure vessel using the filling system shown in Figure 9. The bomb was heated to 650 F in an oven and held at this temperature for 30 min. Upon removal from the oven, the bomb was cooled in a water bath. Figure 10 shows a trace of the temperature and pressure in the bomb during a typical test. After cooling to ambient temperature, samples of the gas phase of the bomb were taken and analyzed for hydrogen and hydrocarbons by gas chromatography. The metallic coupons were weighed and examined with optical and scanning electron microscopes.

The coupons used in the Aminco Bomb Tests were punched from 0.020-in. thick rolled sheet. The coupons were 15/16-in. dia circles with a 1/8-in. hole in the center. Each coupon was cleaned, weighed, and photographed before the test. The surface of each specimen was examined under a SEM and micrographs were taken of a point on the middle of the surface of each coupon at 200, 400 and 2000x prior to the tests. After cleaning and inspection, the coupons were suspended on a Type 347SS rack, and the entire assembly sealed and leak tested with nitrogen. After passing the leak test, the bomb was evacuated to < 1 torr for a minimum of 30 min. The bomb was then filled with fuel plus the appropriate additives and heated. When the coupons were removed from the bomb after testing, they were immediately weighed and

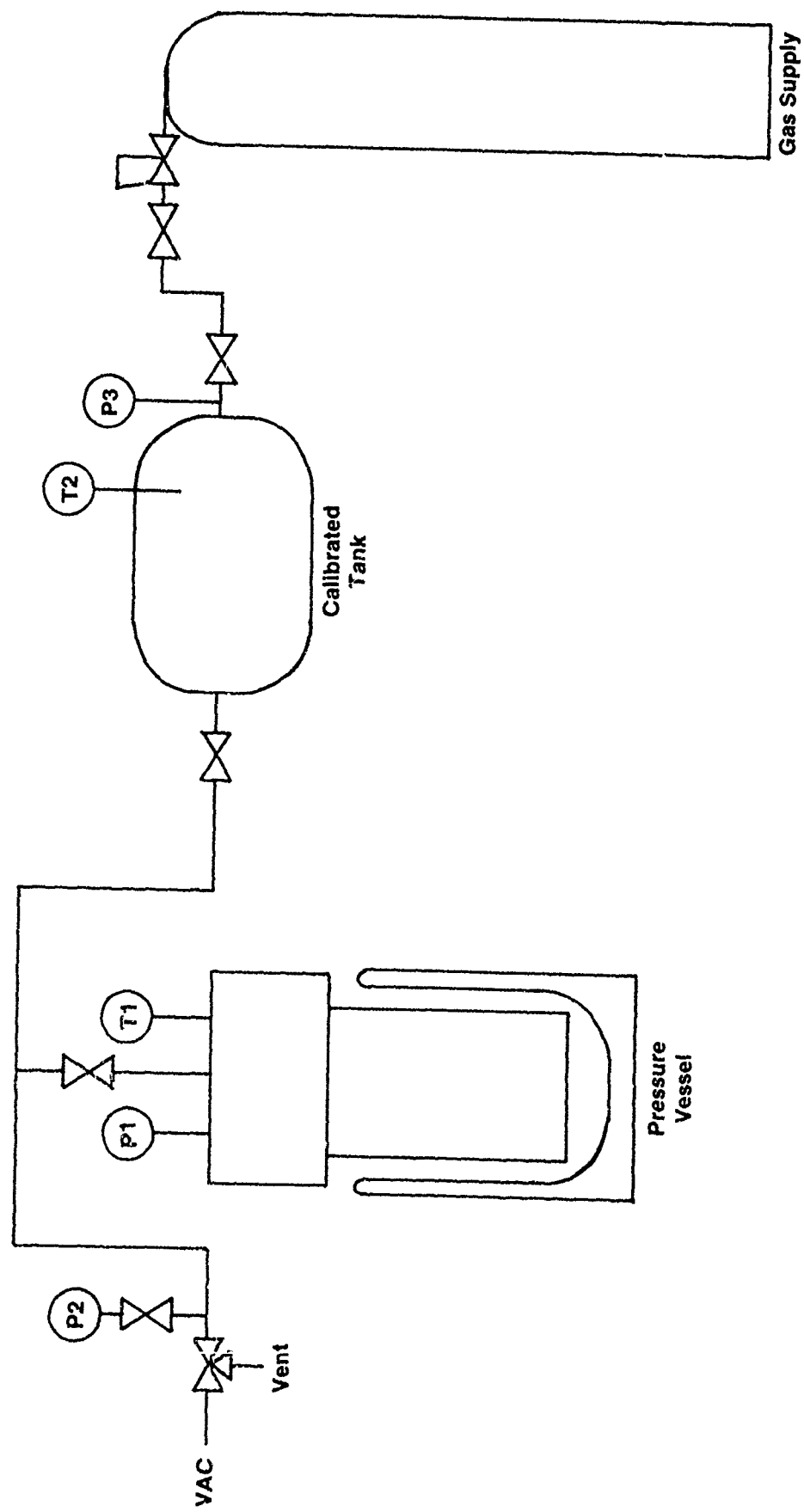


Figure 9. Bomb Loading Apparatus Used in Methane and Propane Static Tests

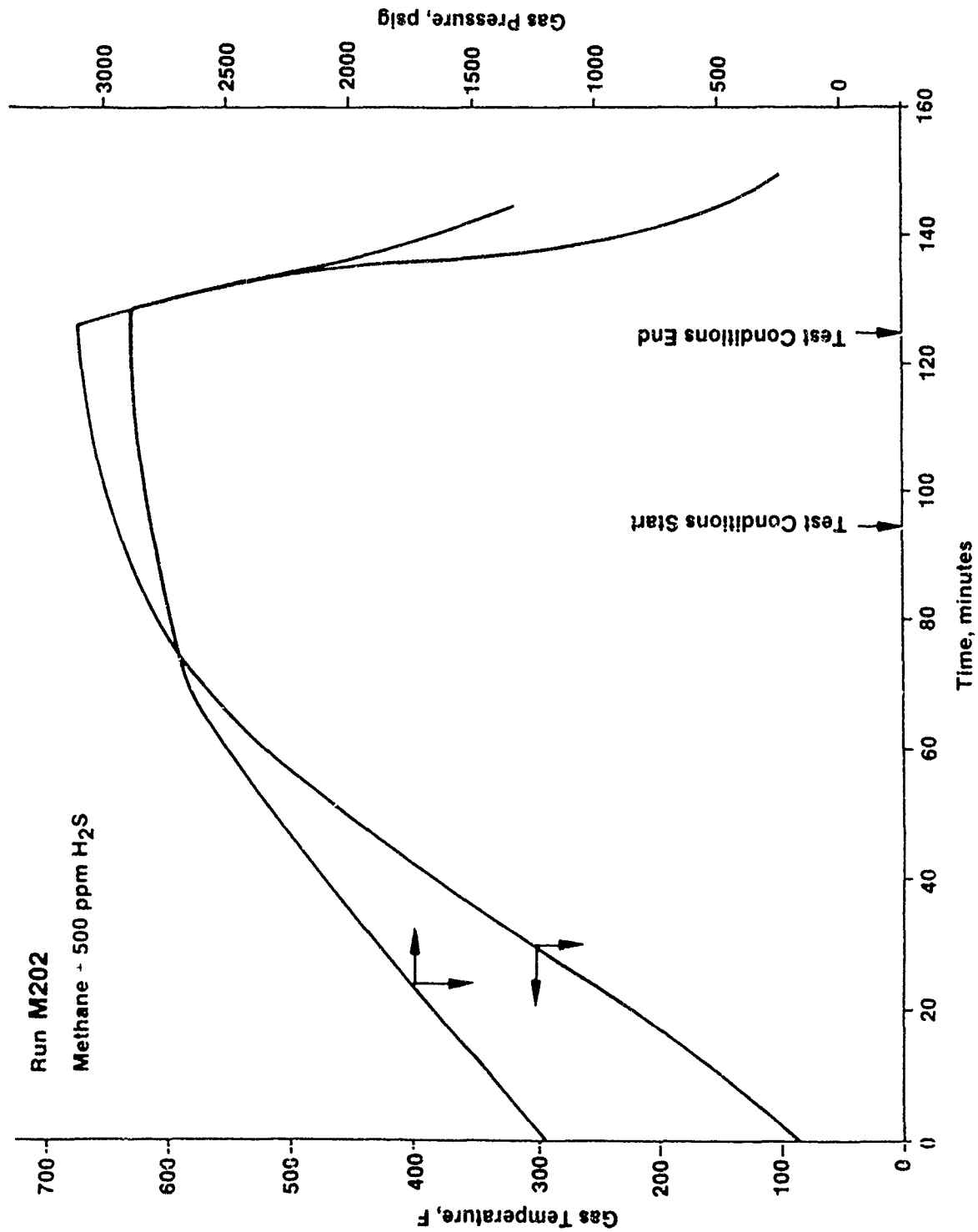


Figure 10. Typical Static Bomb Test Pressure and Temperature Traces

### 3.1, Test Methods (cont.)

photographed, and posttest micrographs were taken of the same spot on the surface, again at 200, 400, and 2000x.

Appendix A of this report details the procedures used to load and unload the Glass Ampules and the Aminco Bomb.

#### 3.1.2 Dynamic Test Methods

Dynamic tests were conducted in the Aerojet Carbothermal Test Facility with four hydrocarbon fuels, Mil-Spec RP-1, n-dodecane, as a high-purity simulant for RP-1, methane, and propane, and three copper chamber materials, OFHC, NASA-Z (3% Ag, 0.5% Zr), and Amzirc (0.15% Zr). Figure 11 presents a schematic diagram of the dynamic test apparatus.

The apparatus incorporates two fuel delivery subsystems, one for high-pressure methane, the other for RP-1, n-dodecane, and propane. The RP-1 and n-dodecane were tested at ambient temperature inlet conditions. The methane and propane were subcooled to between -200 and -100 F enroute to the heated copper test specimen. The test specimen was heated within the Aerojet Carbothermal Materials Tester without the use of direct ohmic heating. The apparatus incorporates appropriate filters, thermocouples, pressure transducers, propellant thermal conditioners, and mass flowmeters to control and measure the test conditions and record the test data on-line. A port is incorporated to provide on-line fuel samples for chemical analysis.

Figure 12 presents a conceptual diagram of the Aerojet Carbothermal Materials Tester. It utilizes a large copper block which is heated by ten electrically insulated cartridge heaters embedded in the block. The heat input into the block is transferred by conduction through a test specimen made of the copper material to be tested. The heat is then withdrawn through a 0.020-in. square cooling channel milled in the bottom of each specimen by fuel flowing through the channel. Figure 13 shows photographs of a typical test specimen used in the Aerojet Carbothermal Materials Tester.

Realistic simulations of cooling channel conditions were produced in this facility without the use of direct ohmic heating of the specimen. Table 4 compares

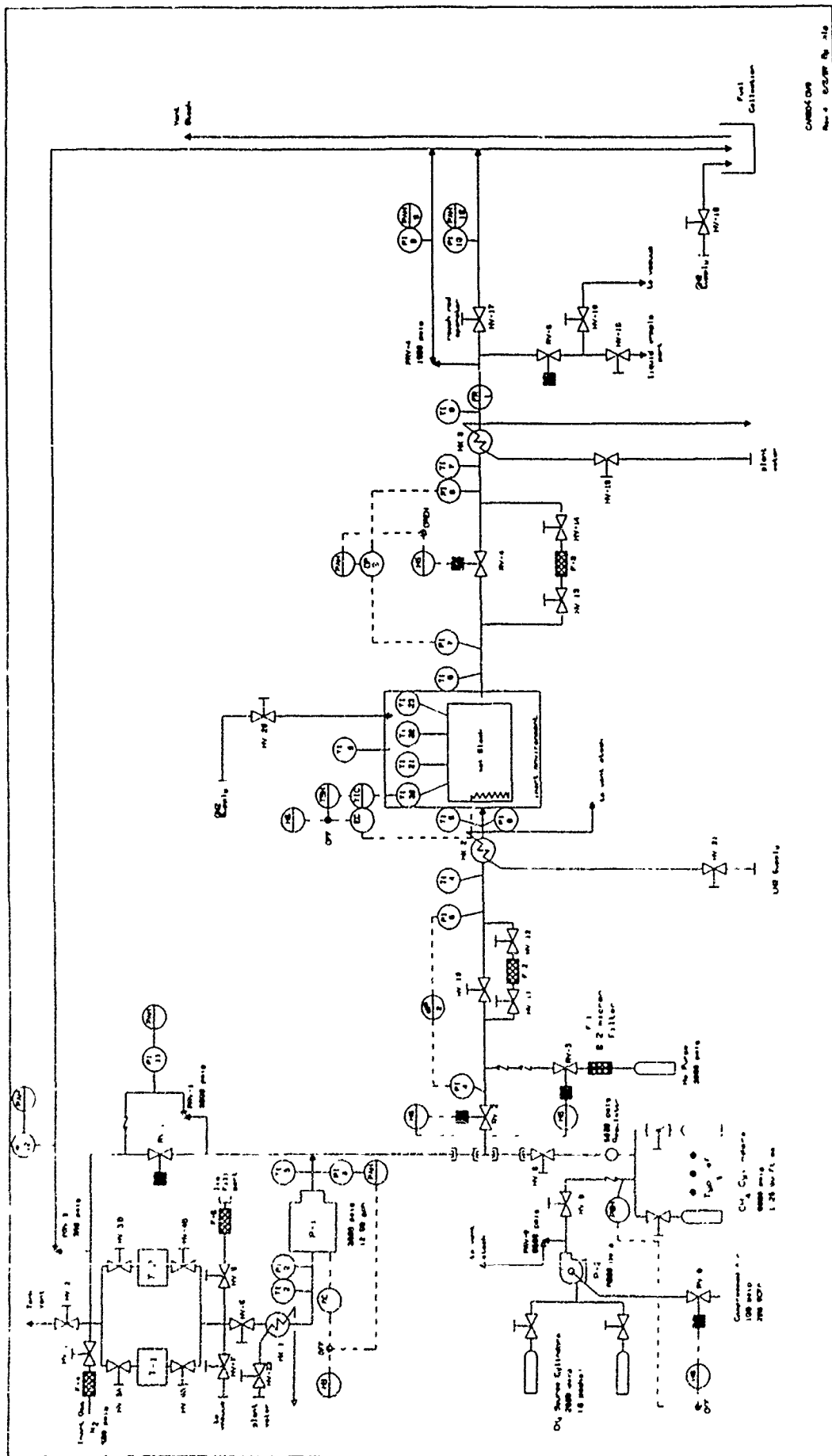
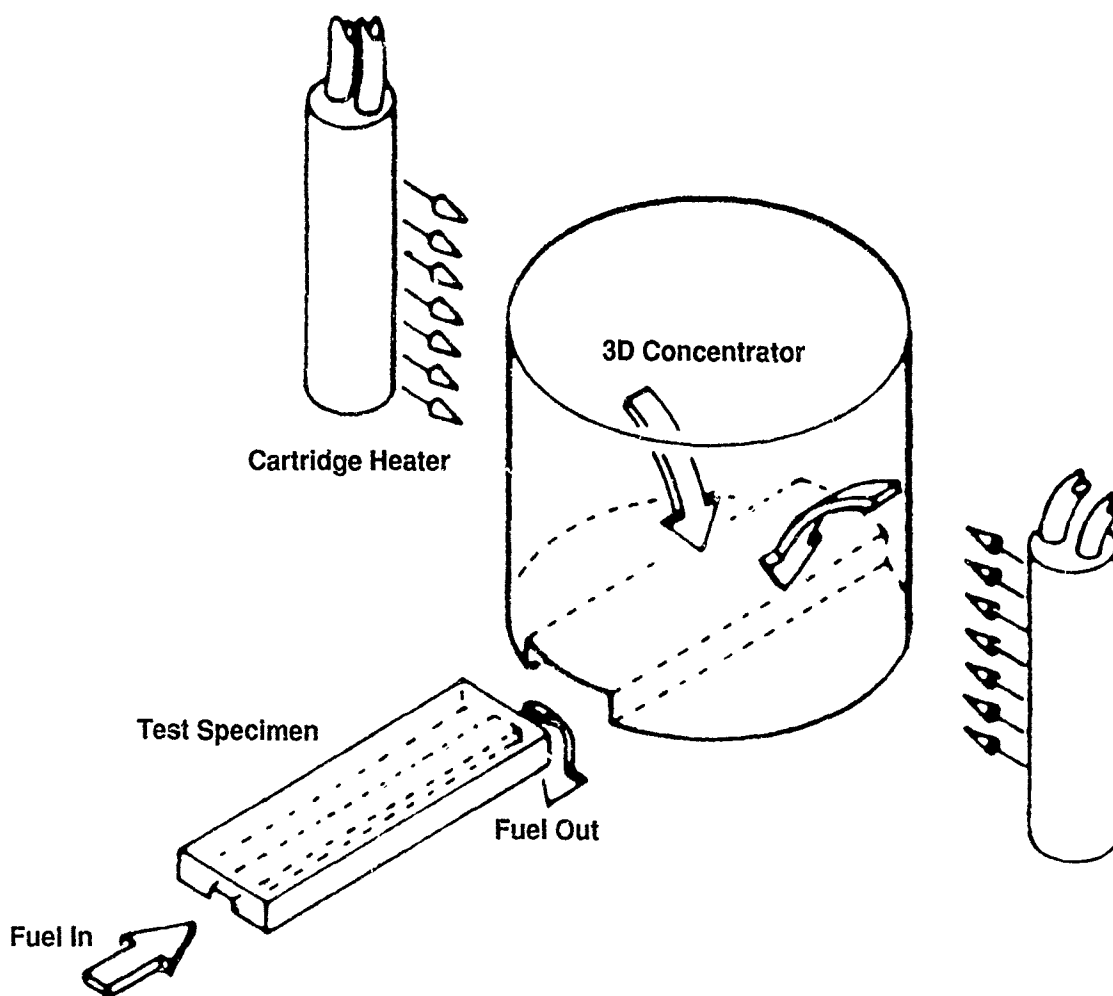


Figure 11. Schematic of Aerojet Carbothermal Test Facility



The Geometric Concentration of Energy is an  
Alternative to Ohmically Heated Test Specimens

Figure 12. Conceptual Design of Aerojet Carbothermal Materials Tester

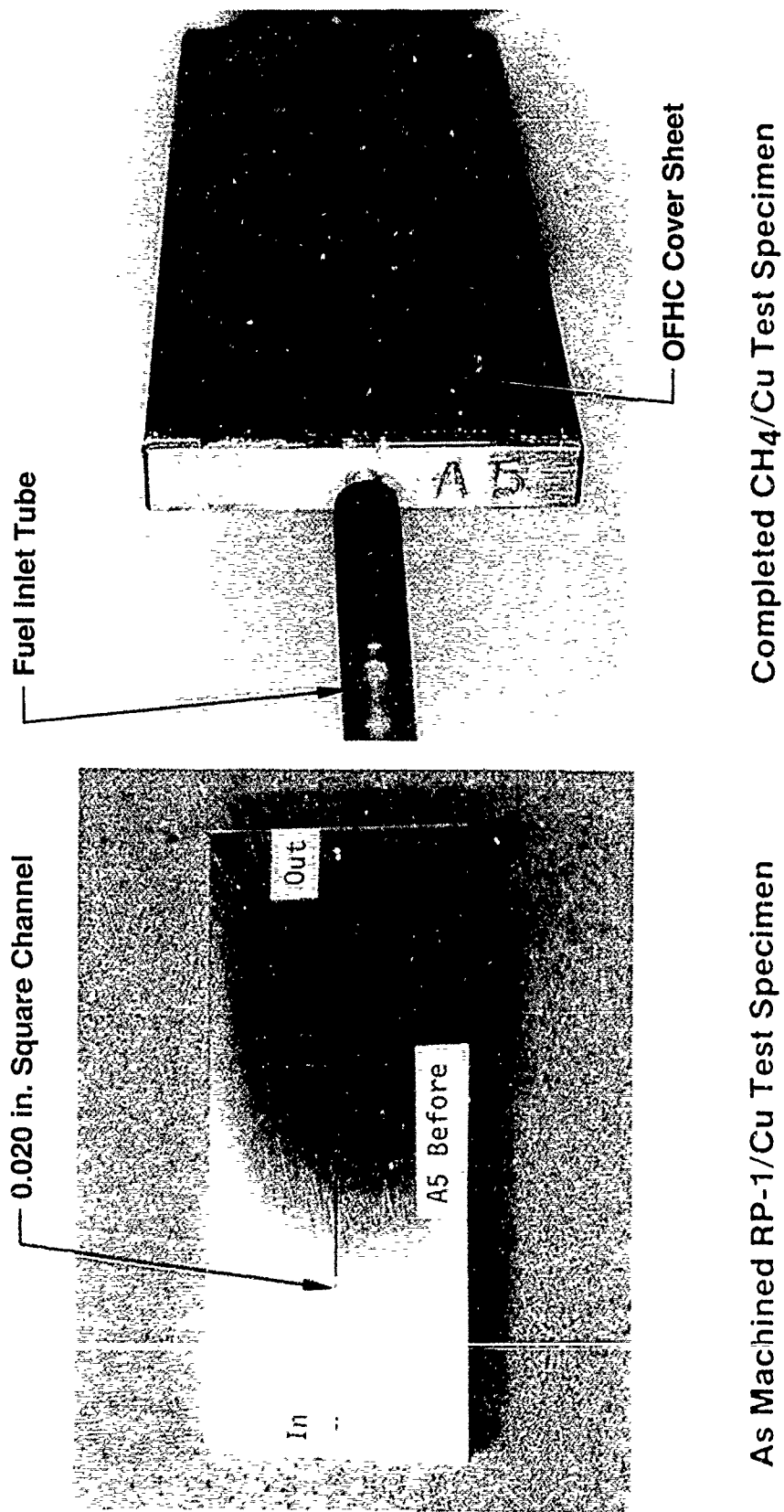


Figure 13. Copper Test Specimen Details

TABLE 4

REALISTIC COOLING CHANNEL CONDITIONS WERE PRODUCED IN  
THE AEROJET CARBOTHERMAL MATERIALS TEST FACILITY

	<u>Methane Test Conditions</u>	<u>STBE Design</u>
Wall Temperature, F	650-930	800
Max Coolant-Side $q/A$ , Btu/in. <sup>2</sup> -s	52	51
Coolant Pressure, psia	4200	4400
Coolant Velocity, ft/s	100 → 1000	300 → 500
Bulk Temperature, F	-150 → +380	-200 → +70
Test Duration, sec	1000 - 1800	160/mission

### 3.1, Test Methods (cont.)

channel conditions produced in the methane tests with design conditions for the STBE methane engine. Note that each of the relevant design parameters were reproduced, including wall temperature, fuel temperature and pressure, fuel velocity, and heat flux through the channel wall.

Another advantage provided by the Aerojet Carbothermal Materials Tester is that examination of the test specimen can be accomplished directly without disturbing the surfaces which were in contact with the fuel. The RP-1 tests used a simple stainless steel fuel manifold pressed into the bottom of the test specimen to close out the channel. After the test, separation of the specimen from the manifold exposed the channel directly. The higher thermal strains encountered in the methane and propane tests required that the channel be closed out with a thin sheet (0.020 in.) of OFHC copper welded around the channel. After testing, a simple end mill operation opened the channel for examination without disturbing either the specimen channel or the closeout which had been exposed to the flowing fuel. This also provided the opportunity to obtain simultaneous compatibility data with OFHC (via the closeout sheet) and ZrCu or NASA-Z (via the machined specimen).

All dynamic test specimens were machined from the billets of material supplied by NASA-LeRC. As in the static tests, all dynamic specimens were cleaned, and photographed prior to testing. SEM photomicrographs of the channel surfaces before testing were taken on three specimens selected at random. No discernable difference was found among these specimens, and it was assumed they were representative of all specimen channels before testing.

Appendix B presents the Test Area checklist which was used in the conduct of the dynamic tests. This checklist describes the sequence of operation that was typically used to conduct a dynamic test.

Each dynamic test was run at a constant wall temperature, as measured by four thermocouples along the channel wall. To achieve this, the power going to the heaters in the Aerojet Carbothermal Materials Tester was manually adjusted during the test with a potentiometer. This was particularly important during testing with RP-1, where the heat transfer performance of the specimen declined by as much as 30% during the course of some tests.

### 3.1, Test Methods (cont.)

Data were collected from the on-line instrumentation of the system through a Daytronics data acquisition system, and stored every 5 sec on an IBM-AT. A data reduction program was written to calculate test conditions and to analyze the hydraulic and heat transfer performance of the specimen during the test. A listing of the data reduction program, along with a typical page of output from a test, is included in Appendix C.

#### 3.1.3 Fuel Analysis

All fuels used in this program were analyzed prior to use. Additives which were used in some tests were either analyzed or certified by the vendor specifications of purity. A summary of all the fuel analyses is included as Table 5.

RP-1 was obtained as a Government Furnished Propellant from Aerojet Test Area J. Two 55 gallon drums were cleaned and filled with RP-1, which provided the fuel for all static and dynamic Task 1 testing. Samples of the RP-1 were analyzed at Aerojet by gas chromatography and X-ray fluorescence. The gas chromatograph resolved over 50 distinct peaks, though the exact molecular species corresponding to each peak was not determined. X-ray fluorescence was used to analyze the RP-1 for sulfur content. No sulfur compounds were detected. Laboratory standards which were made established the detection limit of the instrumentation to be approximately 10 ppm (by weight) of sulfur compounds in the RP-1.

One 55 gallon drum of high purity n-dodecane was purchased from Phillips Specialty Chemicals for Task 1. An independent analysis was conducted by J&A Associates, Golden, CO prior to use on the program. Gas chromatography was used for characterization of the hydrocarbons. In contrast with the analysis of the RP-1, gas chromatography indicated that not more than two species were present in the n-dodecane, namely >99% n-dodecane and <1% n-undecane. Standards established that the n-dodecane contained less than 2 ppm (by weight) each of aromatic, olefinic, or other aliphatic compounds. X-ray fluorescence did not find any sulfur compounds in the n-dodecane, down to a detection limit of 2 ppm.

TABLE 5  
VENDOR SUPPLIED ANALYSES OF PROPELLANTS AND ADDITIVES

<u>Material</u>	<u>Supplier</u>			<u>Analysis</u>
UHP Methane	Linde Specialty Gases	>	99.97	vol % CH <sub>4</sub>
			2.4	ppm O <sub>2</sub>
		<	15	ppm N <sub>2</sub>
		<	5	ppm H <sub>2</sub> S
		<	2	ppm SO <sub>2</sub>
Instrument Grade Propane	Liquid Carbonic	>	99.5	wt % C <sub>3</sub> H <sub>8</sub> (liquid)
		<	2	ppm SO <sub>2</sub>
		<	2	ppm H <sub>2</sub> S
			0.6	ppm O <sub>2</sub>
			200	ppm H <sub>2</sub> O
Ethylene	Linde Specialty Gases	>	99.5	vol % C <sub>2</sub> H <sub>4</sub>
			6	ppm O <sub>2</sub>
			41	ppm N <sub>2</sub>
		<	2	ppm H <sub>2</sub> S
		<	2	ppm SO <sub>2</sub>
Propylene	Linde Specialty Gases	>	99.0	wt % C <sub>3</sub> H <sub>6</sub> (liquid)
			172	ppm H <sub>2</sub> (gas)
			1192	ppm O <sub>2</sub> (gas)
			2.0	vol % N <sub>2</sub> (gas)
Methyl Mercaptan	Matheson Gas Products	>	99.5	wt % CH <sub>3</sub> SH (liquid)
n-Dodecane	Phillips Specialty Chem.	>	99.0	wt % n-dodecane
			1.0	wt % undecane
Dodecanethiol	Aldrich Specialty Chem.	>	98.0	wt % dodecanethiol
Biphenyl	Aldrich Specialty Chem.	>	99.0	wt % biphenyl
1-Dodecene	Aldrich Specialty Chem.	>	95.0	wt % 1-dodecene
Research Grade Propane	Matheson Gas Products	>	99.96	% C <sub>3</sub> H <sub>8</sub>
		<	5	ppm O <sub>2</sub>
		<	5	ppm N <sub>2</sub>
		<	0.1	ppm CH <sub>4</sub>
			270	ppm C <sub>2</sub> H <sub>6</sub>
		<	1	ppm C <sub>2</sub> H <sub>4</sub>
			55	ppm C <sub>3</sub> H <sub>6</sub>
		<	5	ppm i-butane
		<	5	ppm n-butane
		<	2	ppm H <sub>2</sub> O
Technical Grade Methane	Linde Specialty Gases	>	97.0	% CH <sub>4</sub>
			8.8	ppm O <sub>2</sub>
			4.8	ppm H <sub>2</sub> O
		<	2	ppm SO <sub>x</sub>

### 3.1, Test Methods (cont.)

Ultra High Purity (UHP) methane was used in the static tests of Tasks 1 and 2. A complete analysis supplied by the vendor is included in Table 5.

Technical Grade methane was used in the dynamic tests of Tasks 1 and 2. The vendor supplied analysis is included in Table 5. Note that no sulfur compounds were found in the original analysis of the methane, down to a detection limit of 2 ppm by volume.

After Task 1 dynamic tests indicated that even very low (1 ppm by volume) concentrations of sulfur compounds in methane could create significant corrosion problems with copper, additional analysis of the technical grade methane was conducted specifically to lower the detection limit on sulfur compounds. Two stainless steel Hoke cylinders were filled with 1800 psig of methane, one directly from the starting methane stock, and the other from the run tanks of the Aerojet Carbothermal Test Facility, which contained methane plus 1 ppm (by volume) methyl mercaptan. The two were marked with serial numbers and shipped to Air Products Corporation. The two cylinders were analyzed for  $\text{H}_2\text{S}$ ,  $\text{CH}_3\text{SH}$ , and  $\text{COS}$  by gas chromatography down to a detection limit of 0.2 ppm by volume. No sulfur compounds were found, even in the sample which was intentionally contaminated to 1 ppm. Two conclusions are possible. Either the detection limit of the analytical method was not as low as was believed, or the sampling procedure which was used to obtain the contaminated specimen did not produce representative samples. In either case, the ramifications are significant and justify further study of the fuel supplier's sampling and analytical techniques.

Instrument Grade Propane was used during the first static test with propane (test 106) and during all the dynamic tests. Analysis was provided by the supplier prior to use. This analysis certified the liquid phase of the propane to contain >99.5 wt % propane, with the gas phase containing 0.6 ppm oxygen, 200 ppm water, and less than 2 ppm sulfur dioxide and hydrogen sulfide (none detected). After the initial dynamic tests with propane showed the formation small amounts of  $\text{Cu}_2\text{S}$  in the channels, additional analysis was done on one of the propane cylinders. One of the original cylinders was shipped to Drexel University and analyzed by Dr. Alan R. Bandy. He analyzed the head gas of the cylinder by gas chromatography and flame photometric detection for  $\text{COS}$ ,  $\text{H}_2\text{S}$  and  $\text{CH}_3\text{SH}$ . None was found, down to a detection

### 3.1, Test Methods (cont.)

limit of 0.050 ppm by volume. It was possible that the sulfur content of the liquid phase was higher. The liquid phase is more difficult to analyze, and was not analyzed.

Research Grade Propane was used during all other static tests with propane. It was analyzed by the supplier prior to delivery, and the results of this analysis are shown in Table 5. Test results did not indicate any sulfur contamination of this propane.

Additives were also purchased for the program to test the effect of high concentrations of olefins, aromatics, and various sulfur-containing compounds. Additives which were tested included biphenyl, 1-dodecene, and n-dodecanethiol (in selected RP-1 tests), ethylene, methyl mercaptan, and hydrogen sulfide (in selected methane tests), and propylene and methyl mercaptan (in selected propane tests). Analyses of these additives were supplied by the vendors and are included in Table 5.

### 3.0, Task 1 — Corrosive Interaction and Corrosion Rate Determination (cont.)

#### 3.2 RP-1 TEST RESULTS

This section of the report discusses the results of tests with RP-1 and its high purity simulant, n-dodecane. The results of static tests using RP-1 and n-dodecane are covered first, followed by a discussion of the dynamic tests.

##### 3.2.1 RP-1 Static Tests (Task 1.1.2)

As detailed in Section 3.1.1, static tests were conducted using glass ampules filled with RP-1 or n-dodecane and a coupon of Amzirc, NASA-Z, OFHC, or SS304. This section documents the results of these static tests.

A custom set of glassware for loading and unloading the ampules was assembled. Care was taken in the selection of materials used in the system to prevent contamination of the ampules from sources such as stopcock grease, and valve and equipment seals. The only materials in contact with the ampules or their contents were glass, greaseless Teflon stopcocks and Tygon tubing.

Ten ampules were loaded with RP-1 or n-dodecane plus selected additives and metallic coupons. Table 6 records the contents of each ampul. These ten ampules were selected to focus upon the effect of the variables believed to be most important in this study, namely (1) fuel impurities, (2) exposure of the fuel to air, (3) nature of copper-based material, i.e., OFHC vs Zr-Ag-Cu alloys such as NASA-Z, (4) grain size of the material and (5) stress/strain history of the material. Analysis of the contents of these ten ampules, both before and after the incubation period, provide an independent test of the effect of each of these variables.

The ten ampules were placed in a 400 F oven and incubated at constant temperature for 336 hours (14 days). Figure 8 shows the oven temperature during the test.

At the end of the fourteen day incubation period, the ampules were removed from the oven and visually inspected. The RP-1 in the ampules showed a change of color in the liquid phase. The RP-1 loaded into the ampules was a dark pink. After heating during the test, the RP-1 became clear and transparent. This color change

TABLE 6  
CONTENTS OF RP-1 GLASS AMPUL TESTS

<u>Ampul No.</u>	<u>Fuel</u>	<u>Additives</u>	<u>Material</u>	<u>Grain</u>	<u>Strain</u>
1	RP-1	Air	None		
2	n-Dodecane	Air	None		
3	RP-1	Air	316SS		
4	RP-1	Air	OFHC	Fine	No
5	RP-1	None	OFHC	Fine	No
6	RP-1	Air	NASA-Z	Fine	No
7	n-Dodecane	Air	NASA-Z	Fine	No
8	n-Dodecane	Air + 525 ppm S	NASA-Z	Fine	No
9	n-Dodecane	Air + 525 ppm S	OFHC	Large	No
10	n-Dodecane	Air + 525 ppm S	OFHC	Large	Yes

### 3.2, RP-1 Test Results (cont.)

occurred in all of the RP-1 ampules, including those with copper coupons, those with stainless steel coupons, and those with no coupons at all (i.e., the control tests).

The only metallic coupons which exhibited visual changes were those copper coupons (both OFHC and NASA-Z) which were exposed to n-dodecane doped with n-dodecanethiol to a total sulfur level of 525 ppm (ampules 8, 9 and 10). These coupons developed a uniform, dark grey, tarnish or deposit on the surface. No other changes were visible on any of the remaining metallic coupons.

After visual inspection upon removal from the oven, the ampules were stored in a 45 F refrigerator until they were opened 12 days later. No visual changes occurred during the 12 days of refrigeration.

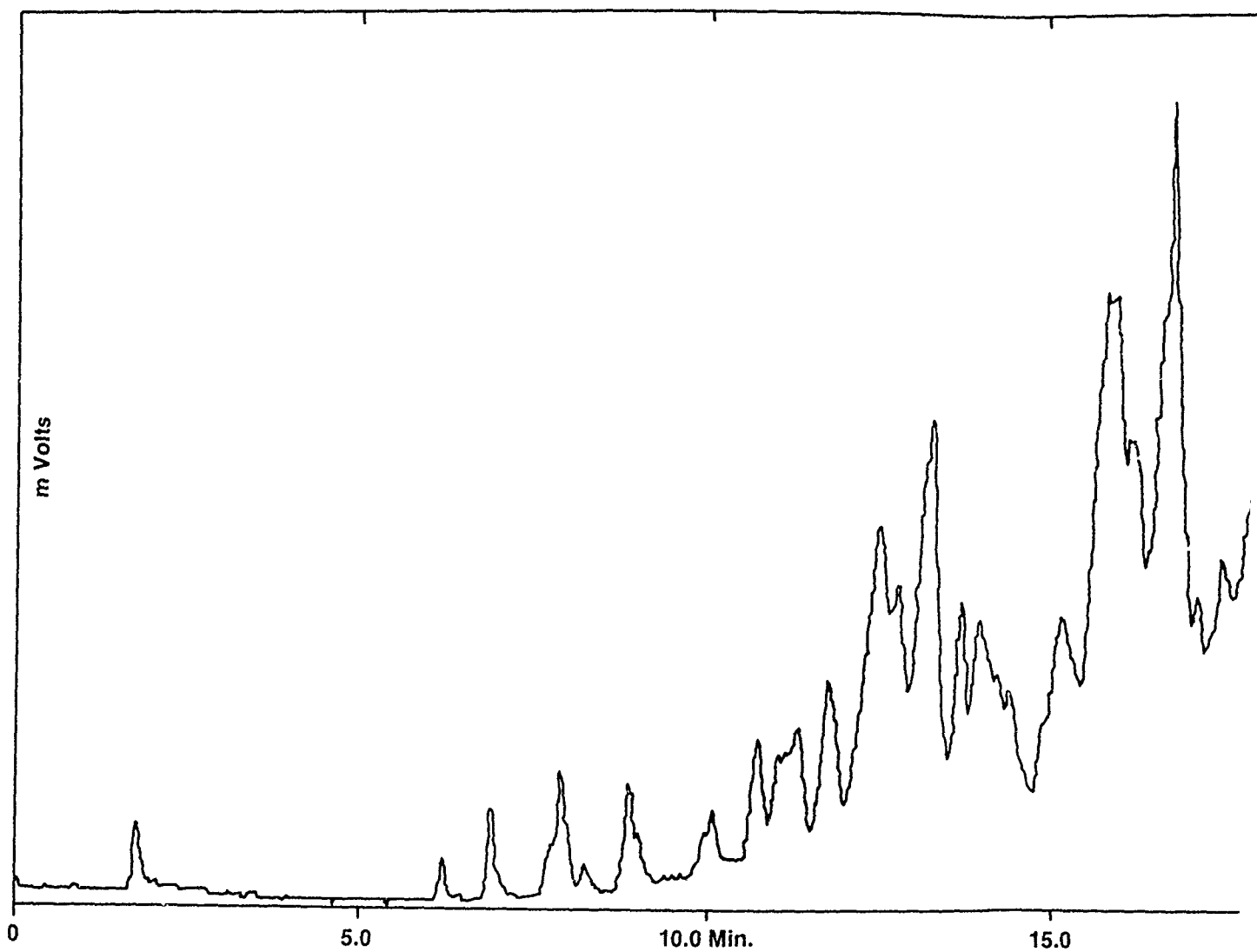
Each ampul was opened into a measured volume so the internal pressure of the ampul could be calculated. Table 7 shows the results of these calculations. Note that none of the ampules showed an increase in pressure as a result of the test, indicating that no insoluble gases were produced during the course of the test.

This conclusion was verified by the fact that no significant amounts of light molecular weight hydrocarbons were detected in the quantitative analysis of the gas phase. Analyses for hydrogen, helium, n-butane, i-butane, n-hexane, propane, ethane, methane, ethylene, propylene, carbon dioxide, and carbon monoxide were carried out by gas chromatography with appropriate calibrated standards. None of the ampules showed the presence of any of these compounds. Oxygen and nitrogen were the only species positively identified.

Similarly, comparison of the before and after analysis of the liquid phase of the ampules for hydrocarbon species and dissolved gases showed little change. Figure 14 shows a trace from a gas chromatograph of a sample of the RP-1 (saturated with air) loaded into ampules 1, 3, 4, and 6. Figure 15 shows a trace from the liquid extracted from ampul 6 after exposure to a NASA-Z coupon. Note that the traces show excellent separation of the various compounds which comprise RP-1, but comparison of the two traces showed no significant difference in the nature of the species separated or their relative amounts. None of the gas chromatograms of the liquid phase showed any difference before versus after exposure to the copper.

TABLE 7  
GAS PRESSURE MEASUREMENTS OF AMPUL TESTS

Test No.	Fuel	Impurities	System Volumes and Pressures					
			Before Opening			After Opening		
			System Volume (in. <sup>3</sup> )	System Pressure (mm)	System Volume (in. <sup>3</sup> )	System Pressure (mm)	Gas Volume (in. <sup>3</sup> )	Gas Pressure (mm)
1	RP-1	Air	2.77	787.0	2.97	777.0	0.20	637.2
2	n-Dodecane	Air	2.73	874.0	2.90	738.0	0.17	<0
3	RP-1	Air						
4	RP-1	Air	2.82	774.0	2.96	744.0	0.15	165.9
5	RP-1	None	2.74	804.0	2.91	767.0	0.17	169.6
6	RP-1	Air	2.76	822.0	2.93	729.0	0.17	<0
7	n-Dodecane	Air		820.0		814.0		
8	n-Dodecane	Air + 525 ppm S	2.76	773.0	2.91	752.0	0.16	380.3
9	n-Dodecane	Air + 525 ppm S						
10	n-Dodecane	Air + 525 ppm S	2.71	822.0	2.87	806.0	0.16	535.9



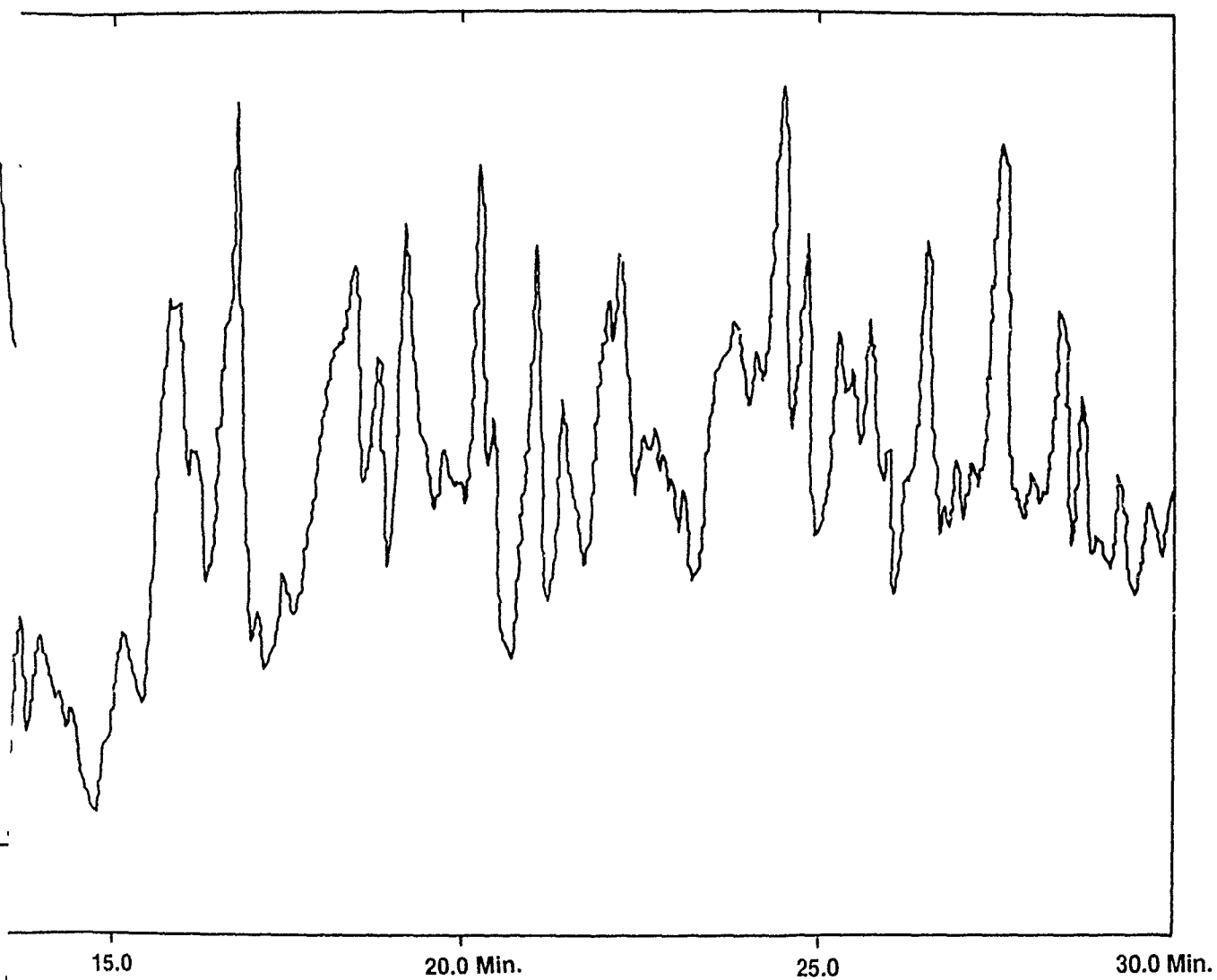


Figure 14. Gas Chromatograph of RP-1 Before Ampul Tests



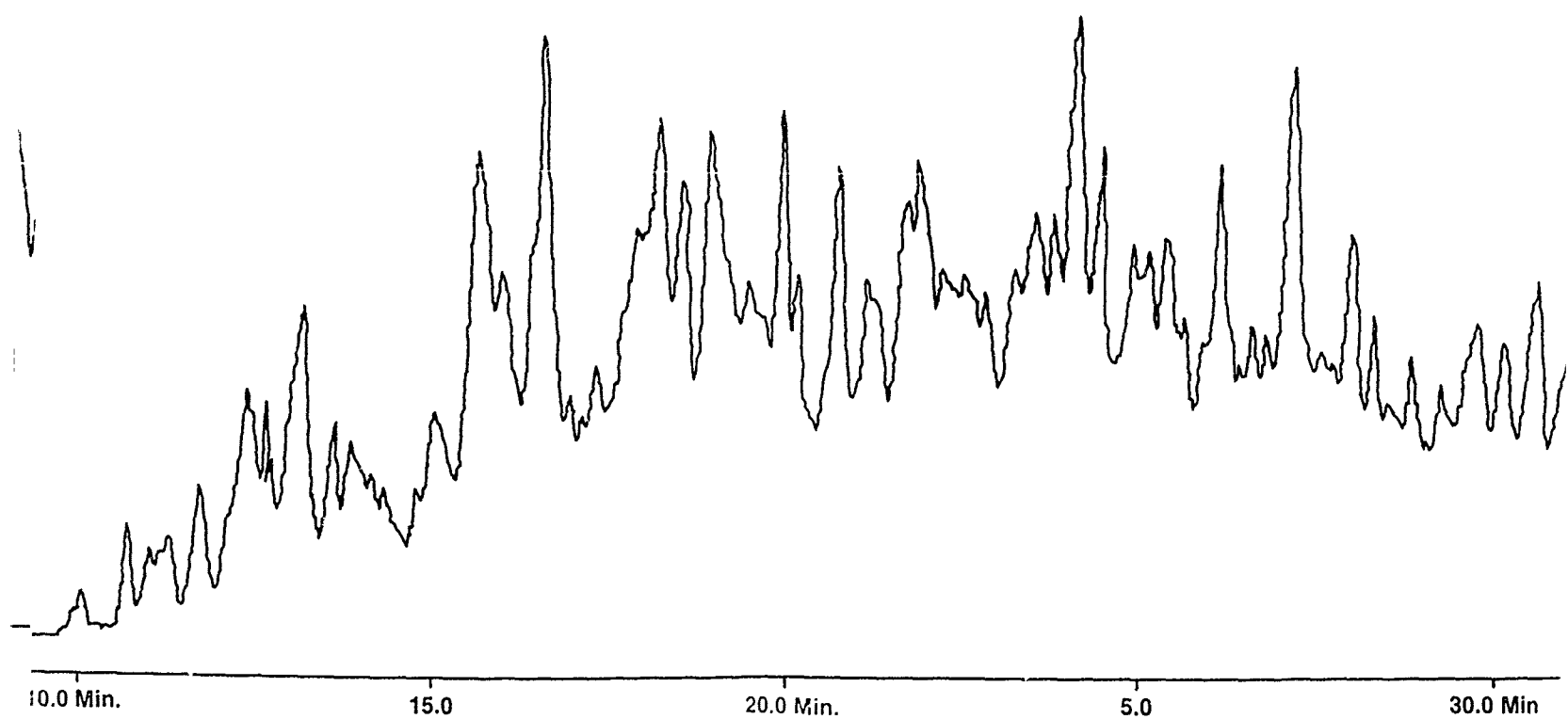


Figure 15. Gas Chroma

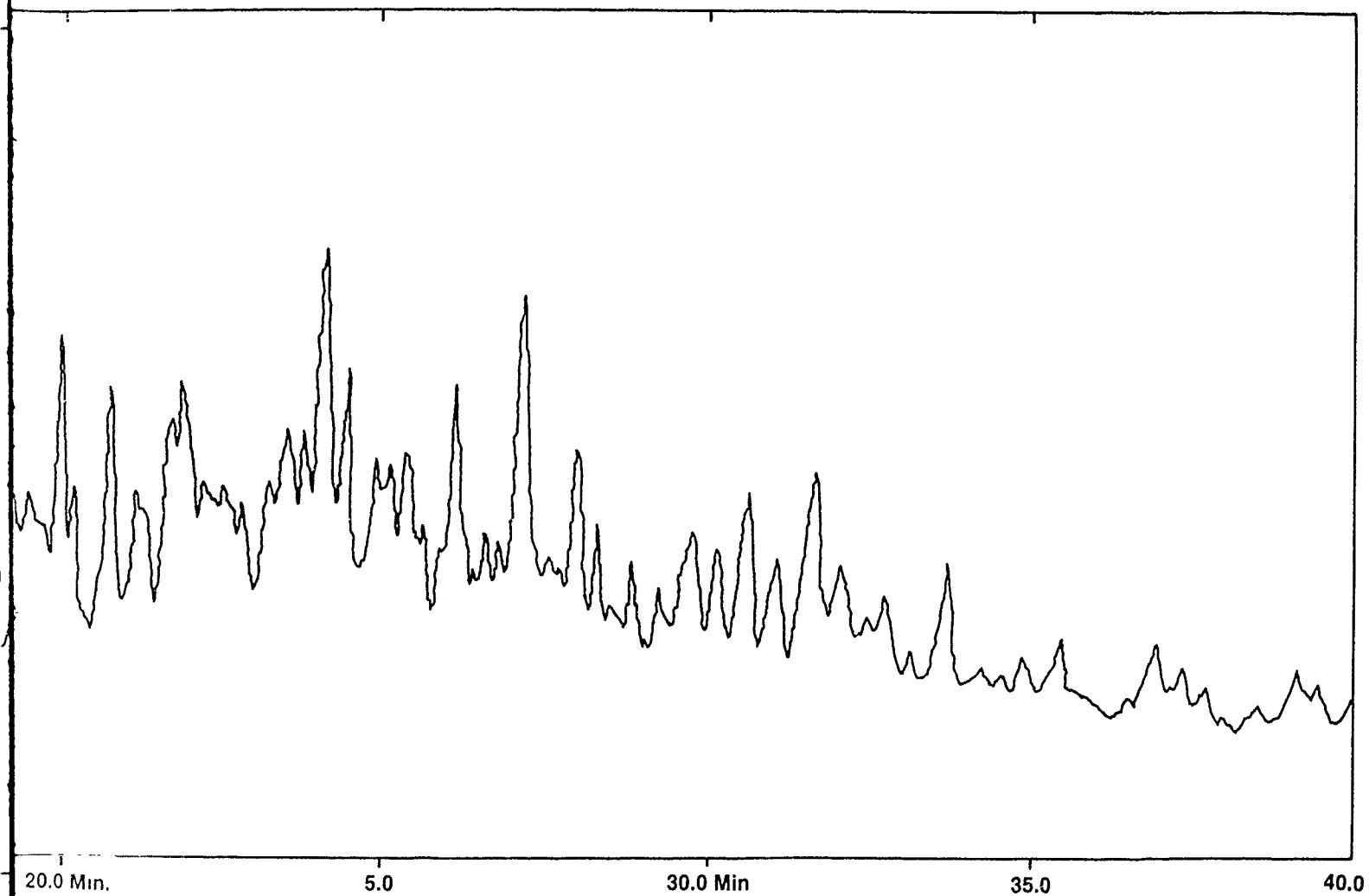


Figure 15. Gas Chromatograph of RP-1 After Ampul Tests

### 3.2, RP-1 Test Results (cont.)

Sulfur analysis of the liquid phase was done by X-ray fluorescence. The RP-1 and the n-dodecane used as starting material contained less than 10 ppm of sulfur (the detection limit of the equipment used to run the analysis — no sulfur was actually found in the starting materials).

n-dodecanethiol was added to n-dodecane in ampules 8, 9, and 10 to a prescribed level of 500 ppm by weight. X-ray fluorescence showed the sulfur content of these ampules was 525 ppm by weight before exposure to the copper. Some of this sulfur in the liquid phase was consumed during the test. The sulfur content of the liquid in ampules 8, 9 and 10 at the end of the tests was 368, 446, and 442 ppm by weight, respectively.

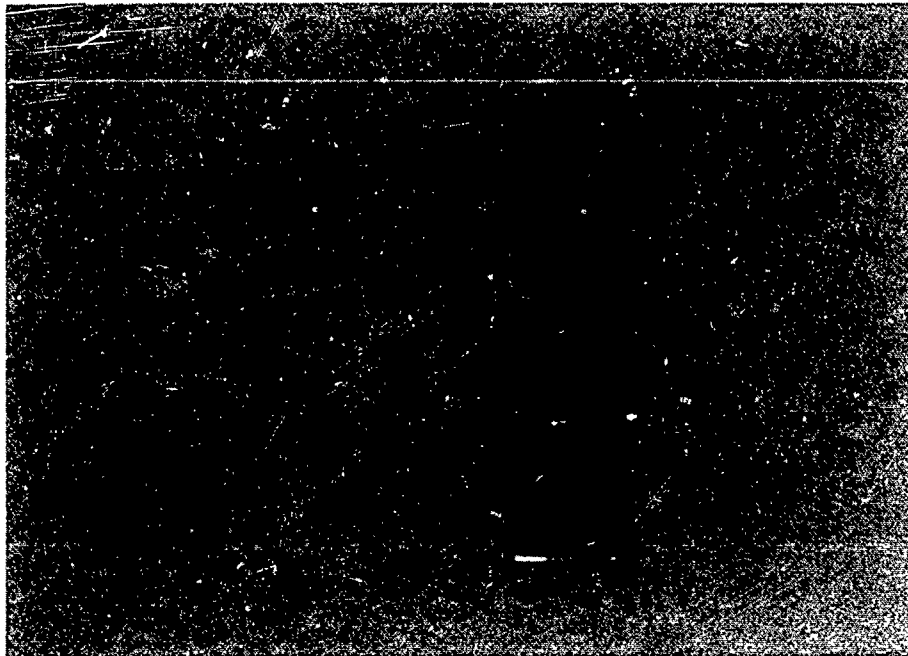
Material balances were performed on the sulfur in each of these ampules. As shown in Table 8, excellent closure was obtained based on the before and after analysis of the liquid phase and the weight gain of the copper coupon. As well as providing assurance of the validity of the analytical procedures and lab techniques of these tests, the fact that the weight gain of the coupon can be entirely traced to the deposition of sulfur on the surface was further indication that no corrosion, pitting, or carbon deposition on the copper took place during the test, other than that caused by the sulfur reaction with the metal.

The only metallic coupons which exhibited visual changes were those copper coupons (both OFHC and NASA-Z) which were exposed to n-dodecane doped with sulfur (ampules 8, 9 and 10). These coupons developed a uniform black tarnish or deposit on the surface. No other changes were visible on any of the remaining metallic coupons.

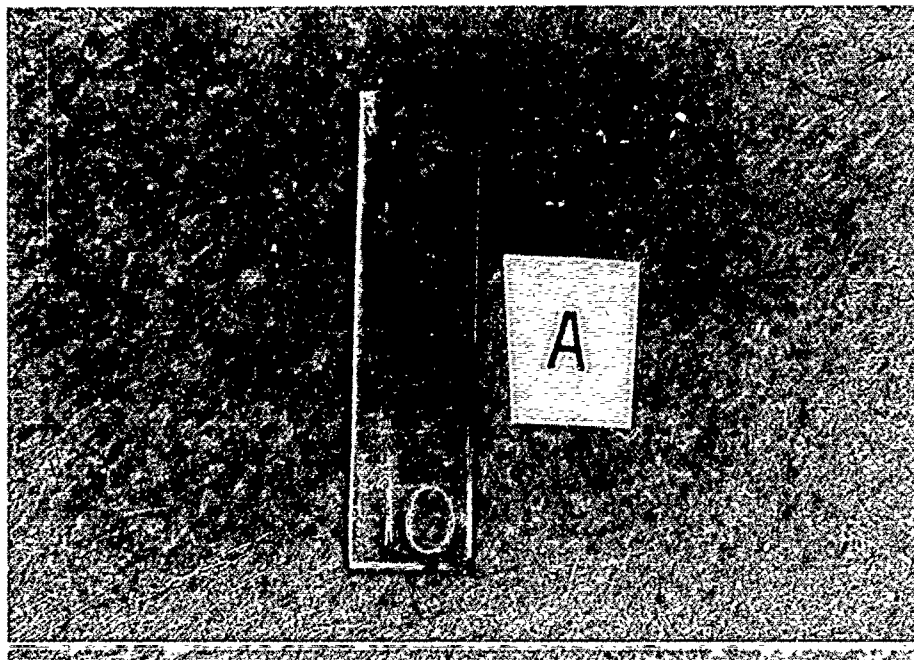
Figures 16 and 17, typical 35 mm photos of the metallic coupons taken before and after exposure, document this change in appearance. Figure 16 shows specimen 10 before and after exposure to RP-1 saturated with air. No visible change was detected. Figure 17 shows specimen 30 before and after exposure to pure grade n dodecane plus 525 ppm by weight sulfur as dodecanthiol. Note the dark, even deposit on the surface which developed during the test. This was identified primarily as cuprous sulfide,  $\text{Cu}_2\text{S}$ .

TABLE 8  
MATERIAL BALANCES FOR SULFUR IN AMPUL TESTS

<u>Ampul Number</u>	<u>Liquid Volume, ml</u>	<u>Sulfur in Liquid Before, g</u>	<u>Sulfur in Liquid After, g</u>	<u>Coupon Weight Gain, g</u>	<u>% Closure (After/Before)</u>
8	3.36	.00142	.00099	.0003	90%
9	3.36	.00142	.00120	.0003	106%
10	3.36	.00142	.00117	.0002	98%

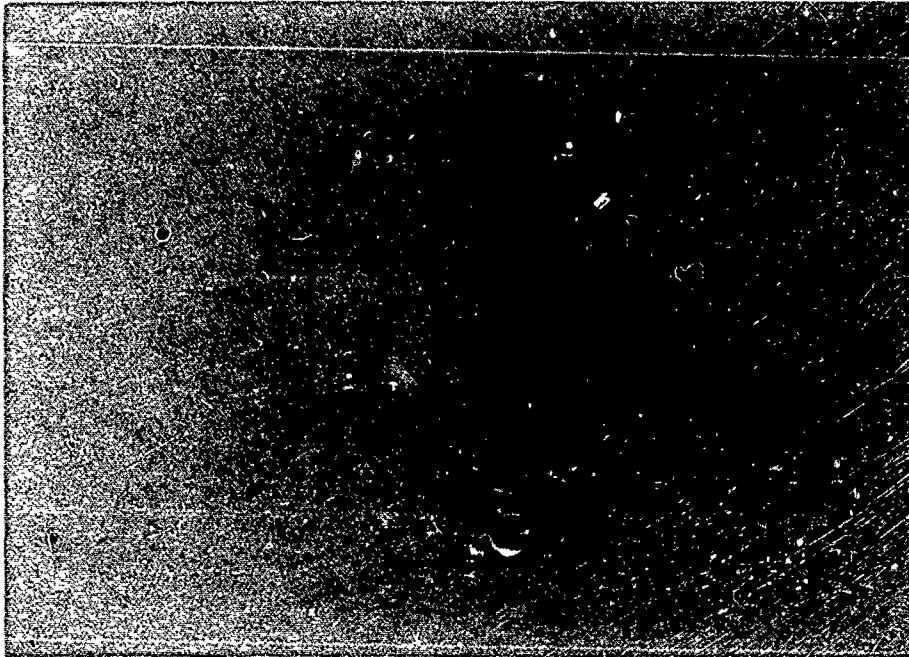


Before Test  
Color: Bright Copper

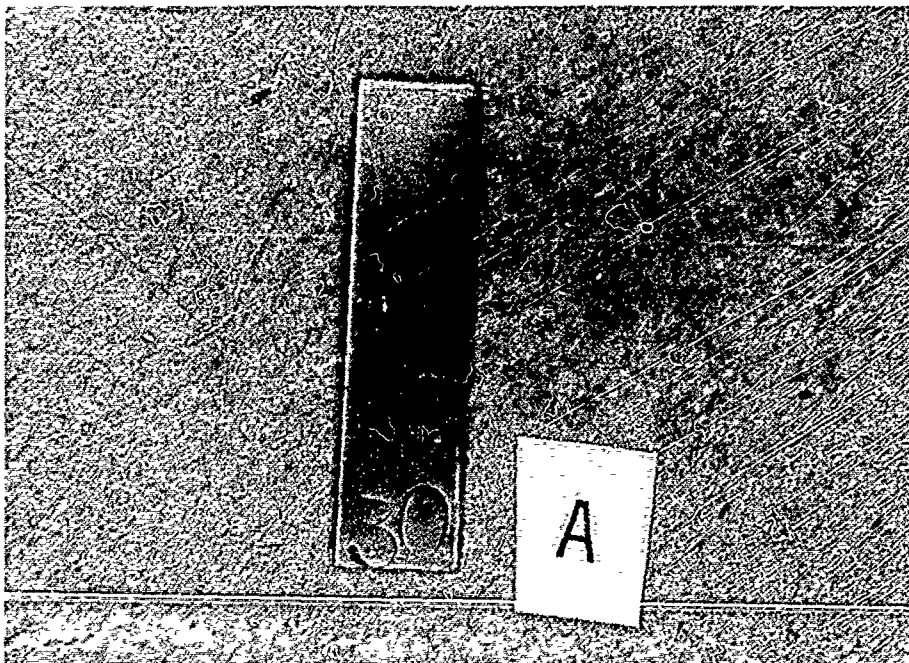


After Test  
Color: Bright Copper

Figure 16. OFHC Copper Specimen Exposed to Air-Saturated RP-1



Before Test  
Color: Bright Copper



After Test  
Color: Steel Gray

Figure 17. NASA-Z Specimen Exposed to n-dodecane Plus 525 ppm Sulfur as Dodecanethiol

### 3.2, RP-1 Test Results (cont.)

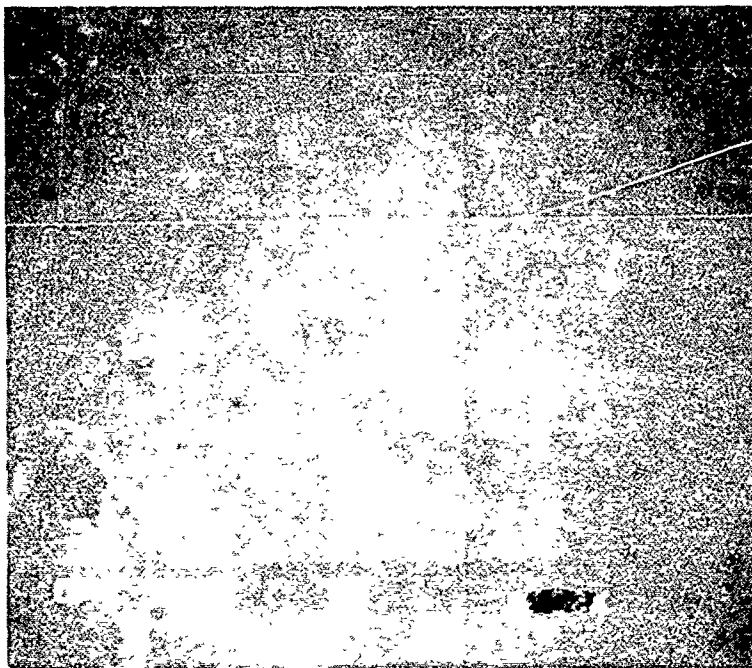
SEM photos of these same coupons are also informative. Figure 18 shows the surface of specimen 10 magnified 50, 400, and 2,000 times before and after exposure to RP-1 saturated with air. A very slight deposit becomes visible at the highest magnification. This small deposit and the fact that it is visible only at high magnification is typical of all the coupons exposed to air-saturated RP-1.

Figure 19 shows a portion of specimen 30 before and after exposure to n-dodecane plus 525 ppm sulfur, again magnified 50, 400 and 2000 times. The  $\text{Cu}_2\text{S}$  deposit, evident with the unaided eye, becomes very dramatic when magnified. The formation of these deposits is typical of all the coupons exposed to n-dodecane with 525 ppm of sulfur added.

Table 9 summarizes the visual and SEM examinations from all the ampul test coupons. By comparing various combinations of tests, it is possible to make a number of conclusions from the results shown in this table. For example, by comparing tests 6 and 7, it can be seen that the test results were not affected by using n-dodecane as the fuel instead of RP-1. Similar reasoning can be used to arrive at the following conclusions regarding the compatibility of RP-1 with copper at 400F:

- (1) RP-1 (degassed and sulfur-free) does not react with copper.
- (2) RP-1 (saturated with air) reacts to form a very minor deposit on copper.
- (3) RP-1 (with 525 ppm by weight sulfur as n-dodecanethiol) reacts to form an even, complete coating of  $\text{Cu}_2\text{S}$ .
- (4) The strain history of the copper had no effect.
- (5) Changing the copper material from OFHC to NASA-Z had no effect.
- (6) The RP-1 used in this series behaved the same as n-dodecane. It is likely that this is dependent on the purity of this particular shipment of RP-1.

Before



50X



400X

After

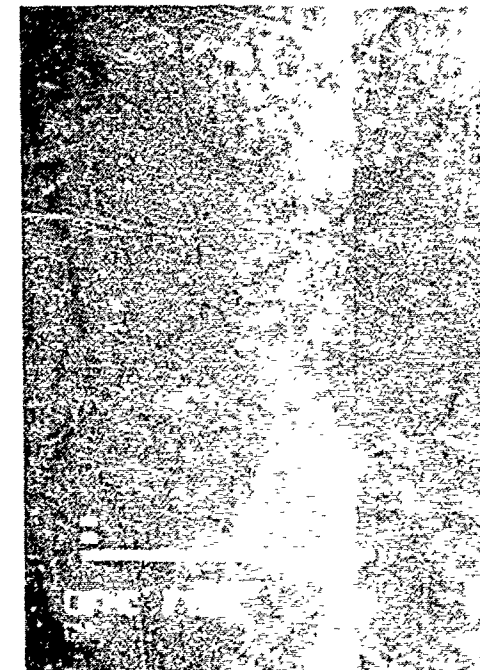
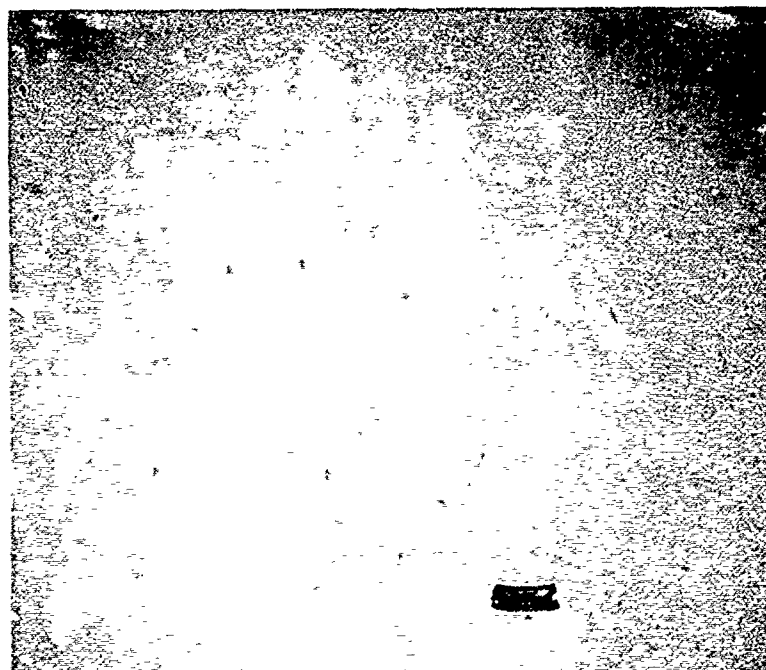
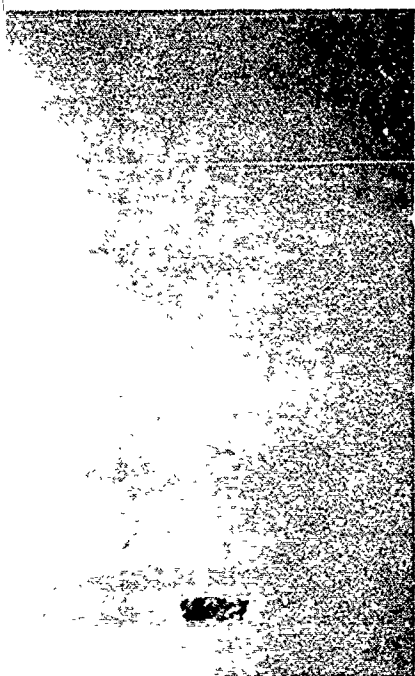
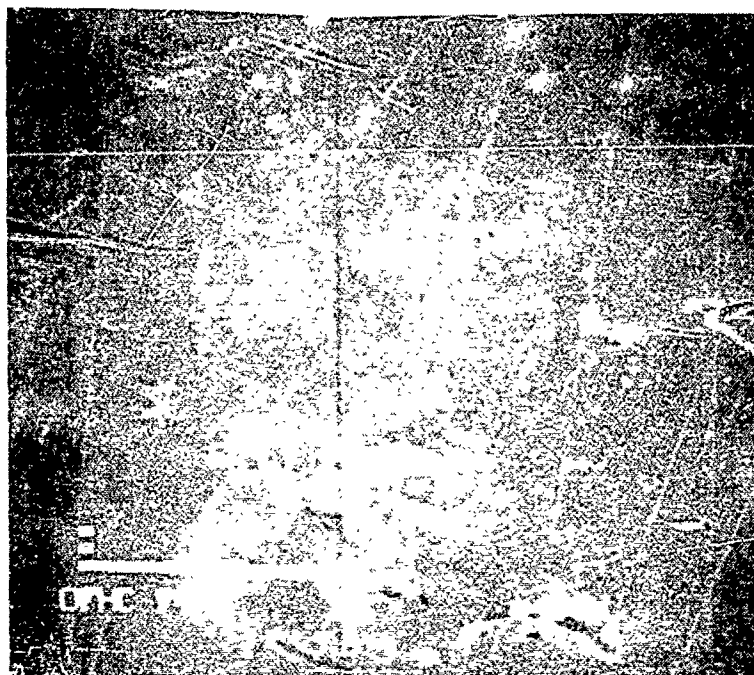


Figure 1



100X



400X

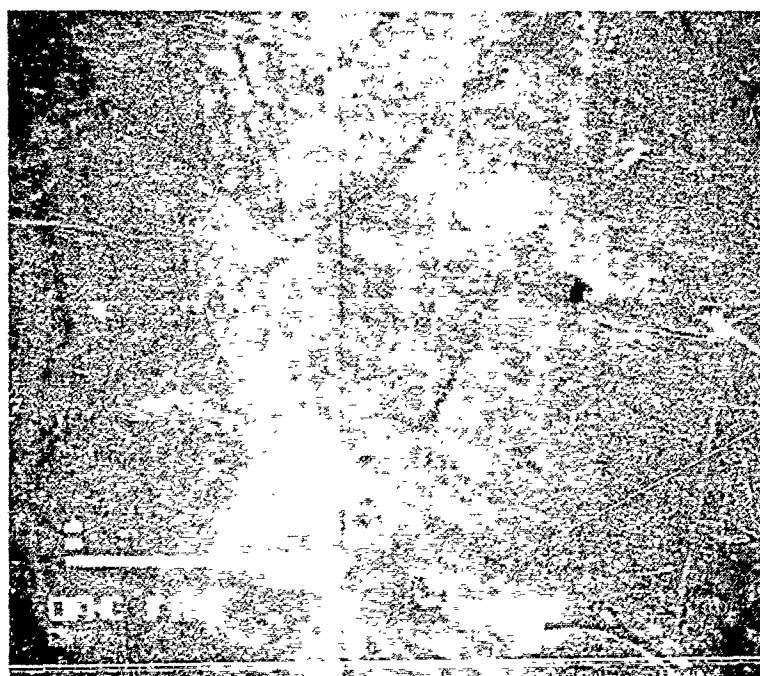
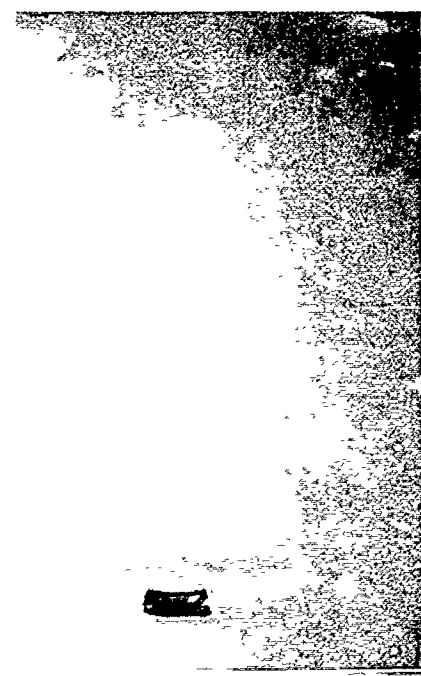
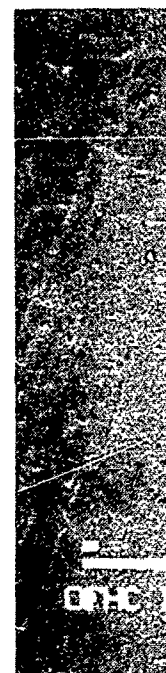
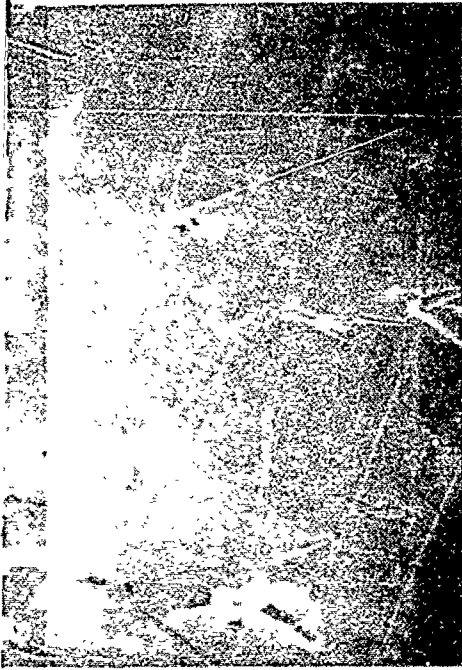
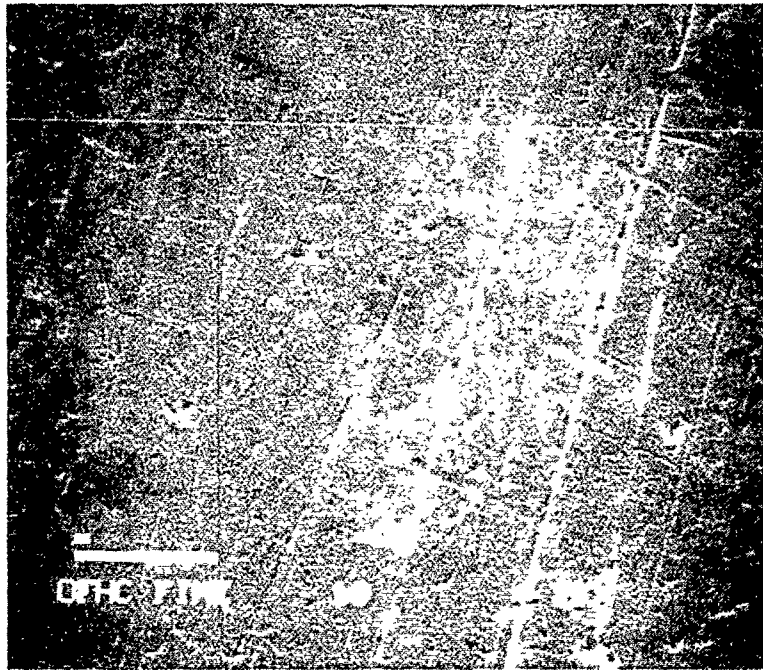


Figure 18. SEM Photos of Specimen #10 Before



400X



2000X

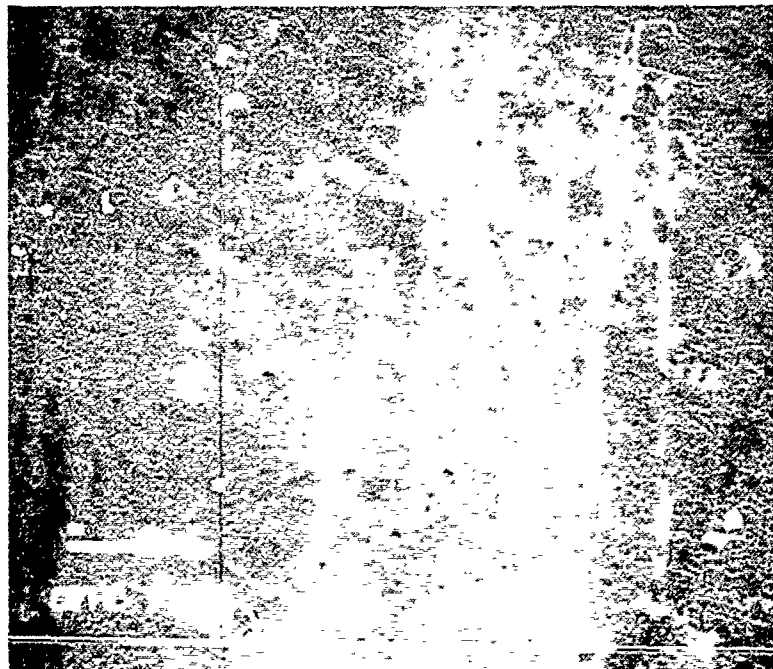
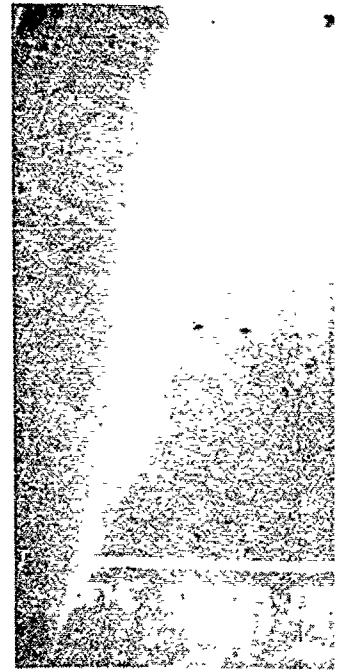
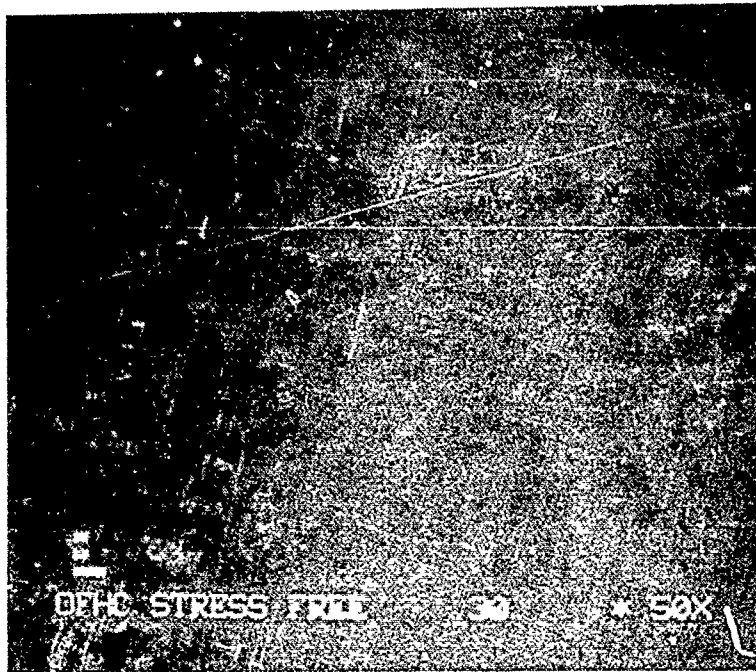


Figure 18. SEM Photos of Specimen #10 Before and After Exposure to Air-Saturated RP-1

Before



50X

After

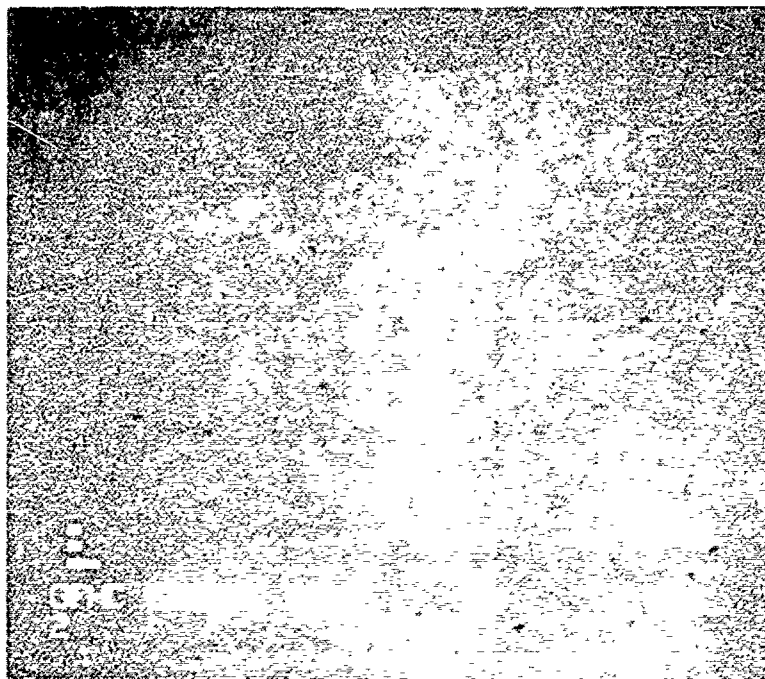
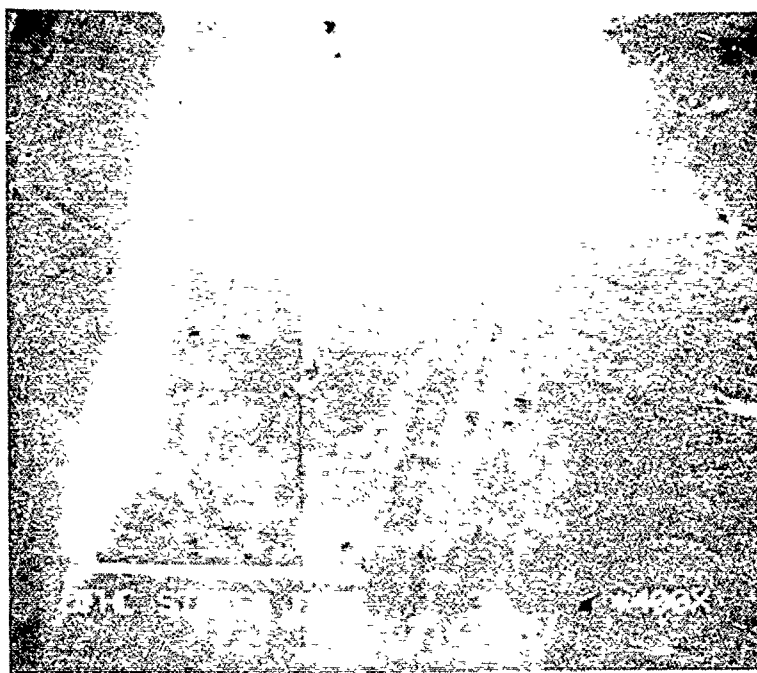
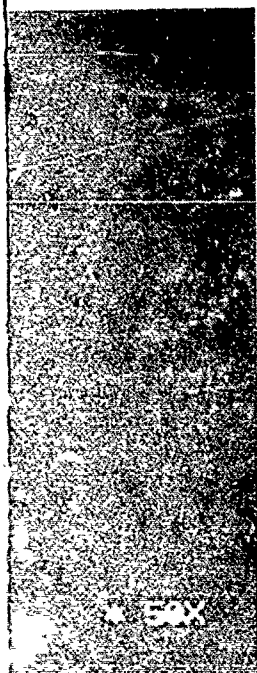


Figure 19. SE



400X

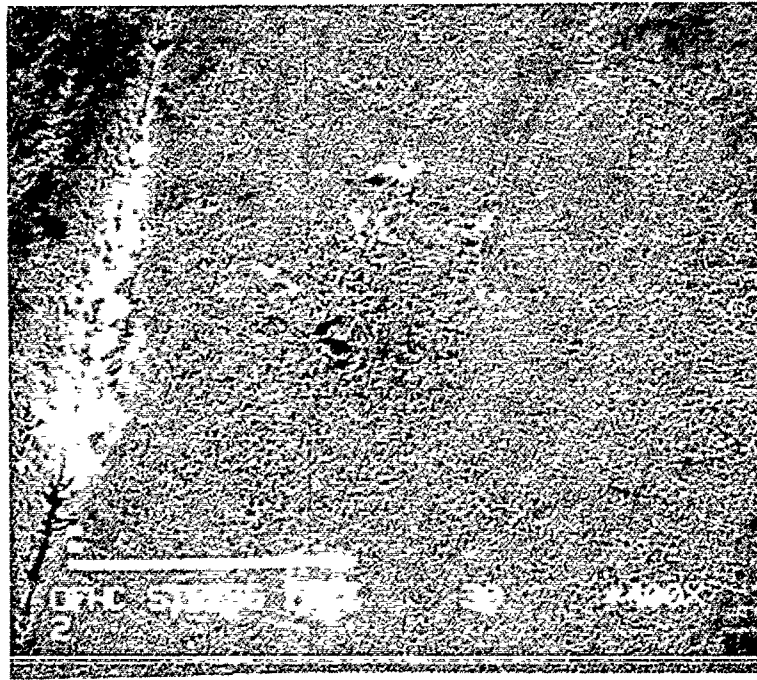
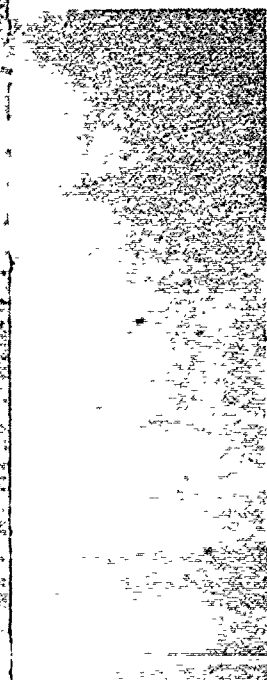
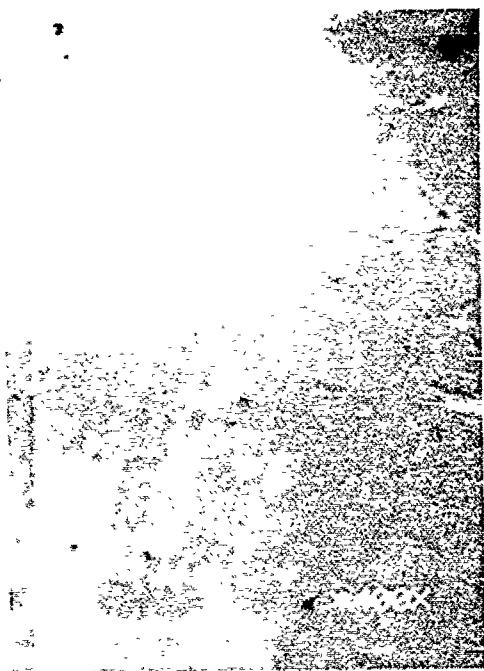
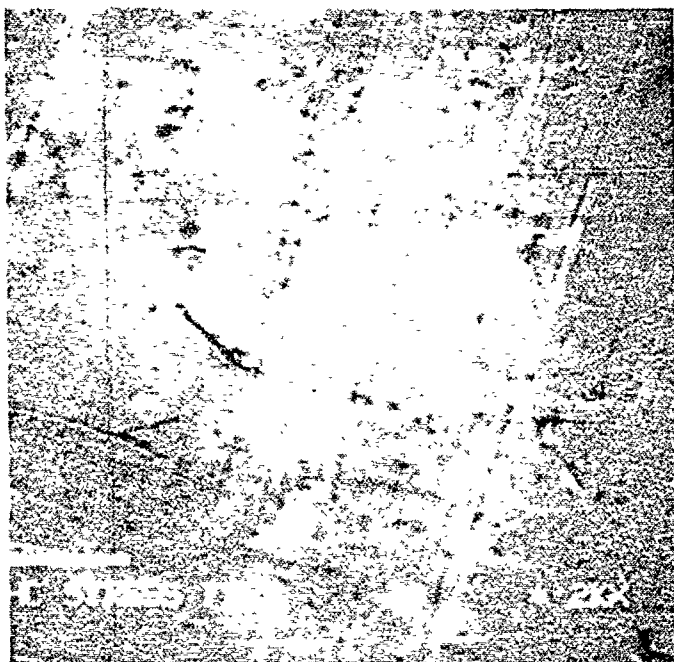


Figure 19. SEM Photos of Specimen #30 Before and After Exposure to



400X



2000X

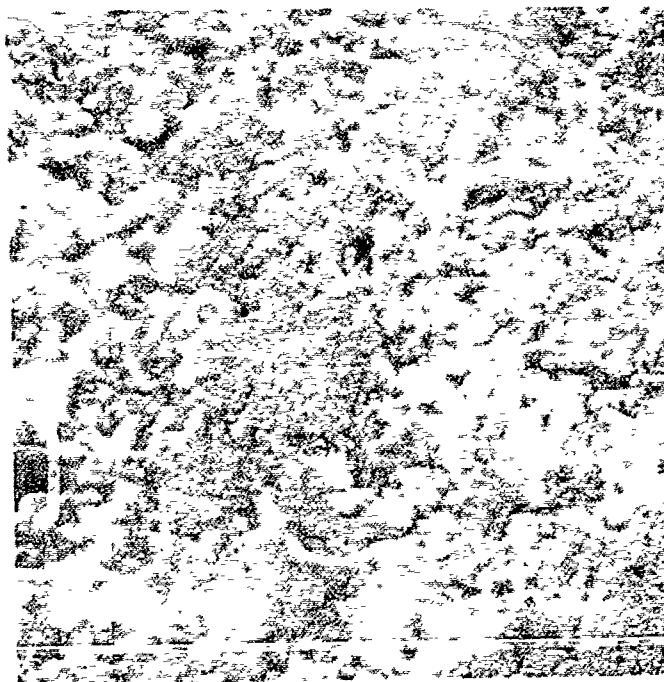
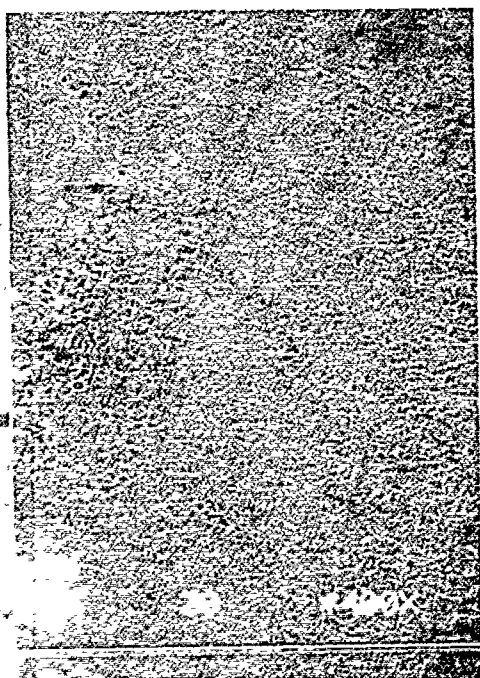


TABLE 9  
SUMMARY OF RP-1 STATIC TEST RESULTS

<u>Ampule No.</u>	<u>Fuel</u>	<u>Impurities</u>	<u>Coupon No.</u>	<u>Coupon Material</u>	<u>Coupon Grain</u>	<u>Coupon Strain History</u>	<u>Coupon Weight Change</u>	<u>Visible Coupon Change</u>	<u>SEM Coupon Change</u>	<u>Fuel Change</u>
1	RP-1	Air	None							None
2	n-Dodecane	Air	None							None
3	RP-1	Air	1	316SS	Fine	None	0.0000	None	None	None
4	RP-1	Air	10	OFHC	Fine	None	0.0000	None	Small	None
5	RP-1	None	11	OFHC	Fine	None	0.0000	None	None	None
6	RP-1	Air	20	NASA-Z	Fine	None	0.0000	None	Small	None
7	n-Dodecane	Air	21	NASA-Z	Fine	None	0.0000	None	Small	None
8	n-Dodecane	Air + 525 ppm S <sup>a</sup>	22	NASA-Z	Fine	None	0.0003	Some	Large	Sulfur Depletion
9	n-Dodecane	Air + 525 ppm S <sup>a</sup>	30	OFHC	Large	None	0.0003	Some	Large	Sulfur Depletion
10	n-Dodecane	Air + 525 ppm S <sup>a</sup>	41	OFHC	Large	2% x 40	0.0002	Some	Large	Sulfur Depletion

as n-dodecanethiol

### 3.2, RP-1 Test Results (cont.)

#### 3.2.2 RP-1 Dynamic Tests (Task 1.2.2)

A series of thirteen dynamic tests were conducted with RP-1 and/or n-dodecane in the Aerojet Carbothermal Test Facility. The objective of these tests was to investigate the compatibility of RP-1 with copper chamber liner materials at conditions simulating those anticipated in the cooling channels of regeneratively cooled LO<sub>2</sub>/hydrocarbon booster engines. Table 10 summarizes relevant test conditions produced in the RP-1 dynamic tests. Table 11 summarizes the 13 dynamic tests which were conducted.

Test R101 was terminated after 185 sec because of a fuel leak. The test used degassed n-dodecane as the fuel. The heater block and test specimen were allowed to heat up to 1000 F before the fuel pump was started and fuel was fed through the test section at 120 feet/sec. During the first 20 sec of fuel flow, the wall temperatures of the specimen decreased by 200 F, while the temperature in the copper heater block continued to slowly increase. Then, 150 sec after the fuel flow was started, steady state temperatures were reached and the pump speed was increased to obtain a flow velocity of 220 ft/sec. This further reduced the wall temperature of the specimen. At 185 sec after initiation of fuel flow, a leak was observed. The heaters and pump were immediately shut off and the test section was purged with high pressure nitrogen gas.

Upon disassembly of the apparatus, blackening of the specimen channel was noted. The discoloration was uniform from channel inlet to outlet and on each of the channel walls. The specimen was weighed (no change), photographed and submitted for metallographic analysis. Due to the short duration of the test, no changes were seen in the heat transfer or roughness of the specimen channel.

Test R102 was conducted with an OFHC specimen and degassed n-dodecane as the fuel. The run duration was 1624 sec, and was entirely operated on recirculation from the recirculation tank. The run was ended by an operating error in which valves were opened in an incorrect sequence, resulting in a loss of suction pressure to the delivery pump. This reduced the flowrate into the block, which required a shutdown of the heaters and the test. The appearance of the specimen when removed from the Carbothermal Apparatus again showed blackening of the channel surfaces in contact with the fuel.

TABLE 10

RP-1 DYNAMIC TESTS INVESTIGATED COMPATIBILITY AT  
REALISTIC COOLING CHANNEL CONDITIONS

	<u>Test Conditions</u>
Wall Temperature, F	560-800
Max Coolant-Side $q/A$ , Btu/in. <sup>2</sup> -s	20
Coolant Pressure, psia	3500
Coolant Velocity, ft/s	250-300
Bulk Temperature, F	70-380

TABLE 11

## SUMMARY OF RP-1 DYNAMIC TEST CONDITIONS

Test Number	Specimen Mat'l (ID#)	Duration (sec)	Coolant Side			Max Velocity (ft/s)
			Max Wall Temp, F	Max Heat Flux (Btu/s-in. <sup>2</sup> )	Fuel	
R101	OFHC (3)	185	810	17.0	Dodecane	--
R102	OFHC (4)	1624	720	15.0	Dodecane	250
R103	OFHC (5)	3483	700	12.2	Dodecane	252
R104	NAS-Z (Z1)	3253	699	16.7	Dodecane	246
R105	OFHC (6)	3118	808	20.2	Dodecane	270
R106	NAS-Z (Z2)	2899	798	19.0	Dodecane	268
R107	NAS-Z (Z3)	3353	701	15.7	RP-1	263
R108	NAS-Z (Z4)	145	493	12.3	RP-1	303
R109	Amzirc (A1)	2853	576	15.1	RP-1	286
R110	NAS-Z (Z5)	257	556	14.8	RP-1	260
R111	NAS-Z (Z6)	2349	576	16.9	RP-1 + Dodecene	276
R112	Amzirc (A2)	2519	579	14.3	RP-1 +Biphenyl	284
R113	NAS-Z (Z7)	2339	576	14.5	RP-1 +Dodecanethiol	267

### 3.2, RP-1 Test Results (cont.)

Test R103 was conducted with an OFHC specimen and degased n-dodecane as the fuel. The run duration was 3483 sec (0.97 hr), including approximately 1300 sec of once-through operation from the run tank to the collection barrel at essentially steady state operating conditions. The remainder of the run was conducted in a recirculating mode. The maximum wall temperature recorded during the run was 700 F.

As shown in Figure 20, the heat transfer coefficient showed a steady decline during the run, first noticed when the wall temperature reached 600 F, and continuing through the last 2800 sec of the run. During this time, the run conditions stayed nearly constant, except for a steady and gradual increase in the channel wall temperature spanning operations in both a recirculating and a once-through operating mode. The pressure drop of the fuel through the channel did not change significantly from the beginning to the end of the run. Visual examination of the OFHC specimen used in Run R103 showed the typical blackening of the channel wall, uniform on all three sides, and from inlet to outlet.

Test R104 was conducted with a NASA-Z specimen and degased n-dodecane as the fuel. The run duration was 3253 sec, consisting of approximately 1600 sec of once-through operation from the run tank to the collection barrel at steady state operating conditions, and the remainder in a recirculation mode. The maximum wall temperature recorded during the run was 699 F.

Again, the heat transfer coefficient declined steadily during the run, beginning when the wall temperature reached 650 F, and continuing through the last 2300 sec of the run. The rate of decrease was almost identical to that seen in test R103, which provided the first indication that there is no difference in the performance of OFHC vs. NASA-Z in the dynamic compatibility tests. The pressure drop of the fuel through the channel did not change significantly from the beginning to the end of the run.

Visual examination of the NASA-Z specimen used in Run R104 showed blackening of the channel wall, but it was unusual in that the discoloration was much more distinct on the outlet of the channel than on the inlet. Figure 21 are 35 mm photographs which document the before and after appearance of the specimen used in

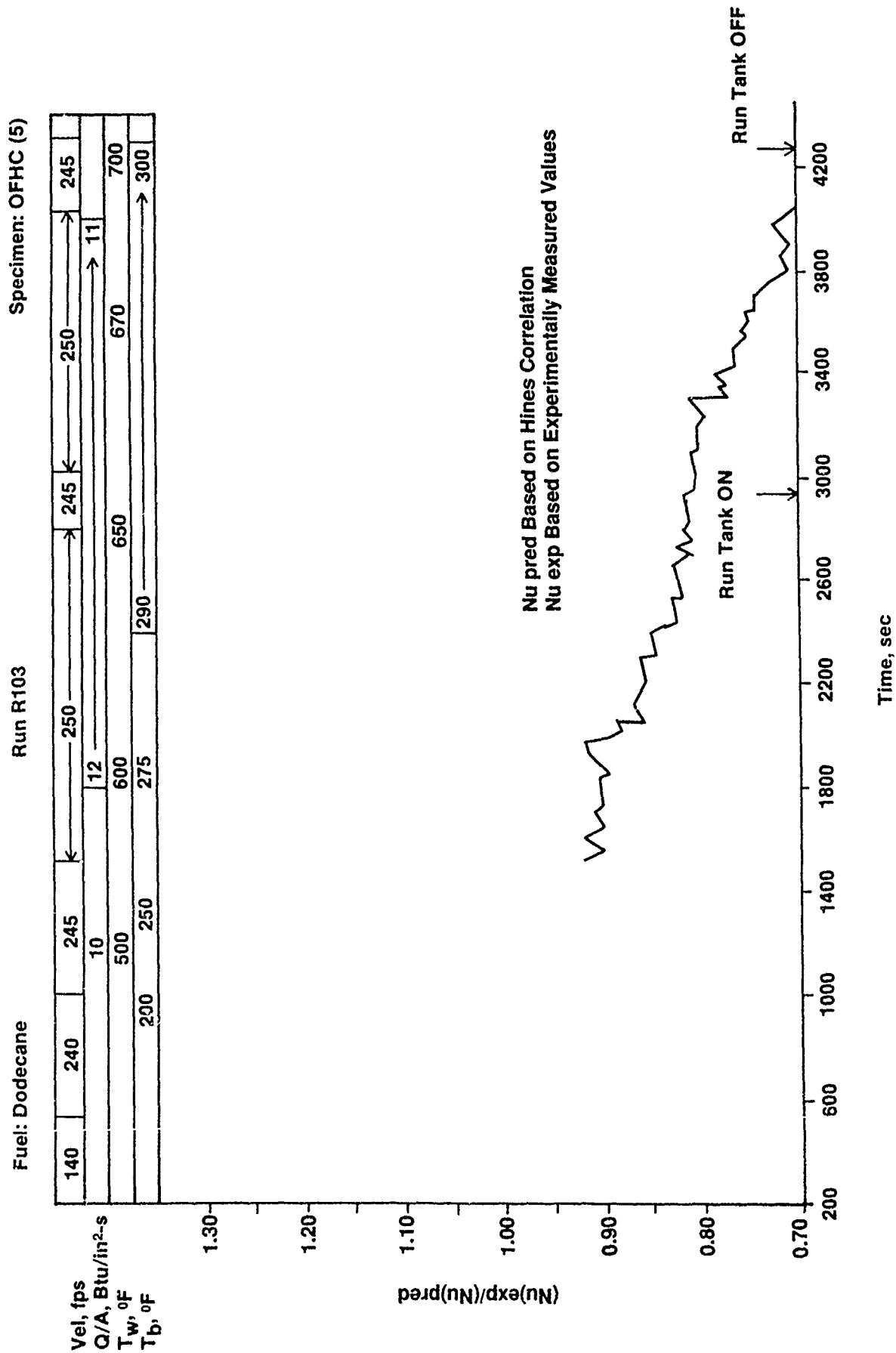


Figure 20. The Heat Transfer Coefficient of the Cooling Channel Decreased Steadily During Run R103

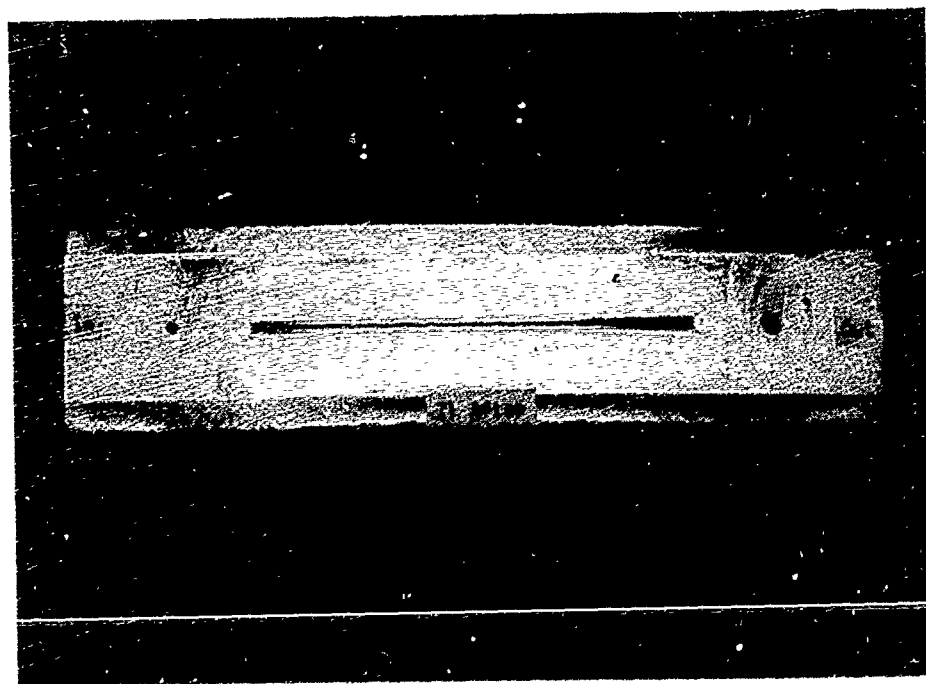
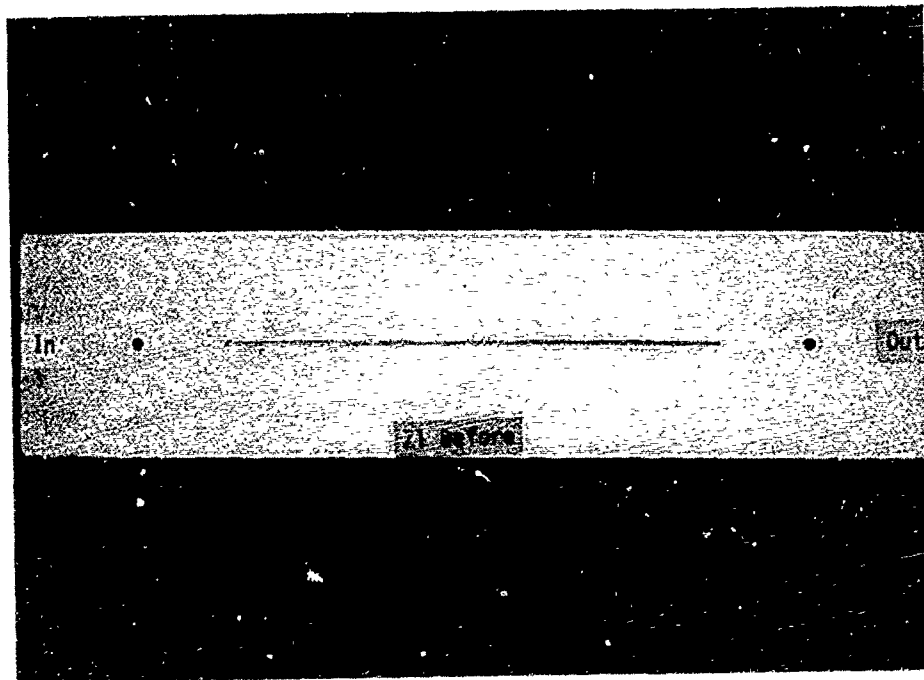


Figure 21. Test Specimen Before and After Dynamic Test R104. Note Black Discoloration of Channel After 3253 sec of Operation With n - Dodecane at a Maximum Wall Temperature of 699°F

### 3.2, RP-1 Test Results (cont.)

this run. The macroscopic view of the specimen and it can be seen that the blackening is much more severe at the outlet of the specimen than at the inlet.

Test R105 was conducted with an OFHC specimen and degased n-dodecane as the fuel. The run duration was 3118 sec, consisting of approximately 1600 sec of once-through operation from the run tank to the collection barrel at steady state operating conditions, and the remainder in a recirculation mode. The maximum wall temperature recorded during the run was 808 F.

As shown in Figure 22, the heat transfer coefficient declined steadily during the run, beginning when the wall temperature reached 700 F, and continuing through the last 2300 sec of the run. The rate of decrease in the heat transfer coefficient was much larger than in either run R103 or R104, probably due to the higher wall temperatures which were used in this test. Again, the pressure drop of the fuel through the channel did not change significantly from the beginning to the end of the run.

Visual examination of the OFHC specimen used in Run R105 showed a uniform blackening of the channel wall. The blackening did not appear to be worse than that seen on the specimens used in the previous runs.

After the run, the 0.4 micron filters both upstream and downstream of the test block were changed, and the filter elements collected for analysis. These filters were used during two runs (R104 and R105). Thereafter, it became standard practice to change the filter elements after each run. The filter upstream of the test block showed a fine black filtrate uniformly covering the exposed surface. The filter downstream of the test block also showed a black filtrate, though the coating on the filter appeared to be much thinner than on the upstream filter. This corresponds to the pressure drops which were observed to increase significantly over the upstream filter during Run R105, but only slightly over the downstream filter.

Test R106 was conducted with a NASA-Z specimen and degased n-dodecane as the fuel. The run duration was 2899 sec, consisting of approximately 1400 sec of once-through operation from the run tank to the collection barrel at steady state operating conditions, and the remainder in a recirculation mode. The maximum wall temperature recorded during the run was 798 F.

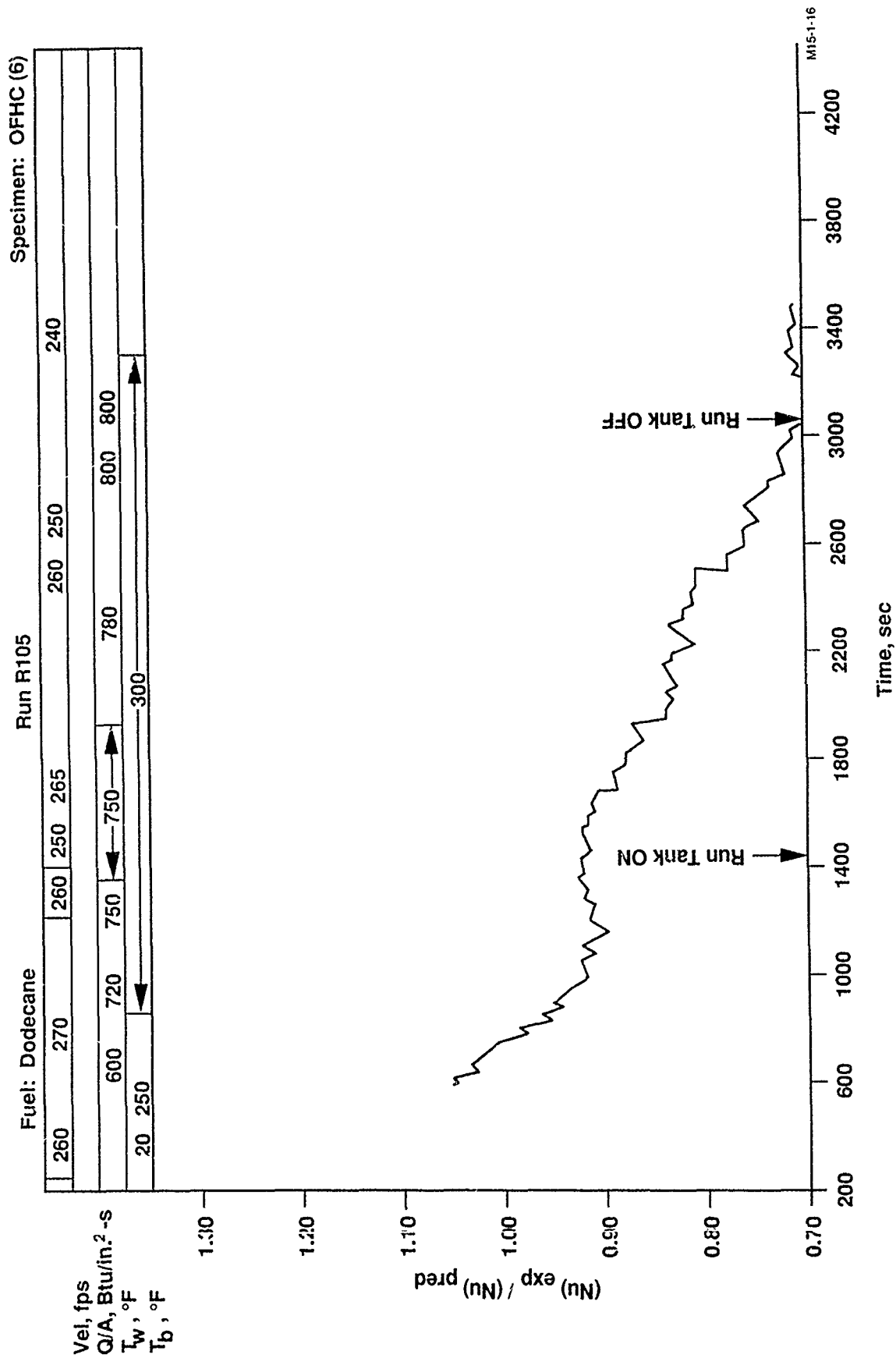


Figure 22. The Heat Transfer Coefficient of Cooling Channel Decreased Rapidly at High Wall Temperature During Run R105

### 3.2, RP-1 Test Results (cont.)

The heat transfer coefficient declined steadily during the run, beginning when the wall temperature reached 700 F, and continuing through the last 2500 sec of the run. The rate of decrease in the heat transfer coefficient was nearly identical to that observed in Run R105, confirming the previous observation made by comparison of Runs R103 and R104 that OFHC and NASA-Z appear to perform identically with respect to their compatibility with n-dodecane.

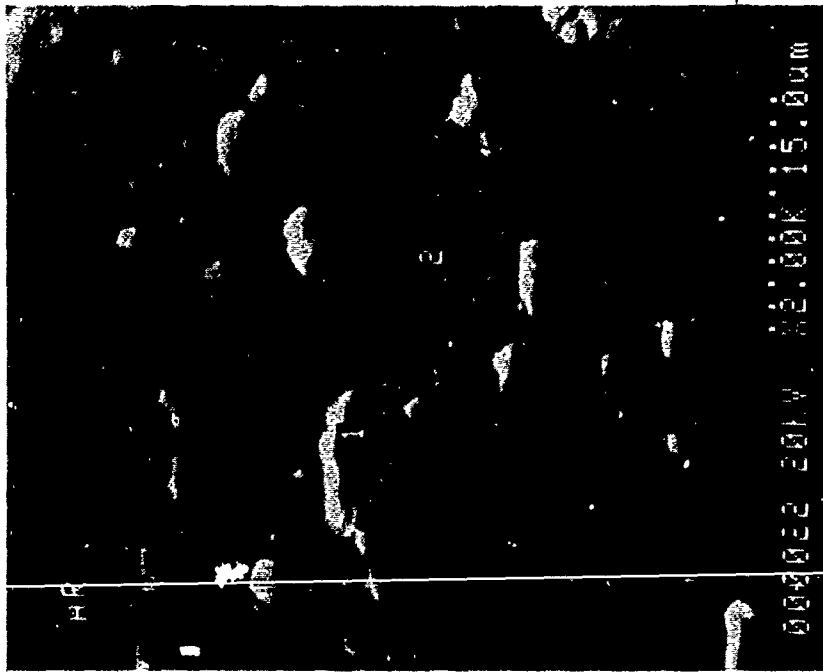
Visual examination of the NASA-Z specimen used in Run R106 showed a uniform blackening of the channel wall. The blackening did not appear to be worse than that seen on the specimens used in the previous runs, in spite of the larger degradation in the heat transfer performance which was seen in this run.

Test R107 was conducted with a NASA-Z specimen and RP-1 as the fuel. No attempt was made to degas the fuel either before or after its introduction into the run tanks of the carbothermal system. The run duration was 3353 sec, consisting of approximately 1350 sec of once-through operation from the run tank to the collection barrel at steady state operating conditions, and the remainder in a recirculation mode. The maximum wall temperature recorded during the run was 701 F.

The heat transfer coefficient declined steadily during the run, beginning when the wall temperature reached 600 F, and continuing through the last 2600 sec of the run. Visual examination of the NASA-Z specimen used in Run R107 showed a uniform blackening of the channel wall, identical in appearance to the specimens used in the n-dodecane runs.

This specimen was selected for further examination under a SEM. Figure 23 shows two photomicrographs looking down onto the surface of the cooling channel. Figure 23a is from a specimen which was machined but not tested, and represents the condition of the specimen surface before conduct of the dynamic tests. Figure 23b is a photomicrograph of the surface of the specimen Z3 after test R107. Note the thin deposits on the surface of the specimen. This is the black tar which was observed in the channel of most of the specimens (including the specimen from Test R107) after testing with RP-1 or n-dodecane.

As  
Received



Post Test  
R107

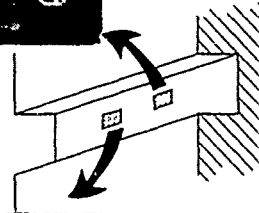
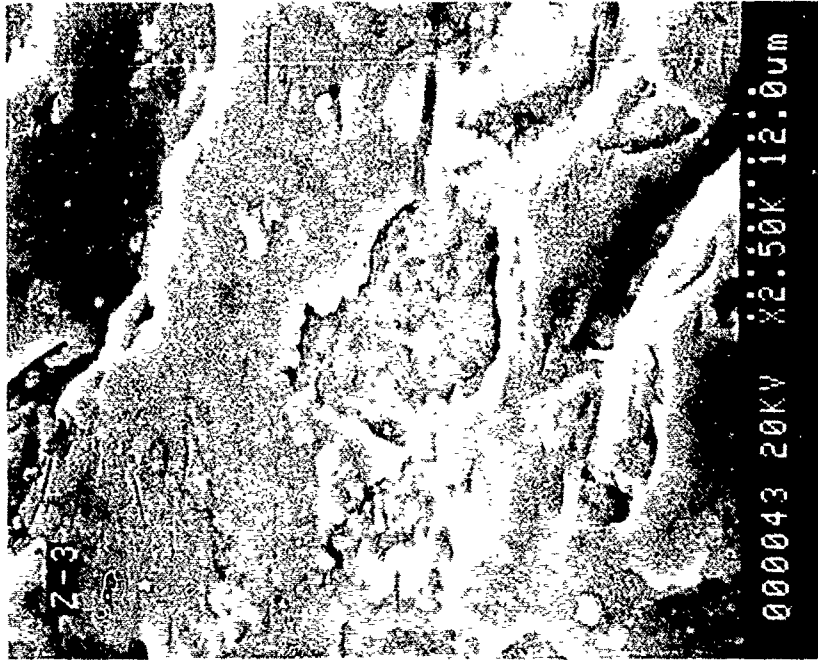


Figure 23. NASA-Z Before and After 3350 sec of Operation at  $T_{wall} = 700^{\circ}\text{F}$ . The Surface Deposits on the Tested Specimen Are Complex High Molecular Weight Hydrocarbons

### 3.2, RP-1 Test Results (cont.)

Electron Spectroscopy for Chemical Analysis (ESCA) was performed by an independent laboratory on the surface of this specimen to determine the elemental composition of the tar-like deposit. ESCA analysis is capable of determining elemental composition (and to a limited extent, bonding structure as well) of very thin, i.e., 100 Angstrom layers of material. A summary of the results of the ESCA analyses which were performed are presented in Table 12.

Test R108 was shutdown after only 145 sec of operation due to failure of the SCR controller used to adjust the power level of the cartridge heaters of the Carbothermal block. Due to the short duration of the test, no attempt was made to analyze the run data. Visual examination of the NASA-Z specimen used in Run R108 showed a uniform blackening of the channel wall, identical in appearance to the specimens used in the n-dodecane runs.

Test R109 was conducted with an Amzirc specimen and RP-1 as the fuel. The fuel was not degassed. The run duration was 2853 sec, consisting of approximately 1450 sec of once-through operation from the run tank to the collection barrel at essentially steady state operating conditions, and the remainder in a recirculation mode. The maximum wall temperature recorded during the run was 576 F.

This run was conducted at lower wall temperatures to find if a test could be conducted in which the heat transfer coefficient did not decline. As seen in Figure 24, the heat transfer coefficient stayed steady during the run, indicating no buildup of a thermal barrier. As in all previous runs, no significant change was observed in the pressure drop through the channel. However, visual examination of the Amzirc specimen used in Run R109 still showed a uniform blackening of the channel wall, identical in appearance to the specimens used in previous runs.

Test R110 was shutdown after only 257 sec of operation because RP-1 was entrained from the collection barrel into the test bay vent by a nitrogen purge. Due to the short duration of the test, no attempt was made to analyze the run data. Visual examination of the NASA-Z specimen used in Run R110 showed a uniform blackening of the channel wall, identical in appearance to the specimens used in the n-dodecane runs.

TABLE 12

ESCA ANALYSIS OF DEPOSIT ON TEST SPECIMEN CHANNELS  
FROM RP-1/n-DODECANE DYNAMIC TESTS

Sample ID Number	Test	C	N	O	Si	S	Cu	Ag	Zr
Z-1	R104	49.	1.9	30.	7.9	1.0	10.0	---	---
Z-3*	R107	63.	2.9	21.	2.0	3.1	8.1	---	---
Z-7	R113	42.	---	35.	---	1.2	21.0	0.2	<0.2

\*The ESCA data from Specimen Z-3 was further analyzed to determine the bonding state of the elements identified. Ester, ether, and olefinic structures were dominant, indicating that the deposit is primarily a complex, high molecular weight polymeric hydrocarbon.

Fuel: RP-1

Run R109

Specimen: Amzirc (A1)

277	→	285	→	275	→	270
Heatup		15.0				14.3 Coolin
Q/A, Btu/in <sup>2</sup> -s		540		560		576
T <sub>w</sub> , °F		212				218
T <sub>b</sub> , °F		200				

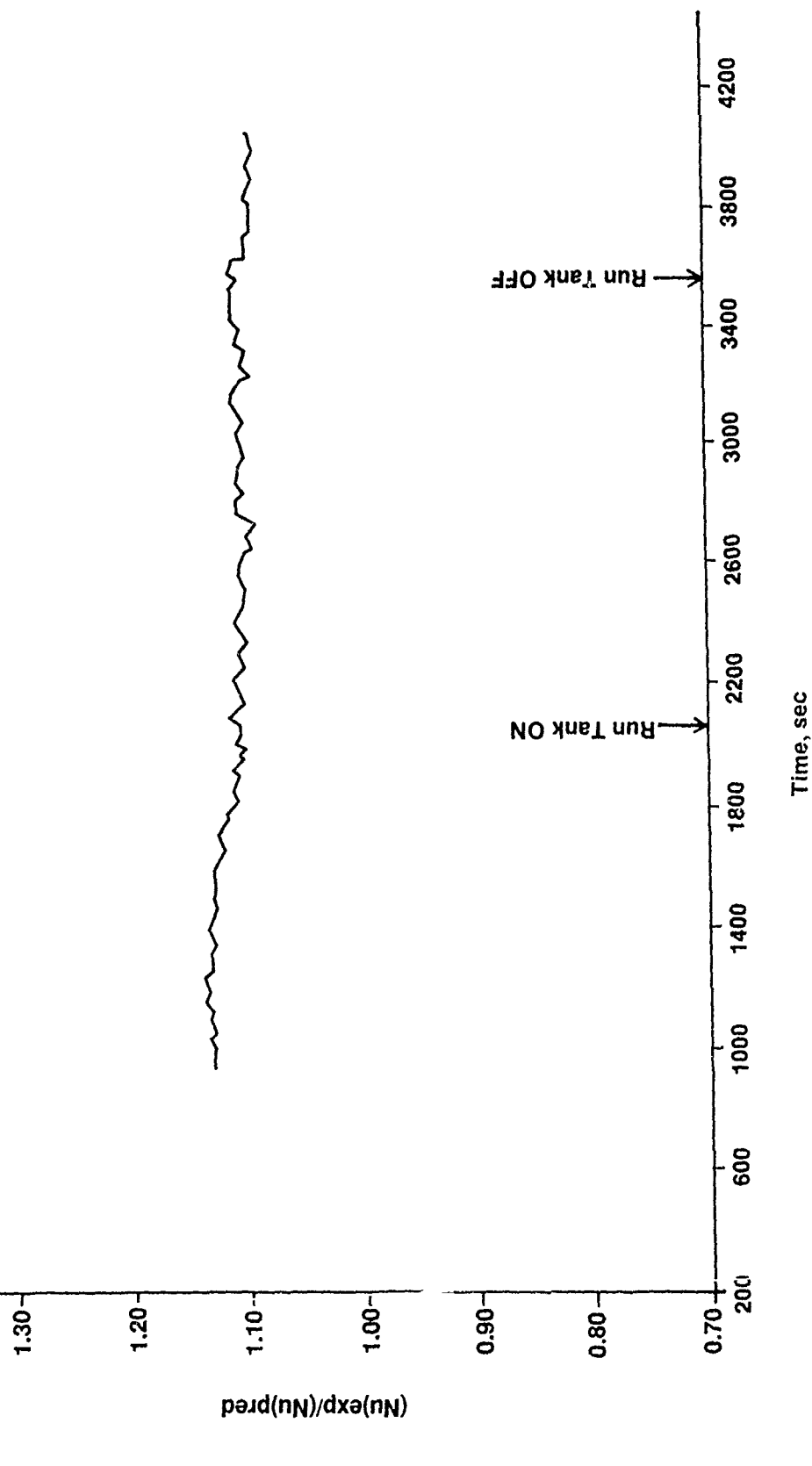


Figure 24. Operation at Lower Wall Temperatures Led to Almost Steady Heat Transfer Performance of Cooling Channel During Run R109

### 3.2, RP-1 Test Results (cont.)

Test R111 was conducted using a NASA-Z specimen and RP-1 with 1% (by wt.) 1-dodecene added to examine the effect of a high olefinic content in the fuel. As was typical with all the RP-1 tests conducted with additives, the 1-dodecene was added only to the run tank. The recirculation tank was left uncontaminated and contained only air-exposed Mil-Spec RP-1.

The total test duration was 2349 sec, consisting of approximately 1340 sec in a once-through mode of operation with the doped RP-1, and the remainder in a circulating mode with uncontaminated RP-1. The maximum wall temperature recorded during the run was 576 F.

The heat transfer coefficient declined during operation from the run tank. However, it is not clear if this was due to the buildup of a thermal barrier, or simply attributable to the steadily decreasing velocity of the fuel through the channel which was observed during the run. The measured heat transfer coefficient declined by 15% during operation from the run tank. The Hines Correlation predicted a decline of about 10% during this same period, primarily because of the declining fuel velocity.

For the first time in the test series, the pressure drop through the channel increased during the run. As seen in Figure 25, the apparent channel roughness (as calculated from the pressure drop through the channel) was near 0 (i.e., a smooth channel) at the beginning of the run. By the time the run tank was switched on, the apparent channel roughness had increased to approximately 130 micro-inches. The calculated roughness continued to increase during once-through operation to a maximum of 350 micro-inches before finishing at approximately 250 micro-inches.

Visual examination of the NASA-Z specimen used in Run R111 showed the typical uniform blackening of the channel wall. Examination under a 40X optical microscope did not show evidence of material loss or roughening of the channel surface.

Test R112 was conducted with an Amzirc specimen and RP-1 with 1% (by wt.) biphenyl added to examine the effect of a high aromatic content in the fuel. The biphenyl was added only to the run tank. The recirculation tank was left uncontaminated and contained only air-exposed Mil-Spec RP-1.

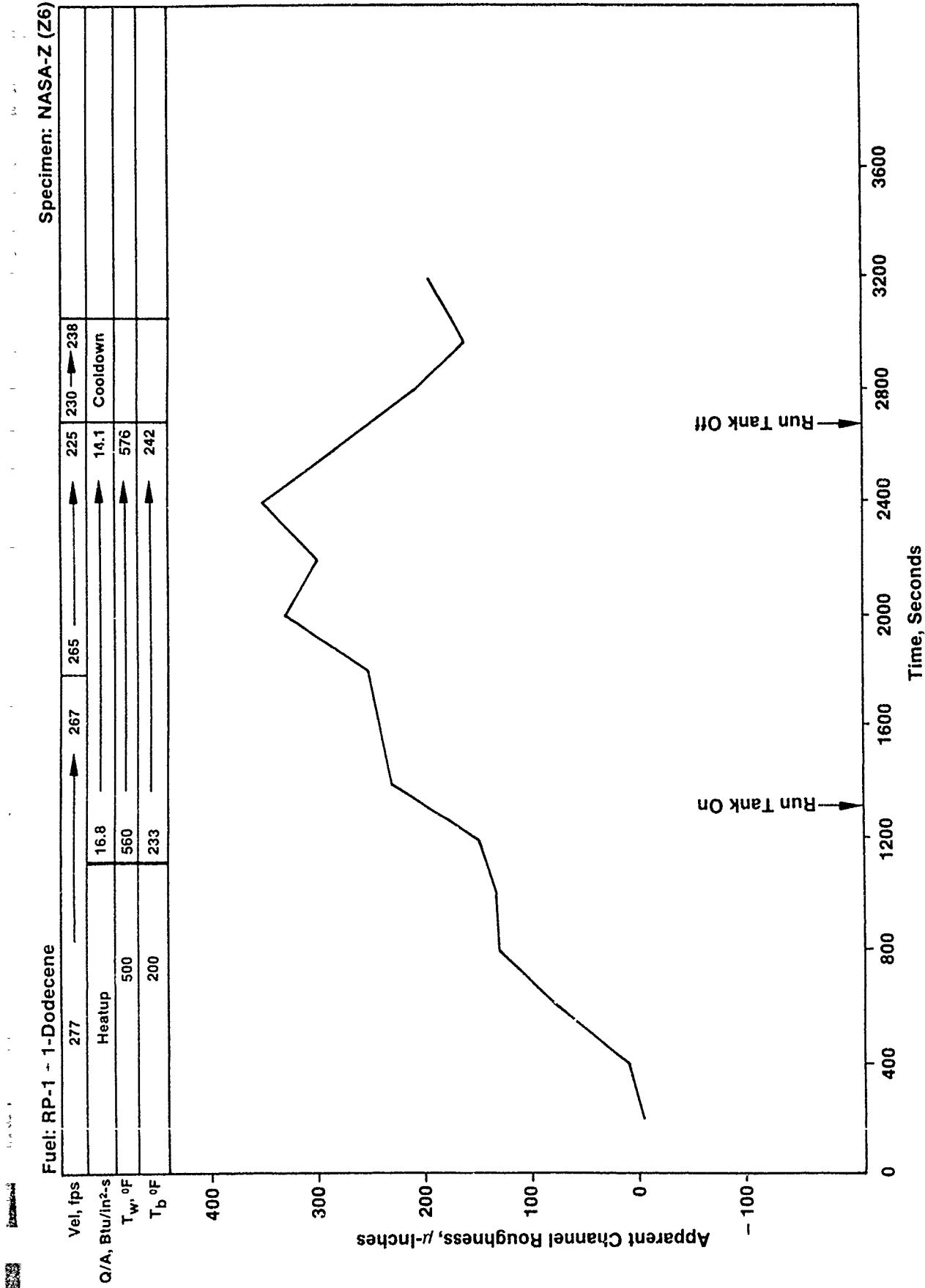


Figure 25. The Apparent Channel Roughness Increased Significantly During Run R111

### 3.2, RP-1 Test Results (cont.)

The total test duration was 2519 sec, consisting of approximately 1536 sec in a once-through mode of operation with the doped RP-1, and the remainder in a recirculating mode with uncontaminated RP-1. The maximum wall temperature recorded during the run was 579 F.

As shown in Figure 26, the heat transfer coefficient declined 10% during operation from the run tank, while the Hines correlation predicted almost no change. No similar decline in heat transfer performance was measured during this test while running Mil-Spec RP-1 from the recirculation tank through the specimen, nor had other test runs conducted with RP-1 at approximately the same temperature and flow conditions measured a decline in the heat transfer performance.

The pressure drop through the channel increased slightly during the run. Figure 27 shows the apparent channel roughness (as circulated from the pressure drop through the channel) throughout the run. From the beginning to the end of the run, the apparent channel roughness increased by 40 micro-inches, which occurred during operation with the RP-1 plus biphenyl.

Visual examination of the Amzirc specimen used in Test R112 showed the typical uniform blackening of the channel wall. Examination under a 40X optical microscope did not show evidence of material loss or roughening of the channel surface.

Test R113 was conducted with a NASA-Z specimen and RP-1 with 50 ppm of sulfur as n-dodecanethiol added to examine the effect of the presence of mercaptan sulfur in the fuel. As was typical with all the RP-1 plus additive tests, the n-dodecanethiol was added only to the run tank. The recirculation tank was left uncontaminated and contained only air-exposed mil spec RP-1.

The total test duration was 2339 sec, consisting of approximately 430 sec in a once-through mode of operation with the doped RP-1, and the remainder in a recirculating mode with uncontaminated RP-1. The maximum wall temperature recorded during the run was 576 F.

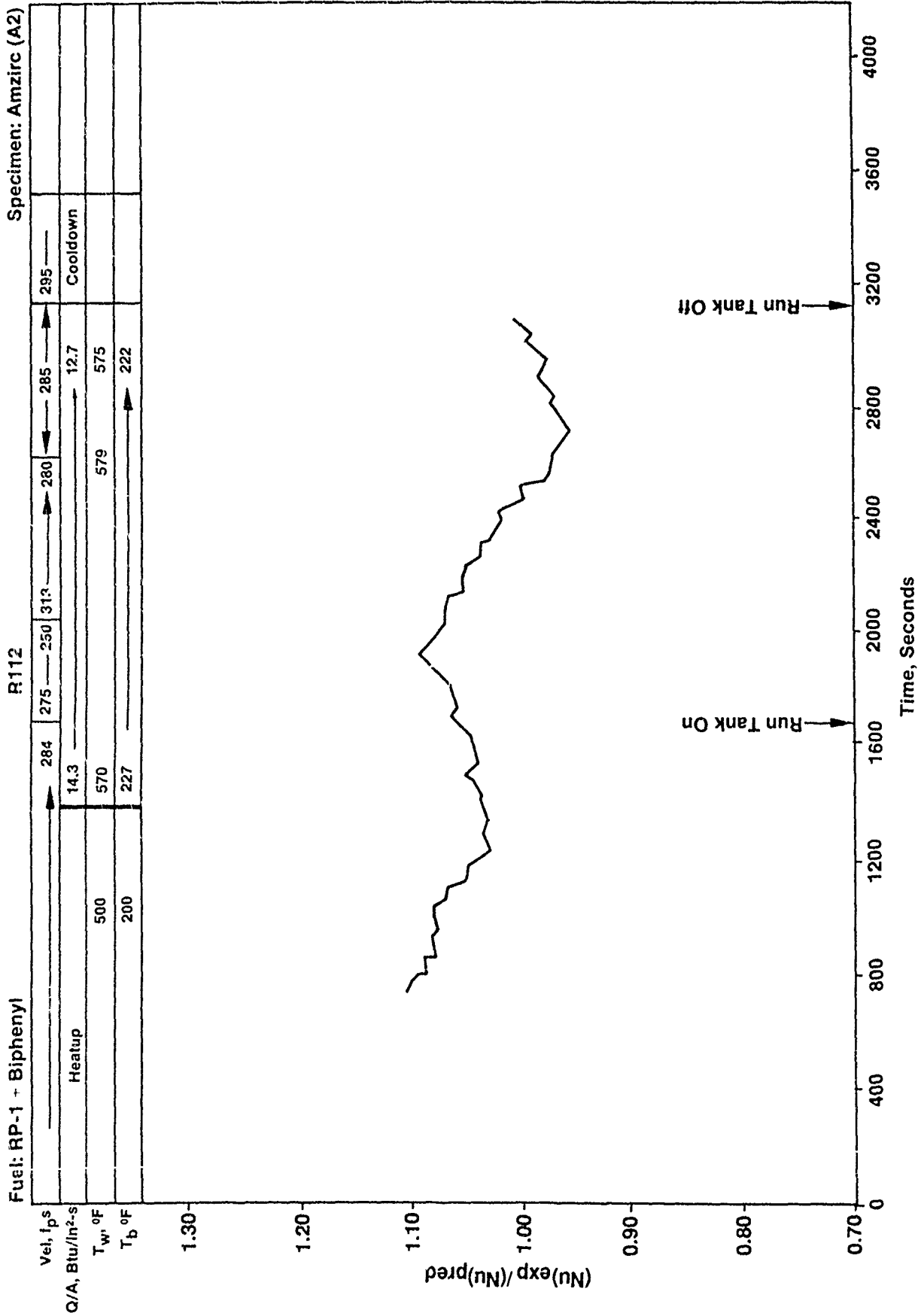


Figure 26. Heat Transfer Coefficient of Cooling Channel During Run R112

Fuel: RP-1 + Biphenyl

R112

Specimen: Amzirc (A2)

275	284	275	250	313	280	285	295	285
Heatup								
14.3						12.7		Cooldown
570	500				579	575		
227	200					222		

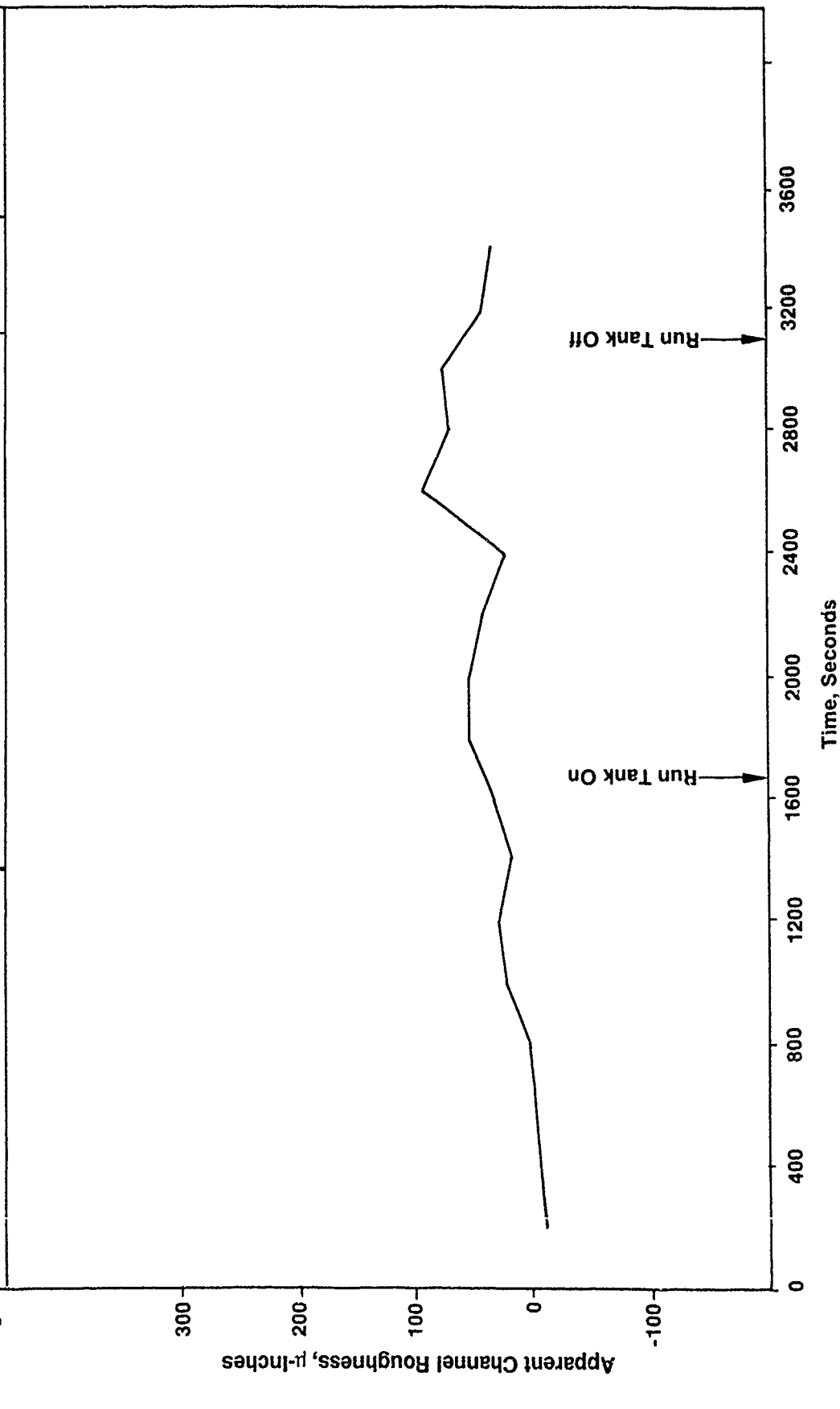


Figure 27. The Apparent Channel Roughness During Run R112 Increased Slightly

### 3.2, RP-1 Test Results (cont.)

As shown in Figure 28, the heat transfer coefficient increased slightly during operation from the run tank. Again, the increase in heat transfer performance was attributed to the additive in the RP-1 (in this case, the sulfur compound n-dodecanethiol), as tests with uncontaminated RP-1 at similar conditions did not exhibit this behavior.

The pressure drop through the channel showed a definite increase during Test R113. As seen in Figure 29, the apparent channel roughness increased 250 micro-inches during the 1430 sec of operation with the mercaptan-containing RP-1. This translates into a 20% increase in the pressure drop through these 20 mil channels in turbulent flow.

Visual examination of the NASA-Z specimen used in Test R113 showed the typical uniform blackening of the channel wall, though the blackening seemed to be more dense and heavy than that seen with other specimens in the series. Examination under a 40X optical microscope did not show evidence of material loss but did show a definite roughening of the channel surface.

Examination of the specimens used in the RP-1 tests under a SEM confirmed that the channel had been roughened. SEM photos of specimen Z7, the NASA-Z specimen exposed to RP-1 fuels plus 50 ppm of mercaptan sulfur, are included as Figures 30 and 31.

Figure 30 shows two magnifications of a view looking down into the channel. Figure 30a shows the channel and lands on either side at a low magnification (80X). Just outside the raised land area is the impression left by the sealing manifold as it squeezed against the bottom of the channel. Figure 30b shows the same view into the bottom of the channel at 250X. The rough appearance of the surface is more evident at this higher magnification. Also note that no scratches or grooves from machining are visible.

Figure 31 shows three views of a section of the channel wall at high magnification. Figure 31a shows the roughening of the wall at 1000X. A closeup of this area, Figure 31b, shows clearly defined nodes of material rising from the underlying surface. Figure 31c shows a view of one of these nodes. These nodes of material were

Specimen: NASA-Z (Z7)

R 113

Fuel: RP-1 + Dodecanethiol

Vel, f/s	267	257	231	267
Q/A, Btu/in <sup>2</sup> ·s	Heatup	14.5	13.0	Cooldown
T <sub>w</sub> , °F	500	562	576	500
T <sub>b</sub> , °F	200	230	245	200

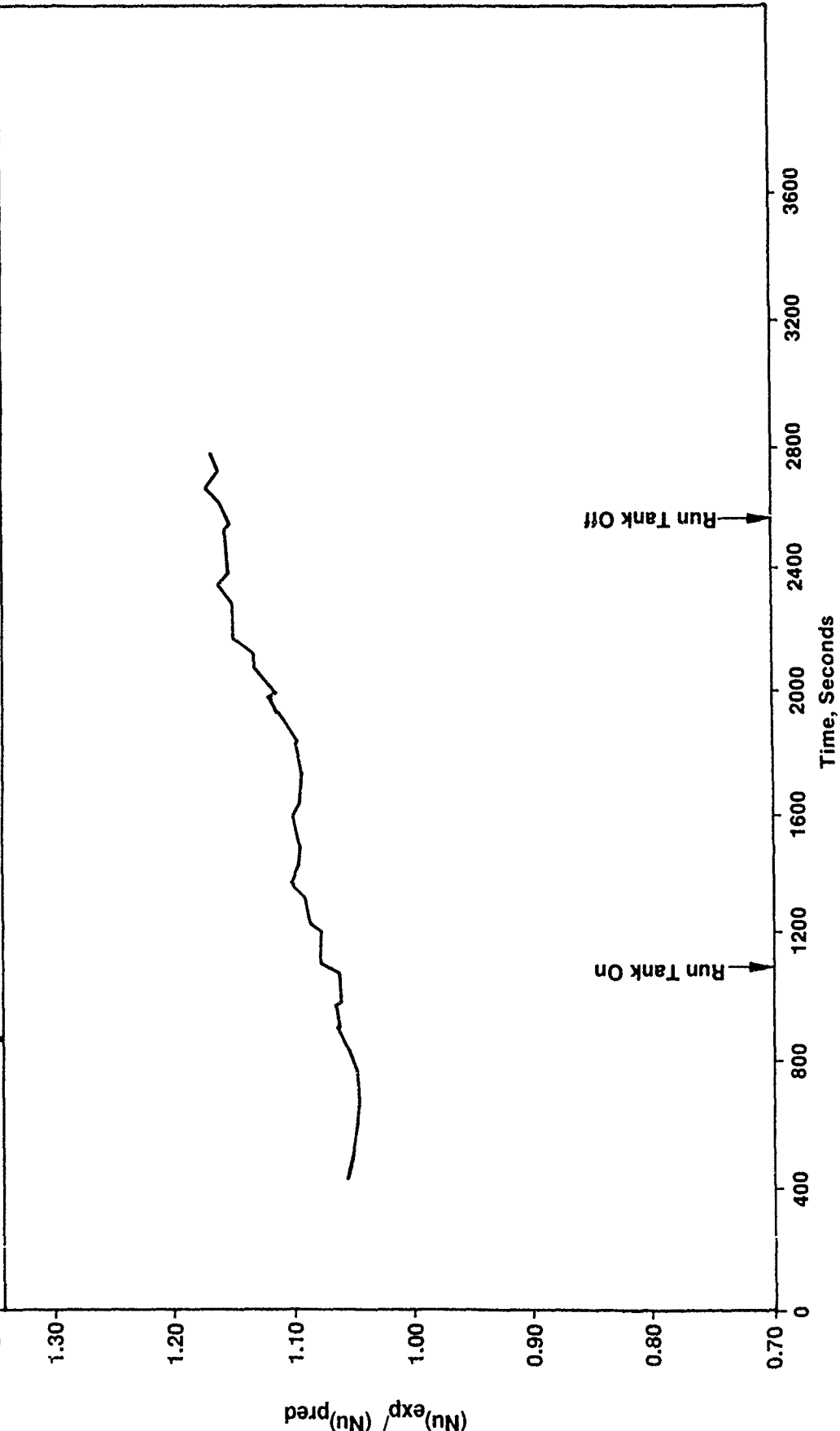


Figure 28. Heat Transfer Coefficient of Cooling Channel Increased Slightly During Run R113, Possibly due to Roughening of the Channel Walls

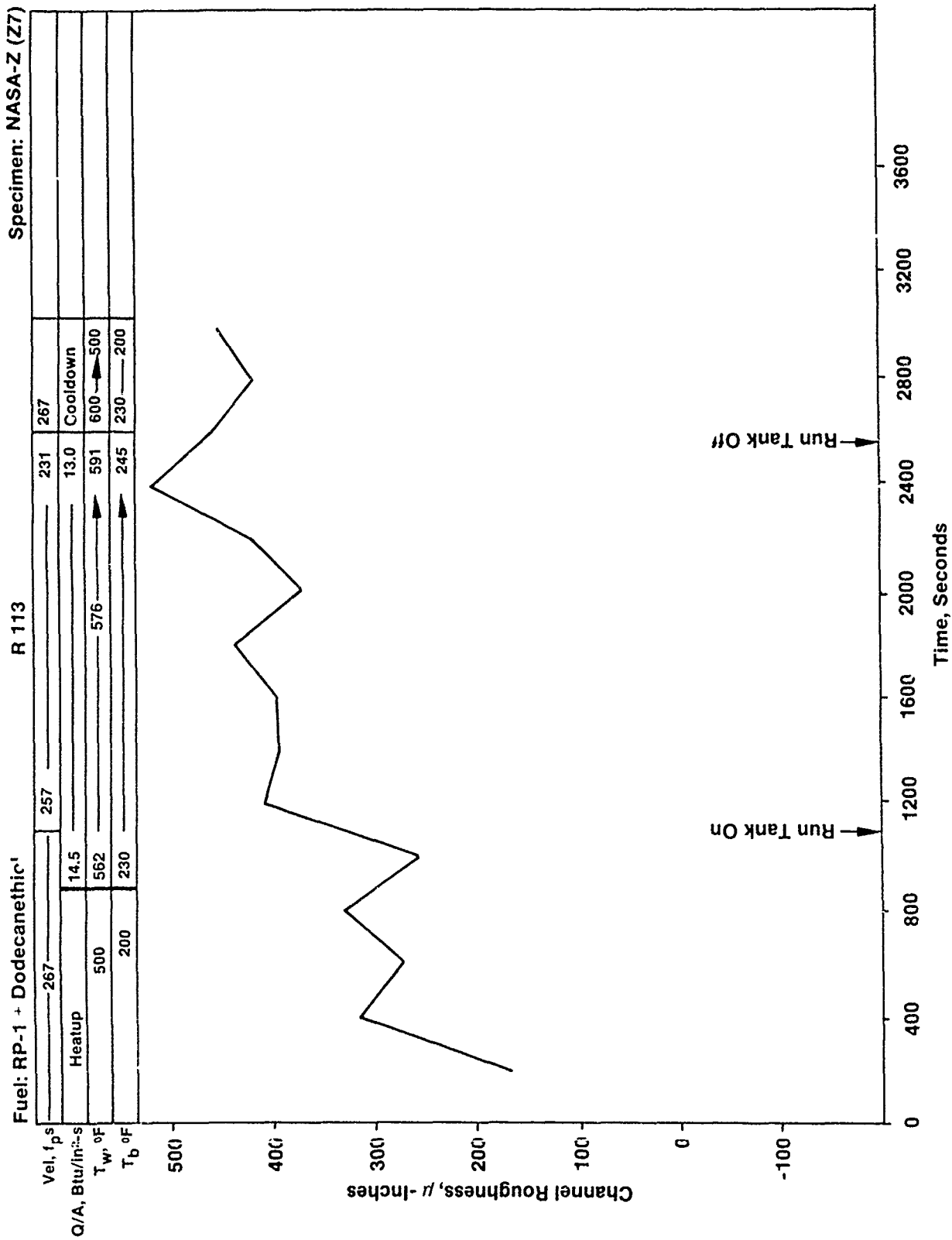


Figure 29. Apparent Channel Roughness During Run R113

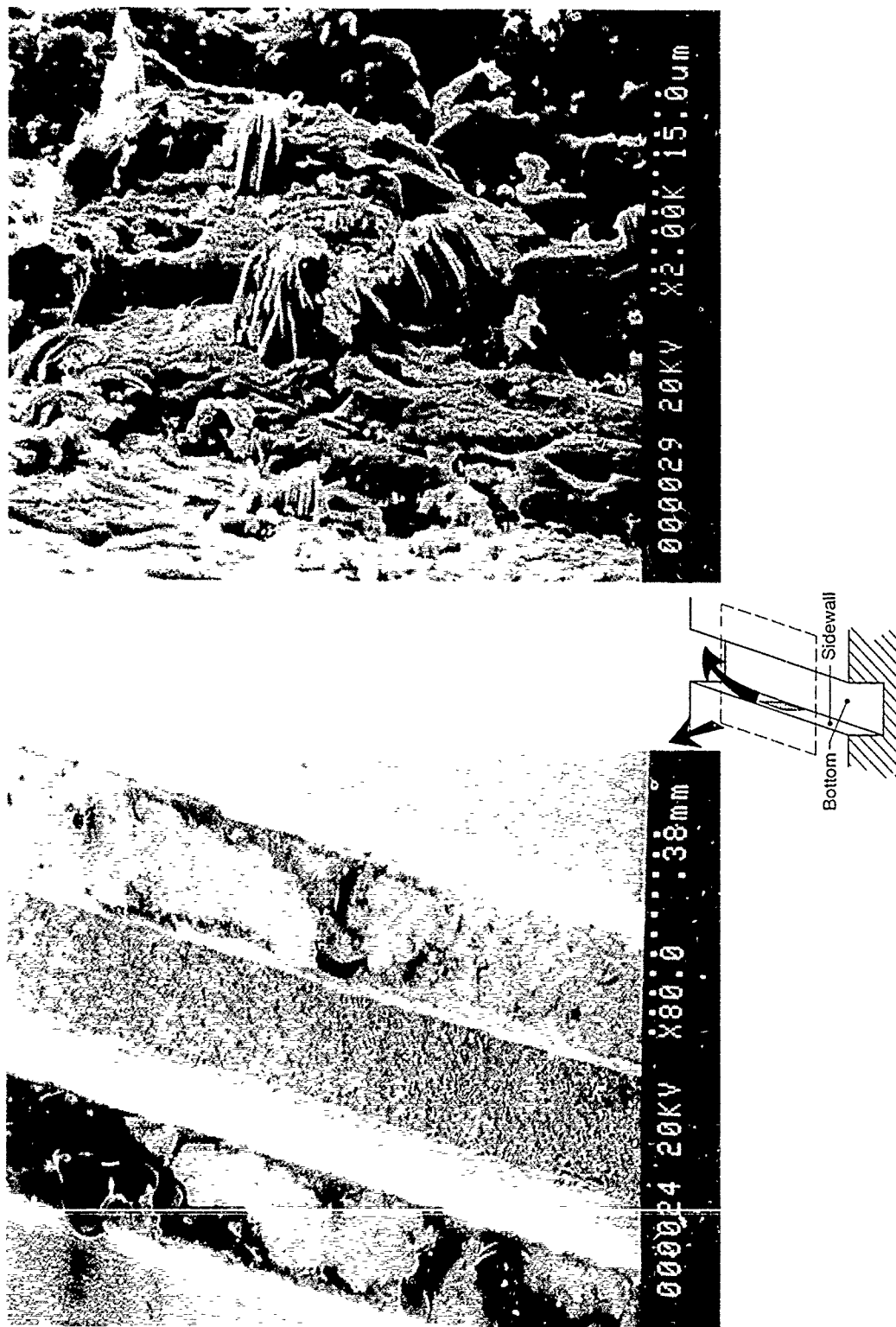


Figure 30. Addition of 50 ppm Sulfur to RP-1 Resulted in Corrosion of NASA-Z Channel, Even at Low Wall Temperature (586°F)

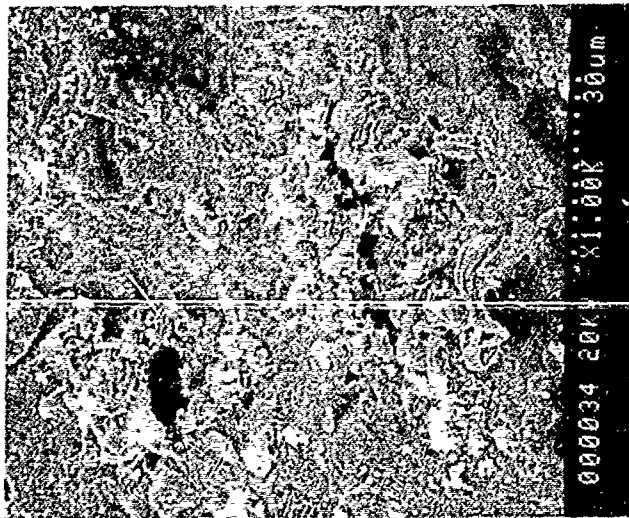


Figure 31a. Channel Wall at 1000x

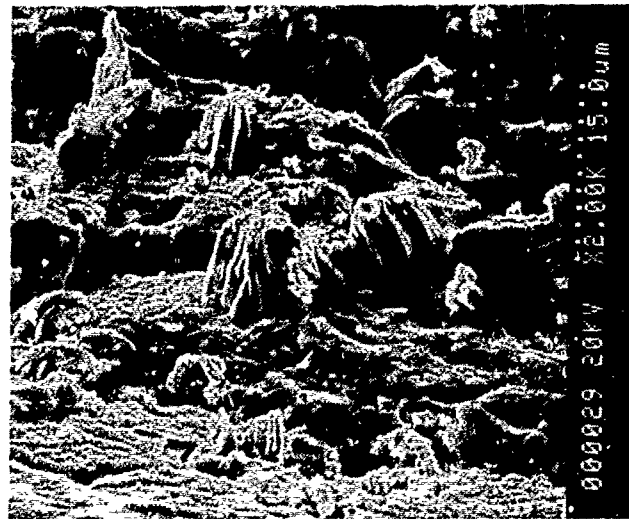


Figure 31b. Channel Wall at 2000x

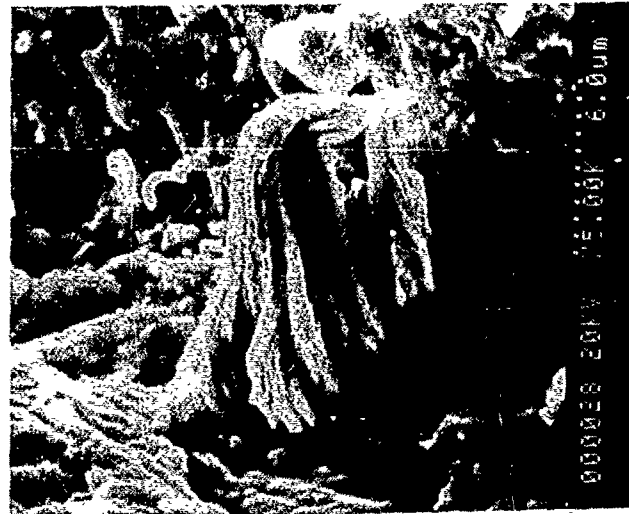


Figure 31c. Channel Wall at 5000x

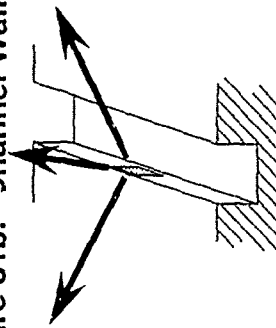


Figure 31. SEM Photos of Channel Wall of Specimen 27 After Dynamic Test with RP-1 Plus 50 ppm of N-Dodecanethiol in Test R113

### 3.2, RP-1 Test Results (cont.)

identified as  $\text{Cu}_2\text{S}$ , formed by a corrosive process in which the copper surfaces of the channel reacted with the sulfur compound added to the RP-1.

A review of all the on-line data from the RP-1 dynamic tests and all the posttest metallographic examinations of the specimen led to the following conclusions:

- 1) When operated at high wall temperatures, RP-1 and n-dodecane deposited a thin, tenacious layer of a complex, high molecular weight hydrocarbon on all copper surfaces.
- 2) These deposits reduced the heat transfer performance of the channel, but had no measurable impact on the pressure drop through the channel.
- 3) The rate at which the heat transfer performance was affected (i.e., the fouling rate) was a strong function of the wall temperature of the channel. The higher the wall temperature, the higher the fouling rate of the channel. On the other hand, it was demonstrated that fouling of the channel by hydrocarbon deposits could be eliminated by operation at wall temperatures below approximately 570 F.
- 4) The fouling rates measured in this program were in good agreement with those measured by previous investigators. Figure 32 presents a plot of correlations developed previously for the fouling rate as a function of inverse wall temperature, along with the data points from this program.
- 5) There was no measurable difference in the performance of the various copper materials tested, i.e., OFHC, Amzirc, and NASA-Z.
- 6) There was no noticeable difference between RP-1 and n-dodecane. The formation of hydrocarbon deposits was demonstrated with both fuels at similar rates. Thus, it does not appear to be feasible

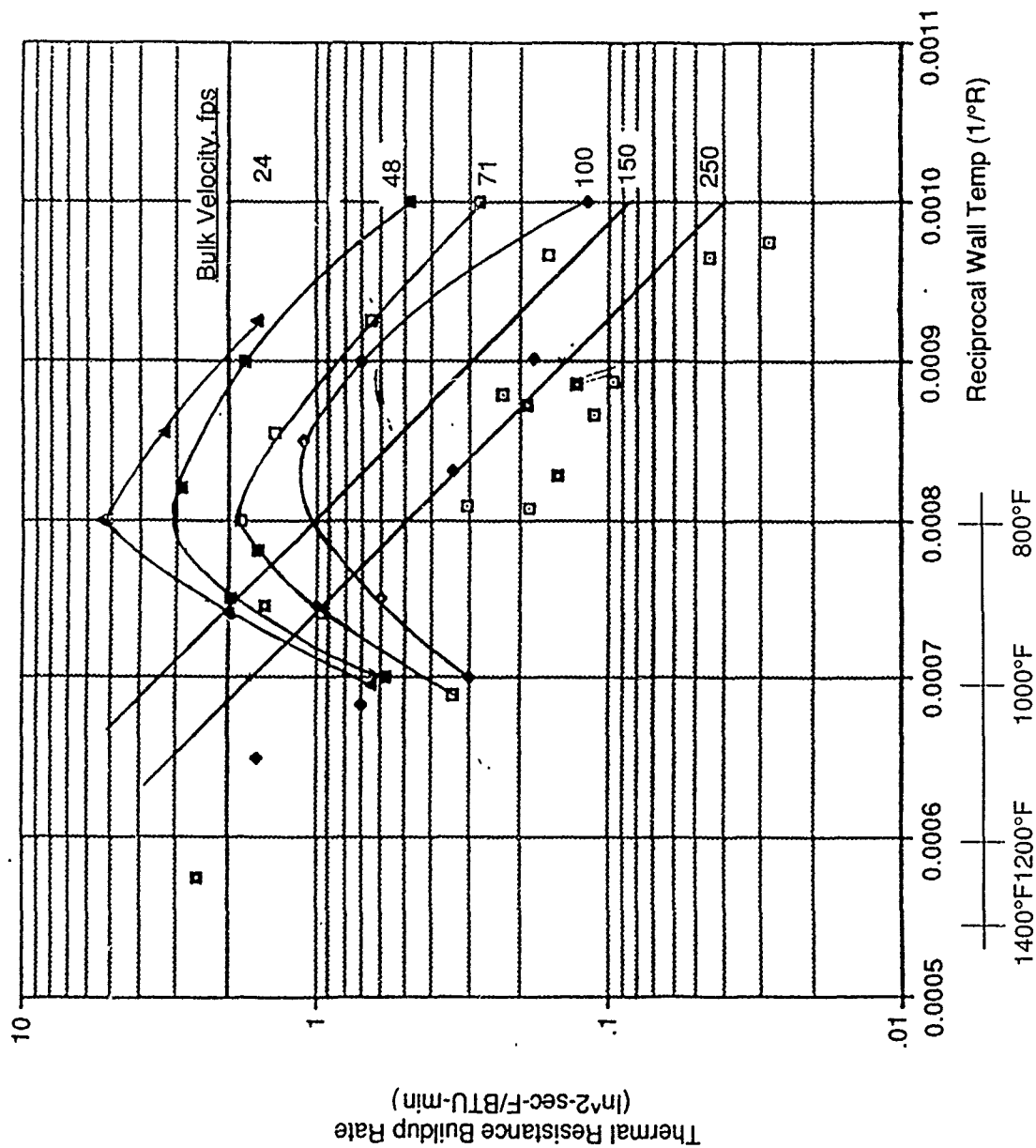


Figure 32. The Current Data on Fouling Rates of RP-1 in Copper Cooling Channels Agrees Well With Previous Test Programs

### 3.2, RP-1 Test Results (cont.)

to alleviate the deposition of the fuel by refining the RP-1 to its major component.

- 7) The addition of 1% (by weight) 1-dodecene to the RP-1 did not appear to affect the heat transfer performance of the test channel, but a 10% increase in the pressure drop through the channel was measured during the test.
- 8) The addition of 1% (by weight) biphenyl impacted the heat transfer performance of the channel during the test, but had only a very small affect on the hydraulic performance.
- 9) The addition of 50 ppm (by weight) sulfur as n-dodecanethiol to RP-1 caused corrosion of the channel which affected the pressure drop through the channel, but had very little impact on the heat transfer performance.

### 3.0, Task 1—Corrosive Interaction and Corrosion Rate Determination (cont.)

#### 3.3 METHANE TEST RESULTS

This section of the report discusses the results of compatibility tests with copper and copper alloys in contact with methane. The results of static tests using methane and methane with contaminants intentionally added is covered first, followed by a discussion of the results of the dynamic tests.

##### 3.3.1 Methane Static Tests (Task 1.1.3)

As described in Section 3.1.1, static tests using methane were conducted in an Aminco Bomb Apparatus. Coupons of NASA-Z were exposed to Ultra High Purity Methane (UHP) and UHP Methane with contaminants intentionally added at high temperature (650 F) and pressure (3000 psig). This section of the report documents the results of these static tests.

Six separate static test runs were conducted with methane in Task 1. Table 13 summarizes the run conditions in each of the tests.

Test 101 established a baseline by filling a bomb containing only UHP methane, with no additives or metal specimen, to nominal test temperature (650 F) and pressure (3000 psig) for 30 min. Analysis of the contents of the bomb was done by gas chromatography both before and after the test. Comparison of these analyses showed no significant changes had occurred during the test. It was concluded, therefore, that the UHP methane was chemically and physically stable in the bomb at these temperatures and pressures, and no reactions occurred which need to be "factored in" to the bomb tests using a copper coupon.

Test 102 exposed a NASA-Z coupon to UHP methane. The bomb was again taken to 3000 psig and 650 F for 30 min. As in Test 101, before and after analysis of the gas showed no changes which had occurred to the methane as a result of this test. No visible changes occurred to the NASA-Z coupon and no changes were seen in the SEM examinations of the coupon conducted before and after exposure. Figure 33 shows SEM photographs of the surface of the NASA-Z coupon before and after this test. Even at the high magnification (2000X), no changes were evident on the NASA-Z surface.

TABLE 13

## SUMMARY OF AMINCO BOMB TESTS

Test No.	Date	Coupon	Starting Fuel Composition	Maximum Test Pressure (psig)	Maximum Test Temp (deg F)	Coupon Weight Before (grams)	Coupon Weight After (grams)	Coupon Weight Change (grams)	Visible Change to Coupon?	SEM Change to Coupon?	GC Change to Fuel?
101	3/17/87	None	UHP Methane	3078	669	--	--		No	No	No
102	3/18/87	Z1	UHP Methane	3056	660	2.2164	2.2165	0.0001	No	No	No
103	3/19/87	Z3	UHP Methane + 1% Air	2373	657	2.2047	2.2047	0.0000	Slight Tarnish	Small	Depletion of Oxygen
104	4/23/87	Z6	UHP Methane + 2% Ethylene	3094	648	2.2253	2.2255	0.0002	No	No	No
105	4/27/87	Z7	UHP Methane	4812	656	2.2472	2.2473	0.0001	No	No	No
107	5/1/87	Z9	UHP Methane + Methyl Mercaptan	2946	656	2.2346	2.2364	0.0018	Grey Deposit	Heavy Deposit	No

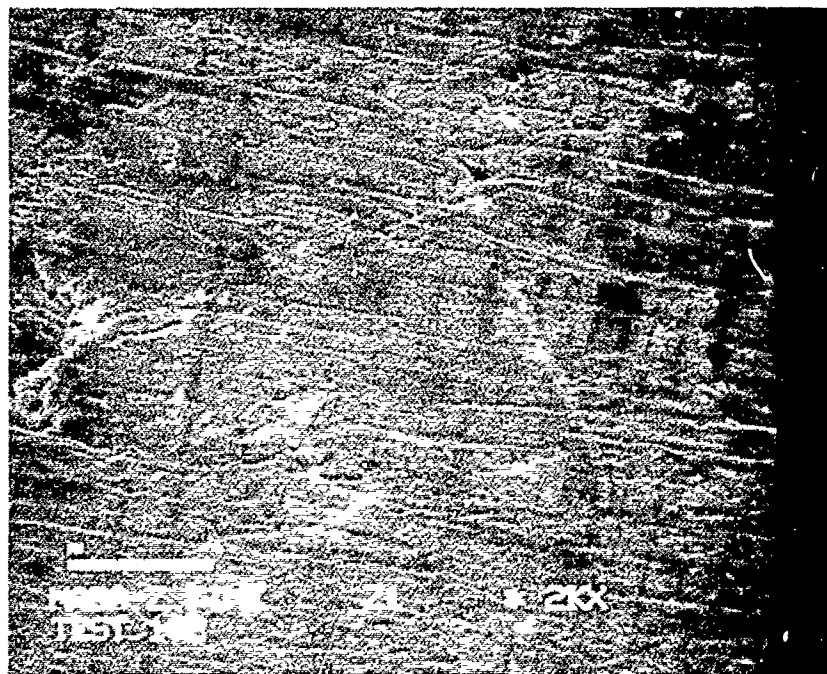
Note:

## Ultra High Purity Methane Analysis:

Methane	99.5%
Sulfur	N.D. (< 0.5 ppm)
Water	N.D. (< 1.0 ppm)
Oxygen	6.0 ppm
Nitrogen	41 ppm



**NASA-Z Before  
Static Test  
(2000X)**



**NASA-Z After  
Static Test  
(2000X)**

**Figure 33. NASA-Z Did Not React With Uncontaminated Ultra High Purity Methane in the Static Bomb Tests**

### 3.3, Methane Test Results (cont.)

Test 103 used a bomb filled with a mixture of 99.0 vol % UHP methane and 1.0% ultra zero air.<sup>(1)</sup> This mixture was made by first filling the bomb with ultra zero air to a pressure of 672 mm Hg at 70 F. Then the bomb was filled to a total pressure by 1234 psig at 70 F with ultra high purity methane.

After exposure, analysis of the gas phase showed significant depletion of oxygen, with no formation of combustion products such as CO, CO<sub>2</sub>, or H<sub>2</sub>O. Visual inspection of the NASA-Z coupon showed some tarnishing of the exposed surface. SEM examinations showed a very light deposit on the surface with no evidence of corrosion or surface attack. Figure 34 documents the appearance of this oxidation layer at high magnification.

Test 104 exposed a NASA-Z coupon to a bomb filled with a mixture of 97.8 vol % UHP methane and 2.2 vol % ethylene. This mixture was made by charging the bomb with 29.19 psia ethylene, and then pressurizing the bomb to 1321.6 psia with UHP methane at 75 F.

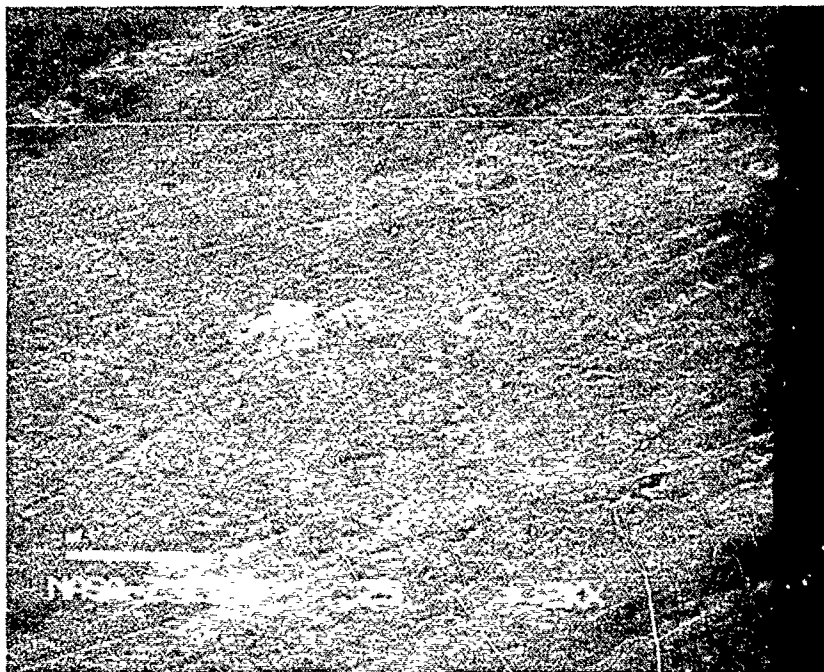
After exposure, analysis of the gas phase showed no change had occurred during the test, and SEM examination of the coupon showed no evidence of deposits or corrosion on the surface of the coupon. Thus, the addition of ethylene did not induce any reactions with the NASA-Z.

Test 105 exposed a NASA-Z coupon to a bomb containing only UHP methane at a pressure of 4800 psig. Analysis of the gas showed no change had occurred during the test, and SEM examination of the coupon showed no evidence of deposits or corrosion on the surface of the coupon. NASA-Z is apparently unreactive with UHP methane, even at these high temperatures and pressures.

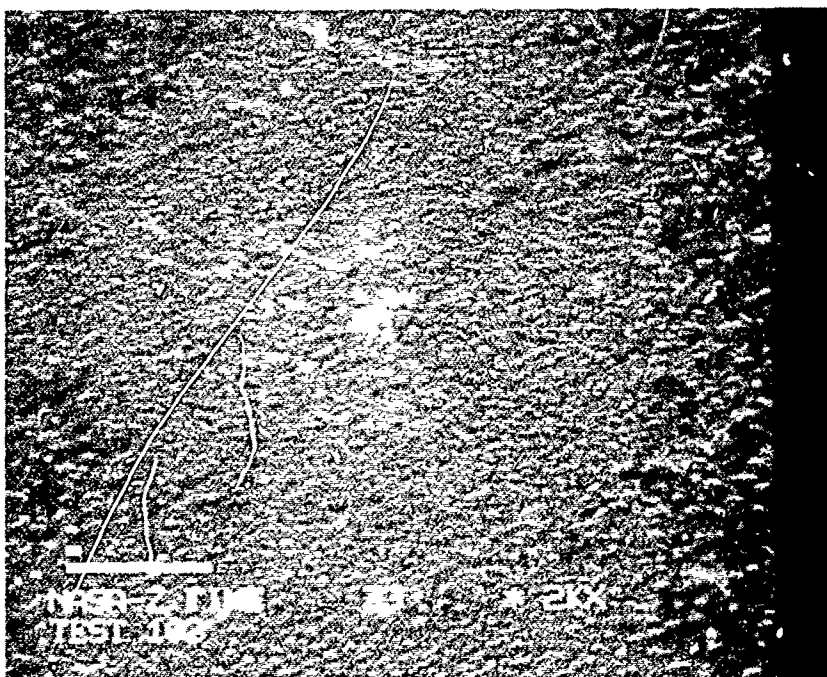
Test 107 exposed a NASA-Z coupon to a bomb filled with 272 ppm by volume methyl mercaptan in UHP methane. This mixture was made by filling the bomb with 18 mm Hg of methyl mercaptan, then increasing the pressure to 1259.7 psia

---

(1) Ultra zero air—compressed air certified to contain less than 0.1 ppm total hydrocarbons as CH<sub>4</sub> and less than 8 ppm H<sub>2</sub>O.



**NASA-Z Before  
Static Test  
(2000X)**



**NASA-Z After  
Static Test  
(2000X)**

**Figure 34. Methane Plus 1% (by vol.) Air Left a Thin, Even Oxidation Layer on NASA-Z in the Static Bomb Tests**

### 3.3, Methane Test Results (cont.)

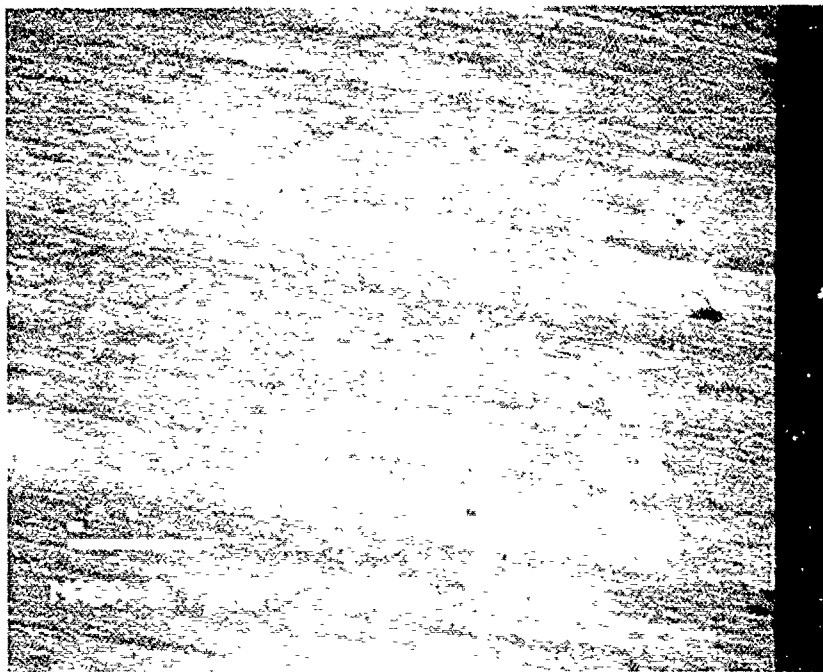
with UHP methane. SEM photographs shown in Figure 35 show the surface of the specimen underwent a dramatic change in appearance during this test. Elemental analysis of the surface by Energy Dispersive Spectroscopy (EDS) indicated the presence of copper and sulfur on the specimen, as shown in Figure 36.

A visible coating formed on the coupon during this test, as a thin, even, grey deposit, much like those deposits observed in the ampul tests using n-dodecane with n-dodecanethiol.

Additionally, this was the only coupon in the methane tests which showed a significant weight change. The coupon weight increased by 0.0018g (0.08%). A complete material balance on the sulfur compound added to the bomb could not be made because the GC was not calibrated to detect any unreacted methyl mercaptan remaining in the bomb after testing. Approximately 0.0094g of sulfur was added to the bomb as methyl mercaptan,  $\text{CH}_3\text{SH}$ , meaning the coupon weight change accounted for 19% consumption of the added  $\text{CH}_3\text{SH}$ .

At the end of the Task 1 static tests with methane, the following conclusions were drawn:

- (1) Ultra High Purity Methane does not react with NASA-Z at 650 F and pressures from 1500 to 5000 psig.
- (2) The addition of 2% (by volume) ethylene had no affect on the test results.
- (3) The addition of 1% (by volume) ultra zero air tarnished the specimen, with the formation of copper oxide.
- (4) The addition of 272 ppm (by volume)  $\text{CH}_3\text{SH}$  produced severe corrosion of the specimen with the formation of  $\text{Cu}_2\text{S}$ .



**NASA-Z Before  
Static Test  
(2000X)**



**NASA-Z After  
Static Test  
(2000X)**

**Figure 35. Methane Plus 272 ppm (by vol.)  $\text{CH}_3\text{SH}$  Dramatically Affected the Surface Appearance of NASA-Z in the Static Bomb Test**

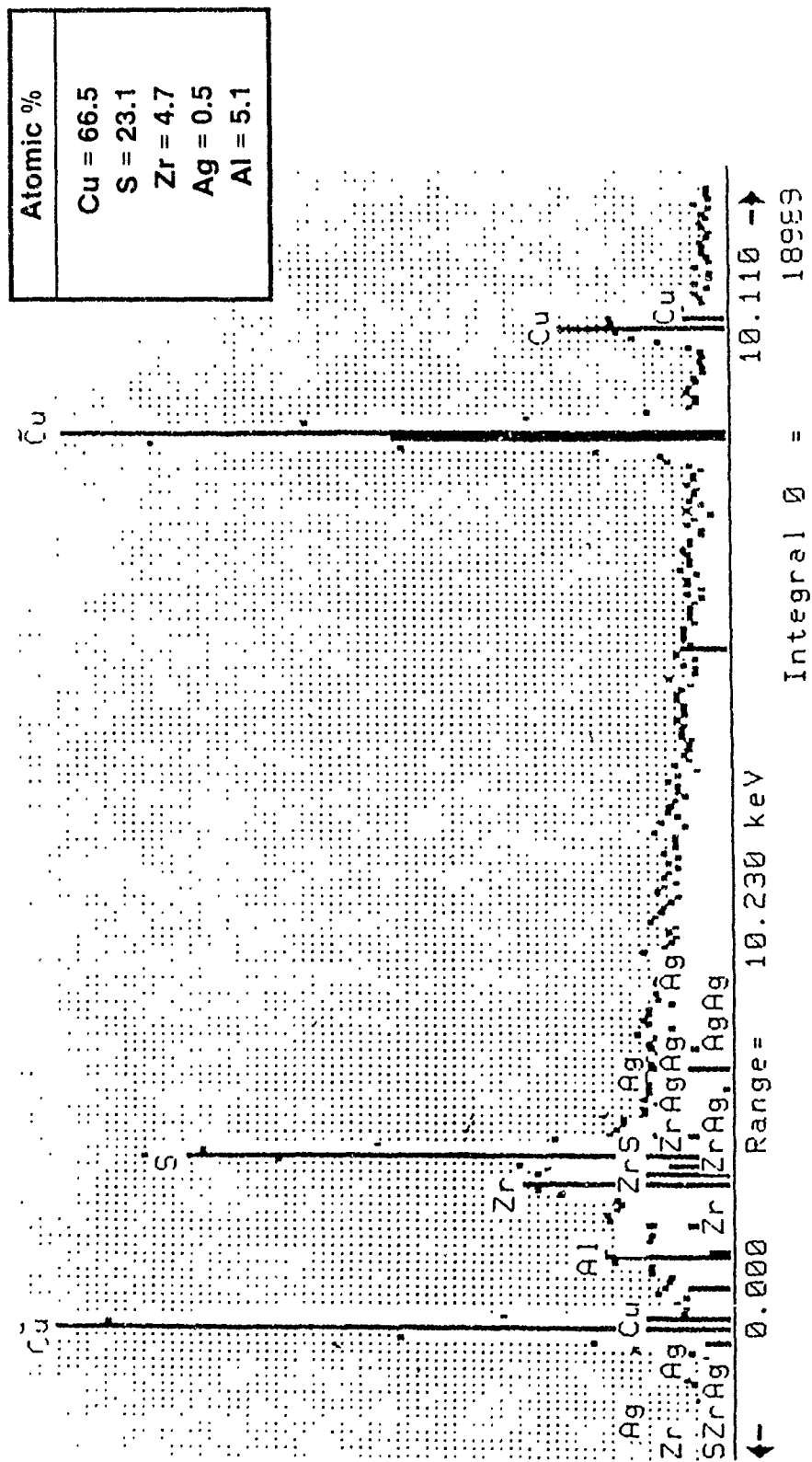


Figure 36. EDS Analysis Shows the Presence of Sulfur on the Surface of NASA-Z After Static Exposure to UHP Methane Plus 272 ppm Methyl Mercaptan (Test M107).

### 3.3, Methane Test Results (cont.)

#### 3.3.2 Methane Dynamic Tests Task 1

Thirteen dynamic tests were conducted with methane fuels and uncoated copper channels. The test conditions simulated operating conditions anticipated in the cooling channels of a regeneratively cooled 750,000 lbF thrust booster engine operating at a chamber pressure up to 3000 psia.

Table 14 summarizes the run conditions of the methane tests conducted to date. All tests were conducted with technical grade (TG) methane which has been analyzed to contain >97% methane, with 8.8 ppm O<sub>2</sub>, 4.8 ppm H<sub>2</sub>O, and less than 2 ppm sulfur.

Test M101 was halted after 92 sec of methane flow because methane froze in the LN<sub>2</sub> preconditioning heat exchanger. The specimen was not changed or examined after this brief test.

Test M102 was stopped after 85 sec because the temperature of the methane exiting the preconditioning heat exchanger rose steadily. When the methane temperature at the inlet to the test specimen reached -20 F, the test was terminated. Again, the specimen was not changed or examined after this test.

Test M103 achieved the desired steady state conditions at the entrance to the test specimen. The inlet fuel temperature and pressure were stable at -125 F and 3950 psig, respectively. Methane flowed through the test specimen for 1325 sec until the supply from the 6000 psig blowdown tanks was exhausted. Outlet fuel conditions averaged 350 F and 1050 psig. The average heat flux during the test was approximately 25 Btu/in.<sup>2</sup>-sec with a maximum wall temperature of 680 F.

The run conditions were very steady during the test. The heat transfer coefficient measured between the channel wall and the coolant increased slightly during the run, as shown in Figure 37. However, the amount of increase is within the accuracy of the technique used to measure this value. Similarly, the pressure drop through the channel did not change perceptibly during the run. This on-line data provided the first indication that the methane did not have a deleterious affect on the copper channel in these dynamic tests.

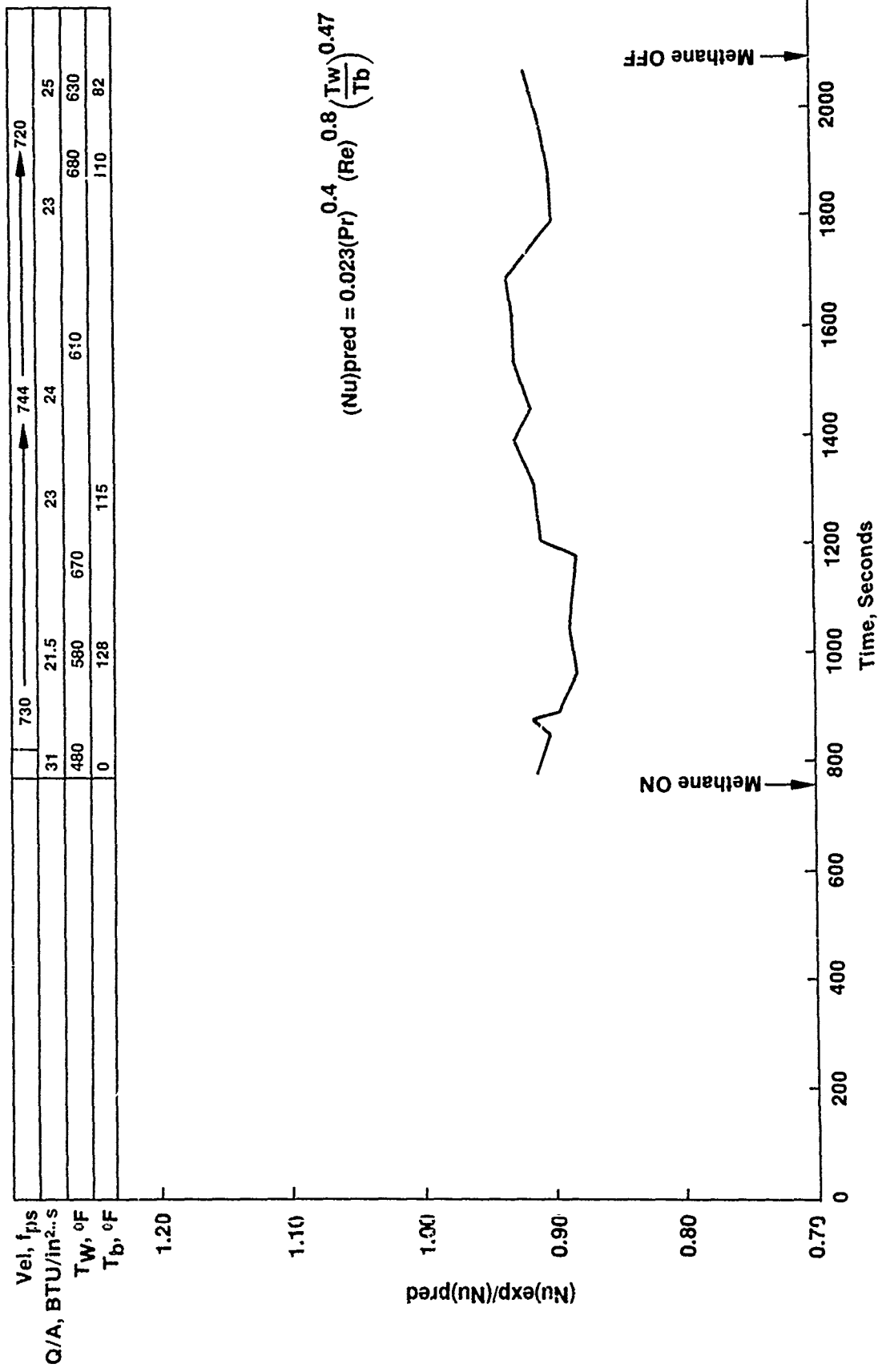


Figure 37. The Data Indicates an Insignificant Increase in Heat Transfer Coefficient Occurred During Test M103. This Behavior Was Typical of Dynamic Tests Conducted With Technical Grade Methane

### 3.3, Methane Test Results (cont.)

After completion of Test M103, the OFHC Cu sheet welded on the bottom of the specimen was removed by carefully cutting the weld with an end mill. This method exposed the entire channel without damage to either the Amzirc test channel or the OFHC Cu which directly covered the channel.

Visual inspection of the Amzirc test specimen showed qualitative evidence of very minor oxidation near the inlet to the specimen channel. The discoloration became less vivid along the length of the channel, with the last two-thirds of the channel appearing to be essentially unaffected by the tests. Figure 38 presents 35 mm photos of the channel taken before and after the Tests M101 through M103.

Examination of specimen A5 under a 40X optical microscope confirmed the visual observations. Small machine marks created when the test channel was cut were still clearly visible. These telltale marks were not covered by any deposition products, or blurred by any corrosive or erosive action.

The specimen was examined in a SEM. It was difficult to find any areas of interest in the channel, as the Amzirc appeared to be unaffected by the tests, even at high magnification. Figure 39 presents two of the SEM photos which were taken looking down into the channel. An EDS analysis of an area in the middle of the channel showed the presence of only Cu and Zr.

Test M104 tested Amzirc specimen A7 with TG methane at a somewhat higher wall temperature. Methane flowed through the test specimen for 1069 sec. Inlet fuel temperature and pressure averaged -110 F and 3980 psig, respectively. Outlet fuel conditions averaged 450 F and 1050 psig. The average heat flux during the test was approximately 30.5 Btu/in.<sup>2</sup>-sec, with a maximum wall temperature of 840 F.

The run data indicated no reactivity of the Amzirc specimen under these conditions. The heat transfer coefficient between the specimen wall and the fuel decreased slightly during the run, though the amount of change is again within the uncertainty of the measurement. The pressure drop through the specimen also remained unchanged during the run.

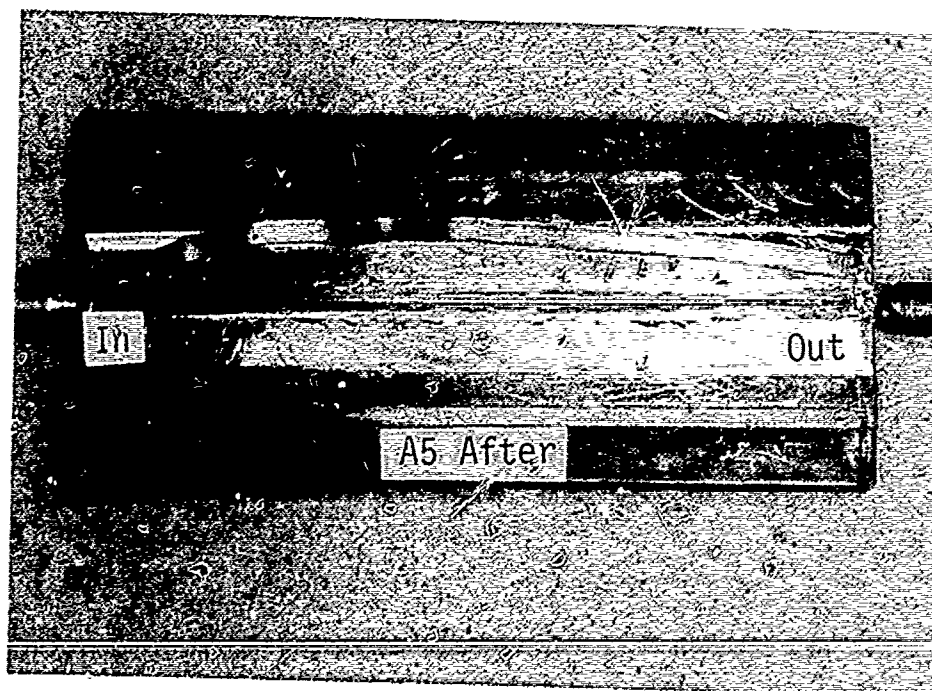
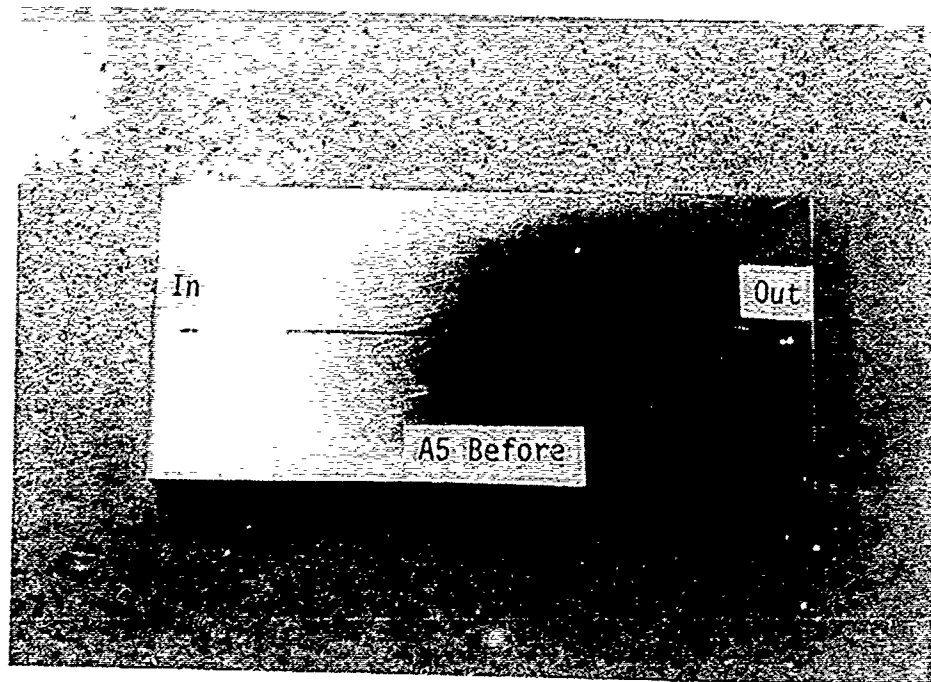


Figure 38. Specimen Tested With Tech Grade Methane at 680°F Shows Little Change

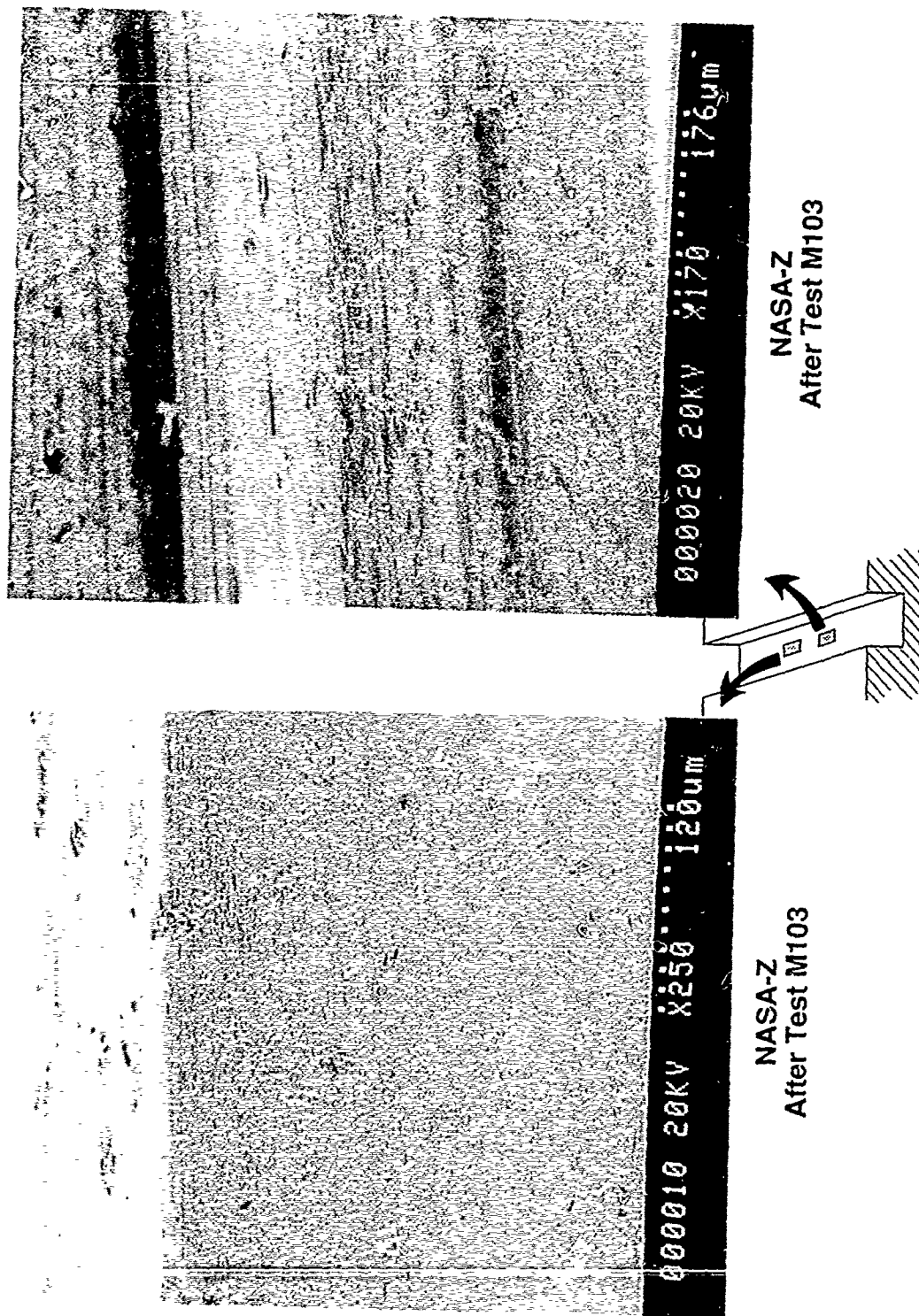


Figure 39. SEM Photos of Specimen A5 Shows No Surface Changes During 1325 sec of Operation With Technical Grade Methane at a  $T_{wall}$  of Up to 680°F (Test M103)

### 3.3, Methane Test Results (cont.)

After the channel cover was milled off, visual inspection showed the channel had developed a slight tarnish in all areas exposed to the fuel. The discoloration was consistent along the length of the channel.

Examination of specimen A7 under a 40X optical microscope showed the formation of a very thin black scale covering the bottom of the channel. In randomly spaced areas along the channel, the scale appeared to have flaked off, revealing the still shiny copper surface underneath the thin deposit. Machine marks could still be seen through the thin tarnish. However, it should be remembered that the deposit was minor enough to have not appreciably affected the fluid flow or heat transfer characteristics of the specimen.

Test M105 tested Amzirc specimen A6 with TG methane at the maximum wall temperature anticipated at the coolant channel wall. Methane flowed through the test specimen for 1394 sec. Inlet fuel temperature and pressure averaged 135 F and 4070 psig, respectively. Outlet fuel conditions averaged 500 F and 1010 psig. The average heat flux during the test was approximately 32.0 Btu/in.<sup>2</sup>-sec with a maximum wall temperature of 918 F.

The run data again indicated no reactivity of the copper specimen under these conditions. The heat transfer coefficient between the specimen wall and the fuel decreased slightly during the run, though it varied less than in the previous two runs. The pressure drop through the specimen also remained unchanged during the run.

After the channel cover was milled off, visual inspection showed the channel had developed a very slight tarnish in all areas exposed to the fuel. The discoloration was less vivid than in the previous test, and slightly more variable from the beginning to the end of the channel.

Examination of the specimen under a 40X optical microscope showed the channel to be nearly free of any deposition products or tarnish, except for an area of oxidation surrounding the inlet to the channel. Some very minor scaling was observed along the channel, appearing as a very thin black layer over an otherwise shiny copper surface.

### 3.3, Methane Test Results (cont.)

Test M106 was conducted for a total of 1383 sec using TG methane and a NASA-Z test specimen (specimen Z8). The primary objective of this test was to examine the performance of a NASA-Z specimen (all previous tests were conducted with an Amzirc specimen) at a nominal wall temperature of 700 F.

The on-line data indicated no reaction occurred during the test, i.e., neither the heat transfer coefficient measured between the channel wall and the coolant nor the pressure drop through the specimen changed during the test. Visual inspection and examination under a 40X optical microscope showed very minor dark discoloration of the last two-thirds of the channel. Small machine marks could still be seen through the discoloration, and there was no evidence of material loss.

As was characteristic of most of the specimens, significant darkening was observed on the land area of the specimen and the OFHC cover sheet. However, the flow and temperature conditions in this area between the channel and the weld are not well known, and almost certainly not representative of any region found in or around an actual cooling channel.

Test number M107 was conducted for a total of 1200 sec using TG methane and an Amzirc test specimen (specimen A9). The primary objective of this test was to examine the performance of an Amzirc specimen under high heat flux conditions at a nominal wall temperature of 850 F.

The steady-state coolant-side heat flux achieved during this test was 40.5 Btu/in.<sup>2</sup>-s at a wall temperature of 849 F. The on-line data indicated no reaction occurred during the test, i.e., neither the heat transfer coefficient measured between the channel wall and the coolant nor the pressure drop through the specimen changed during the test.

Visual inspection and examination under a 40X optical microscope showed almost no discoloration in the channel. Only very localized areas near the inlet and outlet were darkened. All surface details evident on the receipt of the specimen were still clearly visible after the test.

### 3.3, Methane Test Results (cont.)

Test M108 was conducted for a total of 819 sec using TG methane and a NASA-Z test specimen (specimen Z11). The primary objective of this test was to examine the performance of a NASA-Z specimen under high heat flux conditions at a nominal wall temperature of 1000 F. A secondary objective was to determine the maximum attainable heat flux with a 2 in. long channel.

The steady-state coolant-side heat flux achieved during this test was 41.7 Btu/in.<sup>2</sup>-sec and a maximum wall temperature of 934 F. The on-line data indicated no reaction occurred during the test, i.e., neither the heat transfer coefficient nor the pressure drop though the specimen changed significantly during the test.

Visual inspection of NASA-Z specimen showed very minor discoloration in the channel, limited primarily to the second half of the channel. Again, surface details were still visible through the tarnish. The discoloration was not consistent along the length of the channel, appearing as dark patches on an otherwise bright and shiny copper surface.

Test M109 was conducted for a total of 1310 sec using TG methane doped with 5.3 volume percent ethylene and an Amzirc test specimen (specimen A8). The primary objective of this test was to examine the affect of the addition of ethylene to the methane.

The steady-state coolant-side heat flux achieved during the test was 31.0 Btu/in.<sup>2</sup>-s at a wall temperature of 759 F. The on-line data indicated no activity reaction occurred during the test, i.e., neither the heat transfer coefficient nor the pressure drop through the specimen changed during the test.

Visual inspection of the Amzirc specimen showed very little discoloration in the channel. Surface details were still clearly evident. Even areas near the inlet and outlet holes showed little evidence of any activity or discoloration. The entire channel retained its bright and shiny appearance, as documented in Figure 40 which shows the 35 mm photographs taken of the specimen after completion of the test.

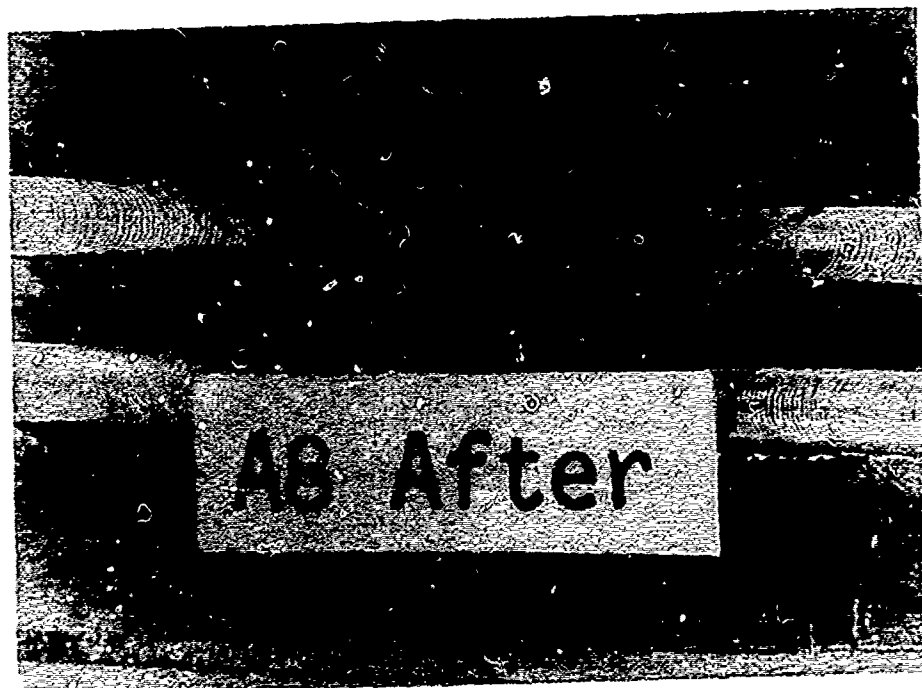
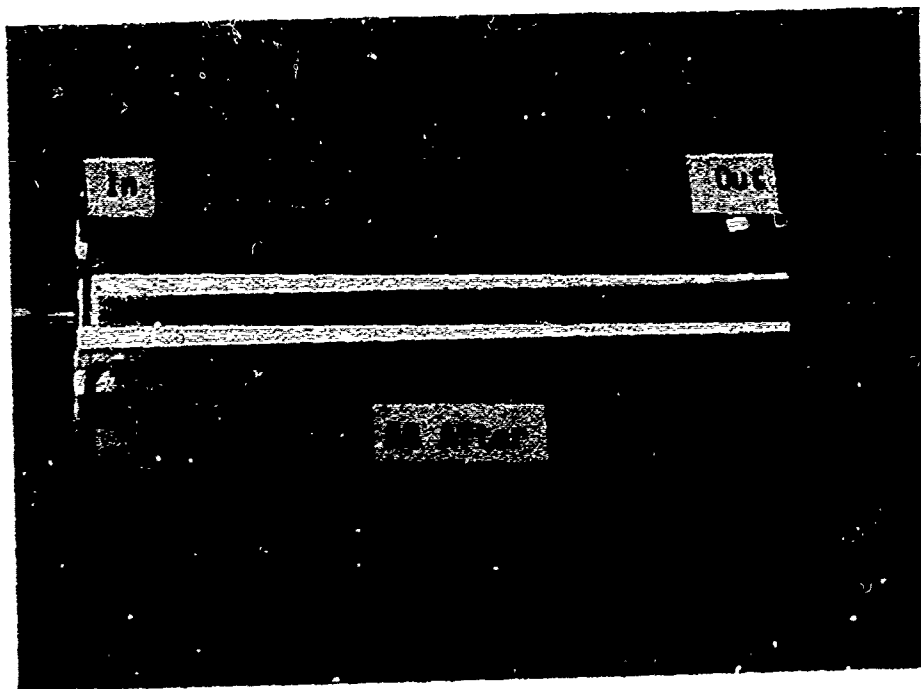


Figure 40. Test Specimen after 1310 sec Test with Technical Grade Methane plus 5% Ethylene at  $T_{\text{wall}} = 740^{\circ}\text{F}$  Shows No Affect on Amzirc.

### 3.3, Methane Test Results (cont.)

Test M110 was conducted for a total of 275 sec using TG methane doped with 201 ppm (by volume) methyl mercaptan and an Amzirc test specimen (Specimen A110). The primary objective of this test was to examine the effect of the addition of a sulfur compound to the methane.

The run conditions were not maintained at steady state for a long duration because a clog developed in the channel during the test. However, a coolant-side heat flux of 41.0 Btu/in.<sup>2</sup>-s was attained for approximately 60 sec before a steady reduction in the flowrate reduced the heat flux. Methane flow was started at a wall temperature of 970 F. As was characteristic of all the methane tests, the wall temperature dropped upon the introduction of methane to the channel, reaching a minimum of approximately 700 F after 10 sec of operation. After this, the wall temperatures recovered as the heating block continued to rise to the desired operating temperature. For this test, the desired steady state wall temperature of 900 F was achieved approximately 30 sec before methane flow was terminated because of the severe reduction in flowrate.

The decrease in flowrate at a constant inlet pressure of 3550 psig was the first time such behavior had been observed with methane. Figure 41 shows the flowrate of methane through the channel measured during Tests M110, M111, and M113.

The reduction in flowrate through the specimen was recognized as a problem after approximately 60 sec of operation by observing the on-line data. After 200 sec of operation with methane, the flowrate, which had been continually dropping since the start of the test, was down to approximately 50% of the initial value. The heaters were shut off in preparation for termination of the test. Methane flow was continued in an effort to cool the heating block and test specimen. However, the flowrate continued to drop and became erratic. After 275 sec of operation with methane, the methane was shut off, and a nitrogen purge through the system was started.

The initial nitrogen flowrate was also reduced from its pretest level, and it continued to decrease. After 10 sec of operation with nitrogen, the flowrate was zero, and nitrogen at a static pressure of 1550 psig was trapped upstream of the specimen. The pressure downstream of the specimen went to zero, which was the first

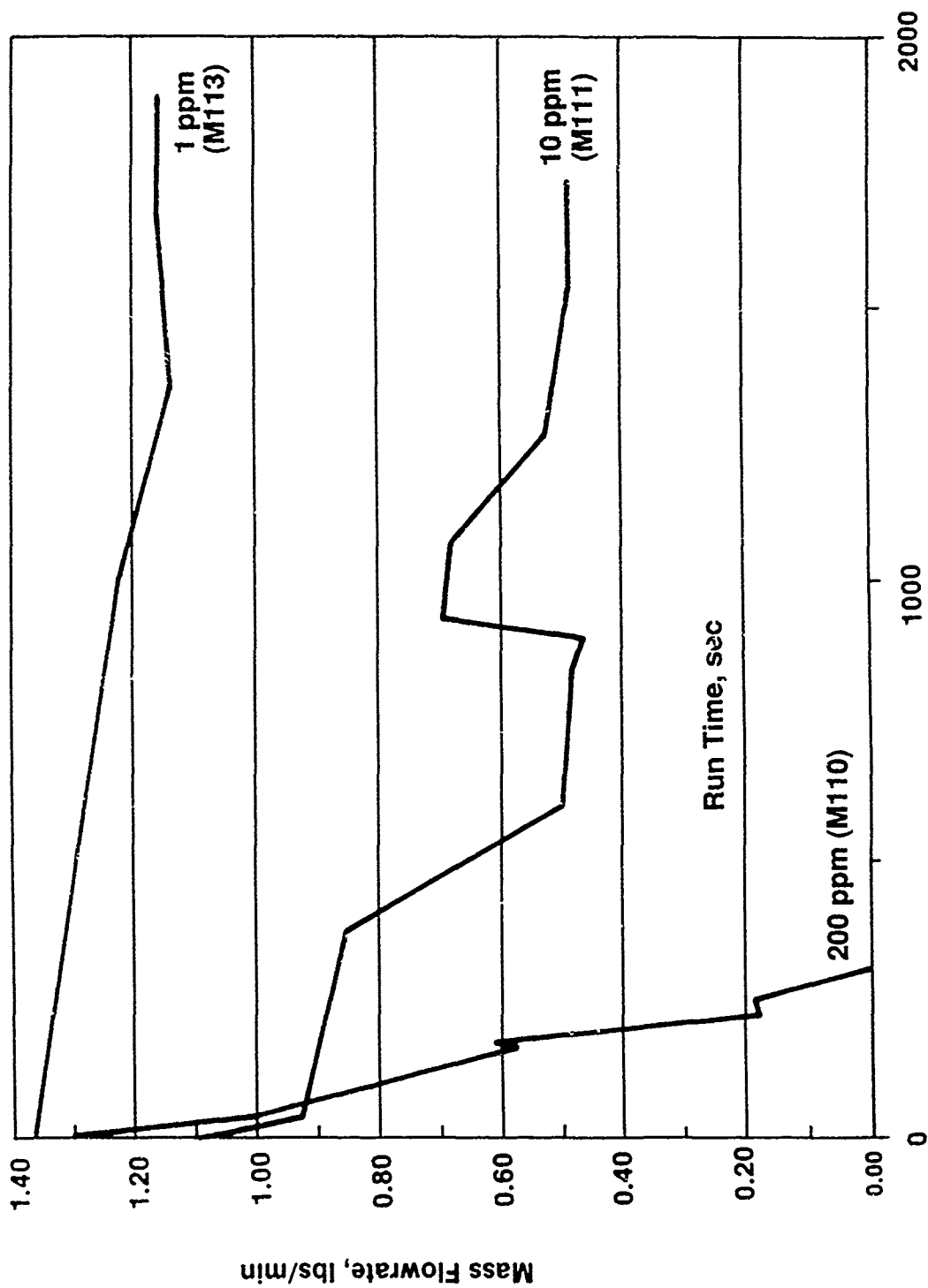


Figure 41. Sulfur in Methane Affected Flow Through Channel

### 3.3, Methane Test Results (cont.)

definitive indication that the flow restriction which had developed during the test was in the specimen, rather than upstream in the preconditioning heat exchanger.

When the flowrate through the specimen stopped, the entire heating block and test specimen became isothermal at 1250 F. The nitrogen trapped upstream of the specimen rose in temperature and pressure, reaching a maximum pressure of 4604 psig at a temperature of approximately 1000 F. Still no flow was observed through the test specimen. Approximately 2000 sec after the start of the test, the heating block and test specimen had cooled to 500 F. The pressure still remaining upstream of the test specimen was vented by opening a manual valve.

When the specimen was removed and the cover sheet milled off, the source of the flow restriction was apparent. The inlet hole into the channel, along with most of the channel, was completely blocked by a heavy, dense, black deposit. This deposit was later identified by EDS as  $\text{Cu}_2\text{S}$ .

Test M111 was conducted for a total of 1798 sec using technical grade methane doped with 10 ppm (by volume) methyl mercaptan and a NASA-Z test specimen (specimen Z9). The primary objective of this test was to examine the affect of the addition of a lesser amount of sulfur to the methane.

As in the previous test, a reduction in the flowrate was observed during the course of the test. However, this time the flow was not completely stopped, and a long duration test, albeit at a reduced heat flux, was conducted. Figure 41 shows the flowrate measured during the test. Again, the inlet pressure was constant during the test at 3500 psig.

The reduction in flowrate was first recognized after approximately 100 sec of operation. The reduction in flow was more gradual than in the previous test, and the flowrate was reduced to one-half of the initial value after 520 sec of operation. The flowrate continued to decrease (and the power to the heaters was correspondingly reduced to maintain a steady wall temperature of 800 F) until at 850 sec of operation, when a sudden recovery in the flowrate was seen. The flowrate increased from 0.43 to 0.67 lb/min over the course of 10 sec.

### 3.3, Methane Test Results (cont.)

As before, the flowrate showed a gradual degradation after this sudden increase, though the flowrate never again fell below 0.50 lb/min.

Examination of the specimen showed heavy black deposits in the channel, similar in appearance to those seen in the previous tests. SEM examination of the specimen identified the deposits as  $\text{Cu}_2\text{S}$ . Figure 42 shows that as much as 30% of the flow area was blocked by the formation of this corrosion product during test M111.

Test M112 was conducted for 1414 sec using technical grade methane and an Amzirc test specimen. The primary objective of this test was to examine the performance of a specimen at a high heat flux. A maximum steady-state wall temperature of 778 F and a maximum steady-state heat flux of 52.7 Btu/in.<sup>2</sup>-sec were achieved. An important secondary objective of this test was to establish that the system was free of sulfur before conducting tests with a very low sulfur concentration added to the fuel and to establish that the apparatus could be decontaminated of sulfur compounds.

Preliminary analysis of the run data showed no evidence of reaction during the test, i.e., neither the heat transfer coefficient measured between the channel wall and the coolant nor the pressure drop through the specimen changed during the test. Visual inspection of the Amzirc specimen showed very minor discoloration in the channel. Figure 43 shows 35 mm photographs of the specimen taken after completion of the test. It must be noted that the specimen label shown in the figure is incorrect. It is Amzirc specimen A24, not NASA-Z specimen Z24.

Test M113 was conducted for a total of 1803 sec using TG methane plus 1 ppm (by volume) methyl mercaptan and an Amzirc test specimen (specimen A22). The primary objective of this test was to examine the effect of very low sulfur concentrations in the fuel on the cooling channel. A maximum steady-state wall temperature of 723 F and a maximum steady-state heat flux of 44.8 Btu/in.<sup>2</sup>-sec were established.

Preliminary analysis of the run data shows a gradual increase in the heat transfer performance during the test. Figure 44 shows the ratio of the experimentally measured Nusselt number to the predicted Nusselt number over the course of the test. Two conclusions are evident from Figure 44. First, there is good correlation

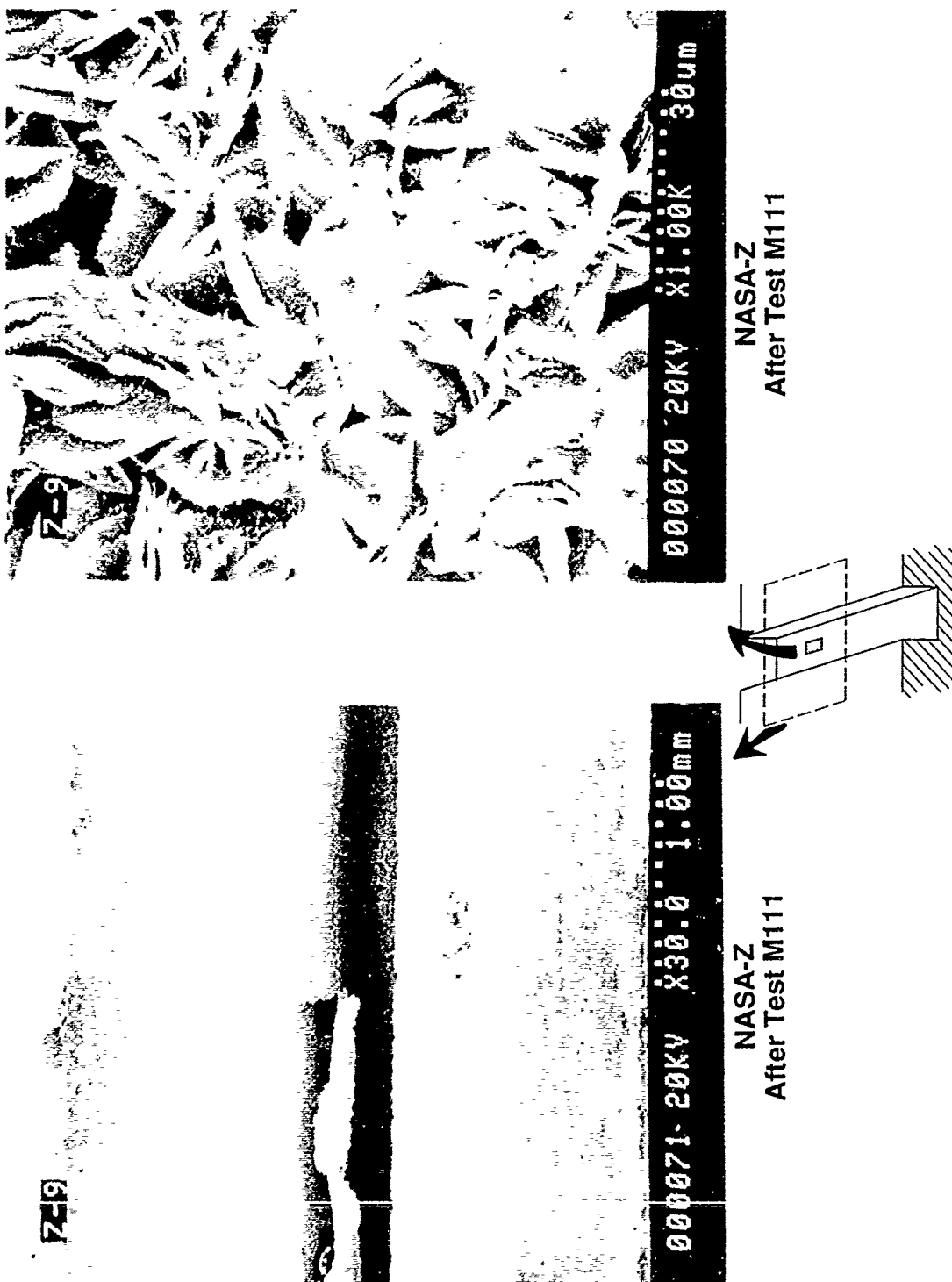


Figure 42. 10 ppm Sulfur in Methane Created Vivid Rosettes of Copper Sulfide in Test M111

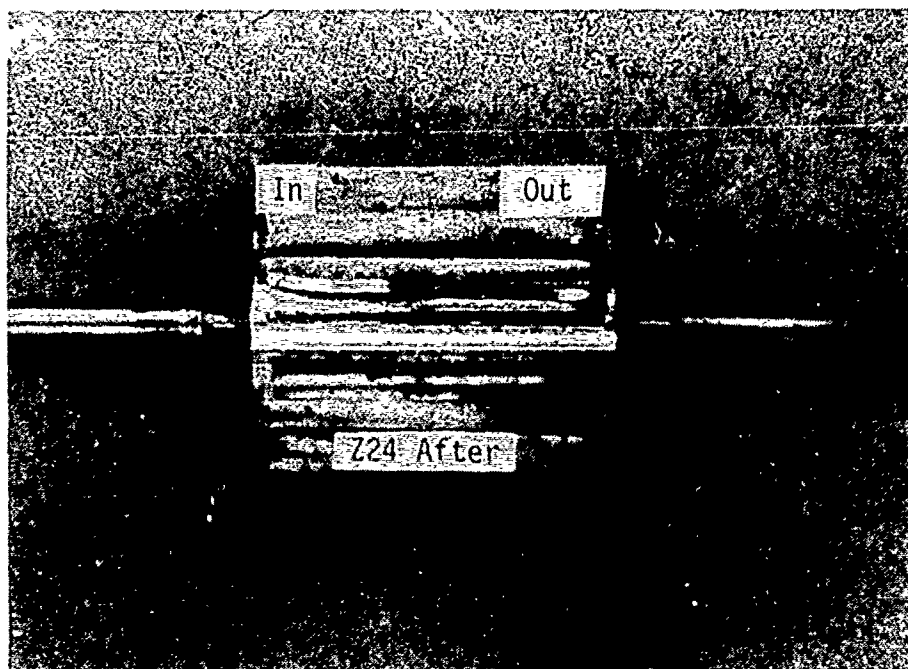


Figure 43. Specimen Tested at Coolant-Side Heat Flux of  $52.7 \text{ Btu/in.}^2\text{-s}$  Shows Only Minor Discoloration of Cooling Channel. No Sulfur Corrosion Was Observed in Test M112, Demonstrating That the Test Apparatus Could Be Cleaned Effectively

Q/A, Btu/in <sup>2</sup> -s	38	43	44	42	37	36
T <sub>w</sub> , °F	530	600	640	665	690	715
T <sub>b</sub> , °F	102	88	130	130	110	70

Run: M113  
 Fuel: Methane + 1ppm Sulfur  
 Specimen: Amzirc (A22)

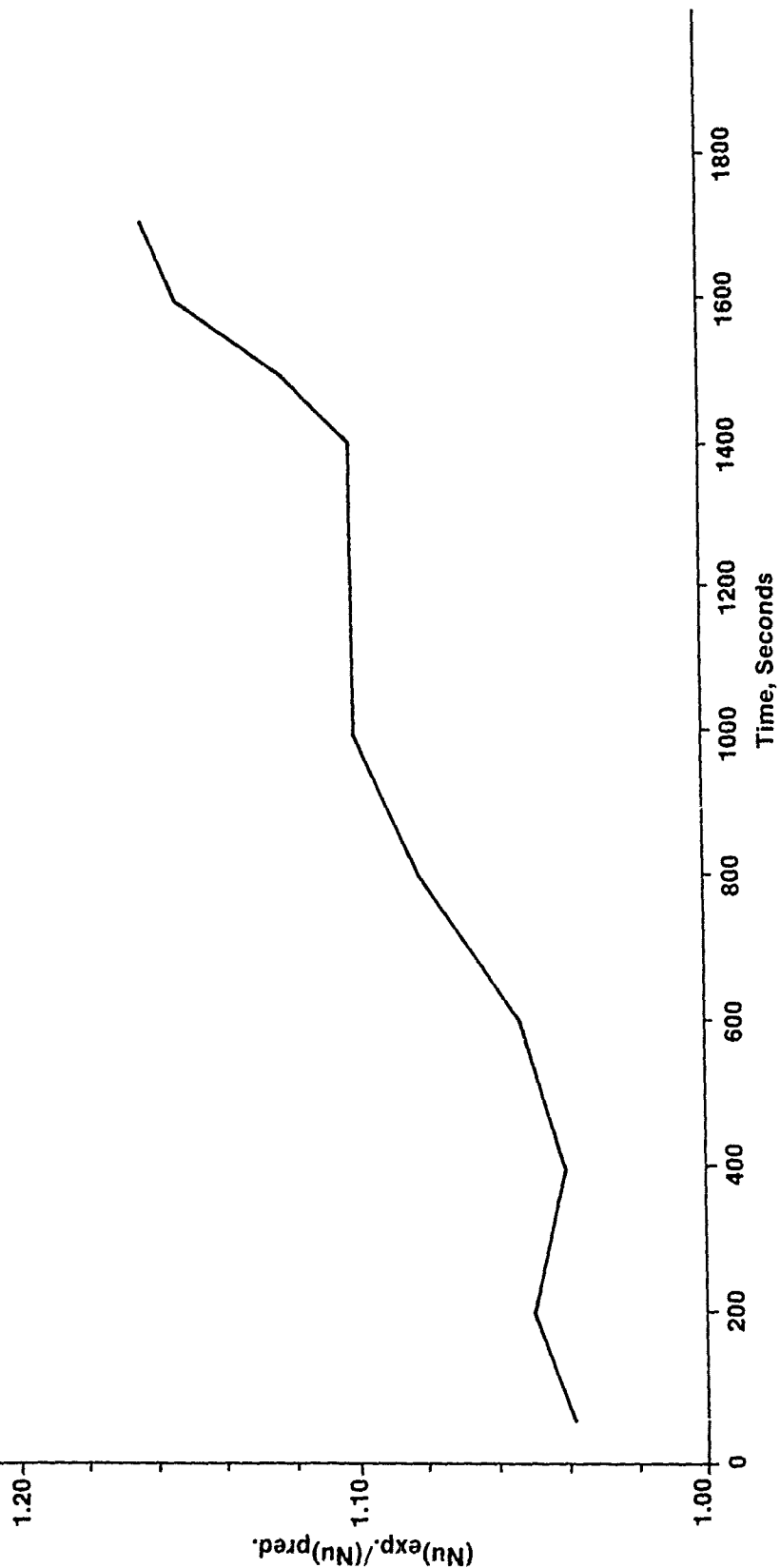


Figure 44. Heat Transfer Increased Slightly During Test Using Methane Plus 1 ppm Sulfur (Test M113)

### 3.3, Methane Test Results (cont.)

between the measured Nusselt number and the form of the Dittus-Boelter correlation recommended by earlier work with methane. This is true for all the methane tests conducted. All heat transfer data fell within a band of  $\pm 30\%$  from predicted values. Secondly, there is an apparent increase in the heat transfer performance of the specimen during the course of the test. This increase in the heat transfer performance is thought to be caused by roughening of the walls of the cooling channel, as evidenced in the SEM photographs.

Posttest visual examination of the specimen showed the channel to be discolored with a thin, grayish, consistent deposit in all areas in contact with the fuel. Figure 45 shows 35 mm photographs of the specimen after the test. SEM examination of the specimen shows evidence of corrosion on the surface of the copper. Figure 46 shows photographs of the bottom of the channel surface taken by the SEM. At low magnification (30X), many "freckles" are seen on the channel surface. Higher magnification (1000X) of one of the freckles shows it to be a crater in the surface of the channel. Also seen at high magnification are irregularly shaped flakes of material lying on the surface. These are believed to be flakes which were scoured from the surface by the flow of coolant and deposited randomly downstream.

EDS analysis of the areas in and around the crater shown in Figure 46 shows the presence of only Cu and S. There did not appear to be a significant variation in composition between the area just outside the crater as compared with the area in the crater or the loose flakes.

A review of all the on-line data from the methane dynamic tests and all the posttest metallographic examinations of the specimen led to the following conclusions:

- 1) Unadulterated Technical Grade Methane showed no compatibility problems with OFHC, NASA-Z, or Amzirc. This included tests at wall temperatures up to 934 F, and coolant side heat fluxes up to 52.7 Btu/in.<sup>2</sup>-sec.
- 2) Addition of 1% (by volume) ethylene to the methane did not affect the test results.

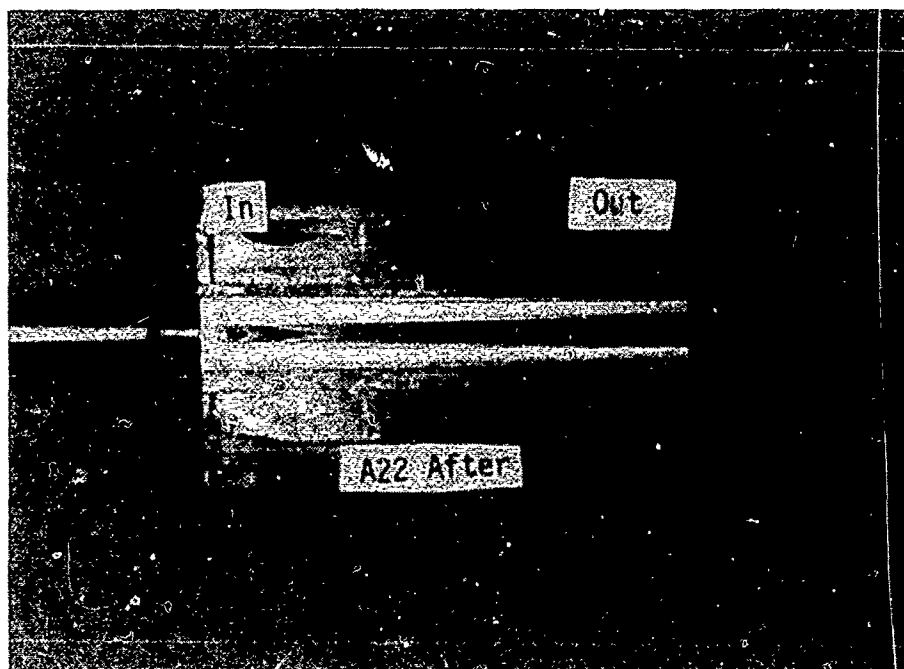


Figure 45. After 1800 sec of Operation with Methane Plus 1ppm Sulfur (Test M113), an Even, Gray Discoloration was Evident

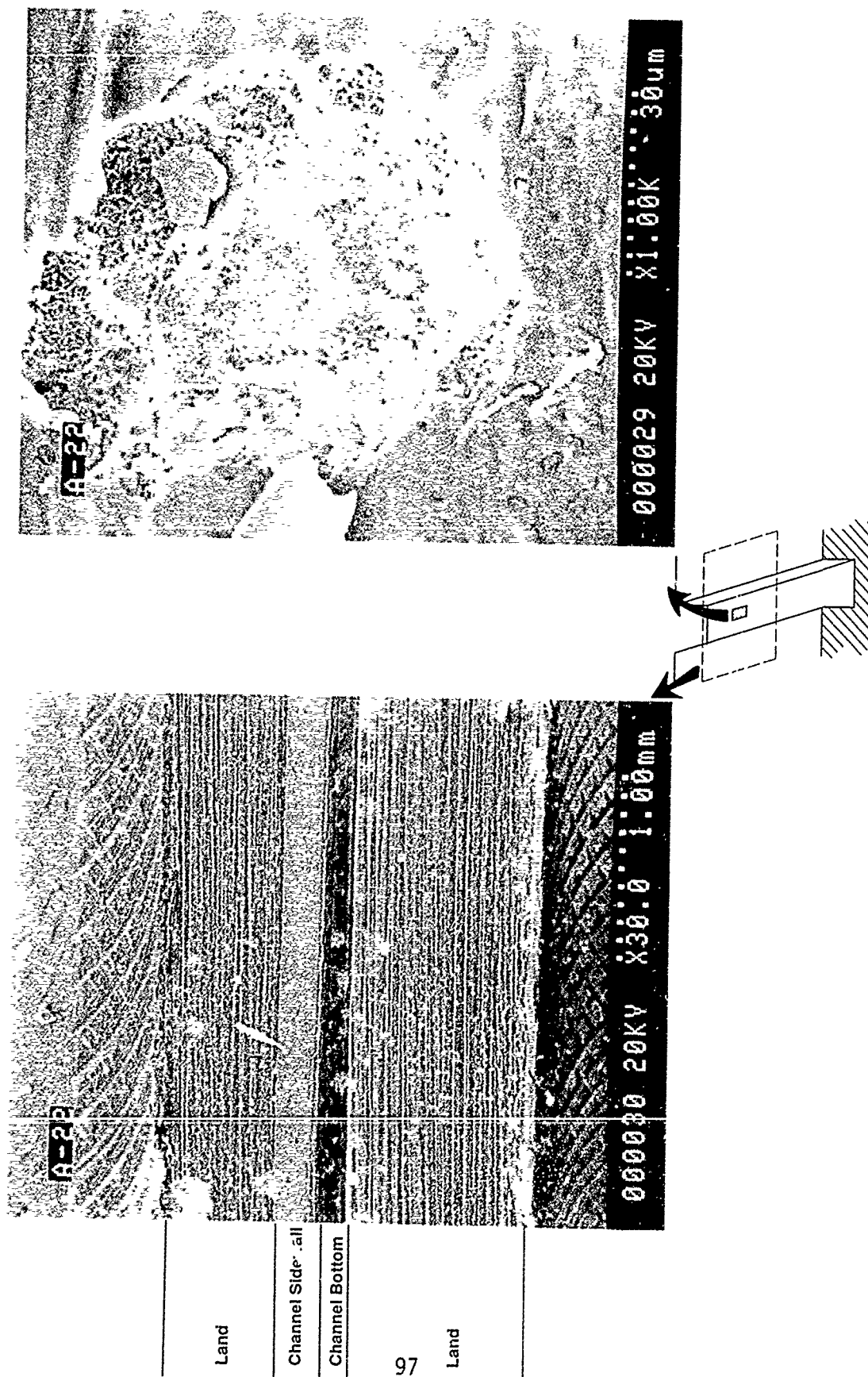


Figure 46. Just 1 ppm of Sulfur in Methane Produced Corrosion of the Amzirc Cooling Channel

### 3.3, Methane Test Results (cont.)

- 3) Addition of 200, 10, and 1 ppm (by volume)  $\text{CH}_3\text{SH}$  to the methane produced severe corrosion of the channel. The sulfur compound reacted with the copper surfaces of the channel (corrosion was observed with all three copper materials tested) to form  $\text{Cu}_2\text{S}$ . In the tests conducted with 200 and 10 ppm  $\text{CH}_3\text{SH}$  in methane, the formation of corrosion products was severe enough to significantly reduce the flowrate through the channel.

### 3.0, Task 1—Corrosive Interaction and Corrosion Rate Determination (cont.)

#### 3.4 PROPANE TEST RESULTS

This section of the report discusses the results of compatibility tests with copper and copper alloys in contact with propane. The results of static tests using Instrument Grade (IG) and Research Grade (RG) propane are covered first, followed by a discussion of the dynamic tests.

##### 3.4.1 Propane Static Tests (Task 1.1.4)

As described in Section 3.1.1, static tests using propane were conducted in an Aminco Bomb Test Apparatus. Coupons of NASA-Z and Amzirc were exposed to Instrument and Research Grade propane at high temperature (nominally 650 F) and pressure (nominally 3500 psig). This section of the report documents the results of these static tests.

Seven separate static test runs were conducted with propane. The run numbers assigned to the propane tests were 106-113 to avoid confusion with the methane static tests numbers which were being run concurrently. Table 15 summarizes the run conditions in each of the tests.

Test 106 exposed a NASA-Z coupon to a bomb filled with IG propane. The bomb was pressurized to 3500 psig at 650 F. Analysis of the gas showed no change, but the coupon was slightly tarnished during the test, as seen in Figure 47. SEM analysis of the surface of the coupon confirmed the presence of a slight deposit on the NASA-Z, but could not identify the elemental composition of the tarnish.

Analysis of the IG propane used in this test showed no sulfur and very little oxygen, but the water content of 200 ppm was much higher than is typical for instrument grade. Further tests were conducted with RG propane, including one conducted to examine if it was indeed the water which caused this tarnish, Test 112.

Test 108 exposed two coupons — one NASA-Z and one Amzirc — to a bomb filled with only RG propane. The temperature was not well controlled during this test, and the gas in the bomb reached a maximum temperature of 685 F.

TABLE 15

## SUMMARY OF PROPANE AMINCO BOMB TEST CONDITIONS

Test No.	Coupon Number	Starting Fuel Composition	Maximum Test Pressure (psig)	Maximum Test Temp (deg F)	Coupon Weight Before (grams)	Coupon Weight After (grams)	Coupon Weight Change (grams)	Visible Change to Coupon?	SEM Change to Coupon?	GC Change to Fuel
106	Z8	Inst. Grade Propane	3526	648	2.2124	2.2125	0.001	slight tarnish	v. slight	None
108	Z4 A51	Research Gr. Propane	3792	685	2.1986 2.0912	2.1987 2.0913	0.0001 0.0001	major discolor		depletion of oxygen
109	Z10 A52	Research Gr. Propane	3666	654	2.1220 2.1085	2.1219 2.1084	-0.0001 -0.0001	v. slight tarnish	v. slight	formed ethane
110	None	R.G. Propane	3664	663	n/a	n/a	n/a	n/a	n/a	formed ethane
111	Z11 A53	R.G. Propane + 2% Propylene	3637	655	2.2158 2.1030	2.2157 2.1029	-0.0001 -0.0001	v. slight tarnish	v. slight	None
112	Z2 A54	R.G. Propane + 200 ppm water	3459	658	2.1782 2.0993	2.1786 2.0996	0.0004 0.0003	heavy tarnish	major	formed ethane
113	Z12	R.G. Propane + Methyl Mercaptan	3551	651	2.1663 2.1046	2.1677 2.1058	0.0014 0.0012	even coating	major	formed ethane

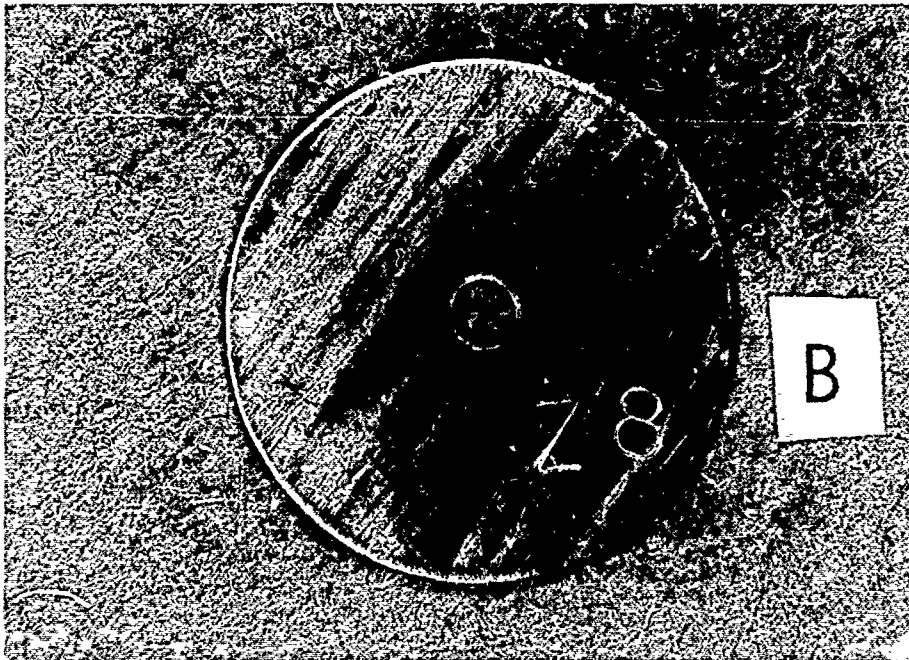
## Notes:

## 1. Instrument Grade Propane Analysis:

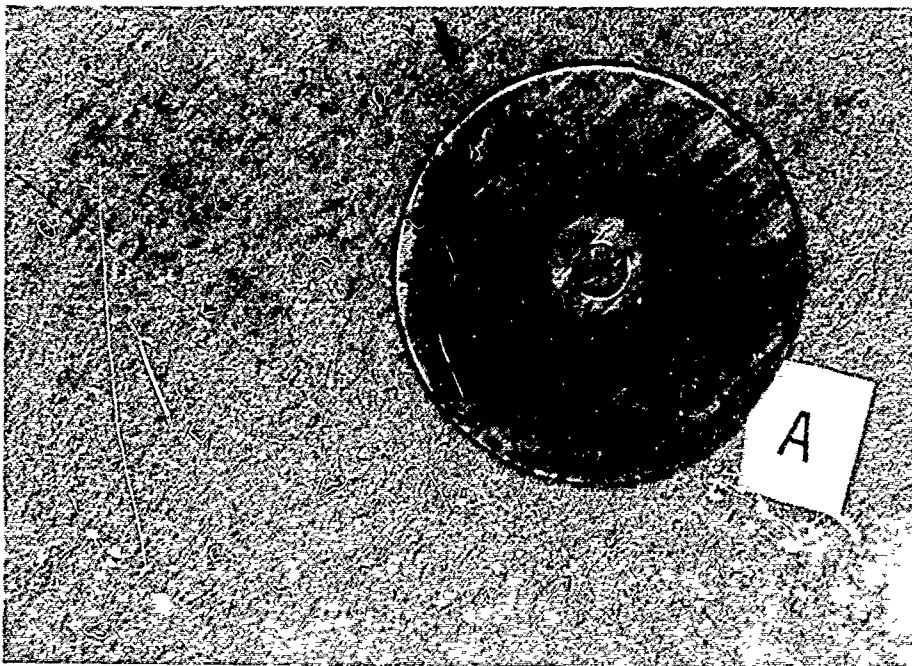
Propane 99.5%  
Sulfur N.D. (< 2 ppm)  
Water 200 ppm  
Oxygen 0.6 ppm

## 2. Research Grade Propane

Propylene 55 PPM  
Ethylene < 1 ppm  
Ethane 270 ppm  
Butanes < 5 ppm  
Oxygen < 5 ppm  
Sulfur < 2 ppm  
Water 2 ppm



Before



After  
Test 106

Figure 47. NASA-Z Coupon Showed a Slight Deposit After Static Testing With Instrument Grade Propane (Test 106)

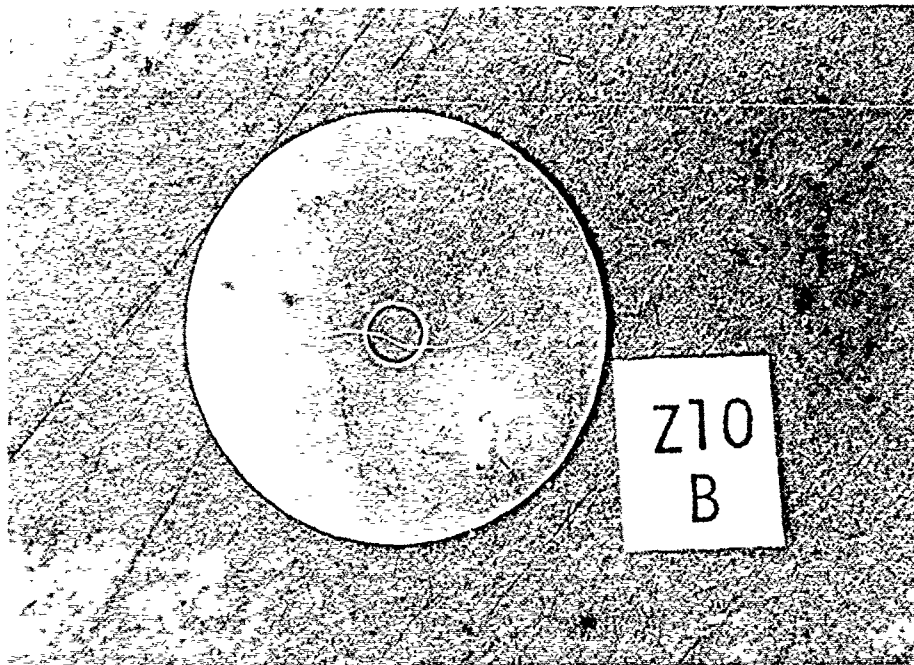
### 3.4, Propane Test Results (cont.)

Both coupons showed evidence of oxidation. Posttest analysis of the fuel indicated a high level of nitrogen (0.8%) and oxygen (0.1%), which are believed to have been introduced by the contamination of the bomb with air. Both coupons showed dramatic discoloration, ranging from dull yellow to bright blue on various parts of each coupon. Both coupons also showed a very minor weight gain of 0.0001 g, through this small change is within the accuracy of the Mettler balance used. The GC analysis of the fuel showed the formation of ethane during the test, from a starting concentration of 270 ppm to a final concentration of 0.3%. This was the first static test in which a measurable change occurred in the fuel other than the consumption of a reactive additive such as oxygen or a mercaptan.

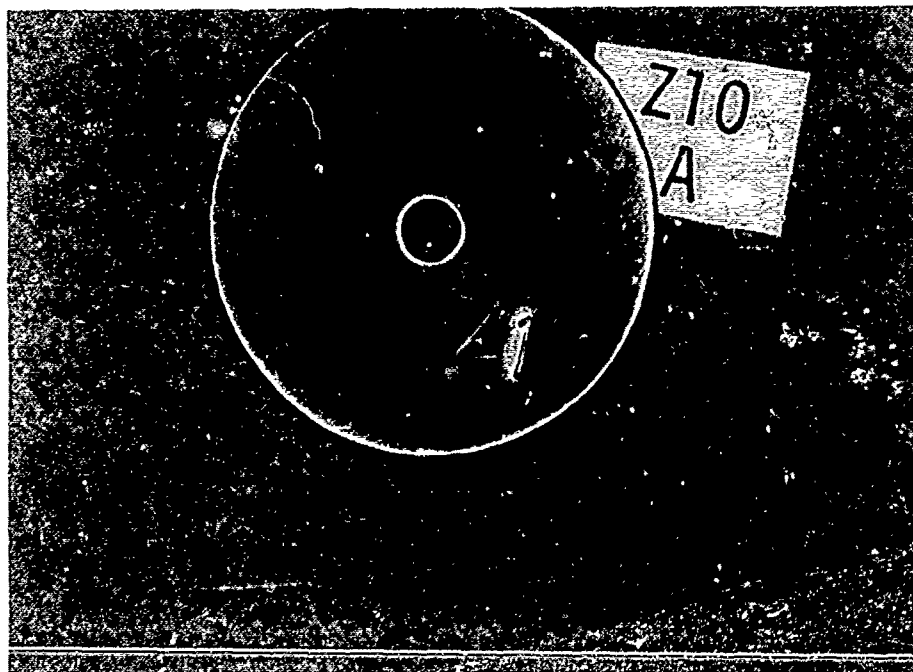
Test 109 repeated the test conditions of the previous run, exposing two coupons to RG propane. At the end of this run, both coupons showed a very, very minor tarnish. Figure 48 shows photographs of the NASA-Z coupon before and after this test. The discoloration of the coupons was somewhat less noticeable than when IG propane was used in test 106, and much less noticeable than that observed in the previous test. Both coupons again appeared to be equally affected by the exposure to the propane and the weight of each decreased by 0.0001 g, though this small of a change in weight may not be significant due to the experimental error of the balance. GC analysis of the fuel at the end of the test again showed the formation of a slight amount of ethane, to a final concentration of 0.3%.

Test 110 investigated the question of whether this change in the fuel was caused by the presence of the copper, or if it was simply a result of heating the fuel under pressure in the bomb apparatus. The bomb was filled with RG propane. No copper coupons were inserted into the bomb. The bomb was subjected to a typical temperature and pressure cycle, and the fuel was analyzed. Ethane was again developed during the test, though the final concentration was lower than measured in tests 108 and 109. The final analysis showed an ethane concentration of 500 ppm. As in previous tests, no other species were formed in a measurable amount.

Test 111 exposed two coupons to a mixture of 2% propylene and 98% RG propane. This mixture was made by first condensing 133 mm Hg of propylene from a measured volume tank into the bomb, and then condensing 129 psi of propane from



Before



After

Figure 48. Research Grade Propane Left a Barely Noticeable Deposit on NASA-Z in Static Test Number 109

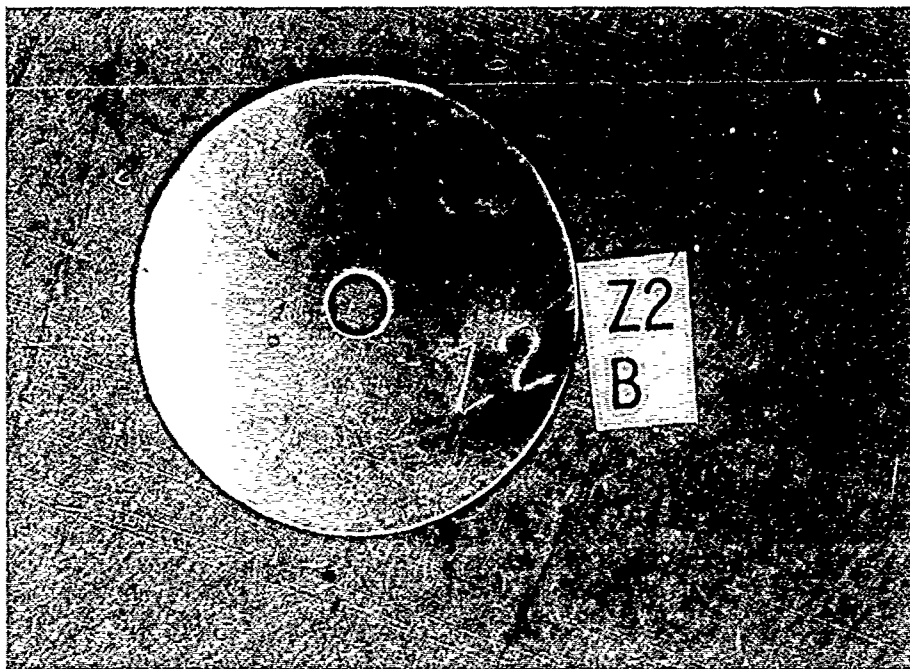
### 3.4, Propane Test Results (cont.)

this same measured volume tank into the bomb. After the test, both again showed a very light deposit, though not any more than when the coupons were exposed to research grade propane without any propylene. The weight of the coupons did not change significantly, both showing a 0.0001 g loss during the test. GC analysis of the fuel did not show a change in the ethane concentration during the test.

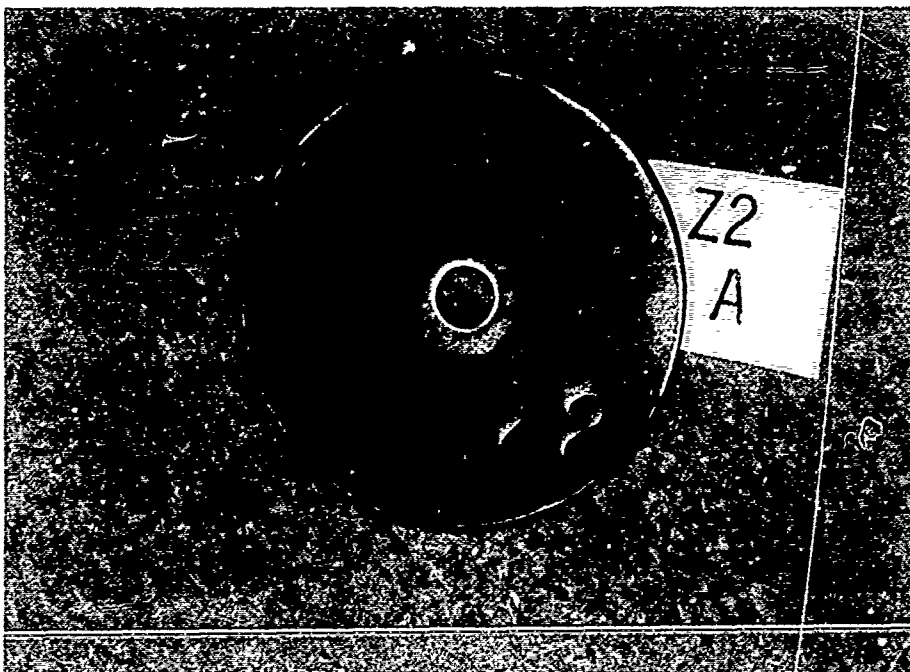
Test 112 investigated the effect of water in the propane. A bomb was prepared containing research grade propane with a water content of 2000 ppm. Two coupons, one NASA-Z and one Amzirc, were placed in the bomb. Deionized water (0.046 microliter) was added and the bomb was cooled to an internal gas temperature of -90 F in Dry Ice to freeze the water and a vacuum was pulled on the bomb to remove any air. The bomb was then chilled by submersion in liquid nitrogen and research grade propane was condensed into it. After heating, the coupons showed the heaviest tarnish of any coupons yet tested in a propane environment. Figure 49 shows photographs of the NASA-Z coupon before and after this test. The NASA-Z and the Amzirc coupons appeared to be equally tarnished, and they showed weight gains of 0.0004 and 0.0003 g, respectively. SEM analysis indicated that the affect of the propane plus 2000 ppm water was minimal on the surface of NASA-Z, as shown in Figure 50. GC analysis of the fuel showed significant formation of ethane, to a final concentration of approximately 0.5%.

Test 113 exposed two coupons to a bomb containing 94 ppm (by volume)  $\text{CH}_3\text{SH}$  in RG propane. This mixture was made by adding 18 mm Hg of  $\text{CH}_3\text{SH}$  to the bomb and then condensing in RG propane from a measured volume tank. The bomb was subjected to a typical heating cycle. Examination of the coupons after the test showed they had acquired an even, dull grey coating (Figure 51), much like those observed during the mercaptan-containing methane and *n*-dodecane tests. The NASA-Z and Amzirc coupons appeared to be equally affected by the test, and they showed weight gains of 0.00014 and 0.00012 g, respectively. The deposits on the surface of the coupons were analyzed to be  $\text{Cu}_2\text{S}$ . Analysis of the fuel showed a small concentration of ethane (0.1%).

The following conclusions were reached regarding the results of the Static Tests with propane:



Before

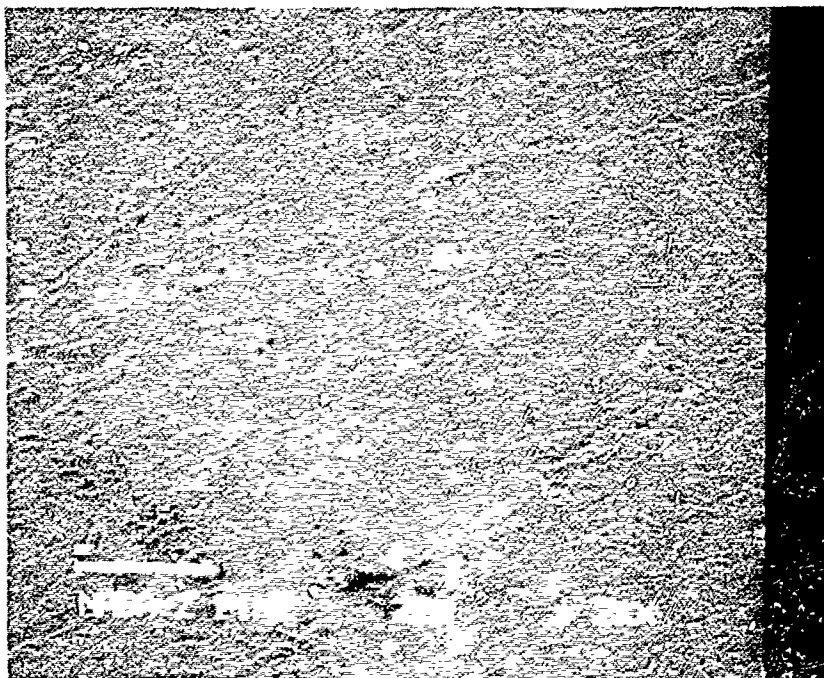


After

Figure 49. Addition of 2000 ppm Water to Research Grade Propane Produced a Heavily Tarnished NASA-Z Coupon in Test 112

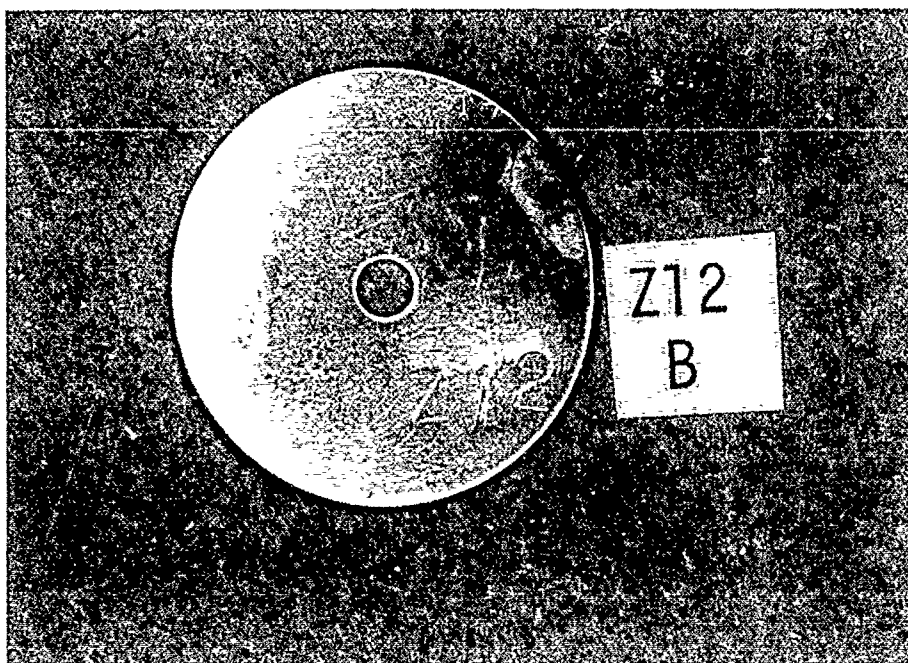


Before



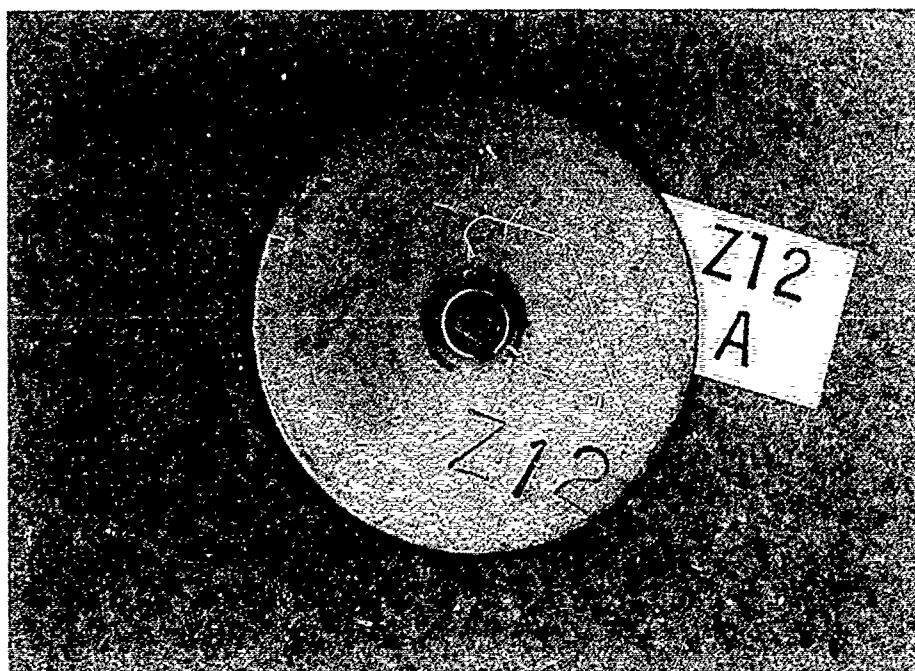
After

Figure 50. Even at High Magnification, It Was Difficult to Discern the Affect of Research Grade Propane Plus 2000 ppm Water on NASA-Z (Static Test 112)



Before

Color: Bright Copper



After

Color: Dark Grey

Figure 51. Propane Plus 94 ppm Sulfur as Methyl Mercaptan Heavily Discolored the Surface of NASA-Z in Static Test 113

### 3.4, Propane Test Results (cont.)

- (1) RG propane forms a very minor deposit on the NASA-Z and Amzirc at 650 F and 3500 psig.
- (2) Addition of 200 ppm water to the propane increases the deposit formation.
- (3) Addition of 2% (by volume) propylene did not affect the test results.
- (4) Addition of 94 ppm  $\text{CH}_3\text{SH}$  produces  $\text{Cu}_2\text{S}$  on the Cu specimen.
- (5) Ethane was formed, but carbon deposition was not observed.

#### 3.4.2 Dynamic Propane Tests (Task 1.2.4)

A series of six dynamic tests was conducted with propane in the Aerojet Carbothermal Test Facility. The objective of these tests was to investigate the compatibility of propane with copper chamber liner materials at conditions simulating those anticipated in the cooling channels of regeneratively cooled  $\text{LO}_2$ /hydrocarbon booster engines. Table 16 summarizes the tests which were conducted.

Test P101 was conducted for a total of 2039 sec using propane and a NASA-Z test specimen (Z23). The primary objective of this test was to checkout the facility with propane at nominal pressure and temperature conditions. A steady state wall temperature of 640 F was maintained at a steady-state heat flux of  $12.5 \text{ Btu/in.}^2\text{-s}$ . The average fuel velocity through the channel was 150 ft/s, and the propane was subcooled to -170 F prior to entering the test channel. Analysis of the run data showed no evidence of reaction during the test, i.e., neither the heat transfer coefficient measured between the channel wall and the coolant nor the pressure drop through the specimen changed during the test.

Figure 52 documents the visual appearance of the NASA-Z specimen after the test. Powdery black deposits were seen in the channel. More dramatic was the discoloration of the filter downstream of the test specimen, which was distinctly blackened with a similar powdery substance.

TABLE 16

## SUMMARY OF PROPANE DYNAMIC TEST CONDITIONS

Test Number	Specimen Matl (ID #)	Duration (sec)	Max T <sub>Wall</sub> (F)	Coolant Side		Additive
				Max Heat Flux (Btu/in. <sup>2</sup> -sec)	Velocity (fps)	
P101	NASA-Z (Z23)	2039	640	12.5	150	None
P102	Amzirc (A20)	3098	710	25.1	210	None
P103	Amzirc (A21)	1394	780	23.1	190	None
P104	NASA-Z (Z20)	3639	806	21.5	185	None
P105	NASA-Z (Z21)	1927	865	20.4	125	None
P106	NASA-Z (Z22)	2229	626	16.5	65	None

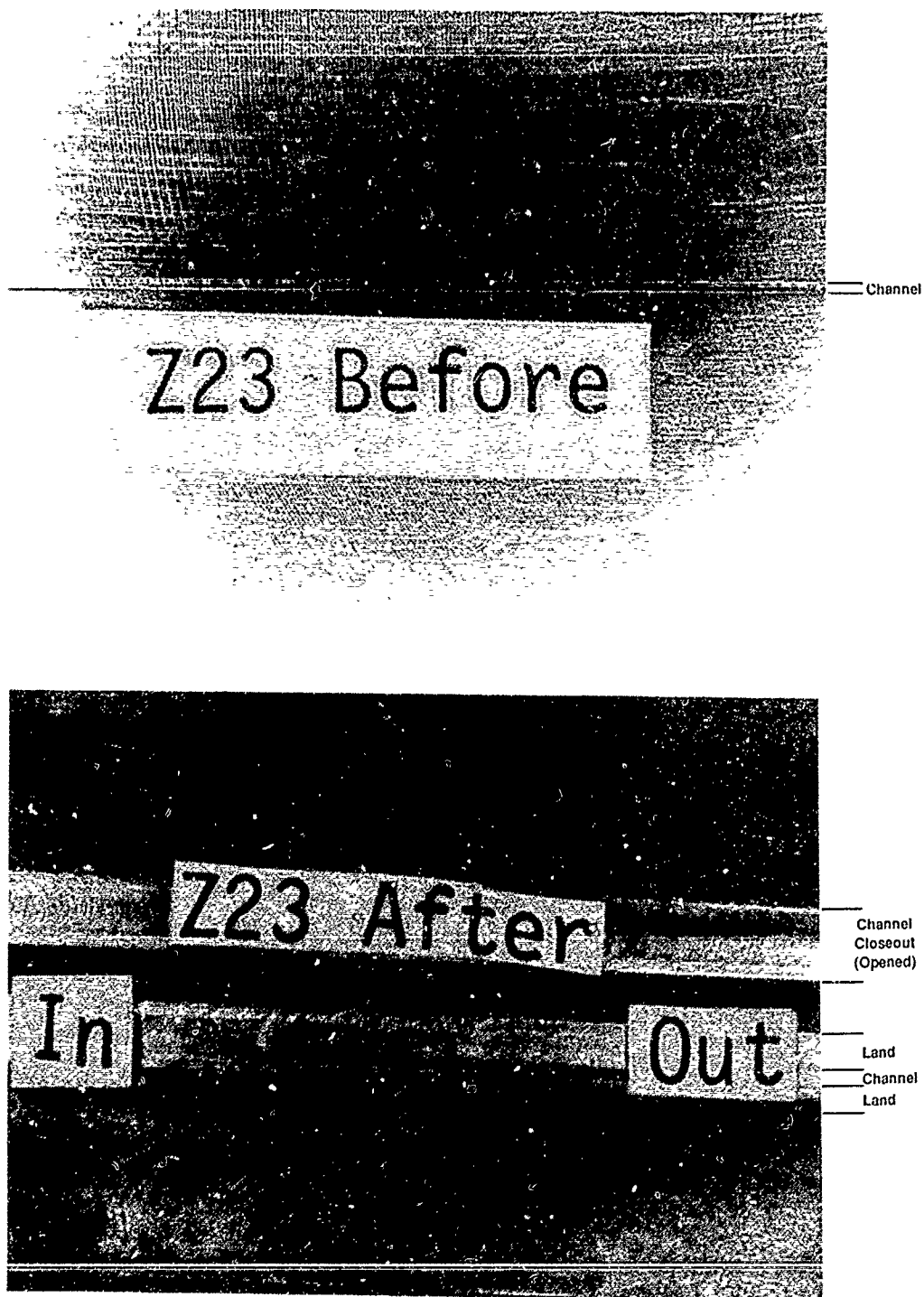


Figure 52. Propane Specimen After 2000 sec at  $T_{\text{wall}} = 640^{\circ}\text{F}$  (Test P101) Shows Blackening of the Channel

### 3.4, Propane Test Results (cont.)

Posttest SEM analysis of the specimen showed the black scale in the channel consisted of many small, round nodes of material (Figure 53). EDS analysis of this scale showed the presence of Cu and S. The atomic ratio of copper to sulfur was almost exactly 2 to 1, indicating the formation of  $\text{Cu}_2\text{S}$ . No carbon or oxygen was detected by EDS analysis.

Test P102 was conducted for a total of 3098 sec using propane and Amzirc test specimen (A20). The primary objective of this test was to operate propane at a higher wall temperature to determine whether this would lead to heavier deposition in the channel and an impact on the heat transfer or pressure drop of the channel. A steady state wall temperature of 710 F was maintained at a steady-state heat flux of 25.1 Btu/in.<sup>2</sup>-s. The average fuel velocity through the channel was 210 ft/s, and the propane was subcooled to -100 F prior to entering the test channel.

Again, no degradation of the channel performance could be detected during the run. Posttest inspection showed the channel to be similarly discolored to that seen in Test P101. As in the previous test, the downstream filter showed more evidence of deposition than did the channel of the specimen. Figure 54 shows photographs of the upstream and downstream filters after this test.

Test P103 was conducted for a total of 1394 sec using propane and an Amzirc test specimen (A21). The intent of this test was to operate at higher wall temperature, as Tests P101 and P102 had not produced conditions which substantially affected the performance of the test specimen. The maximum wall temperature during this test was 780 F. A heat flux of 23.1 Btu/in.<sup>2</sup>-s was attained. Unfortunately, the test was halted prematurely due to operator error during the changeover from operation in a recirculating mode (which is done during heat up and cool down of the test section) to a once-through mode of operation.

The channel and downstream filter again showed discoloration similar to that discussed in the previous two tests. However, because steady state conditions were not established for this test, no conclusions were drawn about the heat transfer and pressure drop performance of the specimen.

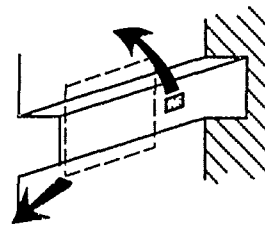
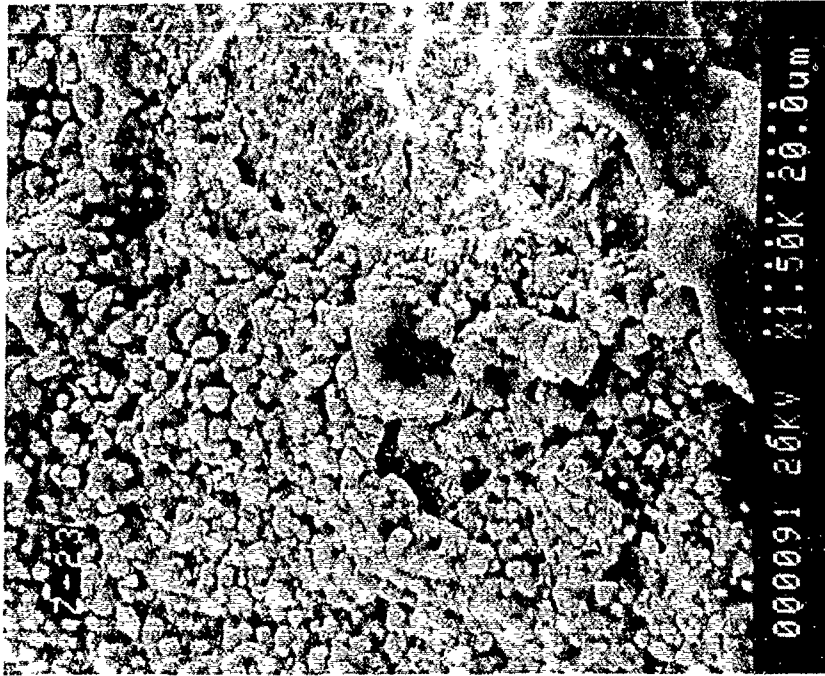
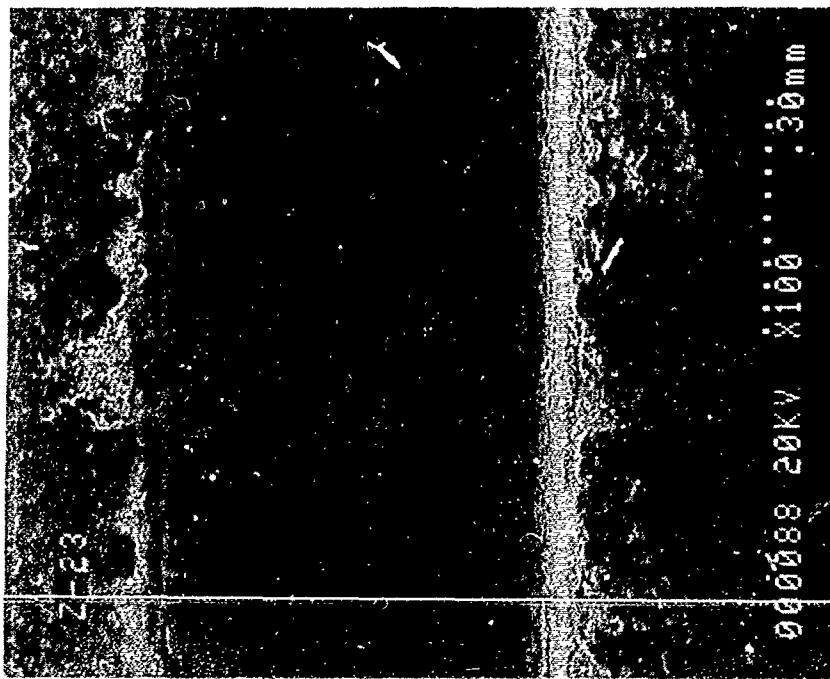


Figure 53. SEM Photos of Propane Specimen After 2000 sec at  $T_{wall} = 640^{\circ}\text{F}$  (Test P101). Scale in Channel Consists of Many Small Nodes of Material. EDS Analysis Shows Only Copper and Sulfur. Scale is Cuprous Sulfide,  $\text{Cu}_2\text{S}$

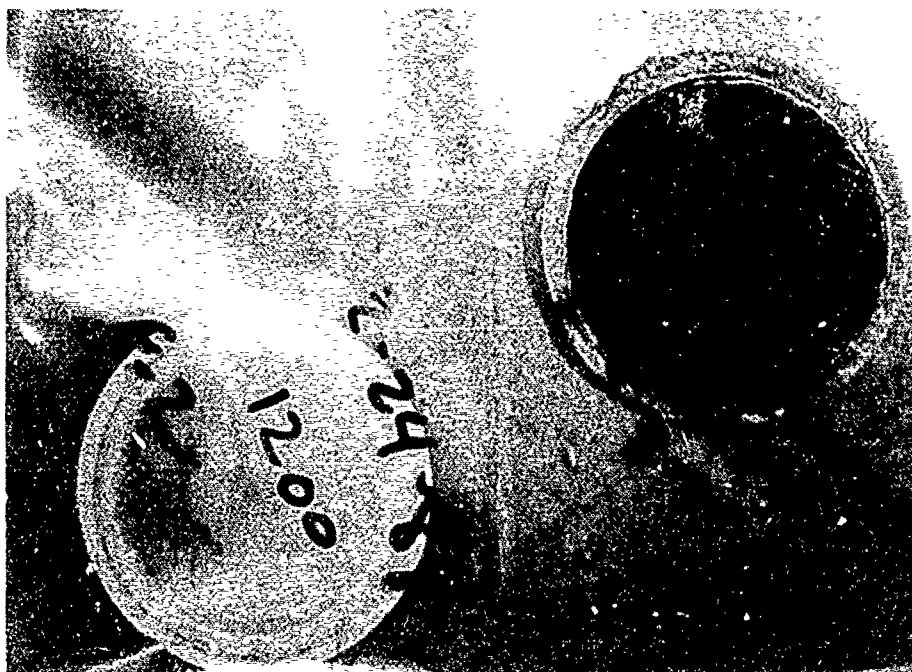


Figure 54. Photos of Upstream (L) and Downstream (R) Filters After Test P102.  
Note Heavy Black Discoloration of Downstream Filter

### 3.4, Propane Test Results (cont.)

Test P104 was conducted for a total of 3639 sec using propane and a NASA-Z test specimen (Z20). The primary objective of this test was to repeat the conditions achieved in the previous test, but this time at steady state conditions. A steady state wall temperature of 806 F was maintained at a steady-state heat flux of 21.5 Btu/in.<sup>2</sup>-s. The average fuel velocity through the channel was 185 ft/s. The propane was subcooled to -130 F prior to entering the test channel.

No degradation of the channel performance could be detected during the run. As seen in Figure 55, posttest inspection showed the channel to be heavily discolored — more so than in the previous testing done at lower wall temperatures. The downstream filter also showed more evidence of deposition than in previous tests. However, there was no evidence that the powdery deposits were impacting the flow or heat transfer through the specimen.

A survey was made of the earlier UTRC and Aerojet propane data to determine why UTRC had reported a significant degradation in heat transfer performance at the same wall temperatures while we had not yet seen the same phenomenon. Two operating parameters were found to be different between the current tests and earlier test programs with propane. The first was subcooling the propane. In tests P101 through P104, the propane had been chilled to between -100 and -170 F prior to its entrance into the test channel. Previous experimentors had typically tested with propane entering at ambient temperature, though UTRC had conducted one test and reported that subcooling the propane reduced the amount of carbon deposits found in the test section by two orders of magnitude. The second important operating parameter was fuel velocity. Tests P101 through P104 were operated at mean velocities between 150 and 210 ft/s. Previous testing had been done at typical velocities between 50 and 100 ft/s.

The objective of the next two tests was to investigate whether these two parameters — fuel temperature and fuel velocity — could impact the results of the current testing. Test P105 was conducted for a total of 1927 sec using propane and NASA-Z test specimen (Z21). The primary objective of this test was to operate without subcooling the propane to determine if this could lead to a degradation in the heat transfer or pressure drop of the specimen. A steady state wall temperature of 865 F was

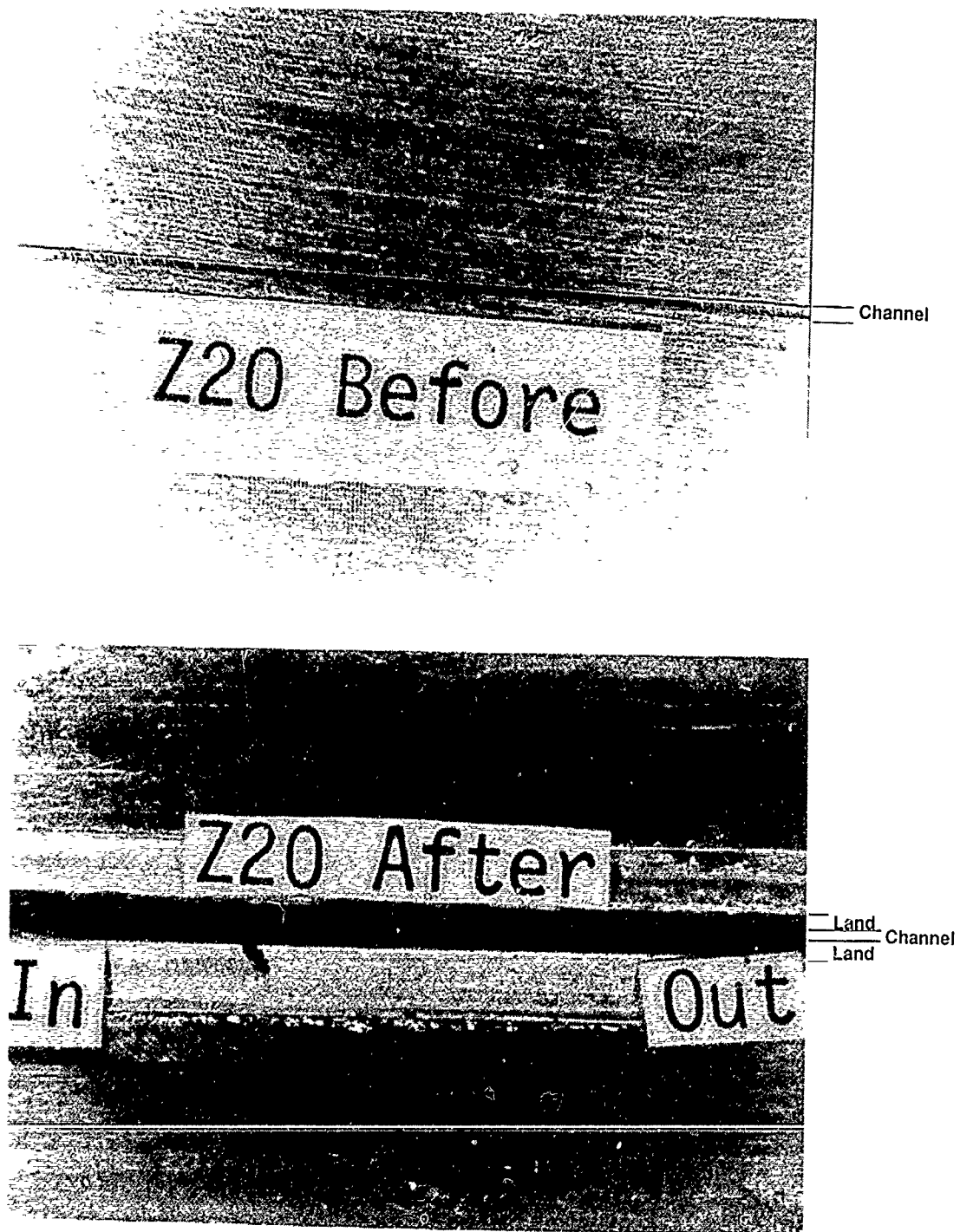


Figure 55. Specimen After Operation With Propane at  $T_{\text{wall}} = 806^{\circ}\text{F}$  (Test P104) Shows More Discoloration. Still, No Degradation in Heat Transfer or Flow Performance

### 3.4, Propane Test Results (cont.)

maintained at a steady-state heat flux of 20.4 Btu/in.<sup>2</sup>-s. The average fuel velocity through the channel was 125 ft/s.

As seen in Figures 56 and 57, a dramatic affect on both the heat transfer and the pressure drop of the channel was produced in this test. The posttest appearance of the specimen was also markedly different from that seen in previous tests using subcooled propane. The deposit formed in the channel was much more massive and tenacious. Figure 58 shows photos from the SEM examination conducted after conclusion of the test series. EDS analysis of the material found in the channel showed the deposit to be only copper and sulfur. Again, no carbon or oxygen was evident. The upstream and downstream filters were similar in appearance to those taken from previous tests. The upstream filter was essentially clean, and the downstream filter was blackened by a powdery substance.

Subcooling the propane, then, did have a beneficial affect on the performance of the cooling channel and in limiting the amount of deposition in the channel.

Test P106 was conducted for a total of 2229 sec using propane and a NASA-Z test specimen (Z22). The primary objective of this test was to operate at a lower fuel velocity through the channel to determine if this could lead to a degradation in the heat transfer or pressure drop of the specimen. A steady state wall temperature of 626 F was maintained at a steady state heat flux of 16.5 Btu/in.<sup>2</sup>-s. The average fuel velocity through the channel was 65 ft/s.

As in Test P105, a dramatic degradation of both the heat transfer and pressure drop performance of the specimen was observed in this test. Posttest inspection of the specimen again showed evidence of heavy deposition in the channel. Figure 59 presents SEM photos of the specimen which show the channel to be bridged by a black deposit. The bridge was hollow and holes could be poked through it easily. Figure 60 also shows a high magnification view of the material in which the nodal shape of the material can be seen. Again, EDS analysis showed copper and sulfur only.

At the conclusion of the propane test series, further analysis of the IG propane was done in an attempt to determine the source of sulfur which appeared in

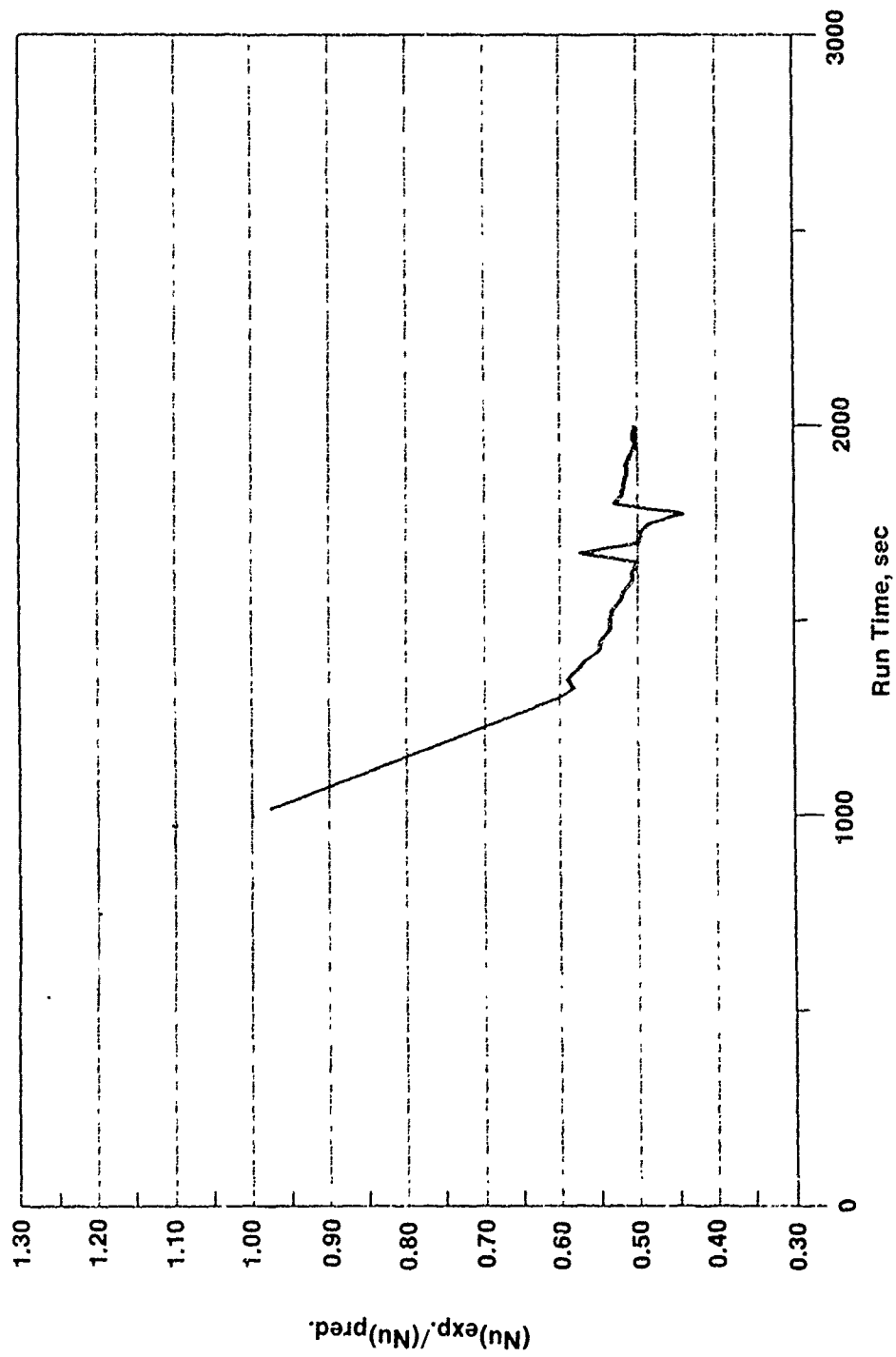


Figure 56. Heat Transfer Performance Degradation Apparent During Operation With Uncooled Propane (Test P105)

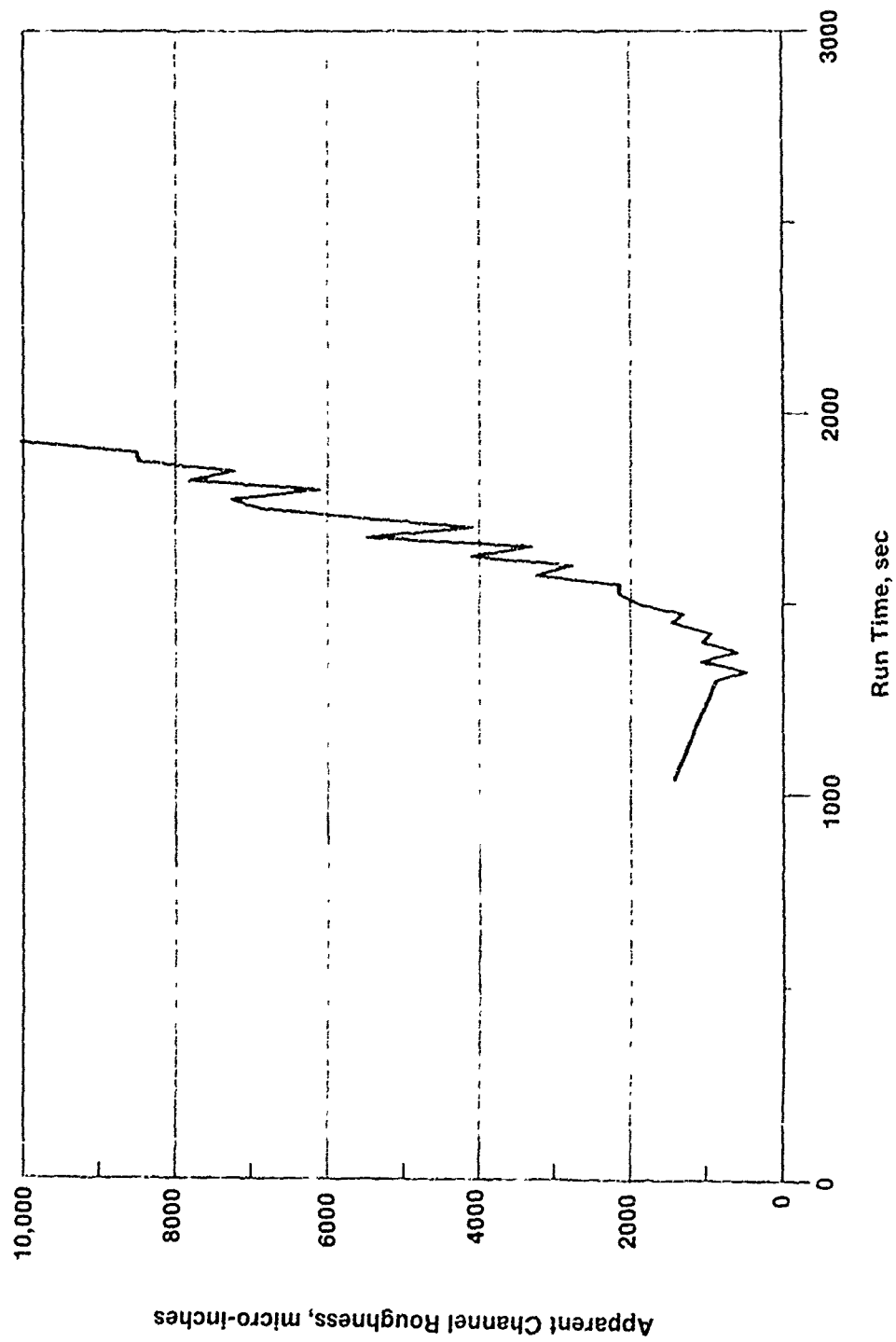


Figure 57. Flow Performance Degradation Apparent During Operation With Uncooled Propane (Test P105).

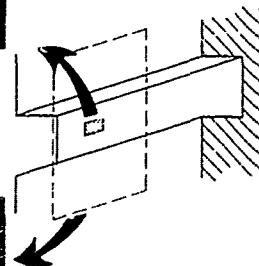
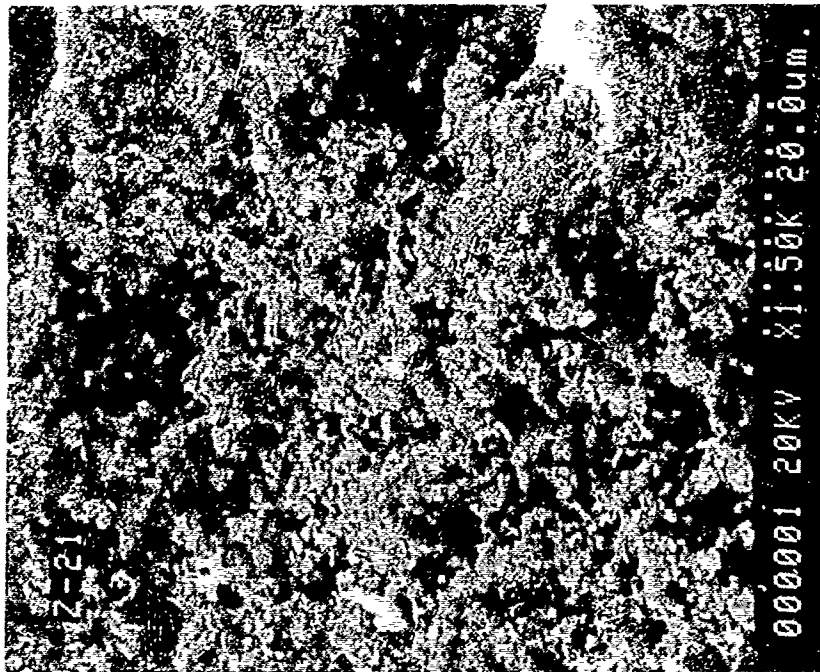


Figure 58. SEM Photos Show Complete Blockage of Channel After Operation With Uncooled Propane (Test P105)

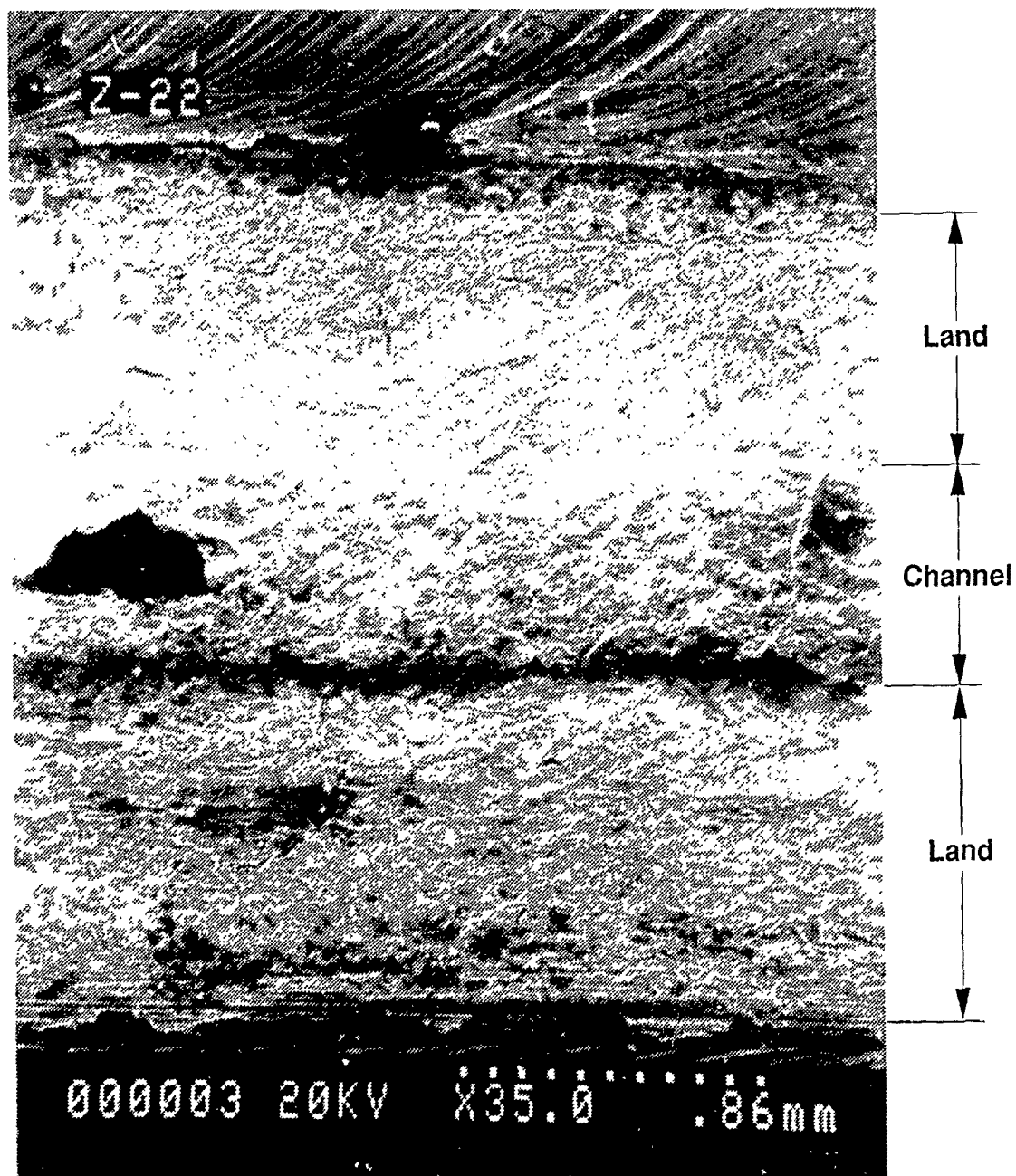


Figure 59. SEM Photo Shows Material Which Bridged Channel During Run Using Sub-Cooled Propane at Low Velocity (Test P106)



Figure 60. SEM Shows Channel Surface After Test With Sub-Cooled Propane at Low Velocity (Test P106). Nodes of Material are  $\text{Cu}_2\text{S}$

### 3.4, Propane Test Results (cont.)

each of the six tests. A cylinder of the IG propane was shipped to Dr. Alan Bandy of Drexel University. Analysis was conducted for  $\text{CH}_3\text{SH}$ ,  $\text{COS}$ , and  $\text{H}_2\text{S}$  by gas chromatography with flame photometric detection. None was found in analysis of the gas phase. Calibration of the instrumentation by standard addition to butane samples demonstrated a detection limit of 50 ppb by volume of each of the sulfur compounds.

Thus, it is still uncertain where the sulfur which affected these tests originated. The apparent increase in the sulfur corrosion observed during the propane test series indicates it was not a remnant of the sulfur contaminants intentionally introduced in previous dynamic tests with methane. This hypothesis is further refuted by the conduct of dynamic test M112, which demonstrated our ability to clean the test apparatus of sulfur contamination completely. A more promising explanation appears to be that the gas which was analyzed was not representative of the propane actually used in the conduct of these dynamic tests because either the particular cylinder shipped for analysis was not representative of the propane used in the tests or the liquid phase of the propane contained very much more sulfur than the gas phase.

A review of all the on-line data from the propane dynamic tests and all the posttest metallographic examinations of the specimen led to the following conclusions:

- 1) All of the propane dynamic tests results were influenced by sulfur corrosion of the test channels. The source of the sulfur contamination was not definitively isolated, but was likely from the IG propane used to conduct the test series.
- 2) Sub-cooling the propane from 70 F to -100 F prior to entering the test channel significantly reduced the formation of corrosion products in the channel. This is consistent with trends of test results reported earlier by UTRC.
- 3) Reducing the velocity of the propane through the test channel from 200 to 65 ft/sec significantly increased the formation of corrosion products in the channel. This is also consistent with trends reported by previous experimenters.

#### 4.0 TASK 2—PROTECTIVE MEASURES DEVELOPMENT AND EVALUATION

Task 1 established that the dominant corrosive process which occurs between hydrocarbon fuels and candidate copper-based chamber liner materials is a result of trace sulfur impurities in the hydrocarbon fuels which react with the copper liner material. The objective of Task 2 was to develop and evaluate protective measures against the corrosive process defined in Task 1. The protective measure chosen was the application of metallic coatings to the copper surfaces of the cooling channels. To be effective, the coating materials chosen must provide resistance to corrosion by sulfur compounds at the temperature and pressure anticipated in cooling channel operation. This was established for a number of candidate materials through a literature search of the chemistry of elemental materials (Task 2.1), and was demonstrated in a series of Static Tests (Task 2.2). Secondly, the materials chosen must be deposited into small, high aspect ratio cooling channels and must be durable enough to bond onto the cooling channel surfaces without spalling or cracking at high temperature while high velocity coolant is forced through the channel. This was demonstrated through a series of Dynamic Tests (Task 2.3). This section of the report discusses the results from Task 2.

##### 4.1 TASK 2.1—CANDIDATE MATERIAL SELECTION

The prime requirement for the initial selection of protective metallic coatings for copper alloys is resistance to attack by sulfur-containing compounds which may be present in hydrocarbon fuels. In the initial selection process, it was assumed that an adequate manufacturing process exists (or can be developed) for coating copper cooling channels with the candidate metal. This assumption was verified by discussions with coatings vendors prior to final selection of the coating materials.

Close coefficient of thermal expansion (CTE) match between the copper alloy and the metallic coating and high thermal conductivity (TC) for the metallic coating are important selection requirements as well. Of these, CTE match is more important than high TC, as the coating is thin enough (approximately 0.1 mil) to avoid a significant temperature gradient. Table 17 shows CTE and TC data for ten of the most promising elements. Copper is shown for comparison.

A survey of metals was made to identify metals with sufficient chemical resistance to sulfur and divalent sulfur compounds to make them suitable as protective

TABLE 17

PHYSICAL PROPERTIES OF CANDIDATE METALS

	<u>Element</u>	<u>CTE (X 10<sup>6</sup>/C)</u>	<u>TC (W/CM/K)</u>	<u>MP (C)</u>
1.	Copper	16.6	4.03	1084.5
2.	Gold	14.2	3.19	1063
3.	Platinum	9.0	0.717	1770
4.	Niobium	7.0	0.533	2477
5.	Tantalum	6.5	0.574	2985
6.	Rhenium	6.1	0.486	3180
7.	Iridium	6.0	1.48	2454
8.	Zirconium	6.0	0.233	1852
9.	Hafnium	6.0	0.232	2222
10.	Nickel	13.0	0.941	1455

#### 4.1, Task 2.1—Candidate Material Selection (cont.)

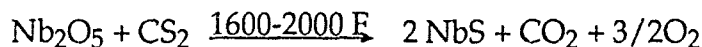
coatings for hot (up to 1000 F) copper exposed to a hydrocarbon fuel containing trace amounts of these materials. A summary of this survey follows.

##### Platinum

Platinum forms two sulfides, PtS and Pt<sub>2</sub>S<sub>3</sub>. These compounds are formed by the action of sulfur on the free metal at elevated temperatures ( $\geq 2200$  F). Platinum is slowly attacked by hydrogen sulfide at 750 F and above. Platinum does not form carbides.

##### Niobium

Niobium forms two sulfides, NbS and Nb<sub>2</sub>S<sub>3</sub>. These compounds are not formed directly from the element, but result from the reaction of the pentoxide with carbon disulfide and hydrogen sulfide.



Niobium reacts with hydrocarbons at 2200 to 2600 F to form carbides.

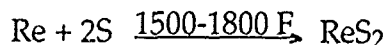
##### Tantalum

There are two known sulfides of tantalum, TaS and Ta<sub>2</sub>S<sub>4</sub>. These sulfides are formed from the pentoxide as described for niobium.

Like niobium, tantalum can form carbides by reaction with hydrocarbons at high temperature ( $\geq 2400$  F).

##### Rhenium

Rhenium forms two sulfides, Re<sub>2</sub>S<sub>7</sub> and ReS<sub>2</sub>. Re<sub>2</sub>S<sub>7</sub> decomposes to ReS<sub>2</sub> above 1500 F. ReS<sub>2</sub> can be formed directly from Re only at high temperature.



Rhenium does not form carbides.

#### 4.1, Task 2.1—Candidate Material Selection (cont.)

##### Iridium

Iridium forms two sulfides, IrS and IrS<sub>2</sub>. These compounds are formed by reaction of iridium oxides with sulfur and hydrogen sulfide at high temperature ( $\geq 2200$  F). The free metal is highly resistant to attack.

Iridium does not form carbides.

##### Zirconium

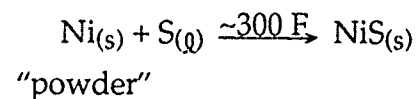
Zirconium is capable of forming a wide variety of sulfides, i.e., ZrS<sub>2</sub>, ZrS<sub>3</sub>, Zr<sub>2</sub>S<sub>3</sub> and Zr<sub>3</sub>S<sub>5</sub>. These compounds are formed by reaction of the hot metal (1220-2400 F) with sulfur vapor or hydrogen sulfide. At lower temperatures, sulfur or sulfur compounds have little effect on the metal. Apparently the sulfur atom is too large to form interstitial solutions with zirconium.

##### Hafnium

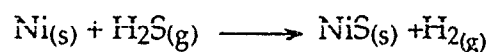
Hafnium is similar in all regards to zirconium.

##### Nickel

Powdered nickel reacts with molten sulfur to form nickel sulfide, NiS.



Nickel is attacked by hydrogen sulfide at elevated temperatures. The grain boundaries are attacked preferentially leading to what is known as "sulfur hardening". The reaction is severe enough that nickel is not recommended for use in a hydrogen sulfide environment above 600 F.



#### 4.1, Task 2.1—Candidate Material Selection (cont.)

Note that molybdenum was eliminated from consideration as it is reported to form  $\text{MoS}_2$  by the action of sulfur vapor on the free metal at 800 F. Tungsten was eliminated from consideration as it is reported to form carbides by reaction with hydrocarbons at 800-1000 F. Titanium was eliminated from consideration as it is reported to be attacked slowly by hydrogen sulfide at room temperature.

#### Tentative Selection of Candidate Protective Metallic Coatings

Based on the critical assumption that suitable fabrication techniques are available for applying these metallic coatings to copper alloys, six metals were recommended for evaluation in Task 2, i.e., gold, platinum, niobium, rhenium, iridium and zirconium. Gold was selected because it appears to have the best combination of chemical inertness, CTE match and TC. Zirconium was selected because it provides the low cost option and appears to resist sulfur attack by a unique mechanism, i.e., apparently the sulfur atom is too large to form interstitial solutions in the zirconium, the first step in the formation of a zirconium sulfide, e.g.,  $\text{ZrS}_2$ . Platinum, niobium, rhenium and iridium were selected because of their apparent chemical inertness and their respective CTE matches (Pt is best), TC (Ir is best), melting points (Re is best) and cost (Nb is lowest).

#### 4.2 TASK 2.2—CHEMISTRY LABORATORY TESTS

Two static tests evaluated the performance of seven materials: gold, zirconium, iridium, platinum, rhenium, niobium, and NASA-Z. Test coupons were cut from thin (1 mil) foils of gold, zirconium, rhenium, platinum, and iridium. Pure niobium coupons were cut from a 40 mil thick sheet, and NASA-Z coupons were made from the 20 mil sheet rolled from the billet of material supplied by NASA-LeRC at the beginning of this program. The NASA-Z coupons were 15/16 in. dia circles with two 1/8 in. holes cut through them to facilitate hanging them on a support stand. All other test coupons were 0.5 in. x 0.75 in. rectangles with a single 1/8 in. hole punched through them.

Each static test was conducted in an environment of UHP methane with 500 ppm of sulfur (by volume). The first test used  $\text{CH}_3\text{SH}$  as the sulfur-containing contaminant, the second used  $\text{H}_2\text{S}$ . The nominal test conditions targeted were identical to the static tests of Task 1, i.e., 650 F at 3000 psig for 30 min. The total duration of each

#### 4.2, Task 2.2—Chemistry Laboratory Tests (cont.)

static test was approximately 2.5 hr, consisting of a 90 min ramp up to temperature, 30 min at nominal test conditions, and a 30 min cool down cycle to 100 F.

Prior to the static tests, each test coupon was degreased, cleaned, rinsed and dried. Scanning electron micrographs were taken of an area on each coupon at 50, 100 and 2000X. The area photographed was marked by a microscopic scratch made in the surface of each coupon, so that the same area could be identified and examined after the tests. Finally, each coupon was weighed to the nearest 0.0001 g on a Mettler balance, placed on a stainless steel support stand, and the stand was inserted into the bomb.

Test M201 tested coupons of the seven candidate materials in a bomb containing UHP methane with 506 ppm (by volume) sulfur as  $\text{CH}_3\text{SH}$ . This environment was established by drawing a vacuum on the bomb, adding 37 mm Hg of  $\text{CH}_3\text{SH}$ , and then pressurizing the bomb to 1217 psia with UHP methane. The bomb was then placed into the oven and the test cycle was started.

During the test, it became apparent that a small leak had developed in the bomb seal. As the temperature increased in the bomb, the pressure did not rise as much as was expected, reaching a maximum of 1938 psia, as opposed to the 2900 psia anticipated. Figure 61 shows the temperature and pressure traces of the test.

After the bomb had been maintained at the nominal test conditions for 30 min, the bomb was removed from the oven, and cooled in air for approximately 10 min, until the temperature reached 500 F. The bomb was then partially submerged in water to cool it more quickly. When the gas temperature inside the bomb reached 100 F, the methane was vented, and the bomb was opened.

Posttest visual inspection of the coupons showed the NASA-Z had developed the characteristic steel grey discoloration resulting from exposure to the sulfur-contaminated methane. The zirconium coupon also showed some slight tarnish during the test. All other materials tested (gold, platinum, iridium, rhenium, and niobium) showed no visible changes had occurred during the test. Photographs of the specimens were taken with a 35 mm camera and with a SEM to document their surface condition.

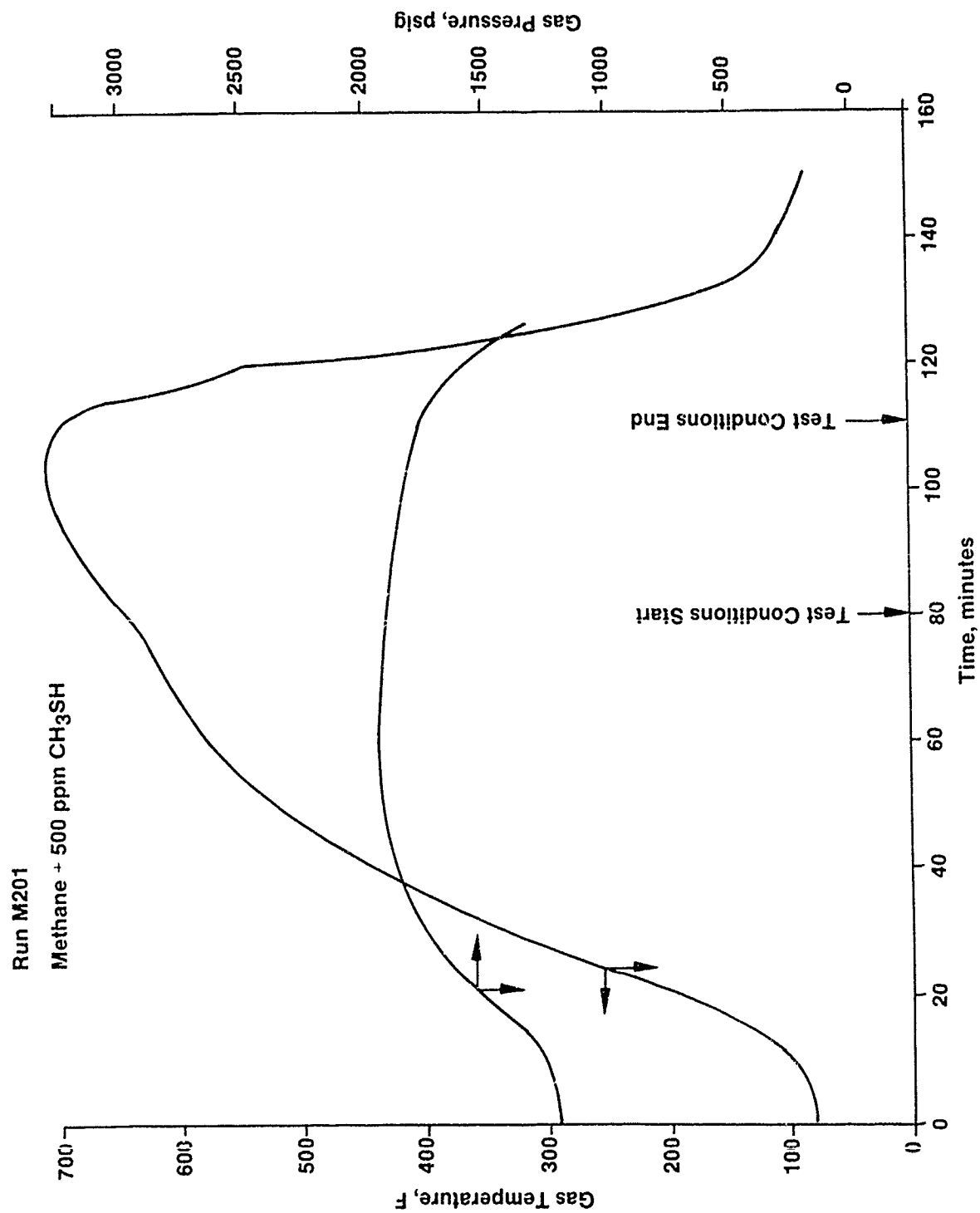


Figure 61. Temperature and Pressure Measurements of Test M201 Indicate Slow Leak in Bomb Seal

#### 4.2, Task 2.2—Chemistry Laboratory Tests (cont.)

Figures 62 and 63 are photographs of the gold specimen taken from Test M201. Figure 62 shows that the specimen was crinkled during the test (the specimen was a very thin, delicate foil), but still appeared shiny and unaffected. Figure 63 shows SEM photographs of the same specimen taken before and after the test. These confirm that the gold was not affected by exposure to methane plus  $\text{CH}_3\text{SH}$  in Test M201.

Figures 64 and 65 are photographs of the zirconium specimen from Test M201. Figure 64 shows that a visible tarnish was formed on the zirconium. However, no evidence of a surface deposit or surface reaction was seen during examination under the SEM, as documented in Figure 65.

Figures 66 and 67 are photographs of the iridium specimen from Test M201. Figure 66 shows that the specimen was not visibly changed during the test. Figure 67 confirms this. Even very small surface features appear identical in the SEM photos taken before and after the test.

The appearance of the gold and iridium are in vivid contrast with the posttest appearance of the NASA-Z coupon, shown in Figures 68 and 69. Figure 68 shows the NASA-Z developed an even grey discoloration during Test M201, and the SEM photographs (Figure 69) show the entire surface has been affected by reaction with the  $\text{CH}_3\text{SH}$  which was added to the bomb.

Table 18 shows the weight of each coupon measured before and after the test. Only the NASA-Z coupon showed a significant weight change, gaining 0.0023 g during the test. Note the iridium coupon decreased by 0.0005 g, but this is probably because the top of the coupon was torn while removing it from the test rack, and the final coupon weight was not valid. The weight of all the other coupons did not change.

Test M202 tested coupons of the seven candidate materials in a bomb containing UHP methane with 497 ppm (by volume) sulfur as  $\text{H}_2\text{S}$ . This environment was established by drawing a vacuum on the bomb, adding 37 mm Hg of  $\text{H}_2\text{S}$ , and then pressurizing the bomb to 1240 psia with UHP methane. The bomb was then placed into the oven and the test cycle was started.



#1 B

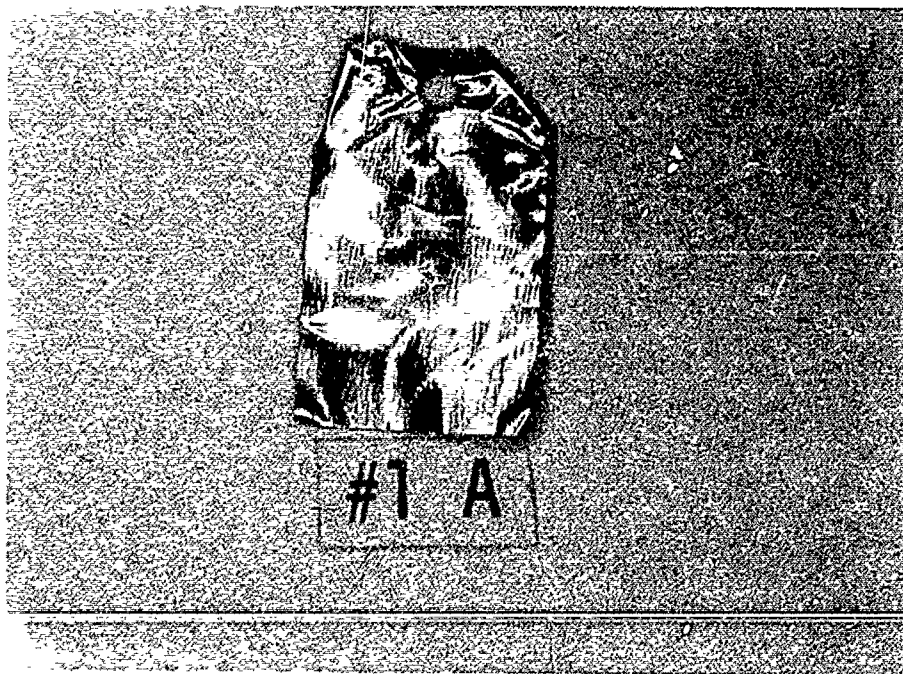
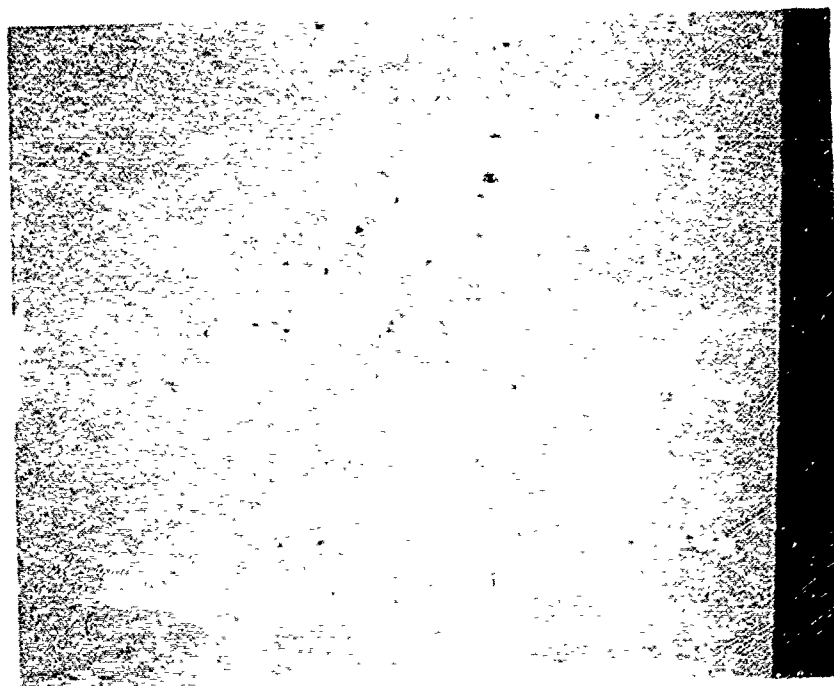
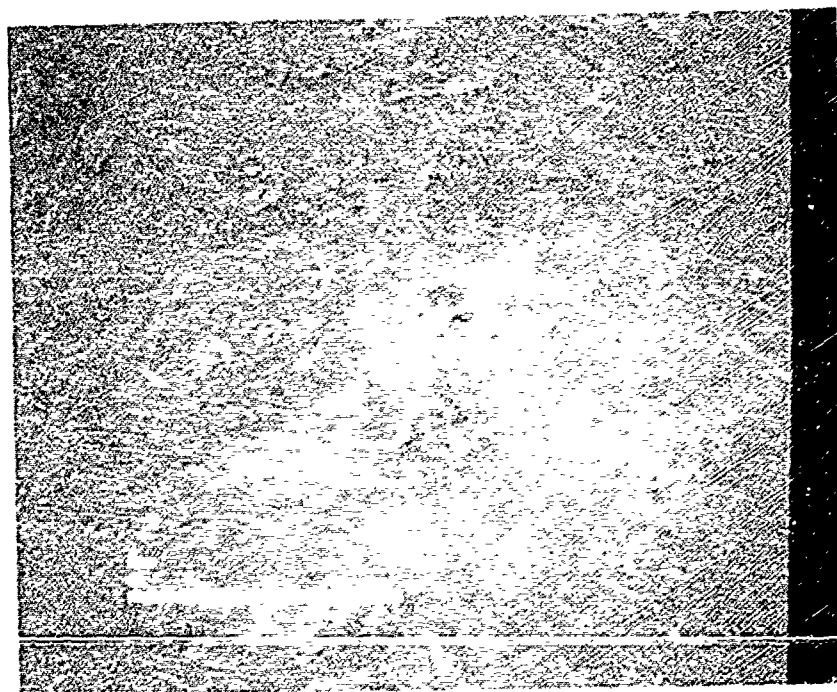


Figure 62. Gold Appeared to Be Unaffected By Exposure to UHP Methane Plus 500 ppm Methyl Mercaptan (Test M201)  
B = Before Test; A = After Test



Gold  
Before  
Test M201  
(400x)



Gold  
After  
Test M201  
(400x)

Figure 63. Gold Showed No Evidence of Reaction With UHP Methane Plus 500 ppm Methyl Mercaptan in Test M201



#4 B

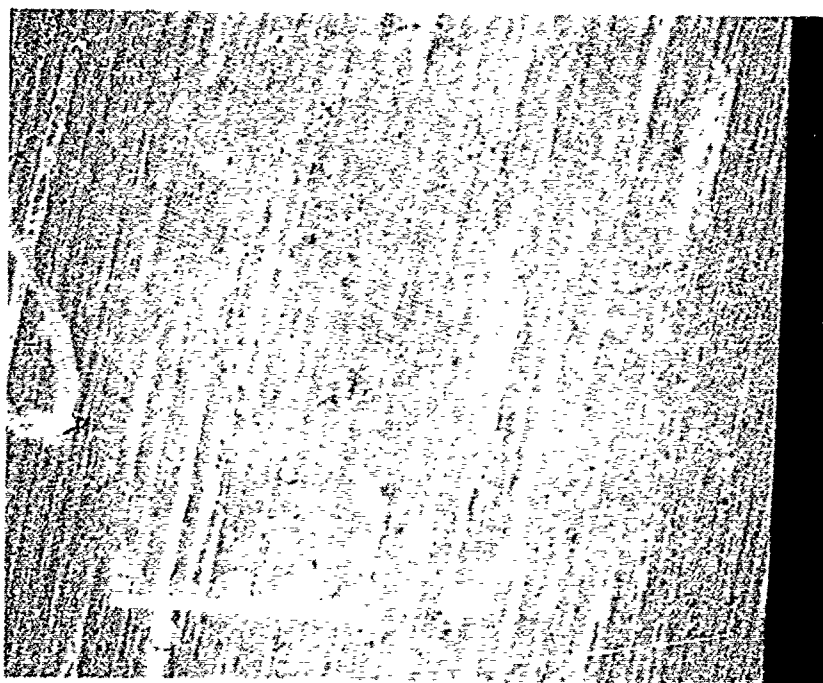


#4 A

Figure 64. Zirconium Developed a Slight Tarnish But No Measureable Weight Change When Exposed to UHP Methane Plus 500 ppm Methyl Mercaptan (M201). B = Before Test; A = After Test

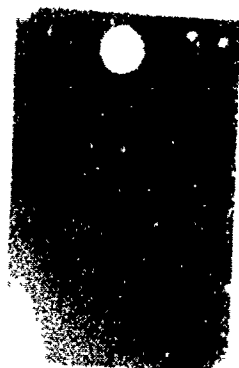


Zirconium  
Before  
Test M201  
(400x)



Zirconium  
After  
Test M201  
(400x)

Figure 65. Though Zirconium Formed a Visible Tarnish, the Surface Looks Unchanged After Test M201



#7 B



#7 A

Figure 66. Iridium Appeared Unaffected By Exposure to UHP Methane Plus 500 ppm Methyl Mercaptan (Test M201)

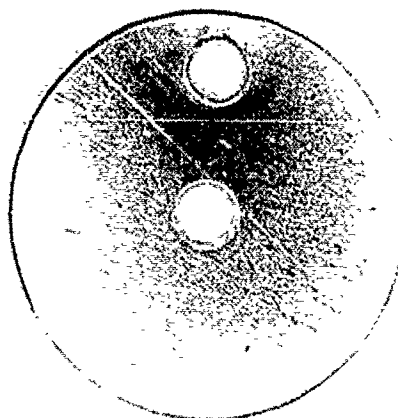


Iridium  
Before  
Test M201  
(400x)

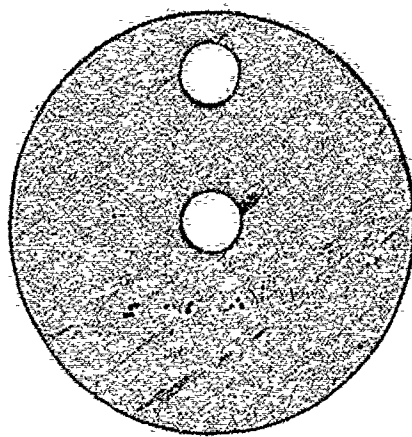


Iridium  
After  
Test M201  
(400x)

Figure 67. Iridium Appeared to Be Unaffected in Test M201

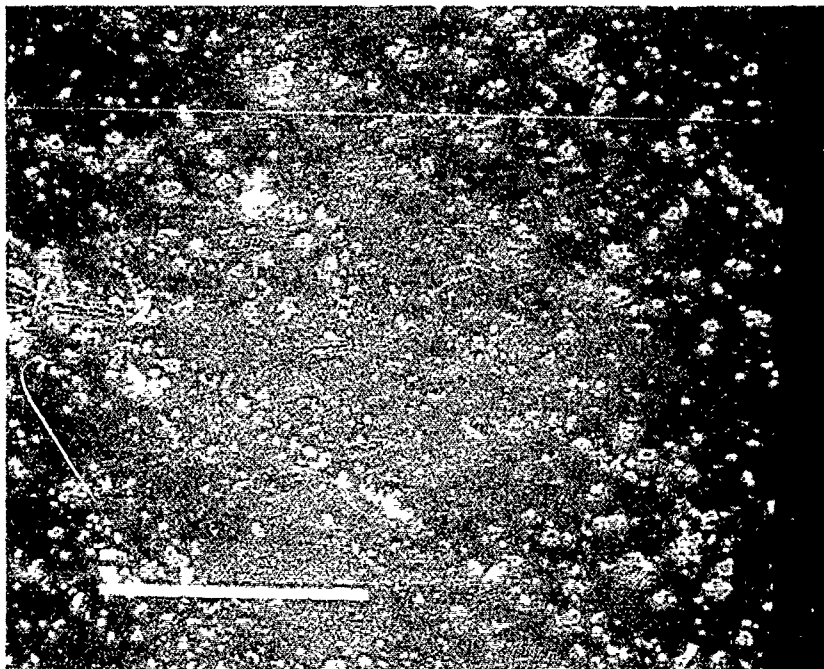


#19 B

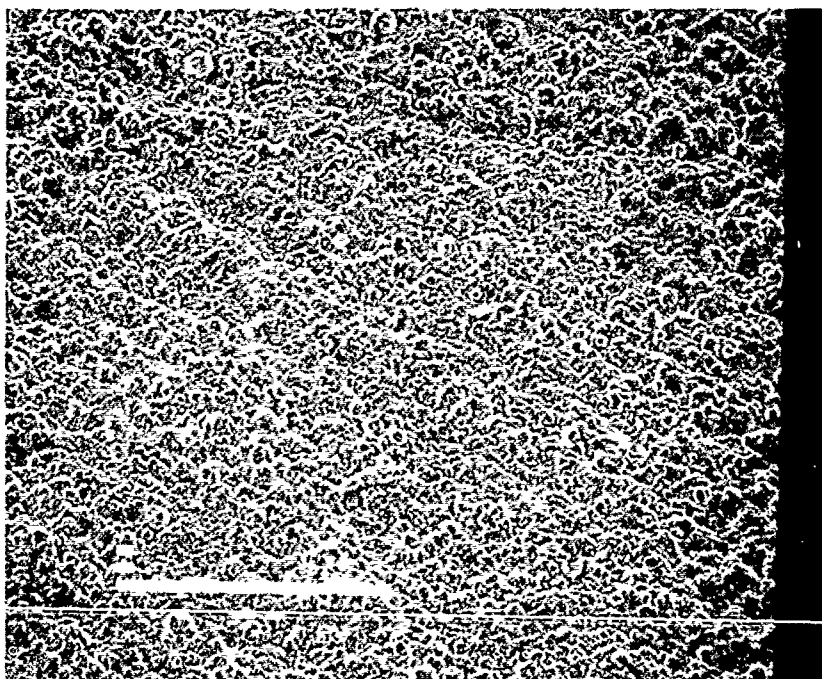


#19 A

Figure 68. NASA-Z Showed Characteristic Grey Discoloration When Exposed to UHP Methane Plus 500 ppm Methyl Mercaptan (Test M201)



NASA-Z  
Before  
Test M201  
(400x)



NASA-Z  
After  
Test M201  
(400x)

Figure 69. A Layer of Copper Sulfide Covered the Surface of NASA-Z After Test M201

TABLE 18  
SUMMARY OF COUPON WEIGHTS

<u>Test M201</u>	<u>Coupon Weight, g</u>		<u>Weight Change, g</u>
	<u>Before</u>	<u>After</u>	
Gold	0.1241	0.1241	0.0000
Zirconium	0.0408	0.0408	0.0000
Iridium	0.1365	0.1360*	-0.0005*
Platinum	0.1528	0.1527	-0.0001
Rhenium	0.0648	0.0647	-0.0001
Niobium	4.7111	4.7112	+0.0001
NASA-Z	1.6718	1.6741	+0.0023
<u>Test M102</u>			
Gold	0.1193	0.1195	+0.0002
Zirconium	0.0429	0.0430	+0.0001
Iridium	0.1394	0.1395	+0.0001
Platinum	0.1485	0.1485	0.0000
Rhenium	0.0647	0.0647	0.0000
Niobium	5.0826	5.0828	+0.0002
NASA-Z	1.6565	1.6614	+0.0049

\*Coupon was torn during removal from bomb. Final weight is too low.

#### 4.2, Task 2.2—Chemistry Laboratory Tests (cont.)

The cause of the leak which occurred during test M201 was eliminated prior to this test, and the pressure and temperature rose as planned. Figure 70 shows the temperature and pressure traces of the test. After the bomb had been maintained at the nominal test conditions of 650 F and 2900 psig for 30 min, the bomb was removed from the oven, and cooled and opened as in the previous test.

Posttest visual inspection of the coupons again showed the NASA-Z had developed the characteristic steel grey discoloration resulting from exposure to sulfur-contaminated methane. The zirconium coupon also showed some slight tarnish during the test. All other materials tested, gold, platinum, iridium, rhenium, and niobium, showed no visible changes had occurred during the test. Again, photographs were taken of each specimen with a 35 mm camera and a SEM.

Figure 71 shows that the appearance of the platinum specimen did not change during Test M202. However, posttest SEM examination revealed one isolated area of reacted material on the platinum specimen, as shown in the photographs of Figures 72 and 73. EDS analysis of this area showed the presence of copper, sulfur, and platinum. EDS analysis of other regions of the specimen did not find any evidence of anything other than platinum. The isolated nature of the area, and the analysis which showed it to contain copper, suggests that the platinum specimen touched the NASA-Z specimen at some point during the test, resulting in a microscopic region of copper contamination on the surface of the platinum specimen.

Figure 74 shows the appearance of rhenium was unaffected during Test M202. SEM examination showed a very minor surface deposit had developed over the entire rhenium specimen, as shown in Figure 75. No analysis was conducted to determine the nature of this deposit.

Figure 76 shows the appearance of niobium was unaffected during Test M202. SEM examination confirmed that there was no evidence of reaction during the test, as documented in Figure 77.

Again, the posttest condition of the NASA-Z specimen exposed in Test M202 offers sharp contrast to the other materials tested. Figure 78 shows the even grey

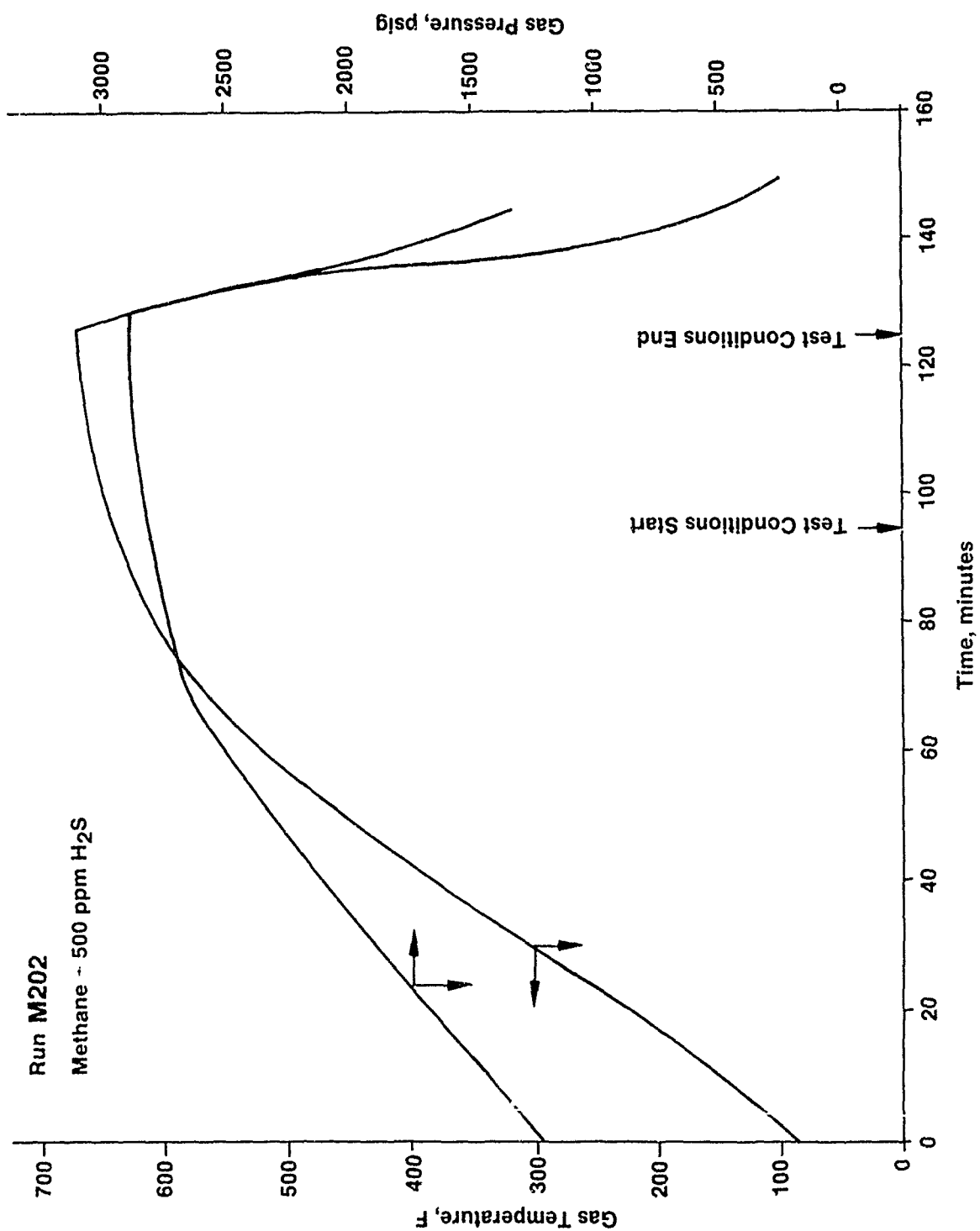


Figure 70. Temperature and Pressure Traces of Static Test M202

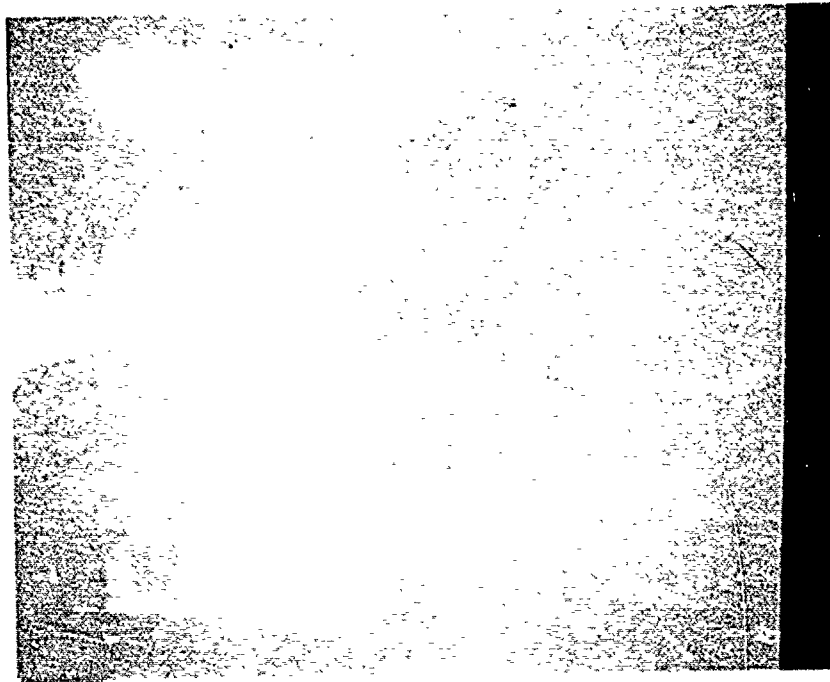


#11 B



#11 A

Figure 71. Platinum Appeared Unaffected When Exposed to UHP Methane Plus 500 ppm Hydrogen Sulfide (Test M202)

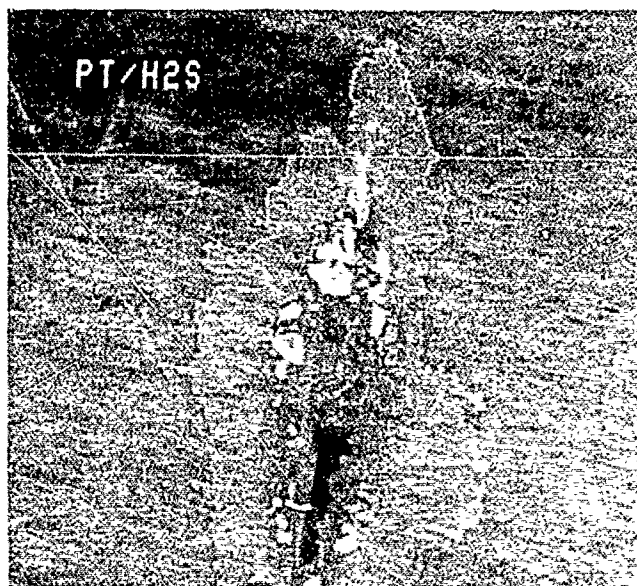


Platinum  
Before  
Test M202  
(400x)



Platinum  
After  
Test M202  
(400x)

Figure 72. Platinum Appeared to Have an Area of Reacted Material in Test M202



Platinum  
Before  
Test M202  
(200x)



Platinum  
After  
Test M202  
(2500x)

Figure 73. Further Inspection and EDX Analysis Showed the Platinum Coupon to Have a Small Region of Copper Sulfide on its Surface



Rhenium  
Before  
Test M202

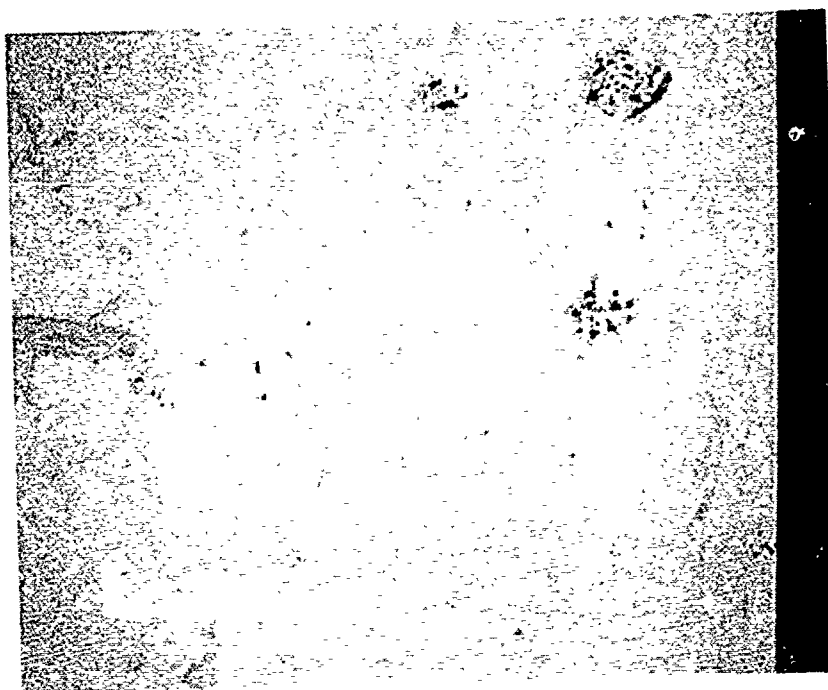
#14 B



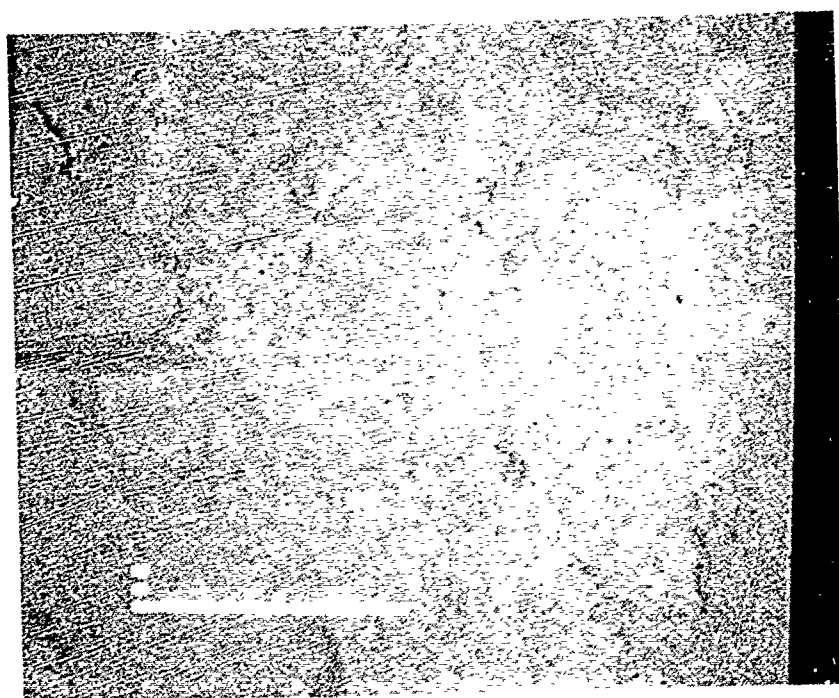
Rhenium  
After  
Test M202

#14 A

Figure 74. The Appearance of Rhenium Did Not Change During Test M202

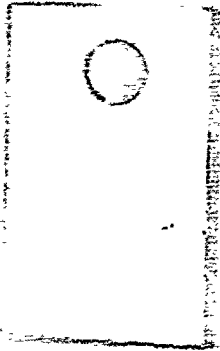


Rhenium  
Before  
Test M202  
(400x)

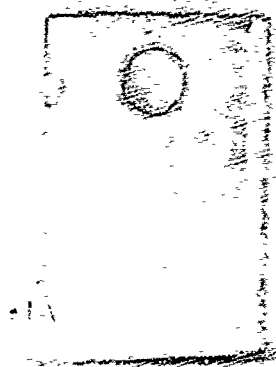


Rhenium  
After  
Test M202  
(400x)

Figure 75. SEM Photos Show a Very Minor Deposit Developed on Rhenium in Test M202

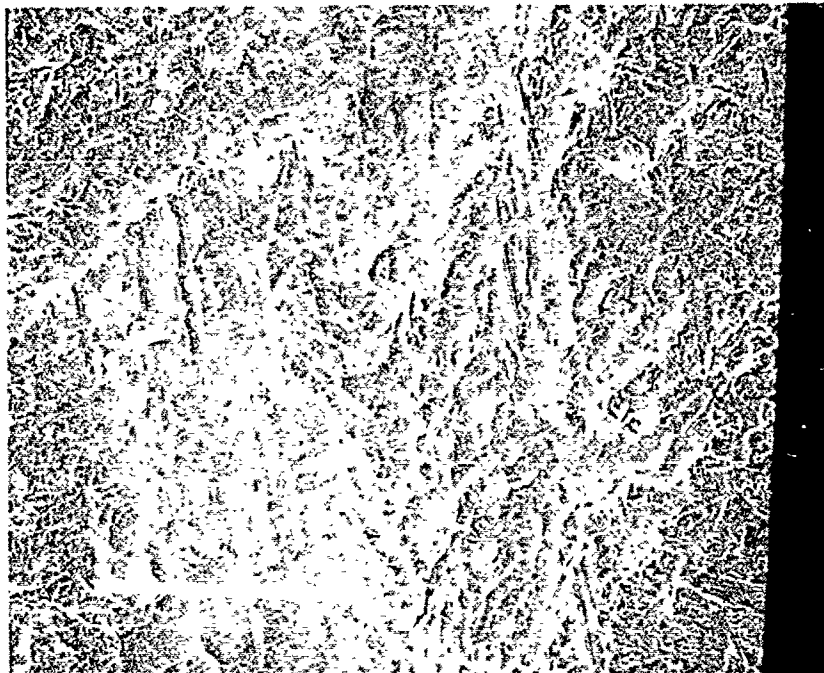


#17 B

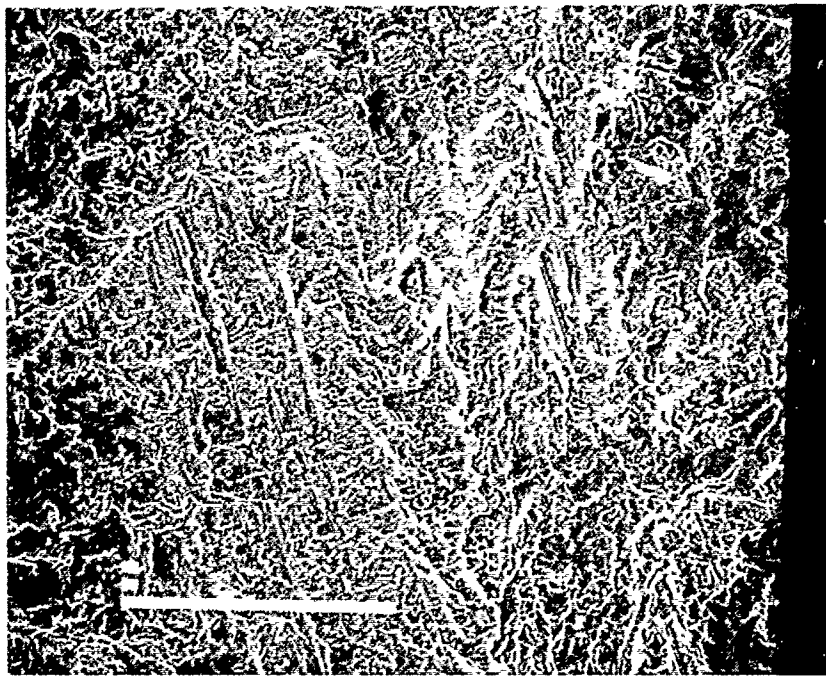


#17 A

Figure 76. Niobium Appeared Unaffected When Exposed to UHP Methane Plus 500 ppm Hydrogen Sulfide (Test M202)

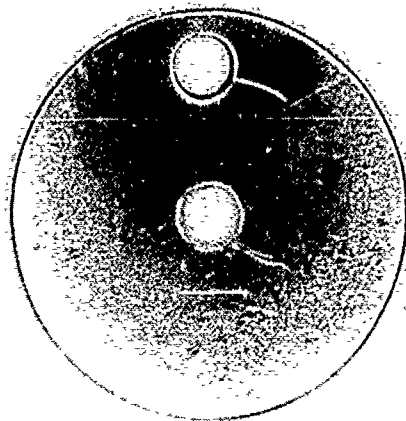


Niobium  
Before  
Test M202  
(400x)

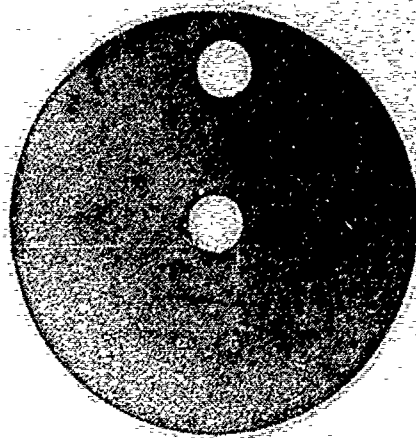


Niobium  
After  
Test M202  
(400x)

Figure 77. Niobium Surface Was Unaffected During Test M202



#20 B



#20 A

Figure 78. Hydrogen Sulfide in Methane (Test M202) Produced the Same Appearance of NASA-Z as Previous Tests With Methyl Mercaptan

#### 4.2, Task 2.2—Chemistry Laboratory Tests (cont.)

discoloration which developed during Test M202. SEM examination (Figure 79) again showed the formation of  $\text{Cu}_2\text{S}$  over the entire surface of the NASA-Z coupon.

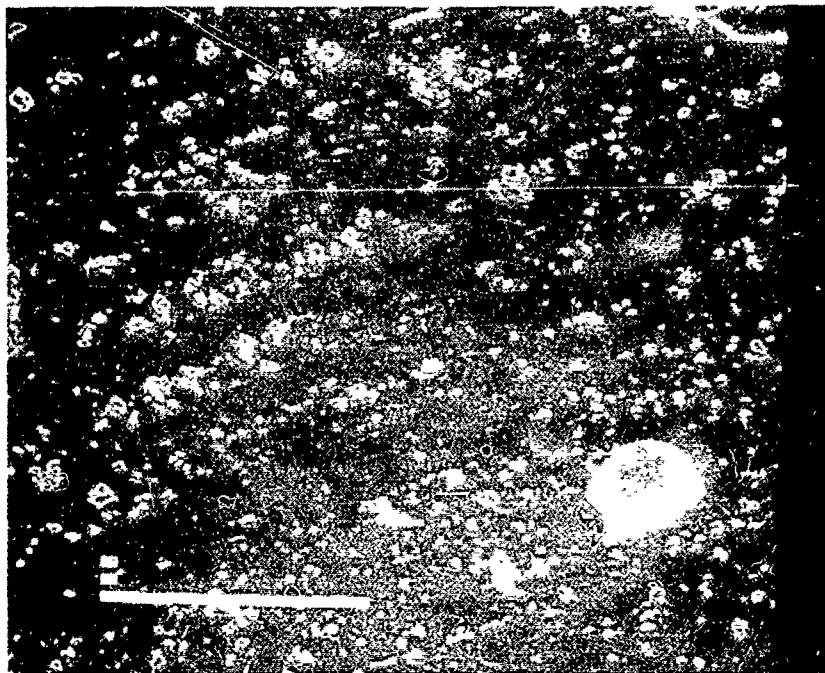
Table 18 shows the weight of each coupon measured before and after the test. Only the NASA-Z coupon showed a significant weight change, gaining 0.0049 g during the test. The weight of all the other coupons did not change.

The Static Tests demonstrated that gold, platinum, iridium and niobium were inert to reaction with sulfur compounds at these temperatures and pressures. Rhenium and zirconium also appeared to withstand the static environment with only minimal change to the surface. A selection of two materials for use in the next phase of the test program was made based on the maturity of the manufacturing processes which existed for the application of these metals to the copper cooling channels. The two metals chosen were gold and platinum, because electrodeposition of these metals onto copper had been demonstrated.

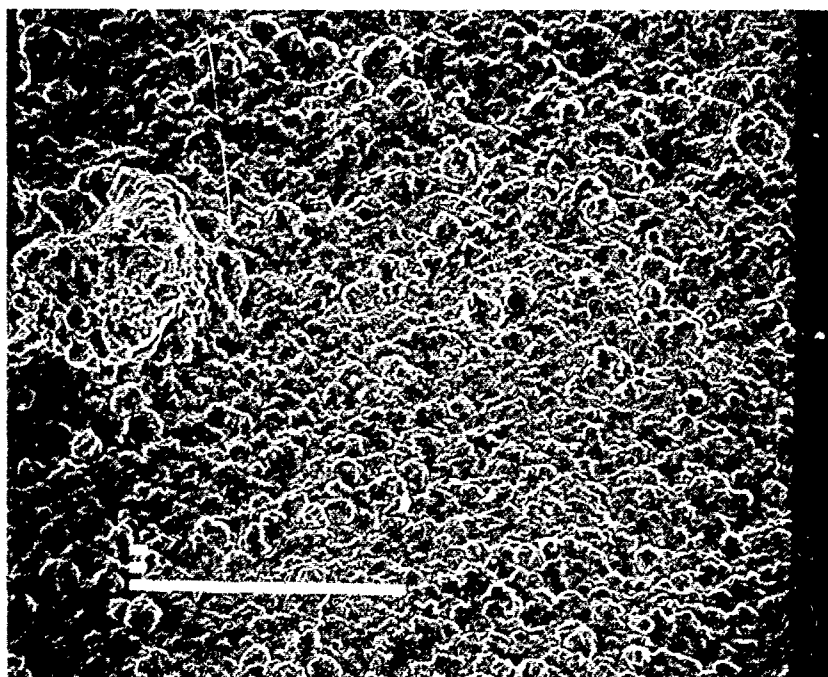
#### 4.3 TASK 2.3—THERMAL SCIENCES LABORATORY TESTS

The next steps in the program were to apply gold and platinum coatings to copper cooling channels and to conduct dynamic tests in the Aerojet Carbothermal Test Facility. The objective of these tests was to demonstrate that coatings could provide corrosion protection from sulfur compounds in methane under realistic service conditions of a regeneratively cooled  $\text{LO}_2$ /methane booster engine.

Two series of dynamic tests were conducted in Task 2. The first series (tests M201 - M206) used specimens with gold and platinum coatings in the channel and an uncoated OFHC closeout. Thus, three sides of the channel were coated, and the fourth side was to serve as a control, demonstrating what would happen to uncoated copper at these conditions. However, corrosion of the uncoated portion of the channel was severe enough to affect the interpretation of test results. It proved to be difficult to determine conclusively the protective ability of the coatings with the presence of the corrosion products. Therefore, a second series of dynamic tests (tests M207 - M208) was conducted with a modified specimen design which eliminated all contact between the fuel and uncoated copper surfaces. The new design replaced the OFHC closeout with a



NASA-Z  
Before  
Test M202  
(400x)



NASA-Z  
After  
Test M202  
(400x)

Figure 79. SEM Photos of NASA-Z Show Formation of Copper Sulfide Over Entire Surface

#### 4.3, Task 2.3—Thermal Sciences Laboratory Tests (cont.)

CRES 304 closeout and fuel inlet/outlet manifold. The other three sides of the channel were protected with gold coatings as before.

All tests were conducted with Technical Grade Methane with between 5 and 10 ppm (by volume) of a sulfur compound. Table 19 summarizes the test conditions in the Task 2 Dynamic Tests.

The dynamic test specimen for tests M201-M206 were machined and stainless inlet and outlet tubes brazed into the ends as in Task 1. Protective metallic coatings of gold and platinum were then applied to selected specimen. The three-sided, open channel and approximately 0.050-in. of land width on either side of the channel were electroplated by dalic plating. Four specimens were coated with gold (with an underlying layer of nickel to serve as a diffusion barrier), and four specimens were coated with platinum (with underlying layers of nickel and gold for protection of the channel while plating with platinum from an acidic plating solution). Figure 80 shows one of the specimens after being coated with nickel and gold.

The coatings were then examined under a SEM. Two purposes were served by this examination. The "before" appearance of each channel was documented, and the examination established that the coatings were free of voids or cracks which extended to the copper substrate. The appearance of the coating showed some variation from specimen to specimen. Representative SEM micrographs of the channel surface is shown in Figure 81. The most prevalent feature of the specimens is the lumpy, uneven appearance of the coating. Subsequent examination of the channels in cross section has shown this to be from a very uneven, lumpy deposition of nickel on the copper. The gold and platinum layers went down relatively smoothly.

After inspection of the channel surfaces, an uncoated OFHC closeout was electron beam welded over the channel at a distance of 0.020-in. outside the coating. One gold coated specimen was sacrificed at this point and sectioned to determine if the welding process had any affect on the condition of the coating.

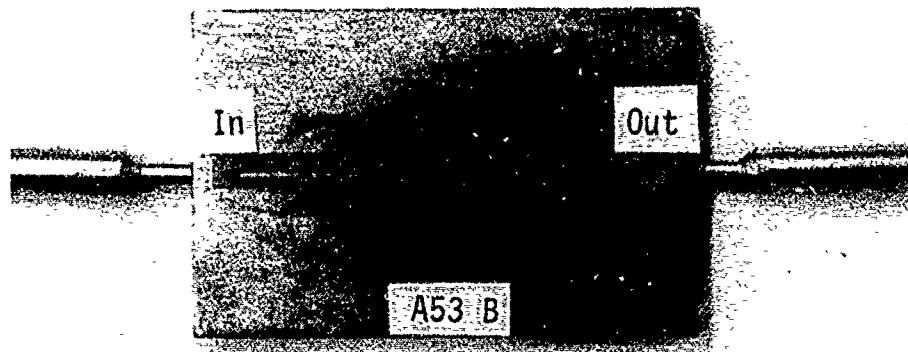
No change in the coating was noted as a result of the welding. However, the post-weld cross section showed a significant variation in the thickness and quality of the coatings from the top to the bottom of the channel, as seen in

TABLE 19

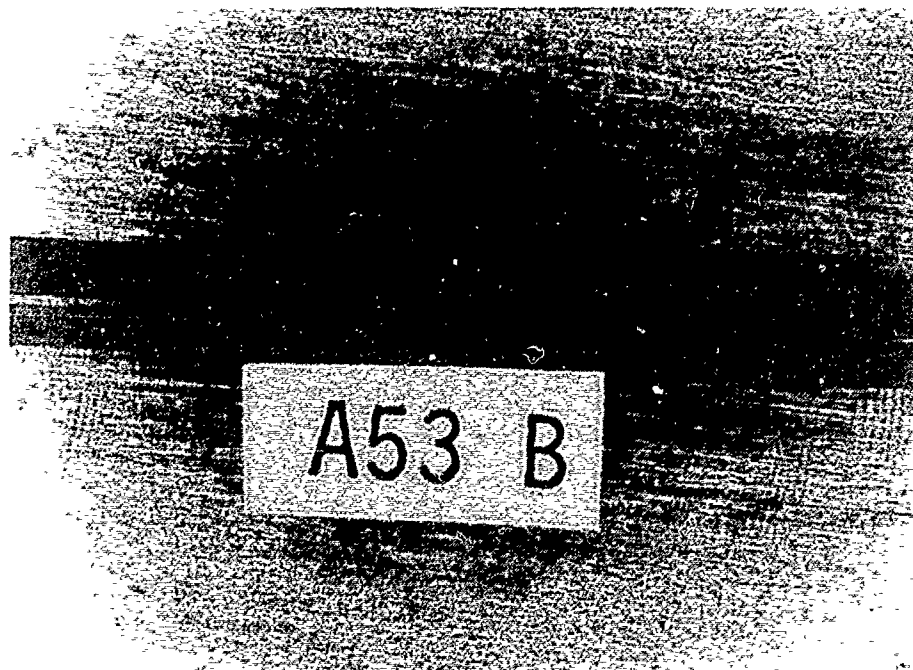
## SUMMARY OF TASK 2 DYNAMIC TESTS

Run No.	Spec ID	Fuel	Additive	Duration (sec)	Wall Temp, F	Plating
M201	Z61	Methane	5 ppm CH <sub>3</sub> SH	1169	730	None
M202	A51			1494	765	Gold
M203	Z53			1160	727	Platinum
M204	A61		5 ppm H <sub>2</sub> S	585	808	None
M205	A52			960	760	Gold
M206	Z50			1344	792	Platinum
M207	Z013		5 ppm H <sub>2</sub> S	1484	751	Gold
M208	Z005		10 ppm H <sub>2</sub> S	1041	735	Gold

Note: Tests M201-M206 were conducted with an uncoated closeout sheet of OFHC.  
 Tests M207-M208 were conducted with a stainless steel closeout.



Amzirc with Ni-Au Coating Pre-Test M201-M206



Amzirc with Ni-Au Coating Pre-Test M201-M206

Figure 80. Dynamic Test Specimen Channels Were Electroplated With a Nickel Flash, Followed by Gold

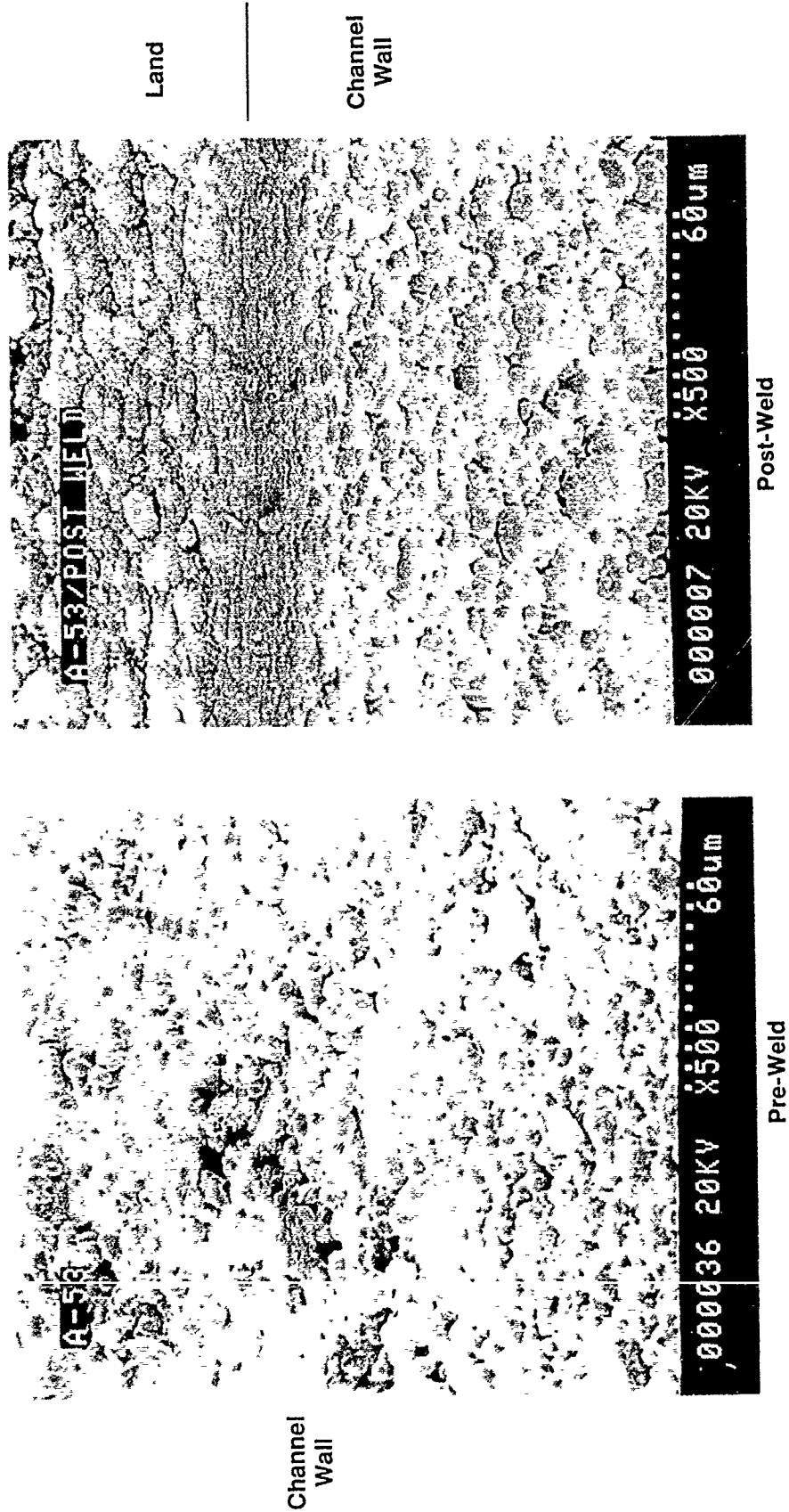


Figure 81. No Difference Was Apparent in the Gold Coating as a Result of Welding on the Channel Closeout

#### 4.3, Task 2.3—Thermal Sciences Laboratory Tests (cont.)

Figure 82. Along the channel land, and for approximately the first 5 mils into the channel, the coating was uniform, and the gold layer was close to the nominal specified 0.00025-in. thickness. Further into the channel, however, the gold thickness decreased substantially, though it did appear to be continuous, even in the corners of the channel. As well, the nickel diffusion barrier, which was relatively smooth, thick (0.0005-in.) and free of voids on the lands and near the top of the channel, was lumpy, poorly adherent, and discontinuous near the bottom of the channel.

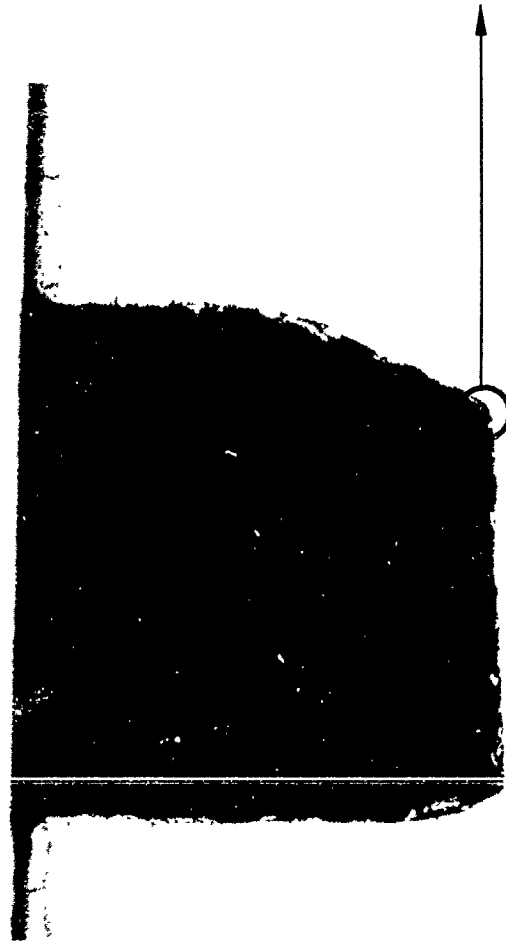
The dynamic test specimen for tests M207 and M208 were fabricated somewhat differently. Figure 83 shows sketches of the modified test specimen. The most important change was to replace the copper closeout sheet with a CRES 304 closeout and fuel manifold which was electron beam brazed into place. This eliminated all contact between the intentionally contaminated fuel and uncoated copper.

Six specimens of this modified design were machined. Two were used for evaluation of alternate plating techniques in an effort to improve the quality of the nickel and gold coatings deposited into the channel. Particular emphasis was placed on improving the nickel coatings.

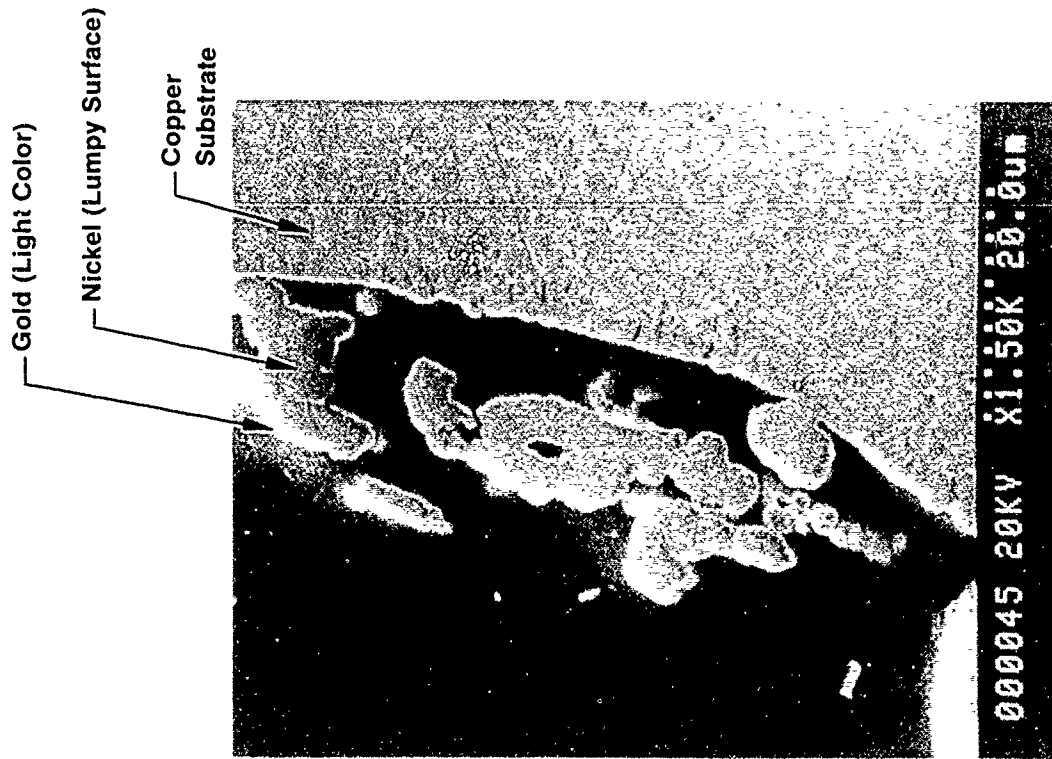
The earlier specimens were electroplated using an alkaline nickel solution. This process was used because it has high "throwing power" which may produce more thorough coverage in the bottom and corners of the channel. Unfortunately, the alkaline nickel baths also deposit material with large grains, leading to the lumpy, uneven surface shown in Figure 81.

Due to the problem with the large nickel grains, it was decided to investigate the use of an acidic nickel plating bath. This plating process produces a deposit with a much finer grain size but has a much slower deposition rate than the alkaline bath. It was expected that the small grain size would cover the bottom of the copper channel but not produce the large nodules that were seen in the earlier parts.

Three samples were prepared in order to compare the different processes. Sample A was prepared using the alkaline nickel plating bath. Sample B was plated using an acidic nickel bath. Sample C used a combination of both the alkaline



Post-Weld



Post-Weld

Figure 82. Cross-Sectioning Revealed a Large Variation in Coating Thickness From Top to Bottom of Channel (L) Though the Gold Layer Does Appear to Be Continuous, Even in the Corner of the Channel (R)

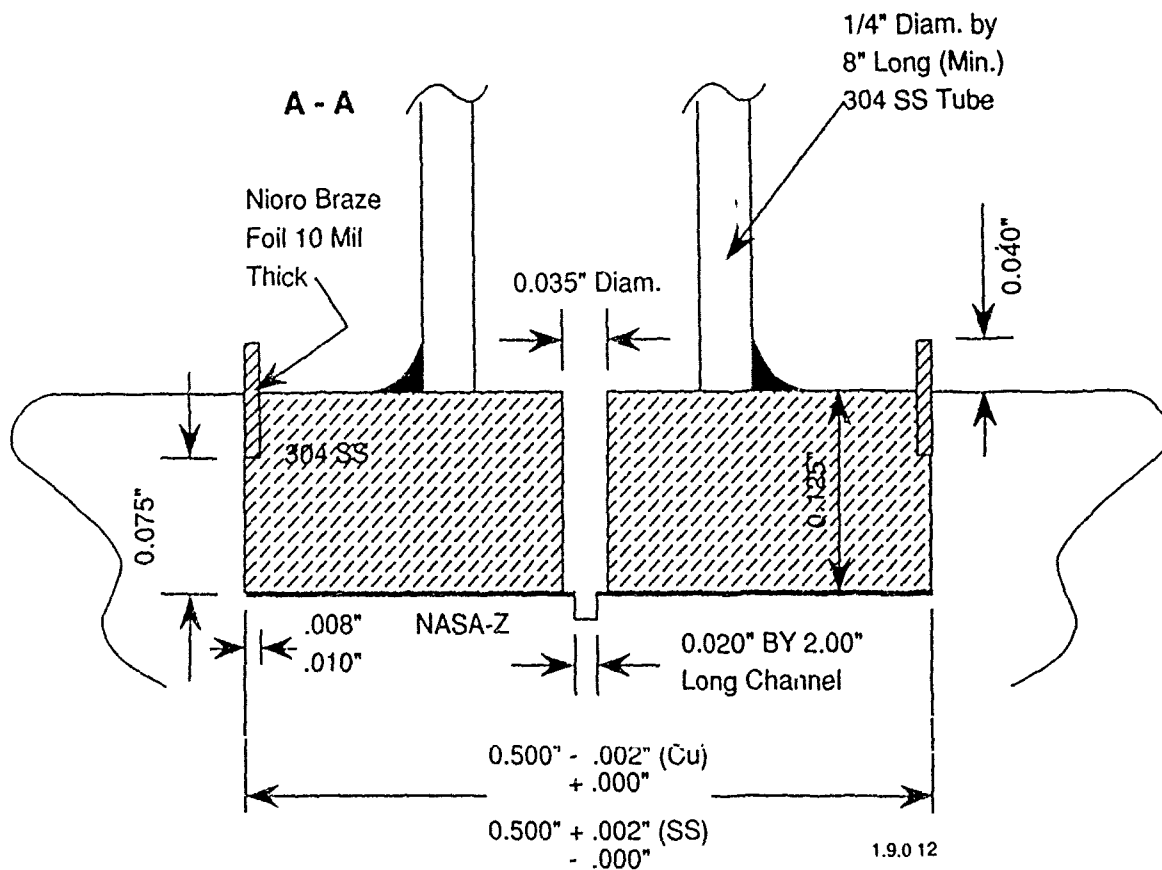
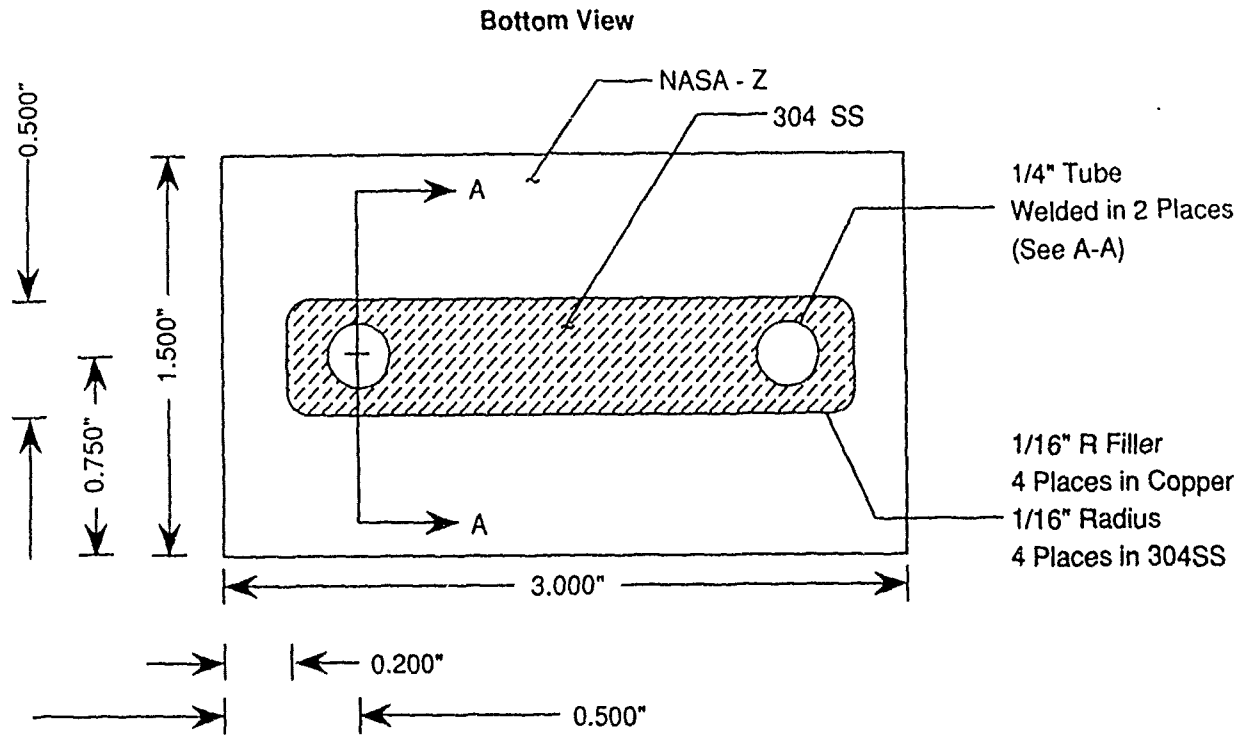


**Figure 83. Revised Test Specimen Design Used in Tests M207 and M208 Eliminated Contact Between Fuel and Unprotected Copper Surfaces**

#### 4.3, Task 2.3—Thermal Sciences Laboratory Tests (cont.)

and the acidic processes. The fine grained acidic technique was used to cover the copper surface and was followed by plating with the alkaline method. All three specimens were then coated with gold as before.

After coating, the three samples were sectioned for metallographic examination. Figure 84 shows results from the examination of Sample A. Figure 84a shows a cross section of a bottom corner of the channel, while Figures 84b and 84c show X-ray dot maps of nickel and gold, respectively. Both the nickel and gold are seen to have reached the corner and the bottom of the channel.

Figure 85 shows results from the examination of Sample B. Figure 85a shows no nickel detected near the bottom of the channel. Figure 85b shows a nickel  $K_{\alpha}$  X-ray trace with no detected nickel. The increase in intensity at the right of Figure 85b is due to the additional background from the copper  $K_{\alpha}$  adjacent to the nickel energy level, not to nickel detection.

Figure 86 shows the cross sections of Sample C. As can be seen, the surface is very uneven and the gold (bright areas) has not covered the channel bottom completely.

It was decided that the original alkaline process for nickel deposition was the best of the three alternatives investigated as a result of these examinations. The remaining four specimens were coated by this process. Pre-test inspections of these specimens will be presented and discussed along with the results from Tests M207 and M208.

Test M201 was conducted with an uncoated specimen as a final checkout of the recommissioned test facility. The test was conducted for 1169 sec at a nominal coolant side wall temperature of 730 F. A slight increase in the pressure drop through the channel was measured during the test, but no significant heat transfer degradation was measured (Figure 87).

After the test, the channel was heavily blackened and scaly deposits had formed on the channel walls. Examination under SEM showed that the channels walls had become roughened and showed that the scaly deposits in the channel consisted of copper and sulfur (Figures 88 and 89).

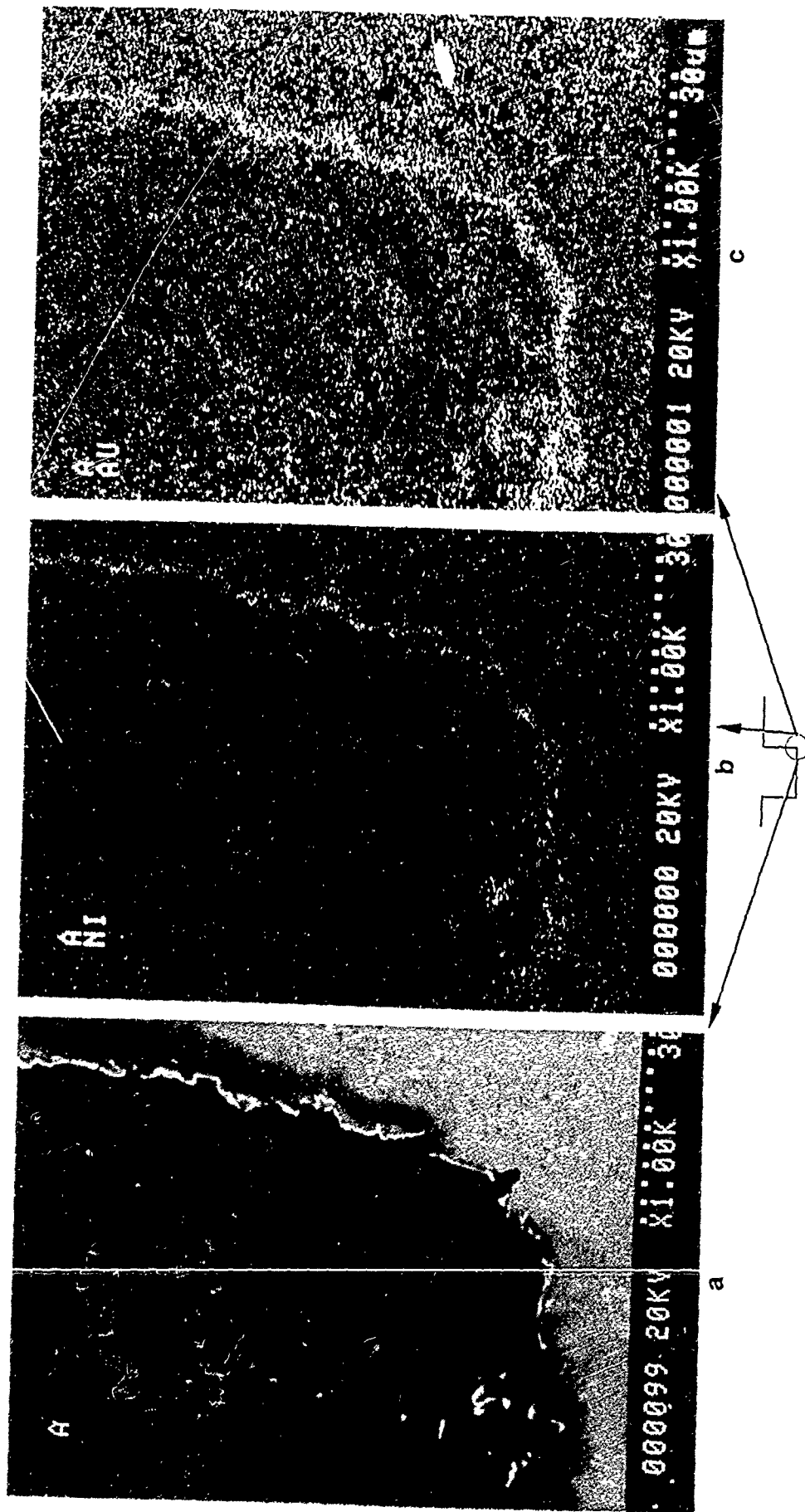


Figure 84. Sample A, Alkaline Nickel Strike Followed by Gold. (a) Cross Section at Bottom Corner of Channel. (b) Nickel Dot Map of (a). (c) Gold Dot Map of (a).

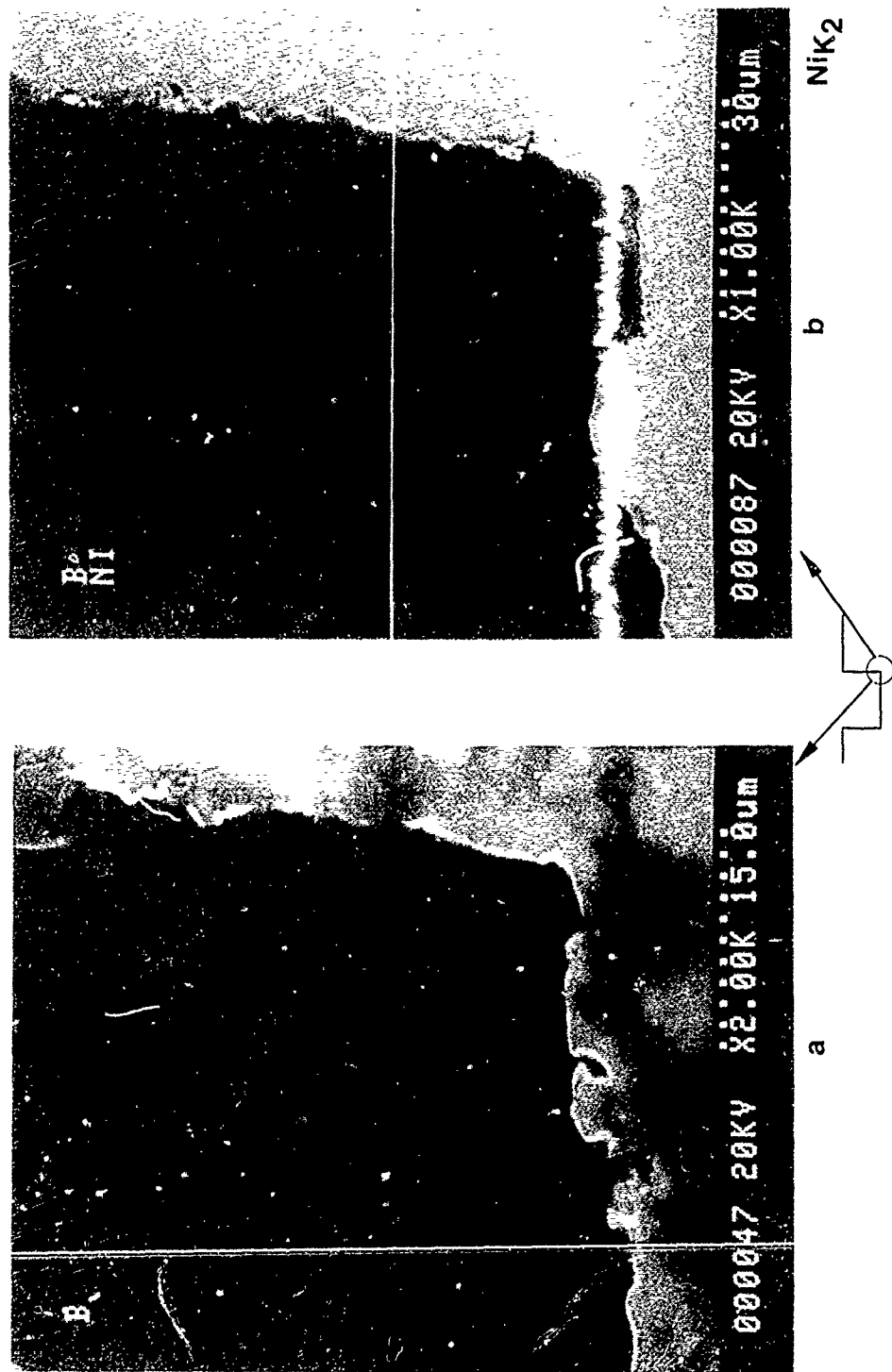


Figure 85. Sample B, Acidic Nickel Strike Followed by Gold. (a) Cross Section at Bottom Corner of Channel, Bright Band is Gold. (b) Nickel K<sub>2</sub> X-Ray Trace. Note: The Increase in Intensity of the Trace is Due to Cu K<sub>2</sub> Peak Width, Not Ni K<sub>2</sub> Detection

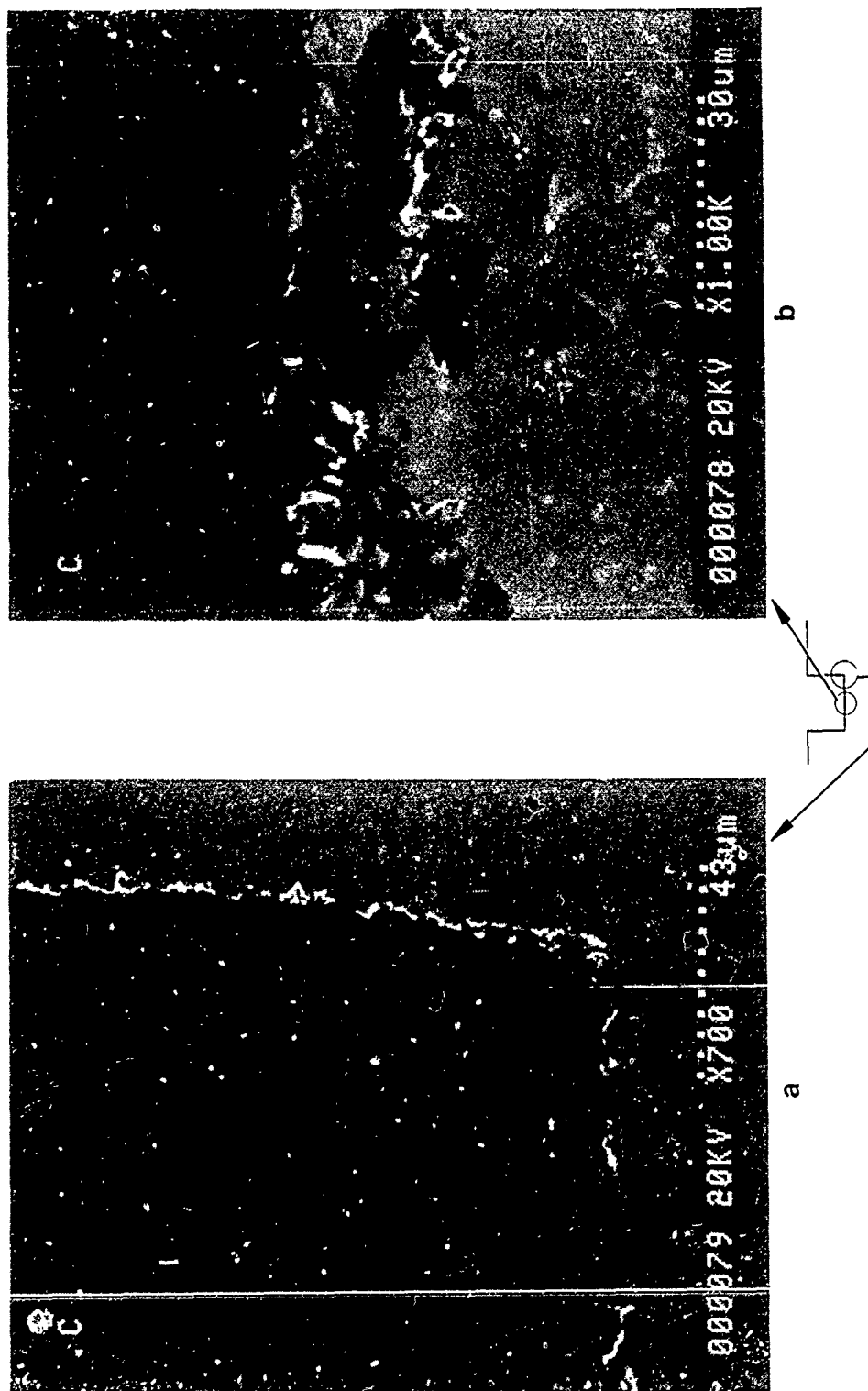


Figure 36. Sample C, Acid Nickel Followed By Alkaline Nickel and Gold. (a) Cross Section of Bottom Corner of Channel. (b) Channel Bottom Note: Bright Spots are the Gold Covered Regions

Q/A, Btu/in <sup>2</sup> -s	20.4		21.0	19.3	19.7		
T <sub>w</sub> , °F	620	650	680	711	719	725	730

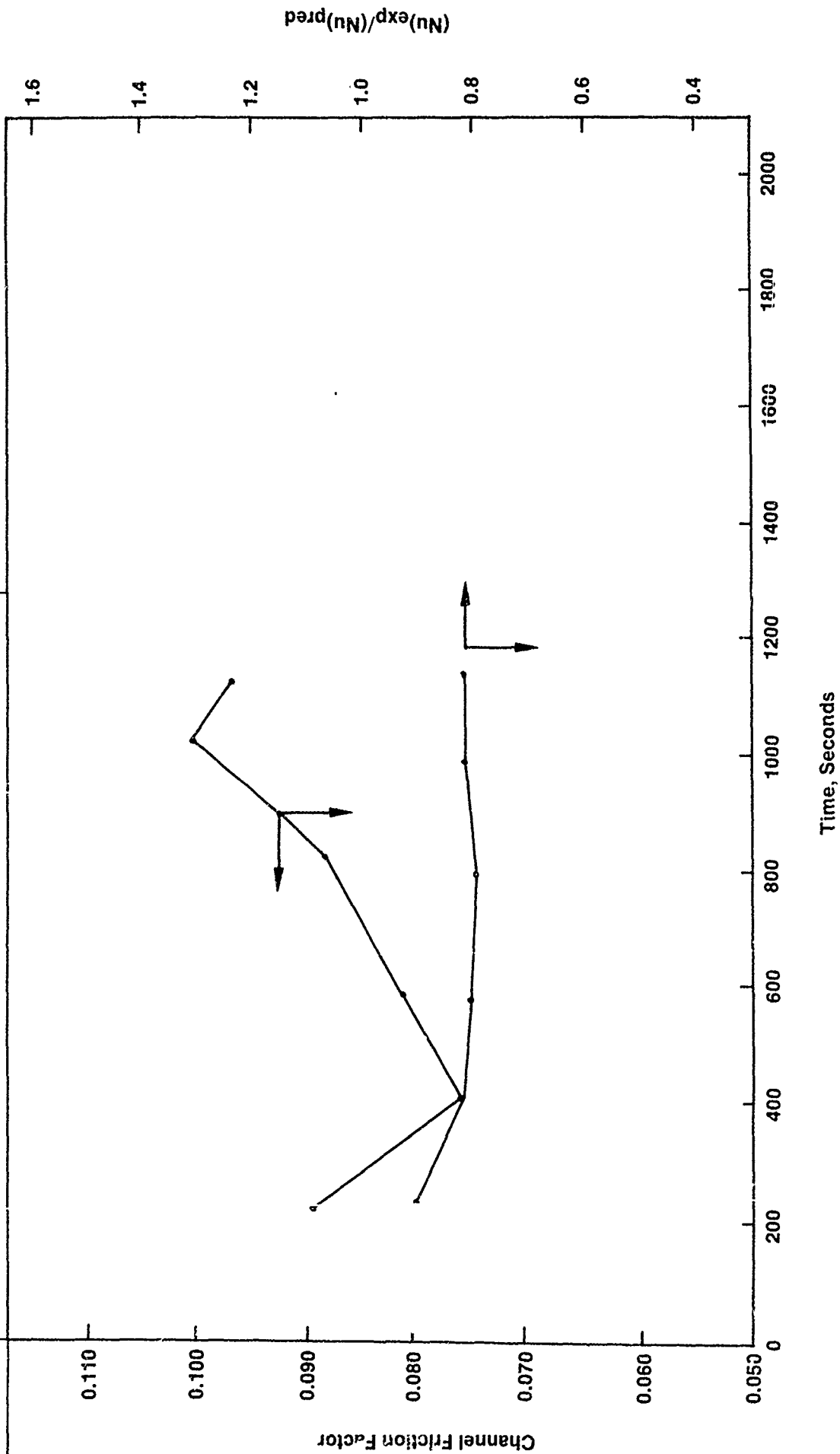


Figure 87. Pressure Drop Increased But Heat Transfer Performance Remained Steady Through Test M201

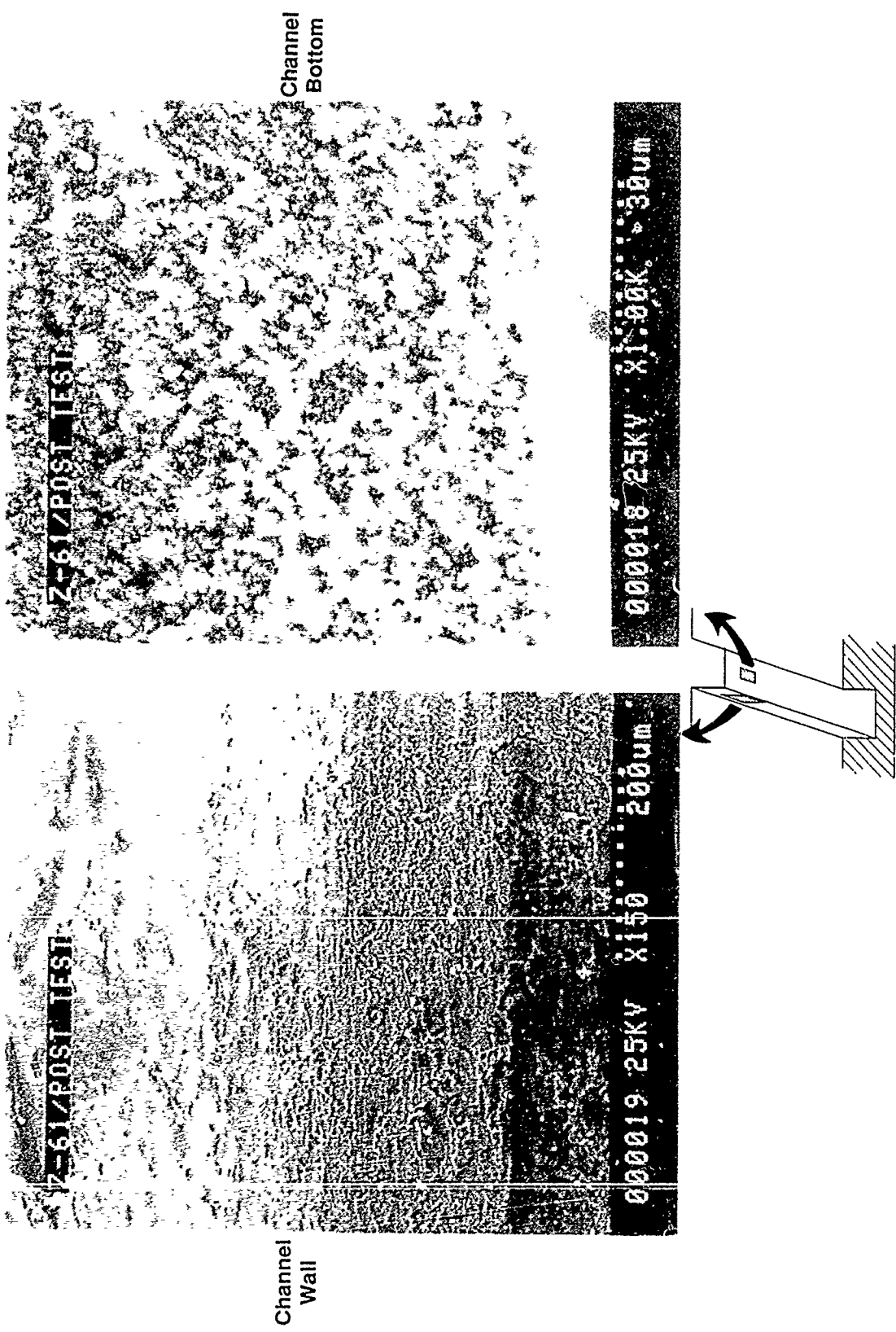
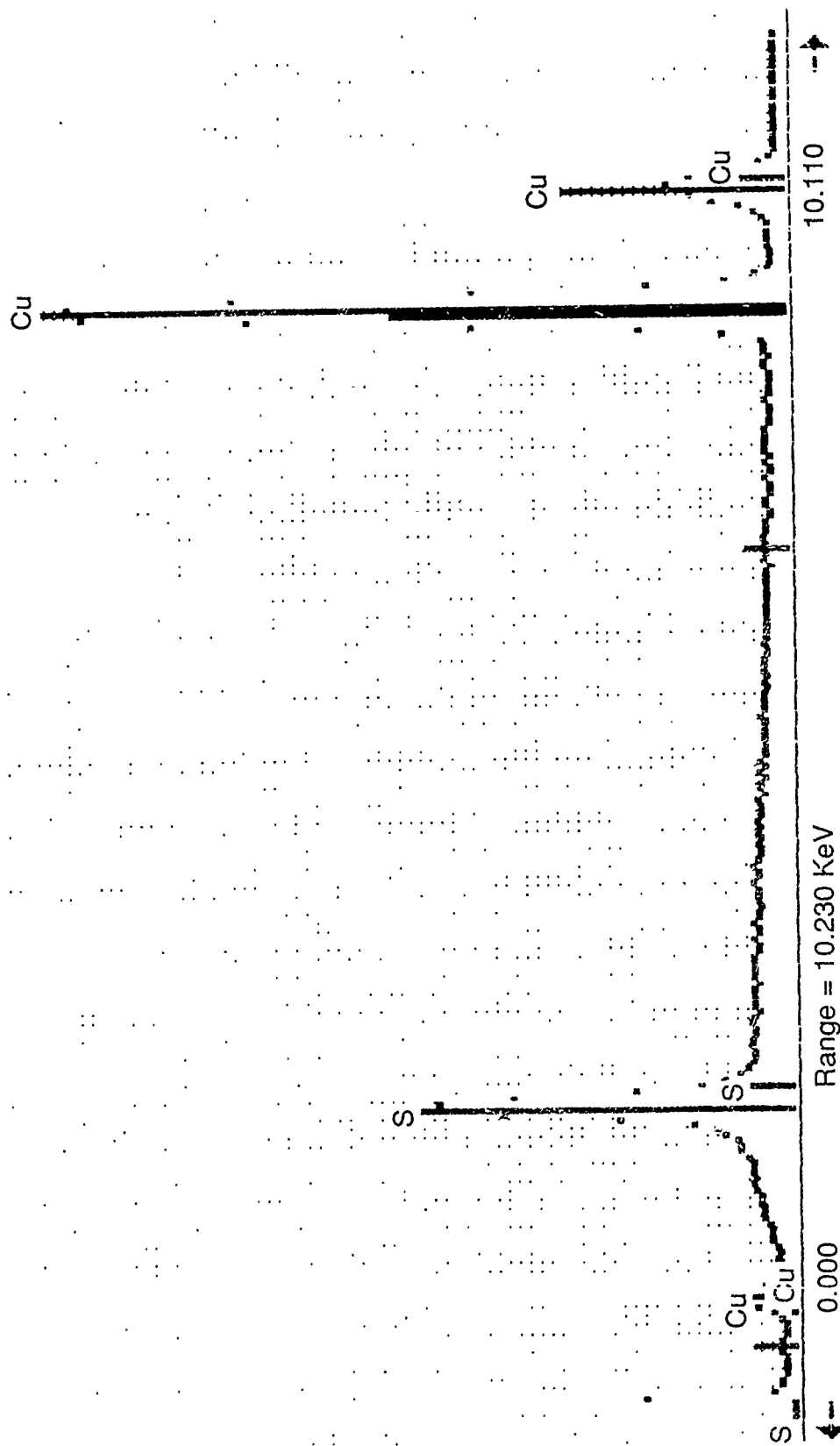


Figure 88. Post Test Examination Shows Wall Toughening and Scale Formation After 1169 sec of Operation with Tech Grade Methane in Test M201

Z-61, Post Test, Bottom  
Vert = 3569 Counts Disp = 1

Preset = Off  
Elapsed = 100 Secs



Range = 10.230 KeV

Integral 0 = 195545

Figure 89. EDS Analysis Showed Scale Formed in Test M201 was Copper and Sulfur

#### 4.3, Task 2.3—Thermal Sciences Laboratory Tests (cont.)

Test M201 indicated that there was a problem with sulfur contamination in the system, but how the sulfur got there was still unknown. Sulfur contaminants intentionally added during the last test series may have not been completely removed from the tubing and/or high pressure tanks of the system, or new sulfur contaminants could have been introduced by the methane which was used in this series of tests.

A simple test showed that the sulfur contamination observed in Test M201 probably originated in the high pressure tanks of the system. The gas vented directly from the high pressure tanks smelled slightly of sulfur. The odor was no worse after the gas was routed from the high pressure tanks through the tubing upstream of the test block. No odor was detected from the methane vented directly from the low pressure cylinders supplied by the vendor. As a result of this first test, the entire system, including all tubing and the high pressure cylinders, was vented and subjected to a 50 micron vacuum for three days. Afterwards, no odor of sulfur compounds was detected in or around the system.

Test M202 was conducted with a gold-plated Amzirc specimen (Specimen A51) and technical grade methane with 5 ppm (by volume)  $\text{CH}_3\text{SH}$  added. The test was conducted for 1494 sec at a nominal coolant side wall temperature of 765 F.

During the test, some degradation was observed in the flowrate through the channel (though not as much as with the uncoated specimen run in Test M201) and a slight decrease in heat transfer performance was also noted (though again, not as much as in Test M201). Figures 90 and 91 show these performance trends for the tests run with methane plus methyl mercaptan.

Posttest metallographic examination of this specimen showed the gold coating was mostly unaffected by the test. Figure 92 shows SEM photographs looking down into the channel at the coated surface, before and after the test. As discussed previously, the rocky appearance of the surface is due to nodules of nickel deposited in the bottom of the channel which were covered with a thin gold coating. At high magnification, it appears that the thin gold coating covering the nickel nodules ruptured during the test. This is documented in Figure 93. Another area of interest was found on the wall of the channel, near the land. In Figure 94, it appears that the coating disbonded from the channel wall. It is not known with certainty if this disbond

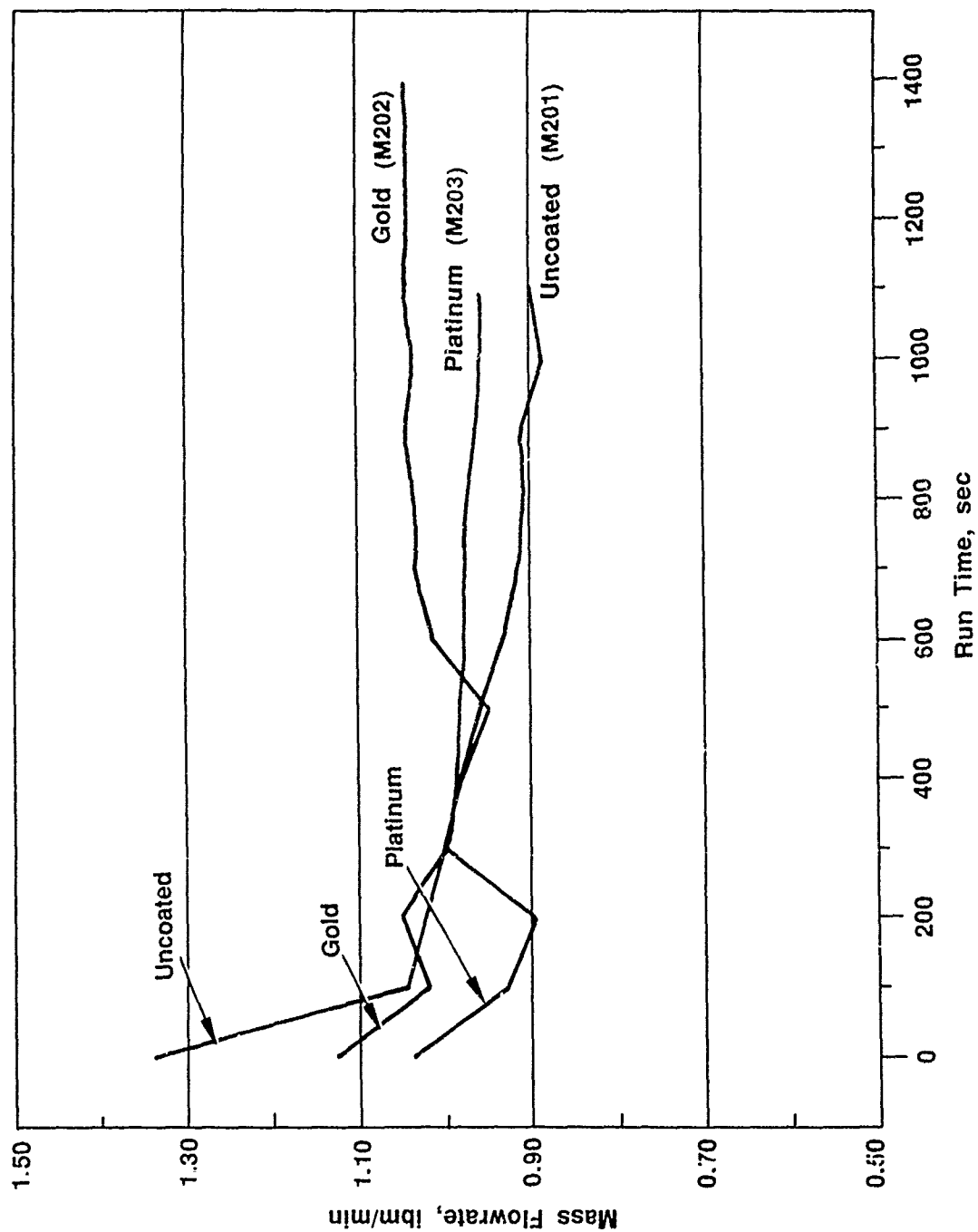


Figure 90. Flowrate Through Channel – Tests M201-M203 (Coatings Helped to Steady the Flowrate Through Channel.)

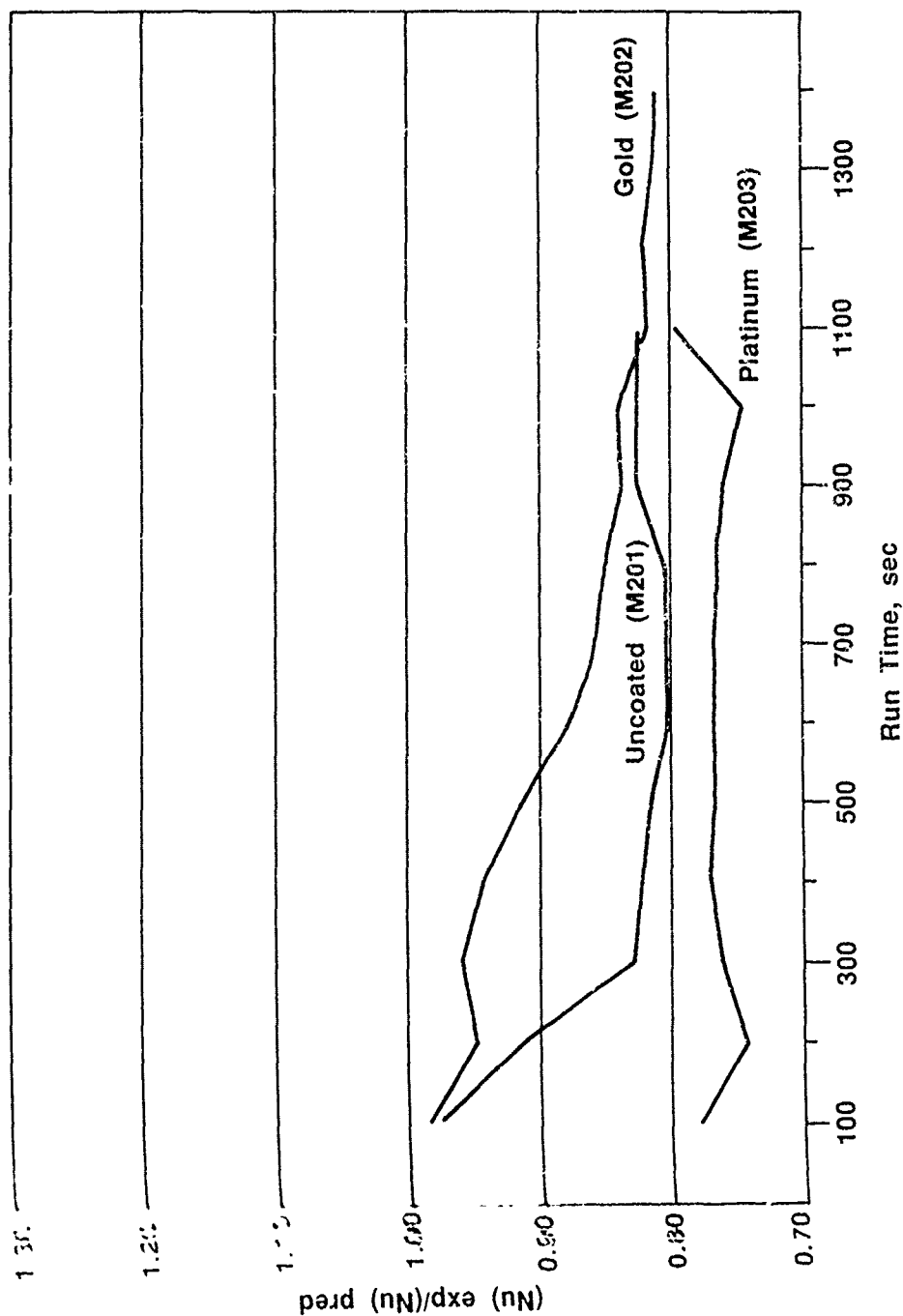


Figure 91. Heat Transfer Performance – Tests M201-M203 (Coatings Had Little Effect on Heat Transfer Performance.)

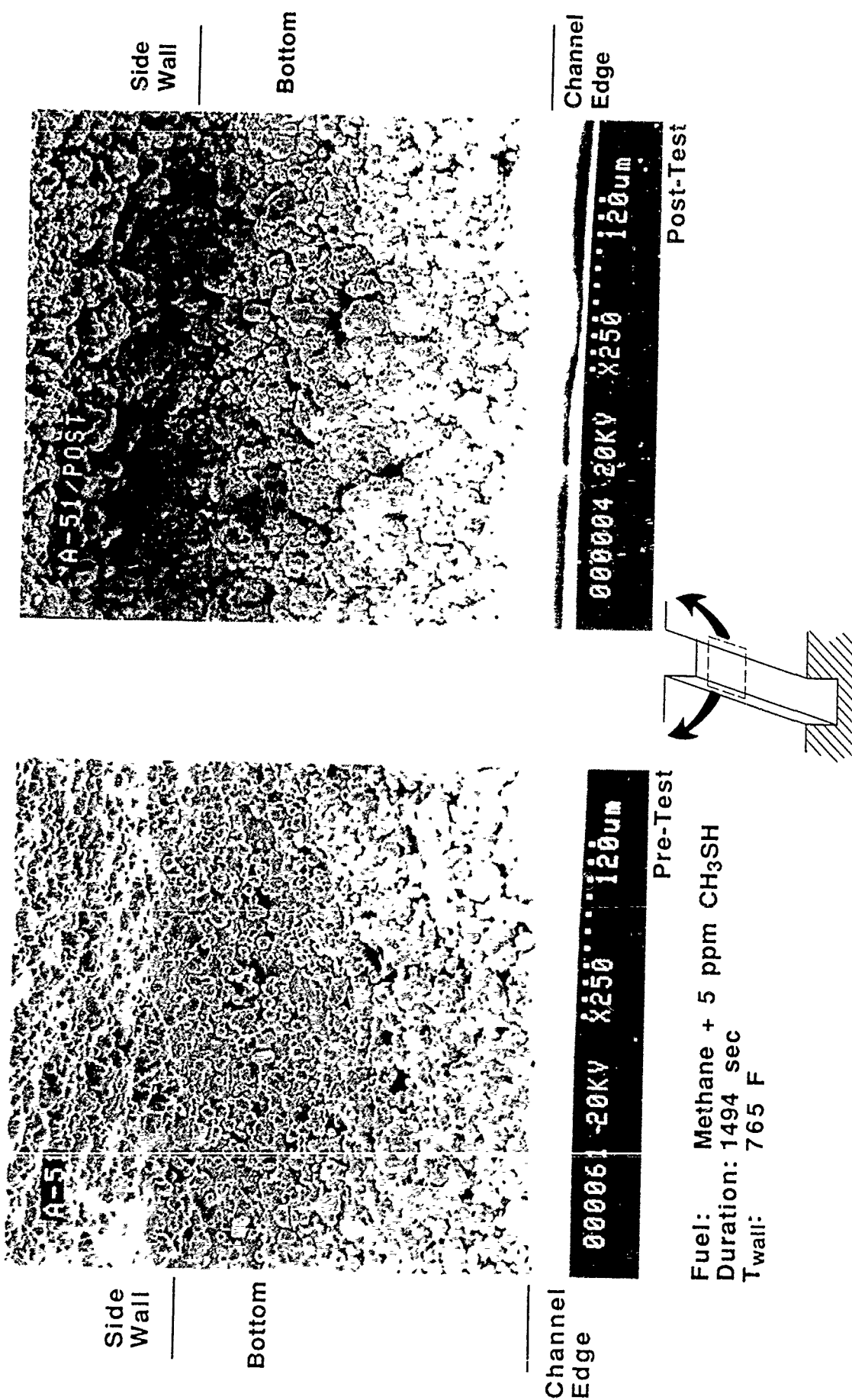


Figure 92. Gold Coating in Channel Provides Protection From Corrosion

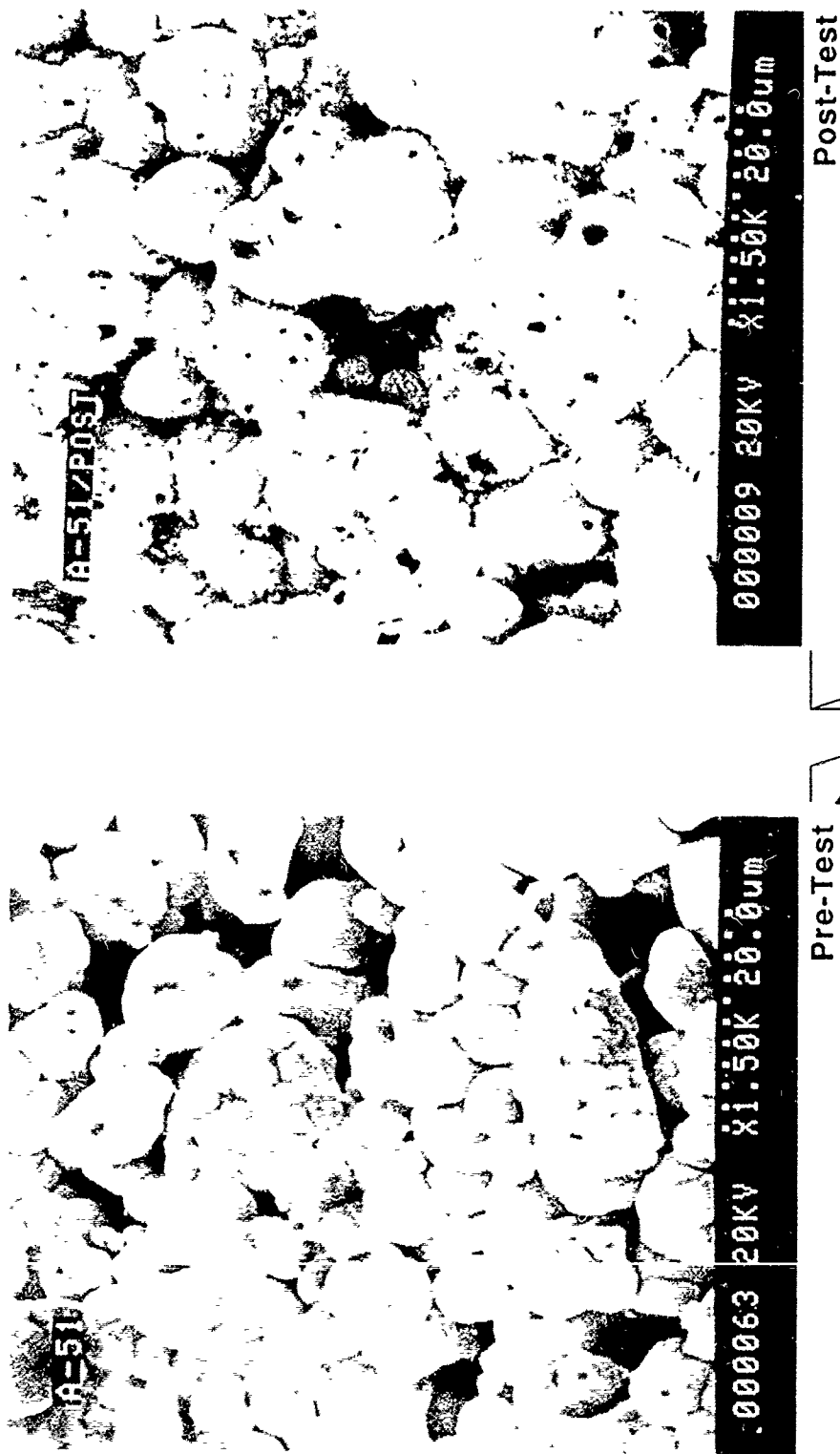


Figure 93. Enlargement of Gold Coating Shows Some Degradation Occurred During Test M202 (Note Fumaroles)

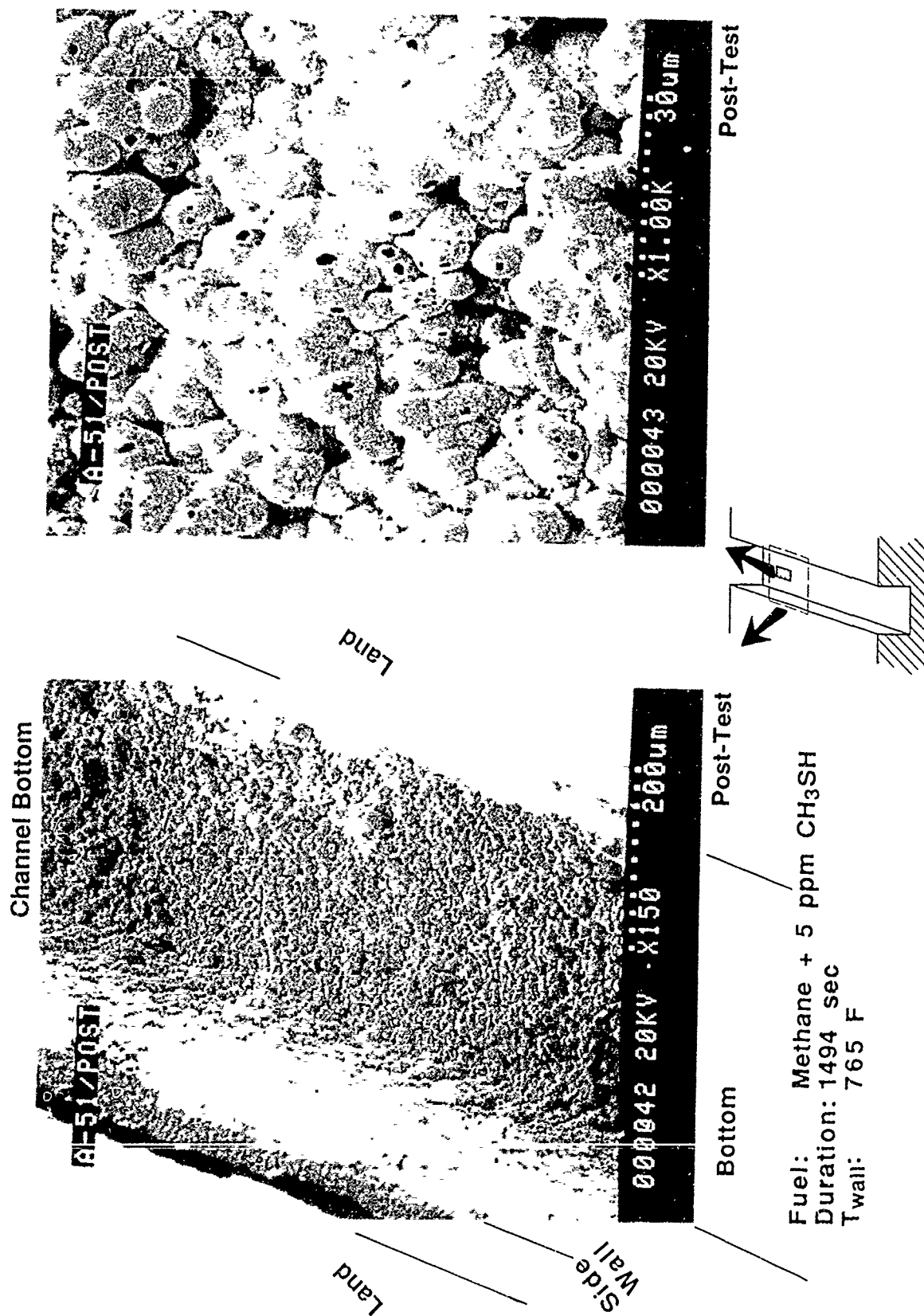


Figure 94. Gold Coating Disbonded At Sidewall and Small Fumaroles Developed During Test M202.

#### 4.3, Task 2.3—Thermal Sciences Laboratory Tests (cont.)

occurred during the course of the test, or if it happened during the removal of the cover sheet. However, EDS analysis of the sidewall underneath the disbonded coating shows the presence of  $\text{Cu}_2\text{S}$ , which appears to have formed during the test. This indicates that the disbond occurred before the removal of the cover sheet.

Test M203 was conducted with a platinum-coated NASA-Z specimen (Z53) and technical grade methane with 5 ppm (by volume)  $\text{CH}_3\text{SH}$ . The test was conducted for 1160 sec at a nominal coolant side wall temperature of 727 F.

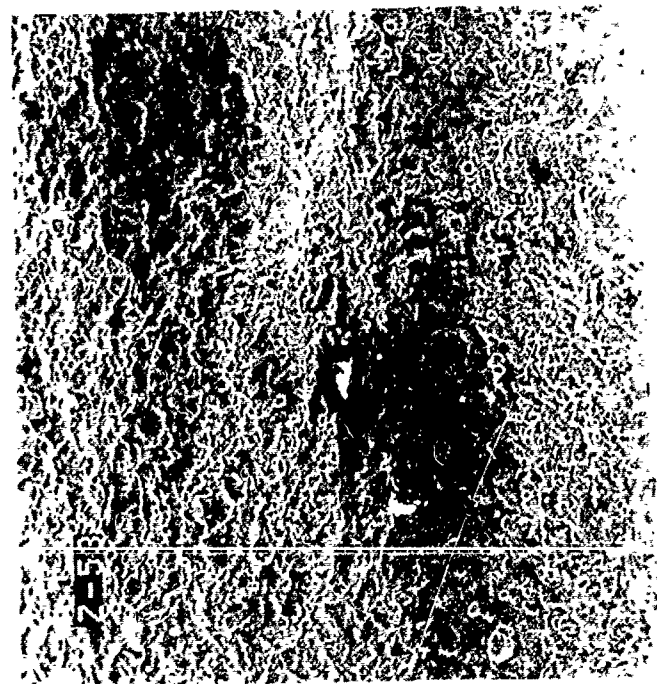
During the test, some degradation was observed in the flowrate through the channel (though not as much as with the uncoated specimen run in Test M201). No degradation of the heat transfer performance was measured. Figures 90 and 91 show these performance trends for the tests run with methane plus  $\text{CH}_3\text{SH}$ .

Posttest metallographic examination of this specimen showed the platinum coating was virtually unaffected by the test. Figure 95 shows a SEM photograph looking down into the channel at the coated surface, before and after the test. At high magnification, Figure 96, there appear to be a number of fuzzy, lichen-like deposits on the platinum surface. EDS analysis did not show a significant difference between the fuzzy deposits and the surrounding areas. Both areas appeared to be primarily platinum, with some copper and sulfur detected. This may be a result of copper sulfide deposits from the uncoated surfaces of the channel.

At the conclusion of Test M203, the run cylinders were vented and the entire system was subjected to a 50 micron vacuum for more than 80 hr in preparation for changing the sulfur contaminant in the system.

Tests M204 through M206 were conducted with  $\text{H}_2\text{S}$  as the sulfur-containing contaminant. Test M204 was conducted with an uncoated Amzirc specimen (Specimen A61) and TG methane with 5 ppm (by volume)  $\text{H}_2\text{S}$ . The test was conducted for 585 sec at a nominal coolant side wall temperature of 808 F.

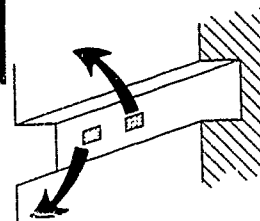
The test duration was much shorter than normal because of severe flow degradation through the channel. At the start of the test, the flowrate through the test specimen was 1.1 lbm/min. However, within 100 sec of the beginning of the test, the



000008 20KV X220 136um

#### Pre-Test

Fuel: Methane + 5 ppm CH<sub>3</sub>SH  
 Duration: 1160 sec  
 T<sub>wall</sub>: 727 F  
 Note: White spot in center of photo is due to film imperfection.



000018 20KV X250 120um

#### Post-Test

Figure 95. Platinum Coating in Channel Also Provided Corrosion Protection in Test M203

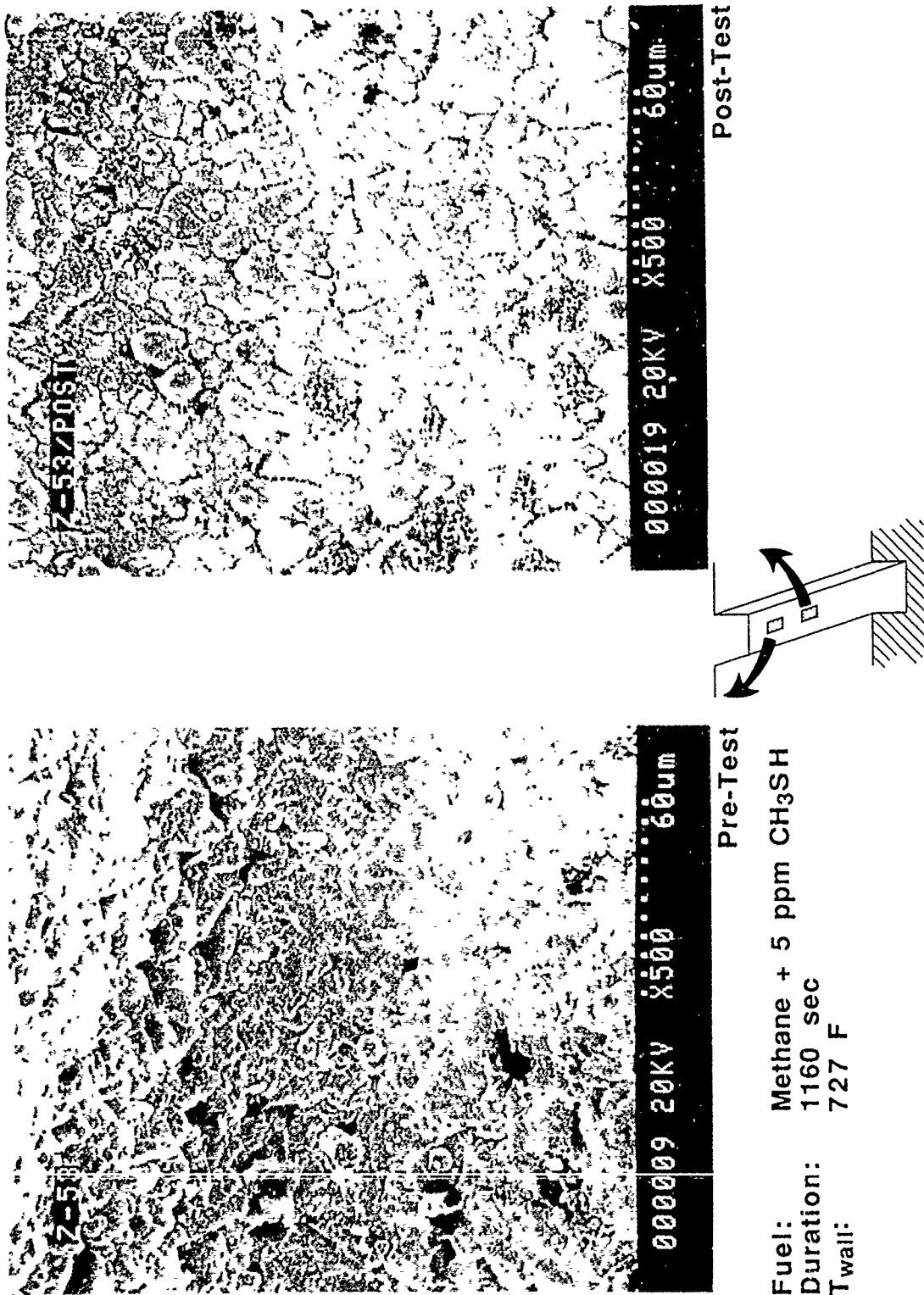


Figure 96. Minor Deposits On Platinum Surface Results in a Fuzzy Appearance With Random Lichen-Like Areas (Test M203)

#### 4.3, Task 2.3—Thermal Sciences Laboratory Tests (cont.)

flow through the channel had decreased to 0.7 lbm/min. The flowrate continued to decrease steadily, dropping below 0.5 lbm/min after 200 sec of operation. Continuous adjustment of the valve controlling the exit pressure of the methane to 1000 psig became necessary as the flowrate continued to decrease. The test block heaters were shut off approximately 450 sec into the test in anticipation of a premature shutdown. After 585 sec of operation, as the flowrate had dropped below 0.2 lbm/min, the methane run valve was closed and GN<sub>2</sub> was run through the system to purge the test specimen.

Figure 97 shows plots of the flowrate through the channel in the test series conducted with methane contaminated with hydrogen sulfide. Figure 98 presents the heat transfer performance measured in this series of tests.

Posttest inspection of the uncoated specimen showed the channel to be filled with Cu<sub>2</sub>S. SEM photographs of the channel surface are presented in Figure 99. Note the characteristic morphology of the material, which EDS analysis showed to be entirely Cu and S. Though the aspect ratio of the deposit structures are different, the morphology is reminiscent of the "barnacles" and the "rosettes" observed in tests with RP-1 plus n-dodecanethiol and methane plus high levels (10 and 200 ppm) of CH<sub>3</sub>SH.

It is also significant to note that only 5 ppm of H<sub>2</sub>S was enough to cause nearly complete blockage of the test channel. The Dynamic Tests of Task 1 with methane plus CH<sub>3</sub>SH under similar conditions of inlet pressure, temperature, and initial flowrate indicated that more than 10 ppm of sulfur was required before complete blockage of the channel would result. In addition, the Static Tests of Task 2 showed that NASA-Z coupons were more reactive (i.e., gained more weight) in a static environment containing H<sub>2</sub>S than in a static environment containing an equal concentration of CH<sub>3</sub>SH. Thus, H<sub>2</sub>S may be an even more harmful sulfur contaminant than CH<sub>3</sub>SH.

Test M205 was conducted with a gold-coated Amzirc specimen (Specimen A52) and TG methane with 5 ppm (by volume) H<sub>2</sub>S. The test was conducted for 960 sec at a nominal coolant side wall temperature of 760 F.

During the test, the flowrate through the channel was very steady as shown in Figure 97, indicating that the gold coating was very beneficial in preventing reaction of the H<sub>2</sub>S with the Cu substrate. However, the heat transfer performance of the

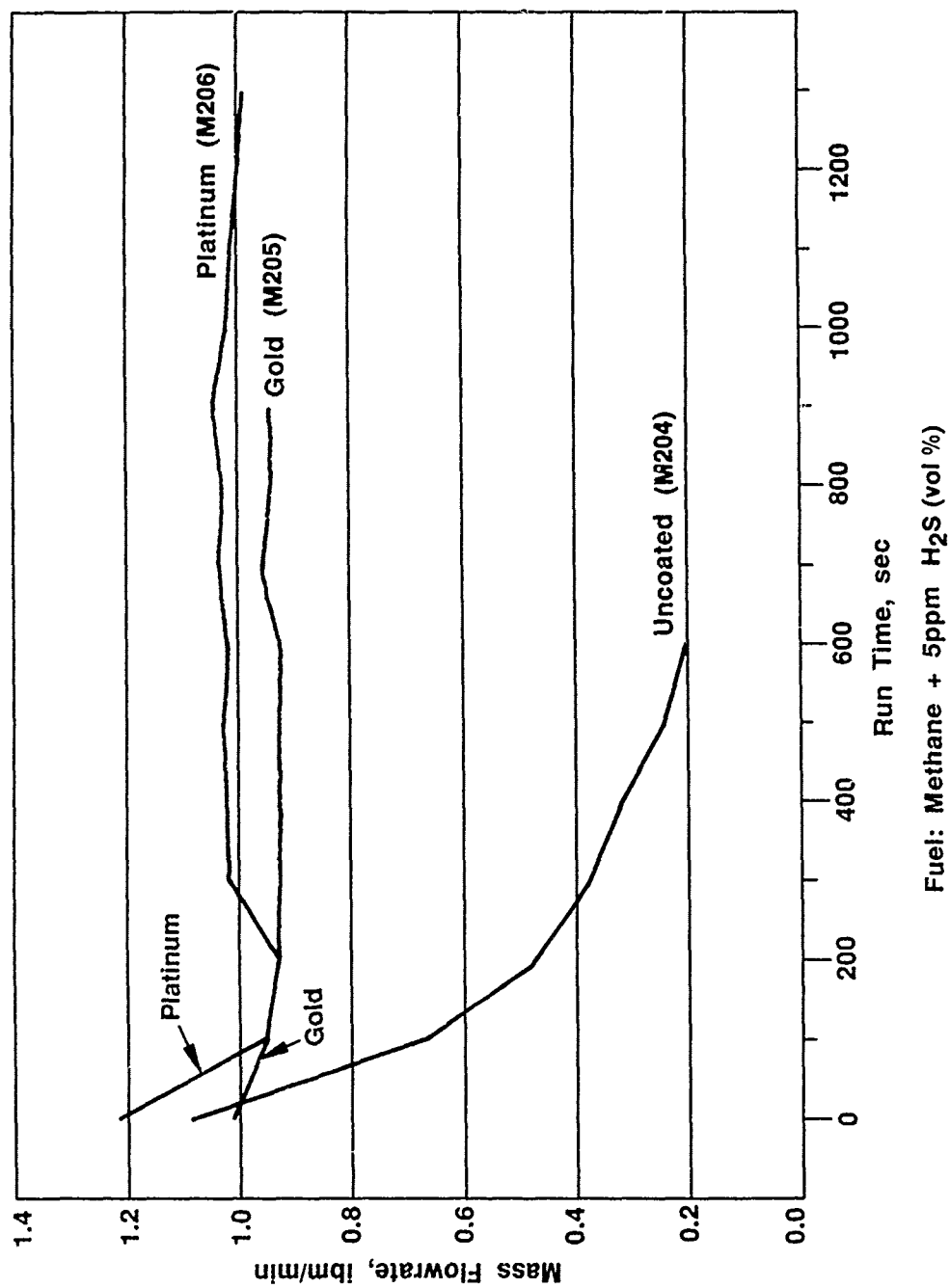


Figure 97. Flowrate Through Channel – Tests M204-M206 (Gold and Platinum Coatings Prevented Degradation of Methane Flow.)

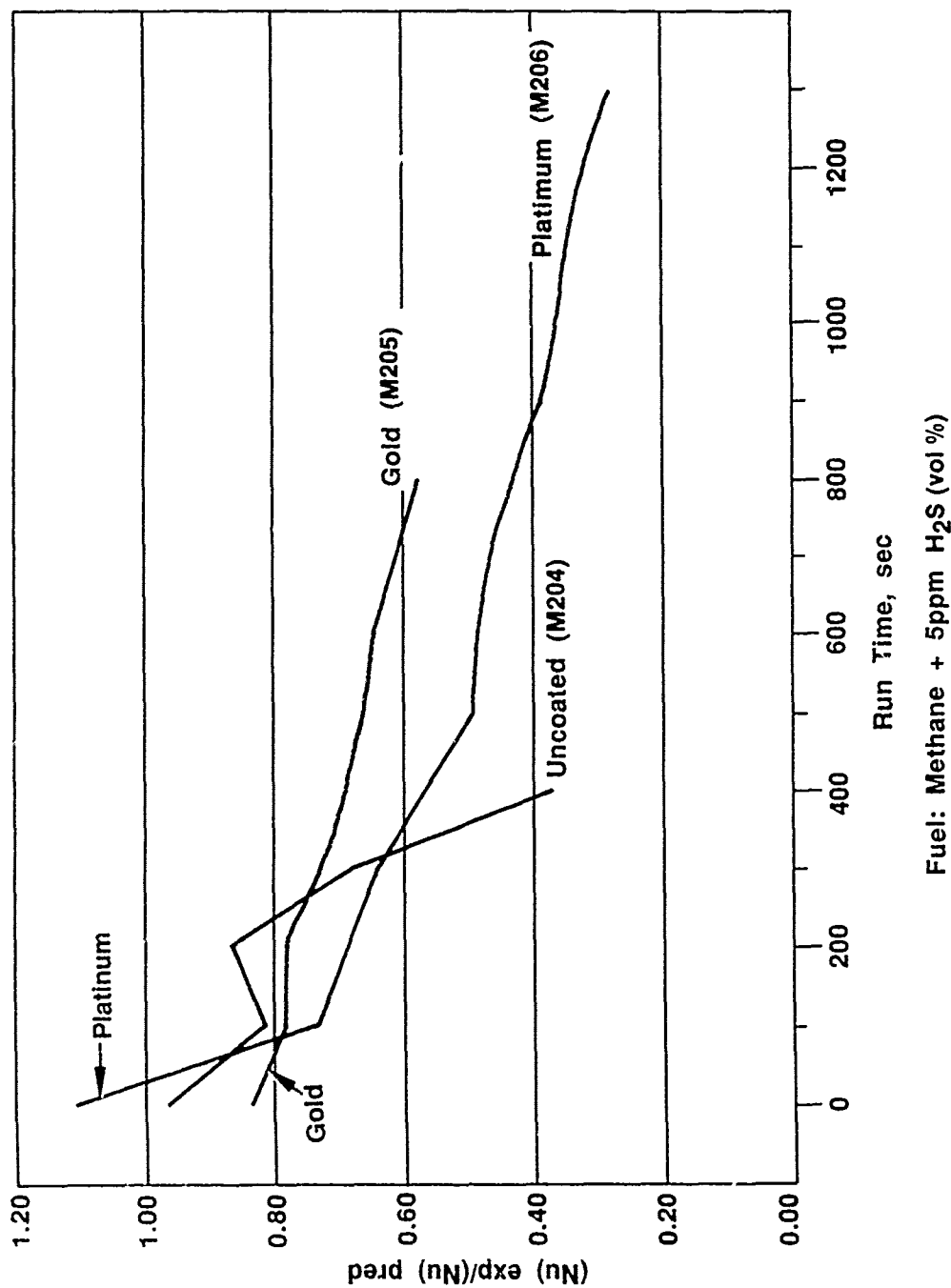


Figure 98. Heat Transfer Performance – Tests M204-M206 (Preliminary Data Indicate Gold and Platinum Coatings Do Not Prevent Decreases in Heat Transfer Performance.)

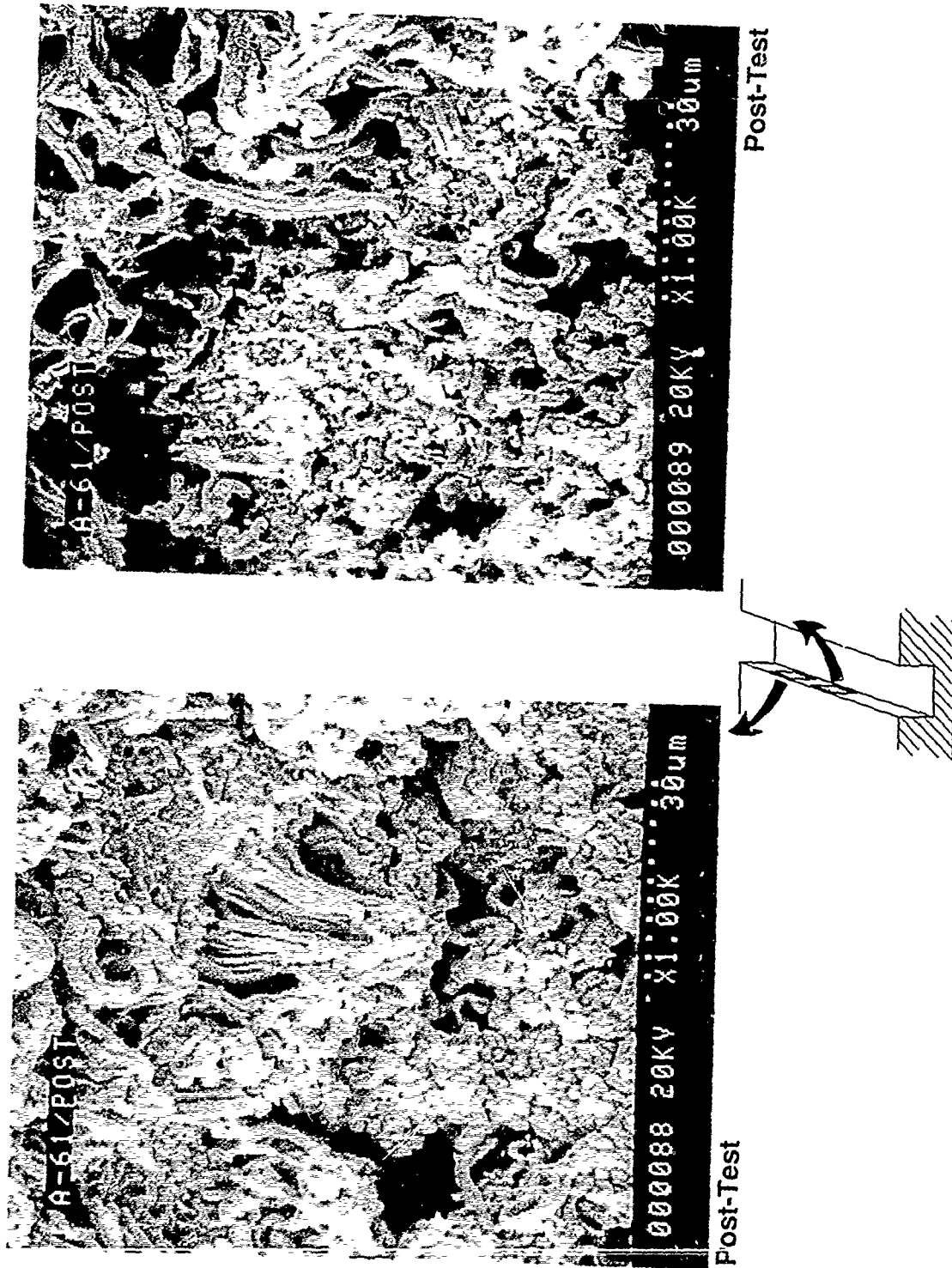


Figure 99. SEM of Uncoated Specimen - Post-Test M205 (Unprotected Amzirc Surface After Operation With Methane + 5 ppm (by vol.)  $H_2S$ . Growths Are Copper Sulfide.)

#### 4.3, Task 2.3—Thermal Sciences Laboratory Tests (cont.)

specimen steadily decreased, as shown in Figure 98. Posttest analysis shows this was probably caused by a thick layer of  $\text{Cu}_2\text{S}$  deposited over all surfaces.

Posttest analysis of this specimen showed that the gold coating had apparently held up well during the test, but that it had become covered by a layer of  $\text{Cu}_2\text{S}$ . Figure 100 documents the appearance of the channel surface before and after the test.

These surface deposits were further examined by preparing a cross section taken from the middle of the channel of the Au plated specimen tested in Run M205 (Specimen A52). Figure 101 shows an overview of the channel cross section. Note how thick and evenly distributed is the dark grey  $\text{Cu}_2\text{S}$  layer, Figure 101. A portion of the Cu closeout sheet is also shown. The closeout sheet is severely corroded, with similar deposits on all exposed surfaces.

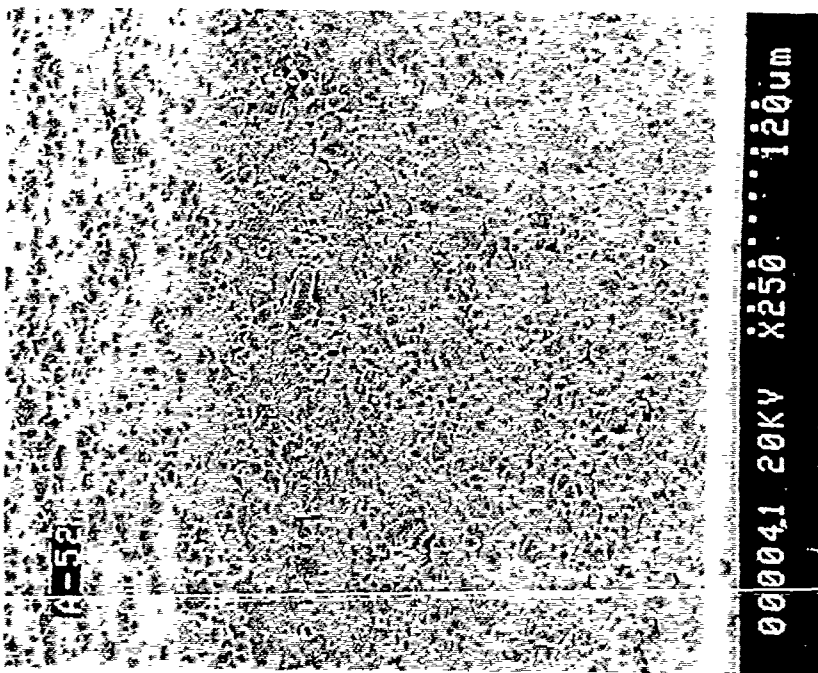
Test M206 was conducted with a platinum-coated NASA-Z specimen (Z50) and TG methane with 5 ppm (by volume)  $\text{H}_2\text{S}$ . The test was conducted for 1344 sec at a nominal coolant side wall temperature of 792 F.

As in Test M205, the flowrate through the channel in Test M206 was very steady, as shown in Figure 97. Again, however, the heat transfer performance of the specimen steadily decreased, as shown in Figure 98.

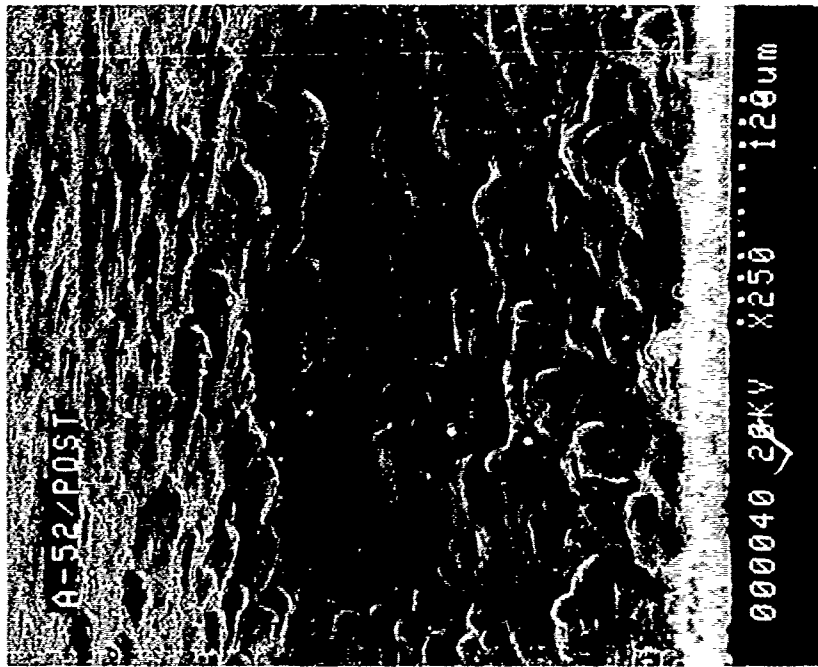
Posttest analysis of this specimen showed that the platinum coating had apparently held up well during the test, but that it had become covered by a thick layer of  $\text{Cu}_2\text{S}$ . Figure 102 documents the appearance of the channel surface before and after the test.

Both the gold and the platinum coatings were of significant benefit in preserving the flowrate through the specimen in the test series with  $\text{H}_2\text{S}$ . However, the formation of the even, consistent deposit of  $\text{Cu}_2\text{S}$  over the entire plated surface in Tests M205 and M206 was difficult to explain with certainty.

The deposit covering the Au layer of the channel was analyzed by X-ray diffraction and was identified unequivocally as  $\text{Cu}_2\text{S}$ . This is consistent with the previous findings from this program and suggests that metallic copper (or copper alloy)



Pre-Test



Post-Test

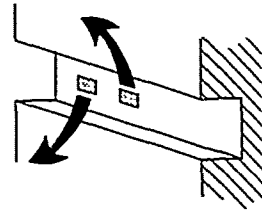
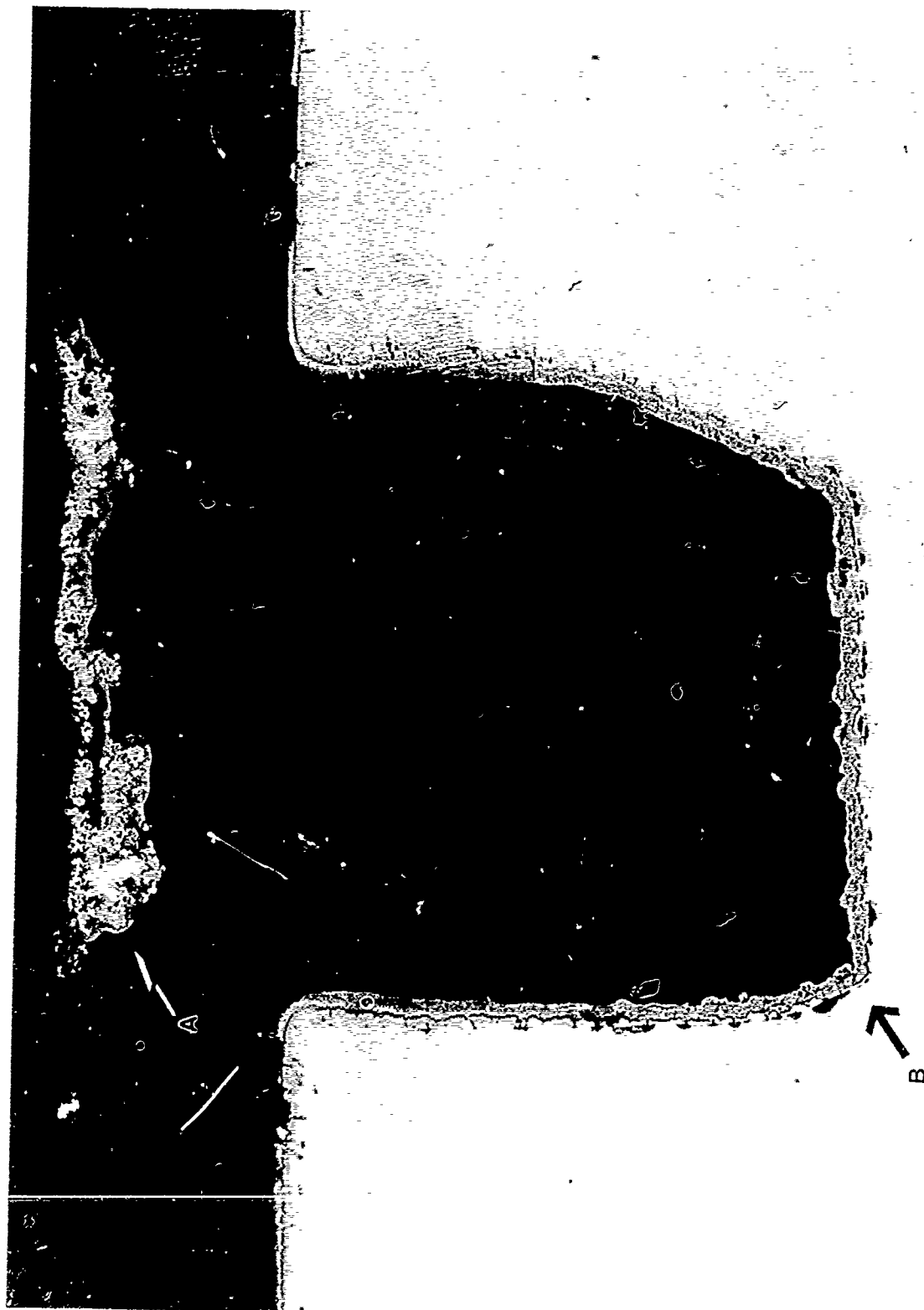
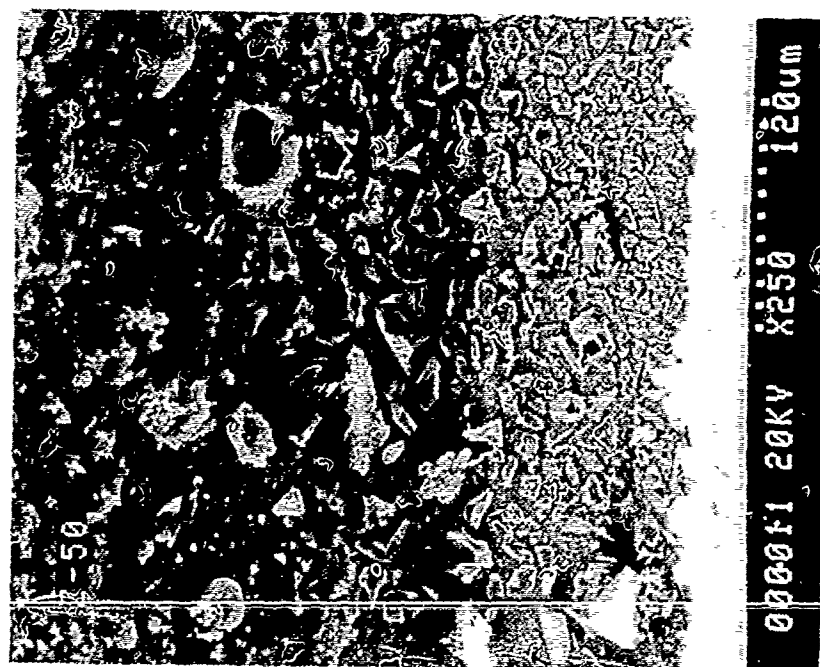


Figure 100. Pre- and Post-Test SEM of Gold Coating Used in Test With Methane + 5 ppm (by vol.) H<sub>2</sub>S (Test M205). Post-Test Surface Has Even Coating of Copper Sulfide.



200X

Figure 101. Cross Section of Specimen A52 After Test With 5 ppm  $H_2S$  (Test M205).  
Note Thick, Even Distribution of Cuprous Sulfide



Pre-Test



Post-Test

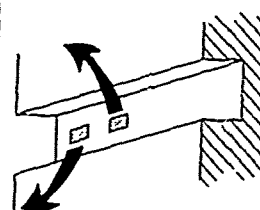


Figure 102. Pre- and Post-Test SEM of Platinum Coating Exposed to Methane + 5 ppm H<sub>2</sub>S (Test M206).  
Post-Test Surface Has an Even Coating of Copper Sulfide

#### 4.3, Task 2.3—Thermal Sciences Laboratory Tests (cont.)

reacted with the  $\text{H}_2\text{S}$  in the  $\text{CH}_4$  to produce this  $\text{Cu}_2\text{S}$ . The focus of this investigation then shifted to determine where the Cu which reacted with the  $\text{H}_2\text{S}$  originated. Three general hypotheses were tested:

- (1) General failure of the coating, by mechanical or corrosive forces, which led to exposure of the substrate.
- (2) Cracks or voids in the as-deposited coating which did not provide a continuous layer of protection to the substrate.
- (3) Reaction of the uncoated Cu surfaces of the close out sheet and inlet and exit holes of the specimen.

It did not appear that the  $\text{Cu}_2\text{S}$  resulted from a general failing of the protective coating. SEM examination of the cross sectioned Au specimen shows the coating held up without evidence of serious deterioration. For example, in Figure 103, the Au coating can be seen underneath the  $\text{Cu}_2\text{S}$  layer. It appears to be smooth and in good condition. As well, the tests conducted with  $\text{CH}_3\text{SH}$  as the sulfur contaminant did not appear to attack the coating materials aggressively.

Cracks in the coatings may have been responsible for at least some of the  $\text{Cu}_2\text{S}$ . As seen in Figures 102 and 103, there are numerous locations around the channel where cracks developed in the coatings. There appears to be a void in the substrate underneath each of the cracks. Figure 104 presents an enlargement of one of the areas. As previously noted, pretest inspection of the coatings did show cracks in the coatings, but no voids in the substrate. Thus, the formation of the void under the coating may have occurred during the test as a result of reaction of the substrate with contaminated fuel. However, the amount of  $\text{Cu}_2\text{S}$  on the surface appears to be much more than that which could have been formed from the reaction of the substrate in the small, localized voids, unless the voids are much larger in other planes of the specimen. It appears that cracks in the coatings may be responsible for some, but not all, of the  $\text{Cu}_2\text{S}$  which was formed on the surface of the specimen.

Reaction of the uncoated copper from the closeout sheet and the inlet and outlet holes was probably responsible for most of the  $\text{Cu}_2\text{S}$  found on the surface. The

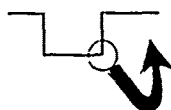
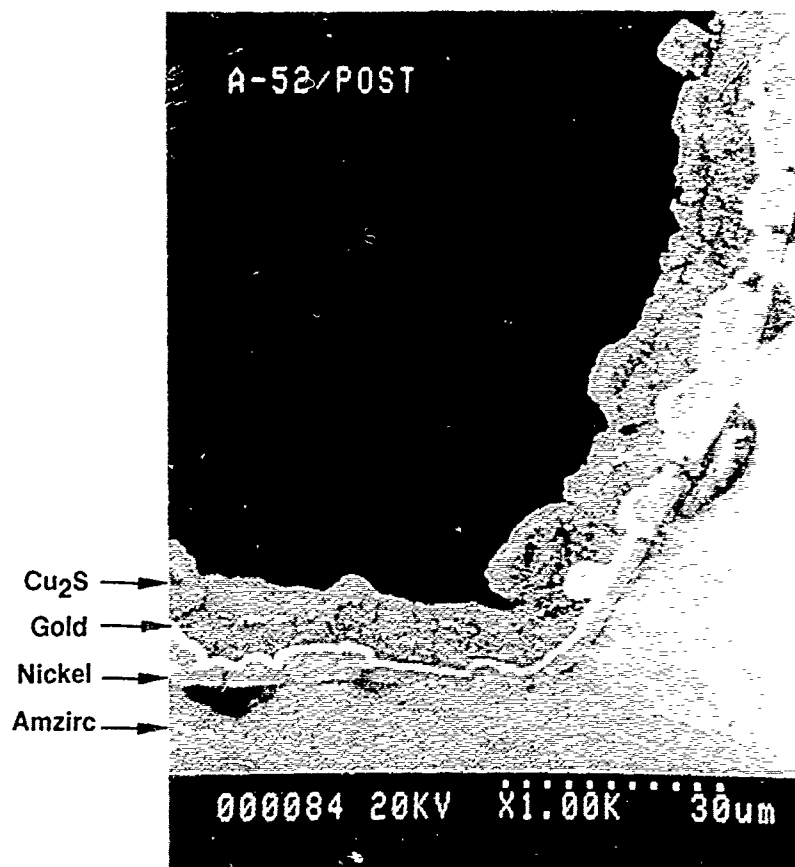


Figure 103. Cross-Section of Channel Corner After Test With 5 ppm H<sub>2</sub>S (Test M205). Note Massive Cu<sub>2</sub>S Layer Over the Bright Gold Coating

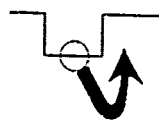
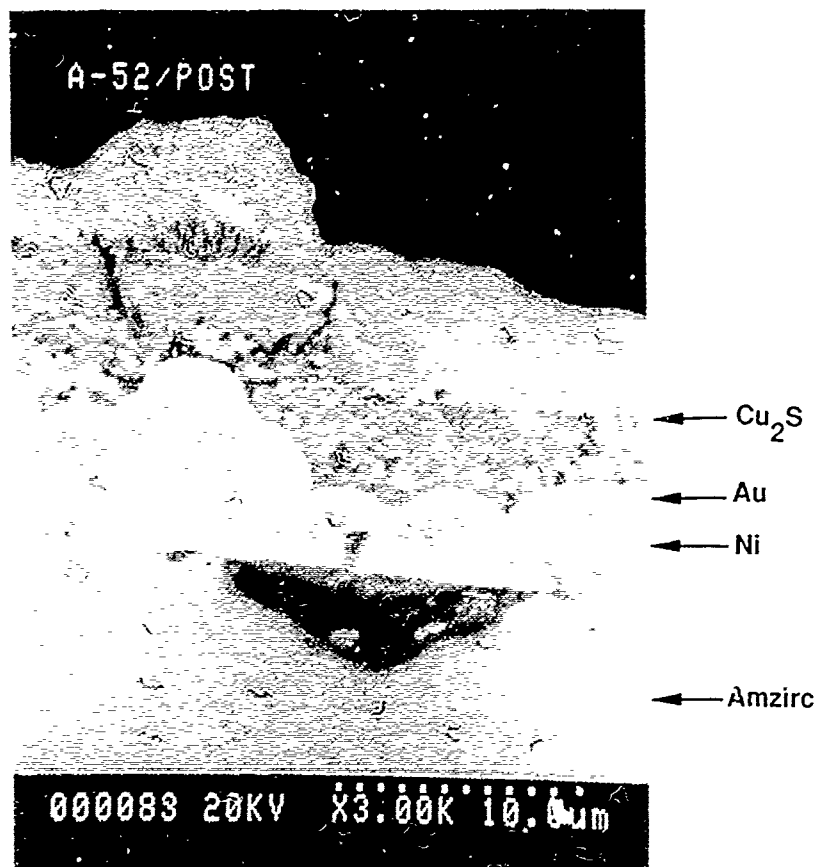


Figure 104. Closeup of Coating Crack and void Created in Substrate, Post Test With 5 ppm  $\text{H}_2\text{S}$  (Test M205).

#### 4.3, Task 2.3—Thermal Sciences Laboratory Tests (cont.)

closeout sheet of the Au coated specimen used in Test M205 was badly corroded by reaction with the  $H_2S$ . Test M204 also demonstrated that uncoated Amzirc was very reactive with 5 ppm  $H_2S$  in  $CH_4$  at these conditions. While the uncoated closeout sheet did provide an opportunity for direct comparison of uncoated versus coated surfaces in this environment, its corrosion also clouded the results of the experiment. Subsequent testing was conducted with coated channels (M207-M208) protected on all surfaces exposed to the contamination fuel.

Test M207 was conducted with a gold-plated NASA-Z specimen (Z-013) and TG methane with at least 5 ppm (by volume)  $H_2S$  added. The test was conducted for 1484 sec at a nominal coolant side wall temperature of 735 F. No degradation was observed in the flowrate through the channel or in the heat transfer performance through the channel during the test.

Test M208 was conducted with a gold-plated NASA-Z specimen (Z-005) and TG methane with at least 10 ppm (by volume)  $H_2S$  added. The test was conducted for 1041 sec at a nominal coolant side wall temperature of 730 F. No degradation was observed in the flowrate through the channel or in the heat transfer performance through the channel during the test.

Detailed posttest metallographic analysis of the specimens was conducted. In preparation for analysis, the stainless steel (CRES 304) cover plates were machined off in order to evaluate the condition for the channels, Figure 105. The CRES 304 cover plate was also removed from one of the untested specimens for comparison, Figure 105a. The dark pattern associated with the channel in Figures 105b and 105c is apparently as a result of the propellant seeping under the cover plate during testing. The transverse dark markings seen in Figure 105c are guide lines drawn on the sample for cross sectioning. The channels were examined with the use of a SEM and energy dispersive X-ray spectroscopy (EDS). In addition, these samples were sectioned and prepared for metallographic evaluation.

Figure 106 shows typical features of the surface of untested specimen. The nodular structure as seen before with gold on nickel is evident. The apparent hole or pit in the gold coating (Location A in Figure 106b) was examined carefully. An EDS spectra at this point is shown to be primarily gold, with traces of copper and nickel. The

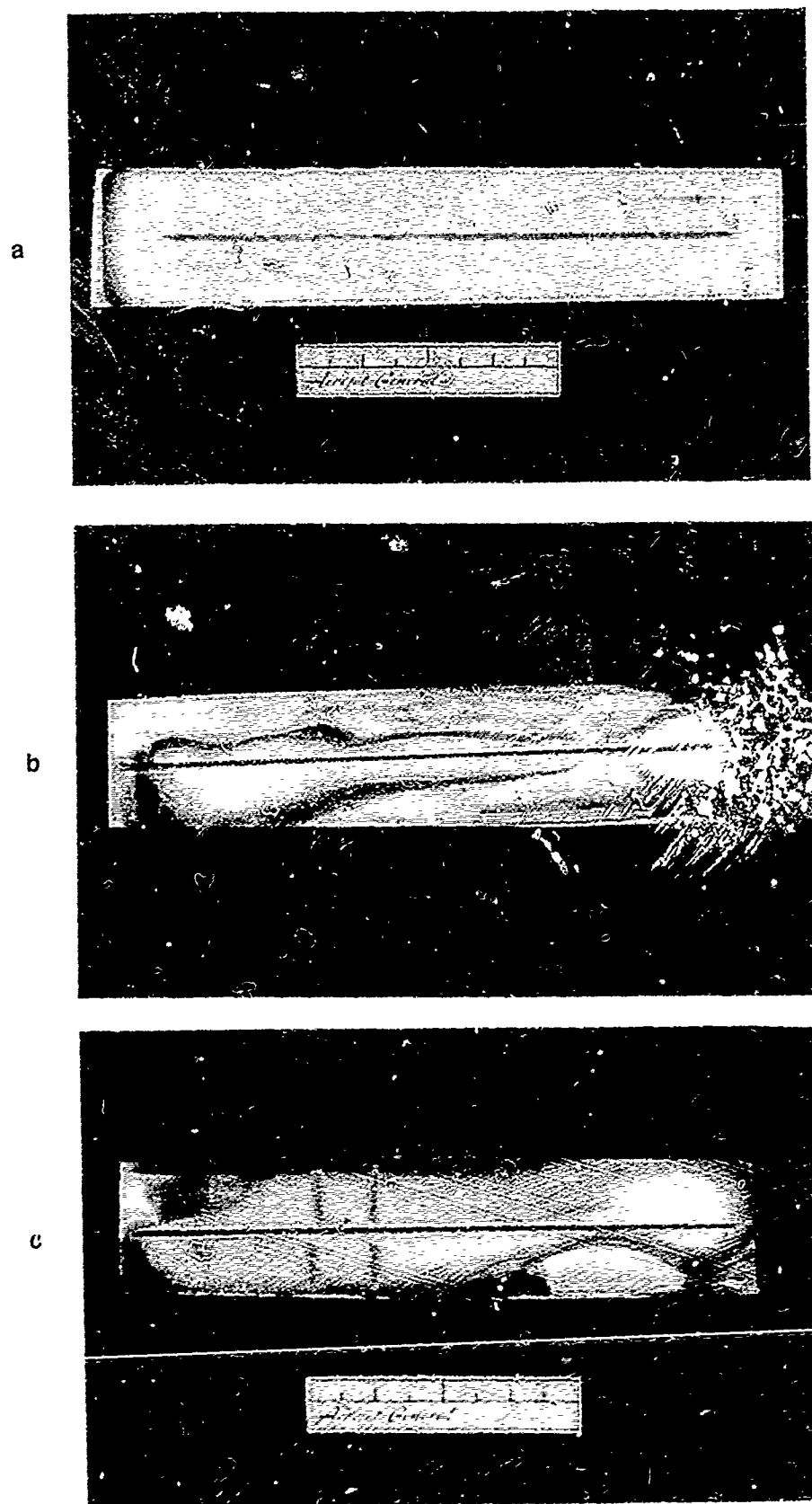
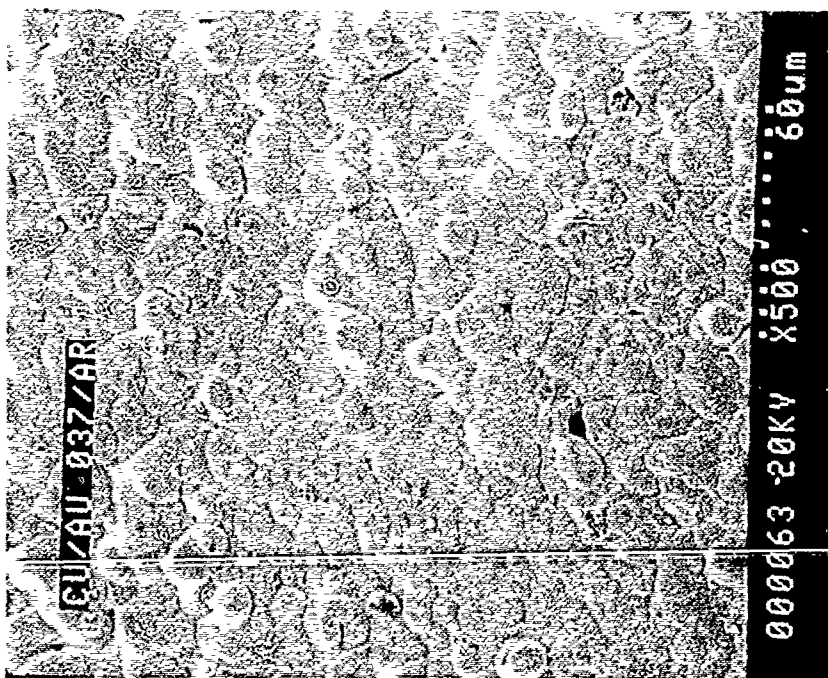
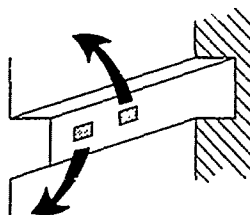
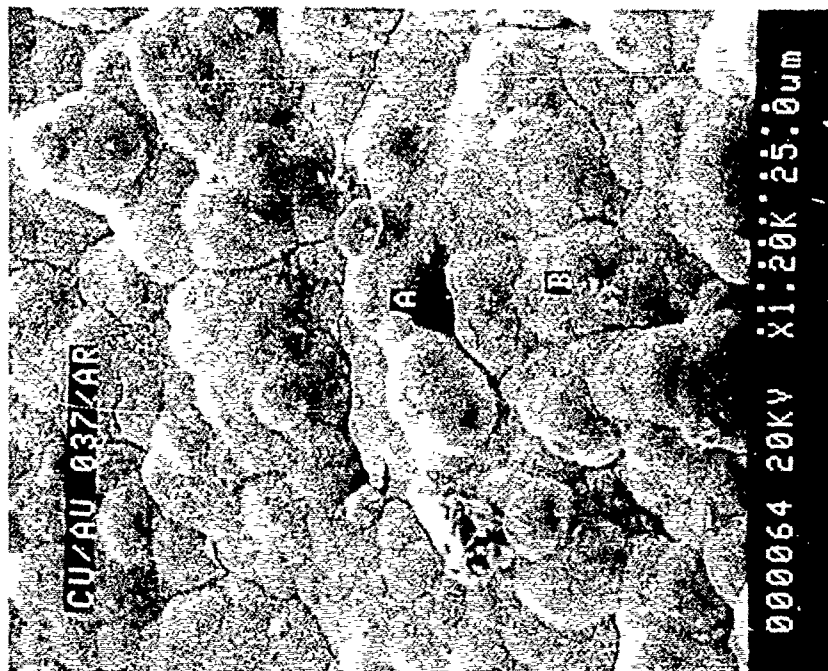


Figure 105. Disassembled Test Specimens Before and After Testing. a) Fabricated But Untested. b) Tested With 5 ppm Hydrogen Sulfide (Test M207). c) Tested With 10 ppm Hydrogen Sulfide (Test M208), Note: Transverse Marks on (c) and Guidelines for Sectioning



Pre-Test M207/M208



Pre-Test M207/M208

Figure 106. Gold Coating at the Bottom of an Untested Sample. Gold Was Found by EDS Analysis Even at the Bottom of the Hole (Location A – Figure 106b)

#### 4.3, Task 2.3—Thermal Sciences Laboratory Tests (cont.)

amount of copper and nickel was not appreciably more than in the EDS of other sections of the coating, indicating that it resulted from penetration of the beam into underlying layers of nickel and copper through the thin gold coating. Copper and nickel were not exposed, even at the bottom of the hole. No sulfur was found on the untested sample, but a small amount of chlorine was detected. The chlorine was most probably a residue contaminant from the plating process.

Cross sections of the untested specimen were also prepared and examined under the SEM to determine if the coverage of the channel surface was complete. Figure 107 shows three photomicrographs of a cross section from the middle of a channel of an untested specimen. A crack in the coatings was evident down the length of the specimen under the top corner of the channel. This crack developed during assembly or disassembly of the stainless steel specimen closeout. However, other than this crack, the coverage of the gold coating was very complete, with no evidence of cracks or voids between it and the underlying nickel diffusion barrier. Particularly impressive was the good coverage of the bottom of the channel, demonstrating excellent "throwing power" of the electrodeposited gold. The nickel diffusion barrier was quite lumpy, consistent with the findings from earlier in the program.

Two interesting features of the coatings are shown in Figure 107c. The first is the thin layer of gold which has apparently diffused through the nickel and into the copper substrate. This diffusion layer was found in the specimens after the stainless steel closeout was electron beam brazed into place. Apparently this process applied enough heat to the part to cause partial diffusion of the coatings into the substrate. Note also in Figure 107a that the region of diffused gold extends about three fourths of the distance up the side of the channel walls, and gradually lessens to zero near the top of the channel, where the nickel diffusion layer is thickest. The second feature of interest is the interface between the copper substrate and the nickel diffusion barrier shown in Figure 107c. It appears that the nickel is poorly bonded to the substrate, with many voids along the interface. In fact, the dark areas are particles of alumina ( $\text{Al}_2\text{O}_3$ ), imbedded in the surface of the copper by the plating vendor, who grit blasted the copper surface just prior to applying the electrodeposited coatings.

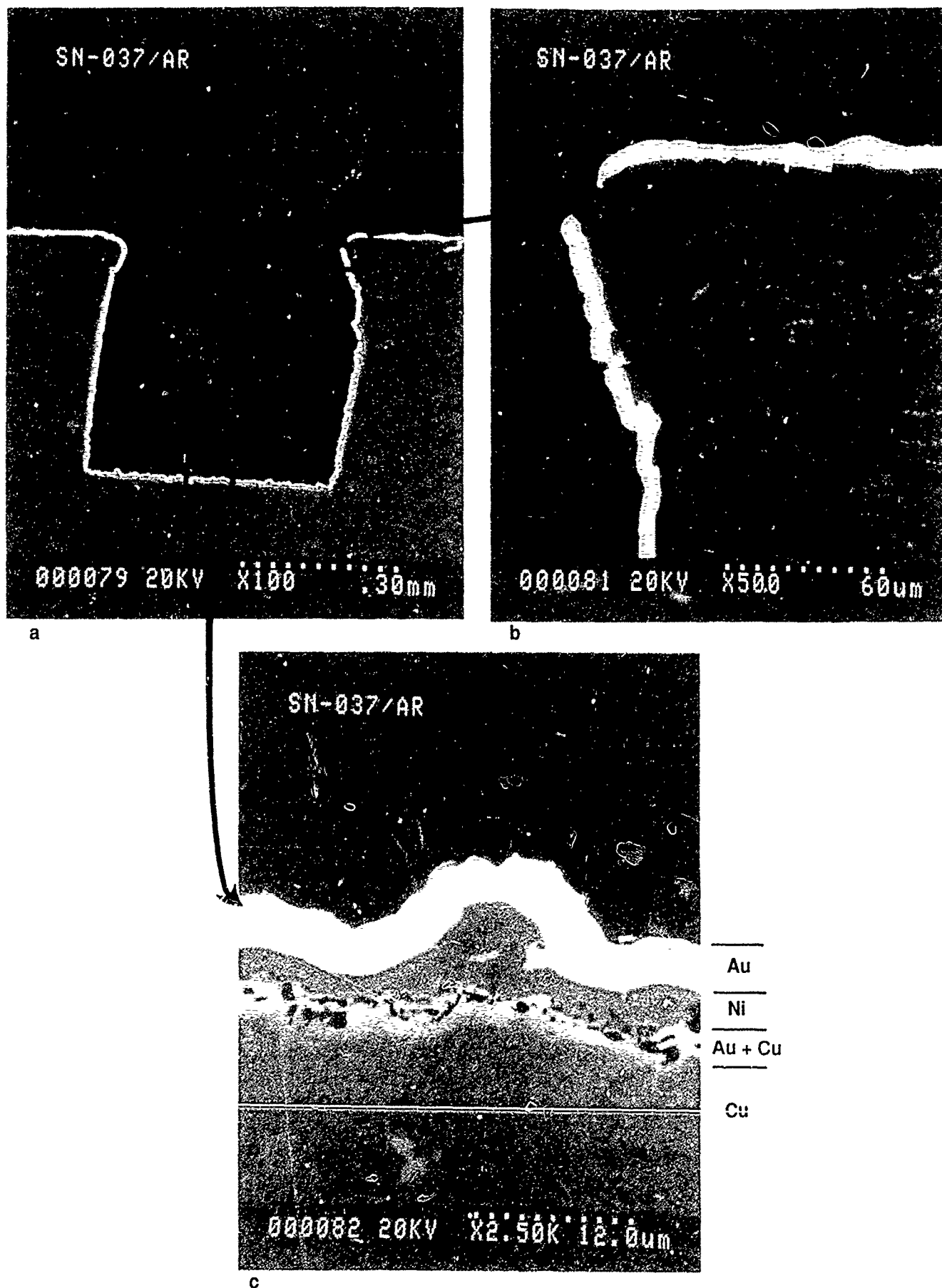


Figure 107. Cross Section of Untested Sample. Crack at the Top Corner is a Result of Mechanical Damage During Specimen Fabrication or Disassembly

#### 4.3, Task 2.3—Thermal Sciences Laboratory Tests (cont.)

Figure 108 shows the surface of the channel after testing with TG methane plus 5 ppm  $\text{H}_2\text{S}$  (Test M207). Note that the surface was virtually unaffected and appeared very similar to the untested surface. Also, a crack in the coatings was evident at the top corner of the channel. Again, this was caused by the mechanical assembly and disassembly of the test specimen, and not a result of the test conditions.

Cross sections of this specimen confirmed that the coating held up well during test M207. Figure 109 presents three photomicrographs of a cross section cut from the middle of the channel. Even at the bottom of the channel, where the coatings were the thinnest, the coating was unbreached and no corrosion of the copper channel was seen.

Figure 110 shows the surface of the channel after testing with TG methane plus 10 ppm  $\text{H}_2\text{S}$  (Test M208). Again, at low magnification (100X) the surface appeared virtually unaffected, with the dominant feature being the crack at the top corner from assembly and disassembly of the specimen. At higher magnification (500X) it appeared that a thin scale has formed evenly over the coating surface. At very high magnification (1200X), some definition of this thin scale was obtained. EDS analysis was performed at locations A, B, and C of Figure 110c. Location A showed a high sulfur content, with evidence of both copper and nickel. This area may be a combination of copper and nickel sulfides, though no analysis was conducted to determine how the sulfur was bound. Locations B and C gave EDS spectra which were close to the nominal spectra of untested coatings, with the exception that there was a very small amount of sulfur found in both locations.

Cross sections of this specimen confirmed that the coating held up well during test M208. Figure 111 presents three photomicrographs of a cross section cut from the middle of the channel. Even at the bottom of the channel, where the coatings were the thinnest, the coating was unbreached and no massive buildup of corrosion products was detected.

One final comparison should be drawn between the posttest condition of the uncoated channel, the channel which had coatings on only three sides, and the channel which had coatings on three sides with a stainless steel closeout. A cross section of each is shown in Figure 112. Each of these specimens was tested with TG methane con-

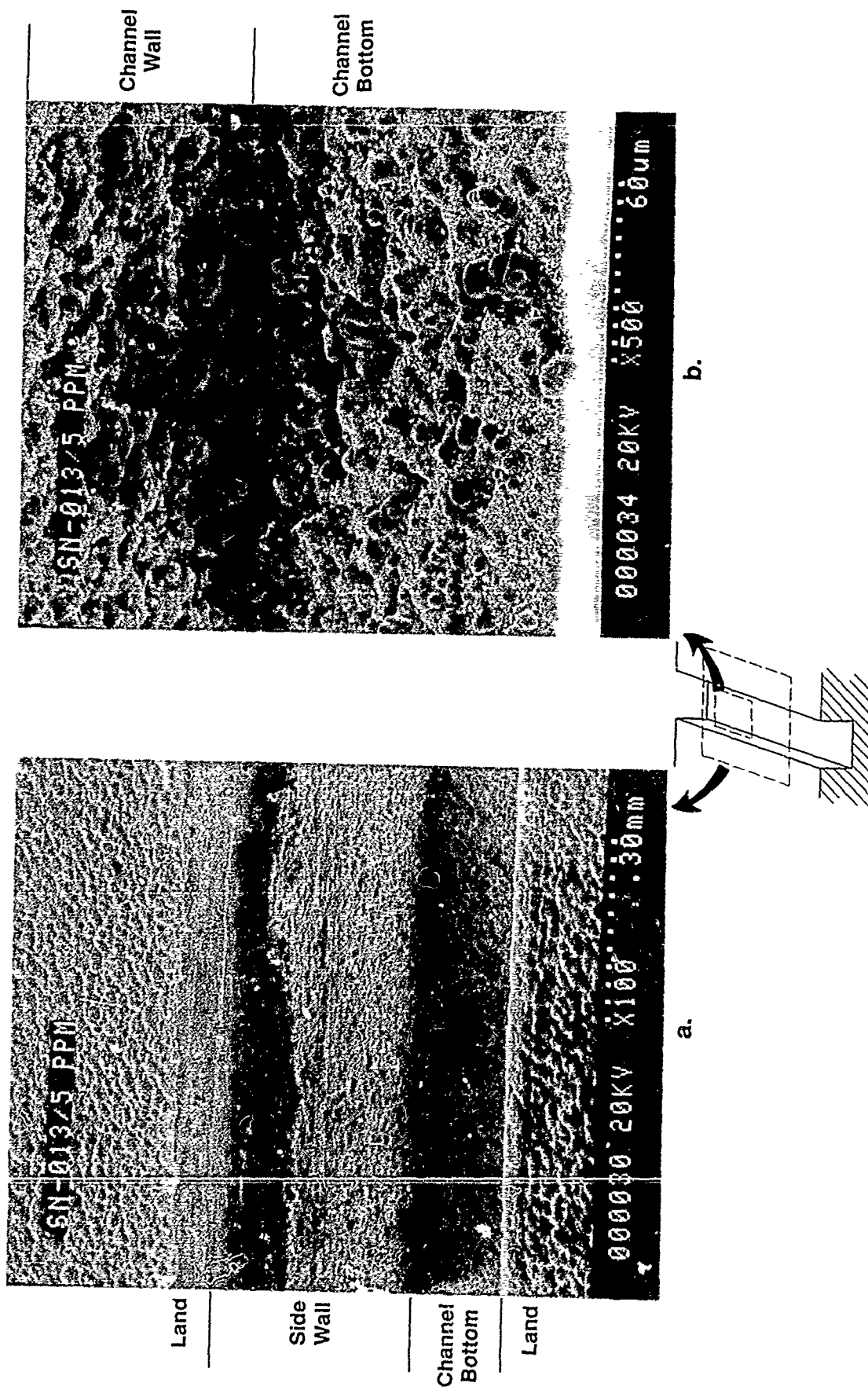
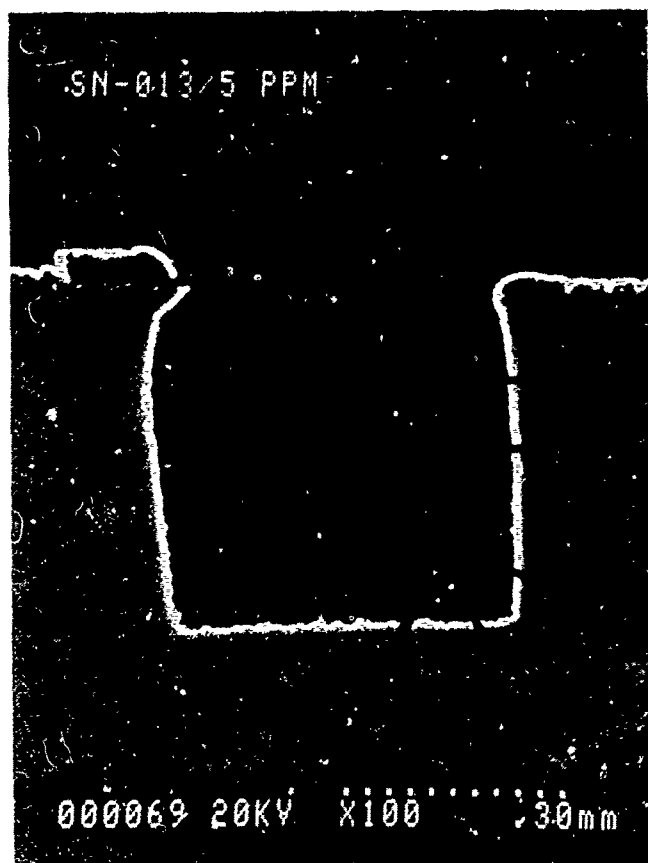
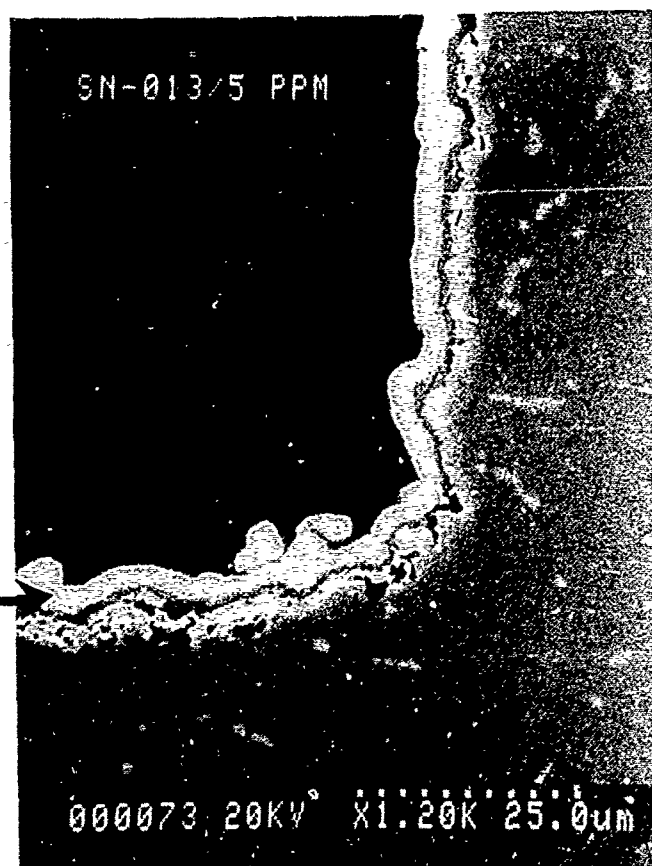


Figure 108. Looking Down at Channel Surface of Specimen After Testing With Methane Plus 5 ppm Hydrogen Sulfide (M207). Note the Coating Appears Mostly Unaffected



a



b



c

Au | Ni | Au + Cu | Cu

Figure 109. Cross Section of Sample After Test With 5 ppm Hydrogen Sulfide in Methane (M207)

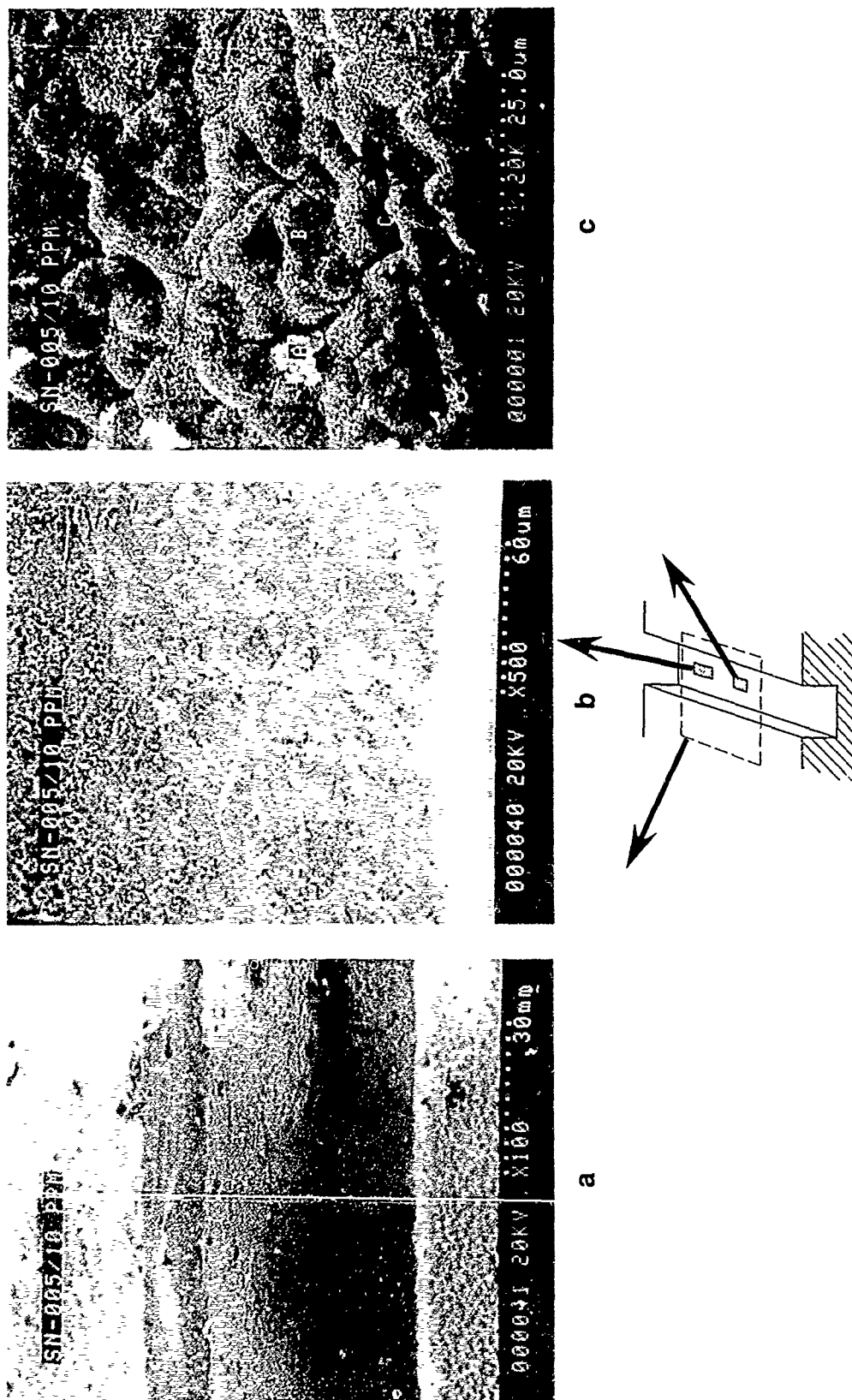


Figure 110. Looking Down at Channel Surface After Testing With Methane Plus 10 ppm  $H_2S$  (M208). Note That Channel Has Thin Covering of Sulfur "Fuzz"

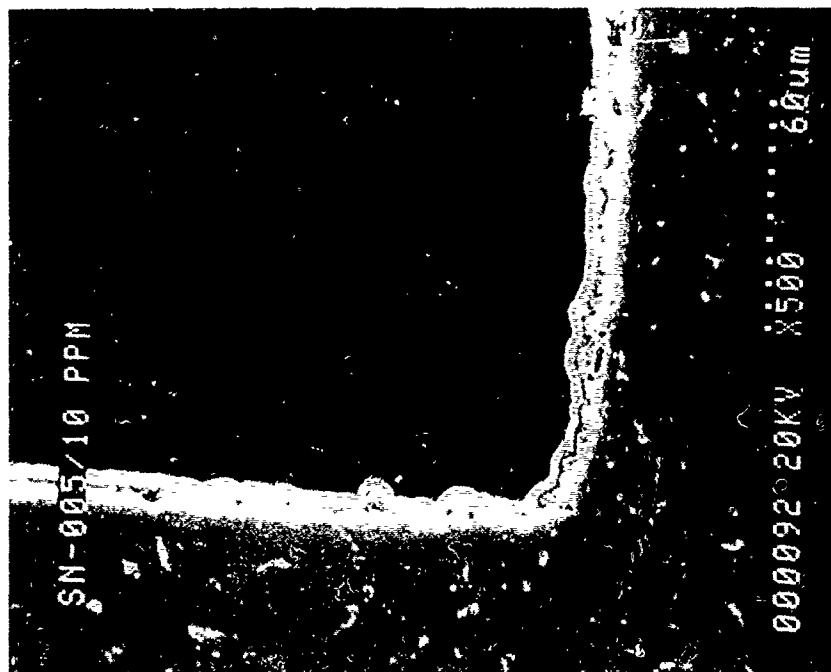
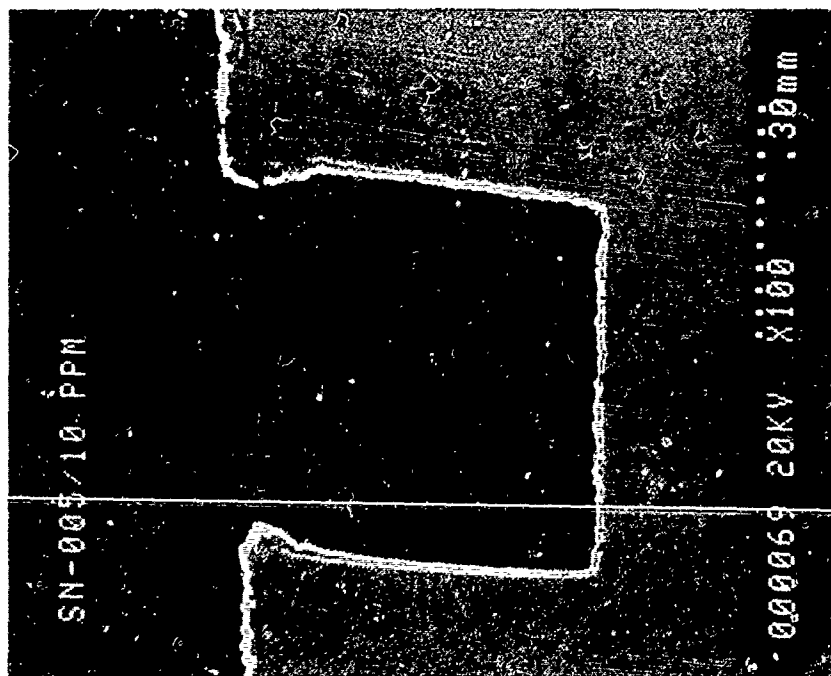


Figure 111. Cross Section of Sample Tested With 10 ppm Hydrogen Sulfide in Methane (M208)

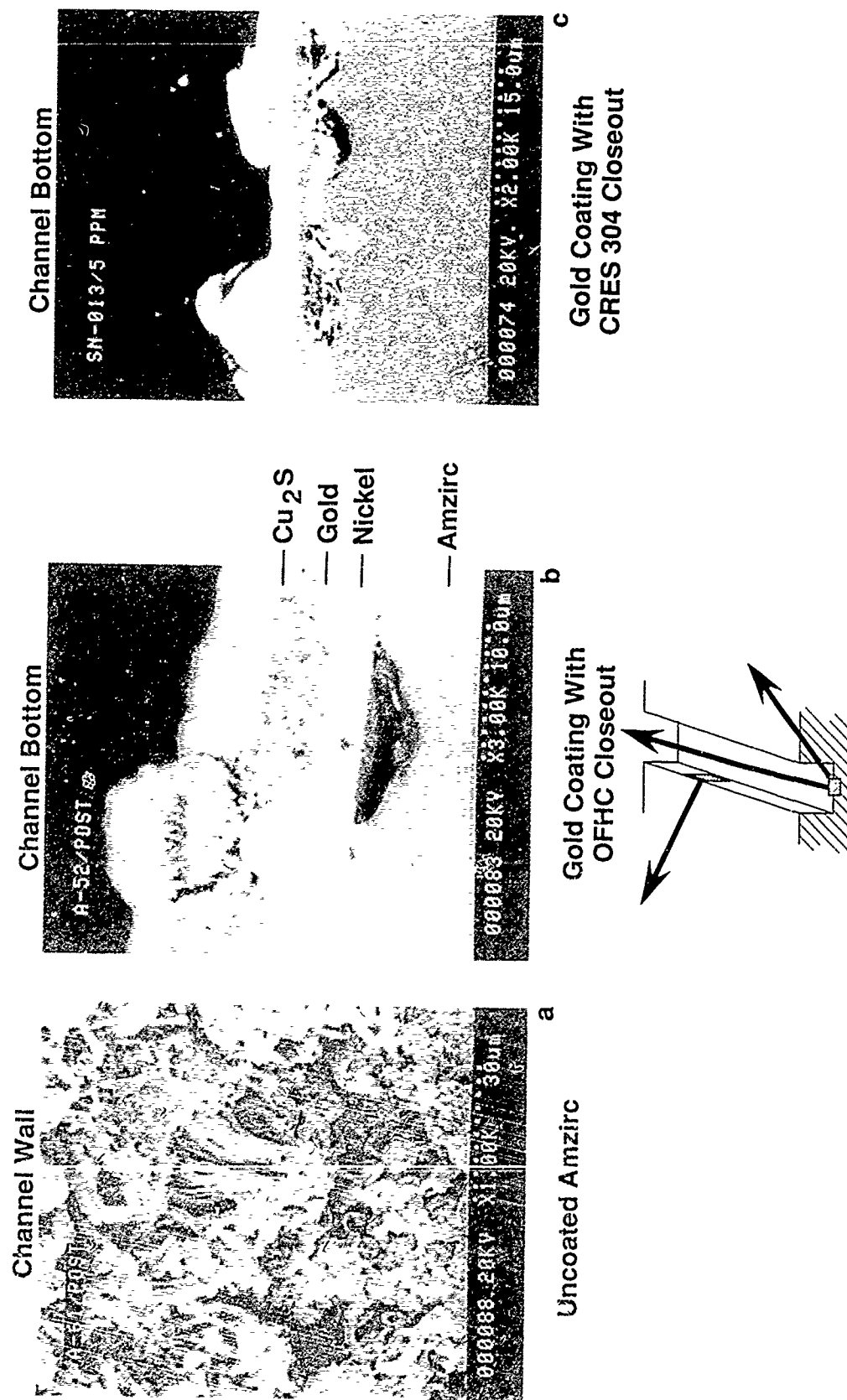


Figure 112. Post Test SEM Photos of Dynamic Test Specimen After Tests With Methane Plus 5 ppm  $\text{H}_2\text{S}$

#### 4.3, Task 2.3—Thermal Sciences Laboratory Tests (cont.)

taining 5 ppm  $\text{H}_2\text{S}$ , at similar temperature, pressure, and flow conditions (Tests M204, M205, and M207, respectively). Note the massive buildup of cuprous sulfide on the uncoated specimen of Figure 112a, which completely blocked the channel flow within 600 sec of operation. In Figure 112b, the coating appeared to resist attack, but was covered with a thick layer of cuprous sulfide, probably from corrosion of the uncoated closeout. Lastly in Figure 112c, a relatively clean coating, i.e., a gold coating with no cuprous sulfide deposit, was found intact after the test using a specimen with a stainless steel closeout. It is concluded, therefore, that the feasibility of using gold to prevent attack of the copper substrate has been demonstrated. However, development of a practical, reliable method for the application of a protective gold coating to the inside of small, high aspect ratio copper alloy channels, remains to be accomplished.

## 5.0 TASK 3—PROTECTIVE MEASURES VERIFICATION PROGRAM

The objective of Task 3 is to recommend and plan a test program for the verification of the protective measures demonstrated in Task 2 under actual engine operating conditions. One subtask was conducted to achieve the objective of Task 3, i.e., Task 3.1, Program Plan Preparation.

### 5.1 TASK 3.1—PROGRAM PLAN PREPARATION

A program plan and cost estimate were prepared for the verification of protective coatings as applied to cooling channels as demonstrated in Task 2.

Task 1 results strongly indicate that the presence of even small amounts of sulfur-containing compounds (<1 ppm) in hydrocarbon fuels (methane, propane, and RP-1) can produce unacceptable corrosion of the cooling channels in copper chamber liners. This corrosion increases the wall temperature and obstructs the coolant flow and thus reduces chamber life and/or increases maintenance costs. It does not appear feasible to circumvent the corrosion problem by reducing the wall temperature through more conservative design. Currently, only completely sulfur-free fuel can be considered for reliable operation with bare, i.e., unprotected, cooling channels.

Comparative tests conducted in Task 2 with gold- and platinum-electroplated copper cooling channels strongly indicate that very thin protective deposits of corrosion-resistant metals eliminates corrosion of copper cooling channels by sulfur-containing impurities.

The objective of this program is to verify that fuels containing measurable amounts of sulfur-containing impurities can be employed for cooling high-pressure booster engines if a thin, protective, corrosion-resistant coating is applied to all surfaces of the copper cooling channels. Figure 113 defines the general approach and program logic. The program will be conducted in five tasks over a 36-month period, as shown in the Program Schedule, Figure 114. Alternative fabrication techniques for applying the protective coatings will be investigated and comparative tests will be conducted. After selection of the best protective material and deposition process, two LO<sub>2</sub>/methane thrust chambers will be fabricated and hot-fire tested to verify the efficacy of the coatings in advanced booster engine service.

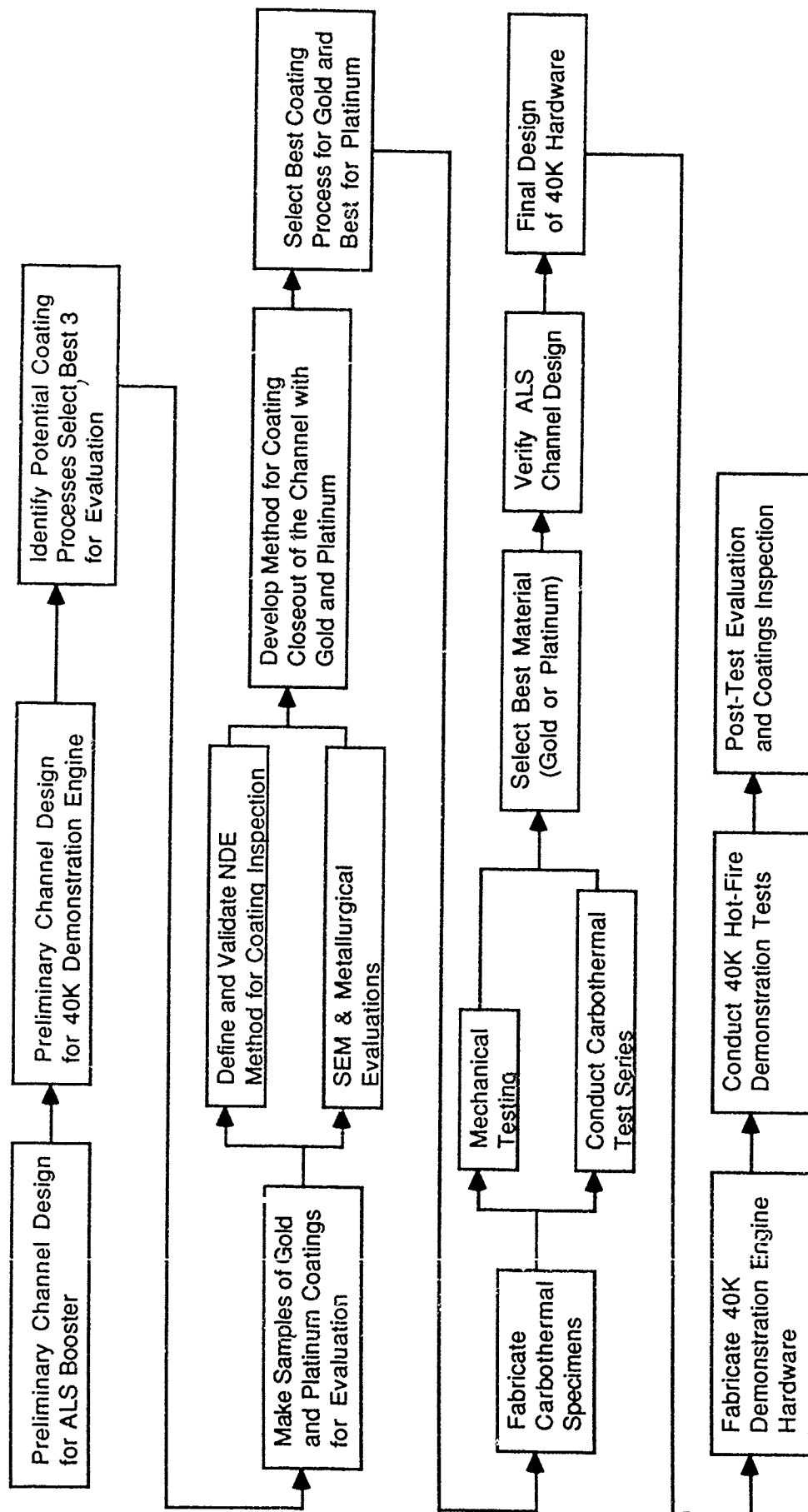


Figure 113. Program Logic: Validation of Protected Copper Liner for Hydrocarbon Cooled Thrust Chamber

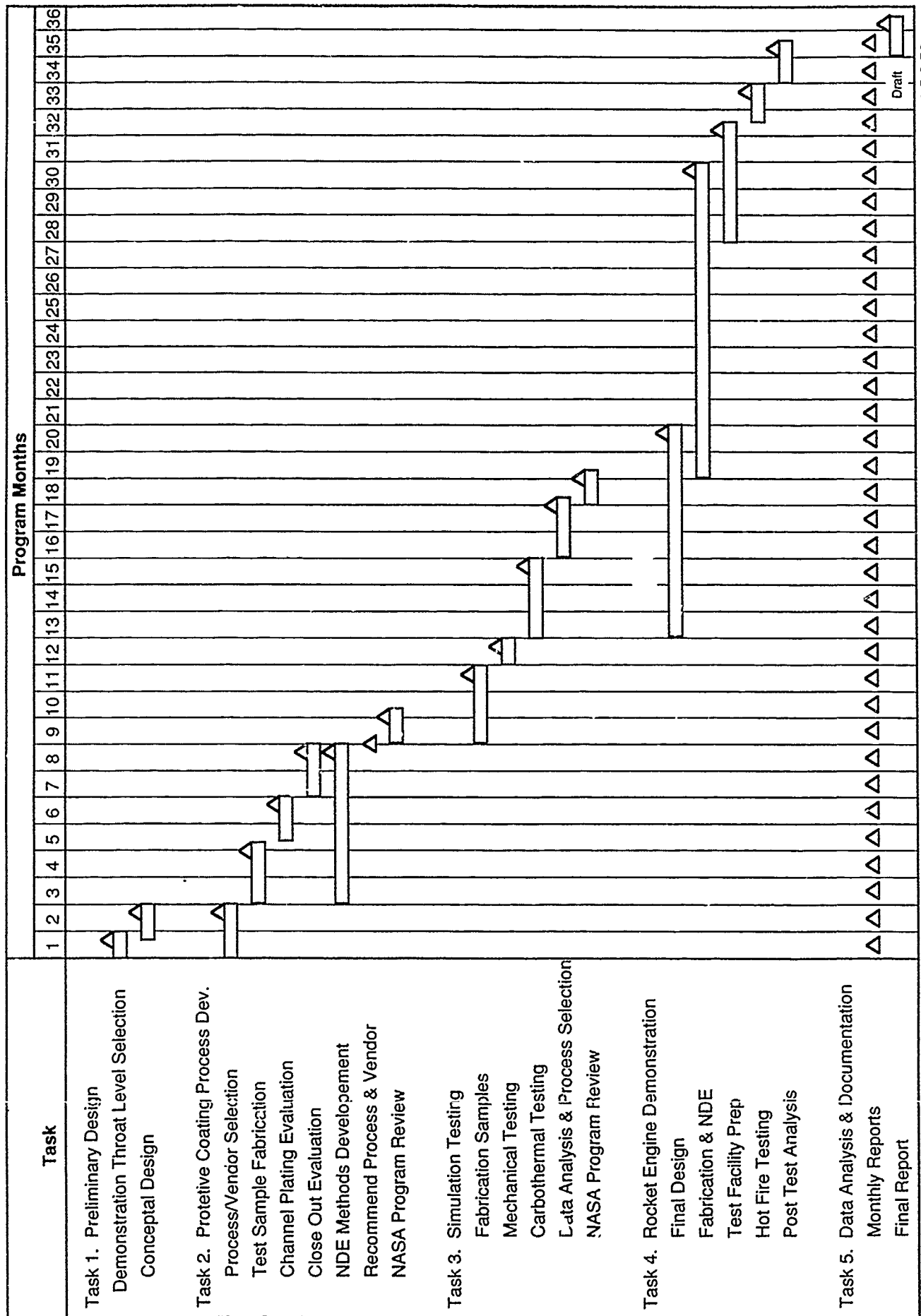


Figure 114. Program Schedule: Validation of Protected Copper Liner for Hydrocarbon Cooled Thrust Chamber 1.5.0.53

### 5.1, Task 3.1—Program Plan Preparation (cont.)

Task 1 will select a suitable thrust level and set of operating conditions which will adequately simulate the heat flux and cooling channel configuration of an advanced booster engine. For planning purposes, we are recommending a 40,000 lbF thrust LO<sub>2</sub>/methane engine configuration operating at a chamber pressure of 2500 to 3000 psia. A conceptual design will be created in sufficient detail to allow selection of the cooling channel width and depth to simulate those of the larger booster engine, e.g., 750,000 lbF thrust.

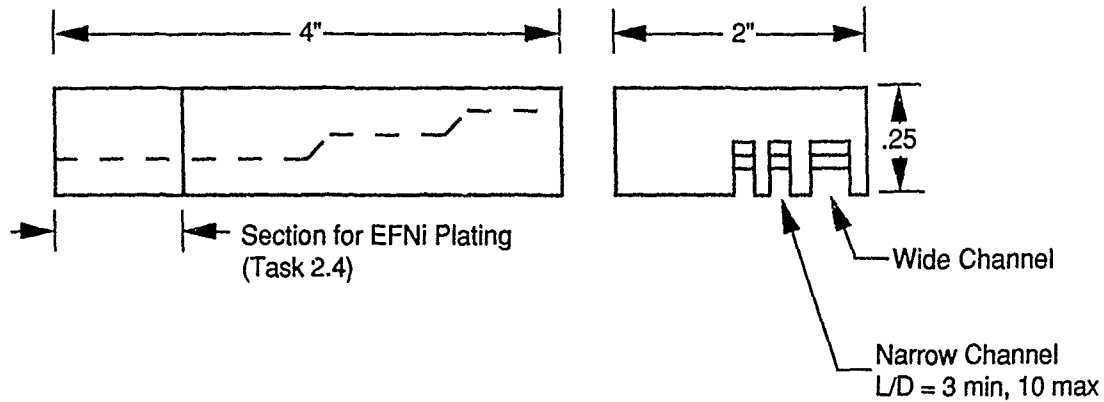
Task 2 will investigate three candidate fabrication techniques for applying protective material to the cooling channels and will develop a suitable nondestructive test method to assure complete, crack-free coverage. Figure 115 defines the scope of work for protecting the three walls of the machined slots. Modification of the electro-forming process may be required to protect the back side of the coolant channel prior to applying the nickel closeout. Figure 116 shows two test methods which will be used to test the closeout bond after application of a protective coating.

Task 3 will subject specimens made by the candidate processes to performance and life simulation tests. The first subtask will be mechanical testing of coated channels which will include pressure testing and simulated cyclic strain testing. The objective of these tests will be to verify the structural integrity of a coated channel system and to demonstrate that the coatings will tolerate the expected strain levels without spalling, cracking, or other degradation. The second subtask will be thermal testing using the Aerojet Carbothermal Test Apparatus. The objective of these tests will be to demonstrate the ability of the coating system to resist corrosion by sulfur compounds systematically added to pure methane. In these tests, methane containing a known quantity of a sulfur-containing compound will be flowed through a coated copper channel. Coolant channel conditions will be maintained for a duration of approximately 1000 sec, which is equivalent to six flights. The performance parameters will include measurement of changes in heat transfer and pressure drop with time. The 12-test program proposed is defined in Table 20. Posttest metallurgical inspection of each tested section will be performed.

Task 4 will consist of a rocket engine demonstration using the thrust level and operating conditions selected in Task 1. The task will be based on the use of an

Apply Protective Coating to 3 Sides of Channel

Fabricate 18 slotted copper plating process evaluation specimens



Task Variables

- Channel width and width to depth ratio
- Coating process options select 2
  - Aqueous bath
  - Fused salt bath
  - CVD
  - Electron beam evaporation
  - Other
- Vendor Selection
- Samples prepared for by 3 vendors for 2 materials, Fabricate 3 samples for each process.  
Sample required  $3 \times 3 \times 2 = 18$

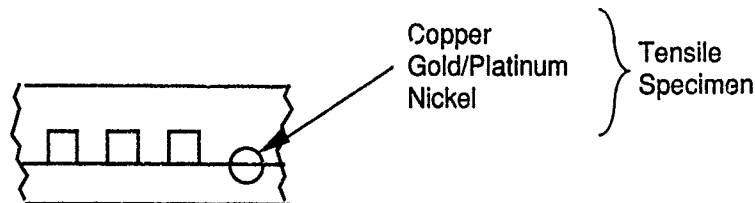
Process Evaluation Criteria -

- Channel coverage in corners
- Depth/width vs. uniformity
- Bond quality
- Local defects and porosity

**Figure 115. Task 2.2 and 2.3: Protective Coating Process Development**

### Apply Protective Coating to Channel Closeout

In addition to plating the 3 sides of the channel, it will also be necessary to plate the protective material on the channel wax filler before the electroformed nickel closeout is applied, as shown below.



The bond between the copper and the protective material must be evaluated. The suggested test method is shown below. Forth-eight (48) tests will be conducted.

### Bond Joint Test Method

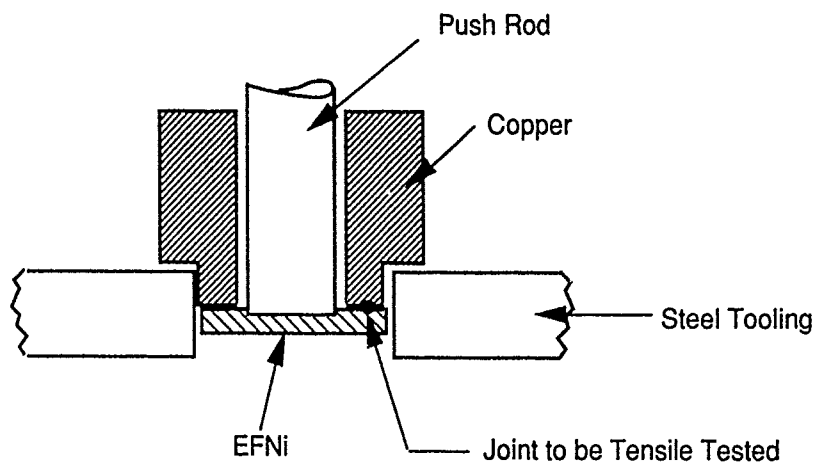


**Figure 116. Task 2.4: Fabrication Experiments in Support of Closeout**

TABLE 20  
PROPOSED CARBOTHERMAL TEST MATRIX

<u>Test No</u>	<u>Fuel</u>	<u>Additives</u>	<u>Level</u>	<u>Coating</u>	<u>T<sub>wall</sub></u>	<u>Comments</u>
1	Methane	None	0	None	700	Baseline
2	Methane	None	0	Gold	700	
3	Methane	None	0	Platinum	700	
4	Methane	H <sub>2</sub> S	2 ppm	None	700	2 ppm Series
5	Methane	H <sub>2</sub> S	2 ppm	Gold	700	
6	Methane	H <sub>2</sub> S	2 ppm	Platinum	700	
7	Methane	H <sub>2</sub> S	10 ppm	Gold	700	10 ppm Series
8	Methane	H <sub>2</sub> S	10 ppm	Platinum	700	
9	Methane	H <sub>2</sub> S	TBD	Gold	900	T <sub>wall</sub> Series
10	Methane	H <sub>2</sub> S	TBD	Platinum	900	
11	Contingency					
12	Contingency					

### 5.1, Task 3.1—Program Plan Preparation (cont.)

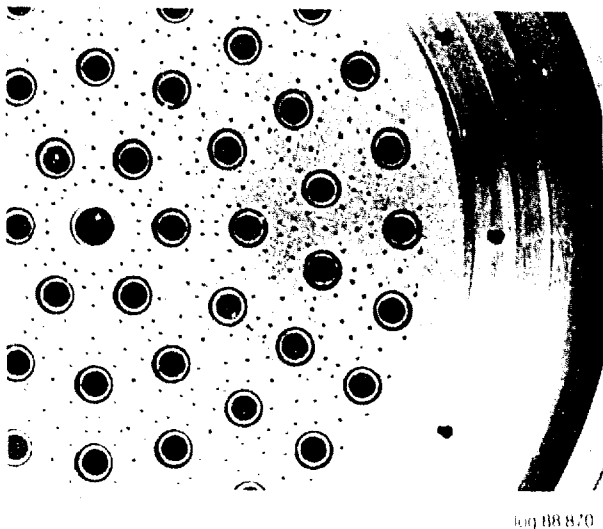
existing, well-characterized LO<sub>2</sub>/methane injector, Figure 117, and the modification of an existing combustion chamber design, Figure 118, to provide the proper cooling channel configurations. Two new thrust chambers will be fabricated using the best protective coating material and deposition process that evolves from the experimental activities of Tasks 2 and 3.

A 10-day hot-fire test program which simulates several full-duration flights will be conducted. The initial checkout tests will be conducted with sulfur-free fuel to verify the design and establish baseline performance characteristics of the chamber. These will be followed by testing with fuel containing a TBD amount of sulfur-containing compounds.

Task 5 is devoted to final data analysis and documentation.

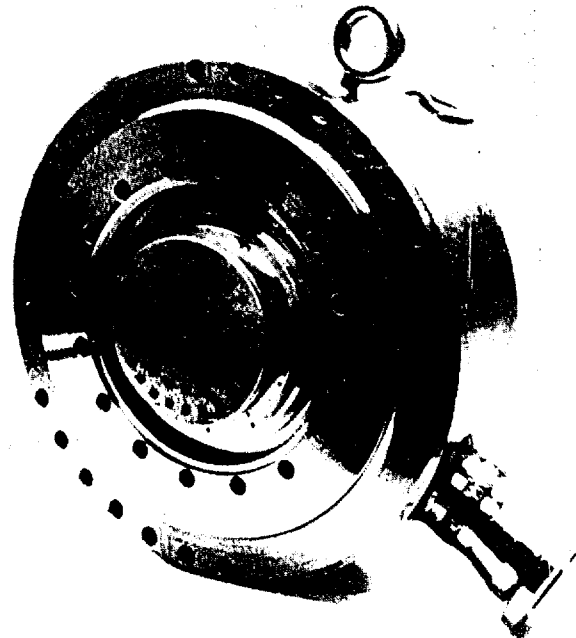
A cost estimate for the program has been prepared and forwarded to the NASA Program Manager under separate cover.

Details of Fuel Cooled Face Using  
Platelet Construction



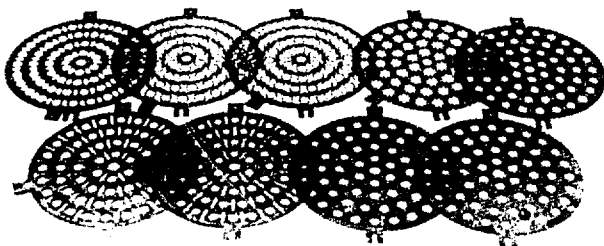
log 88.870

Our 40,000 lbF, 60 Element Swirl  
Coax Injector P/N 1188144 is  
Stable, High Performing and  
Thermally Characterized



log 88.872B

Fuel Cooled Nickel Face Plates  
Assure Long Life and High Per-  
formance



log 88.871

Figure 117. An Existing, Well-Characterized Injector Can Be Used For  
Testing at 40,000 lbf

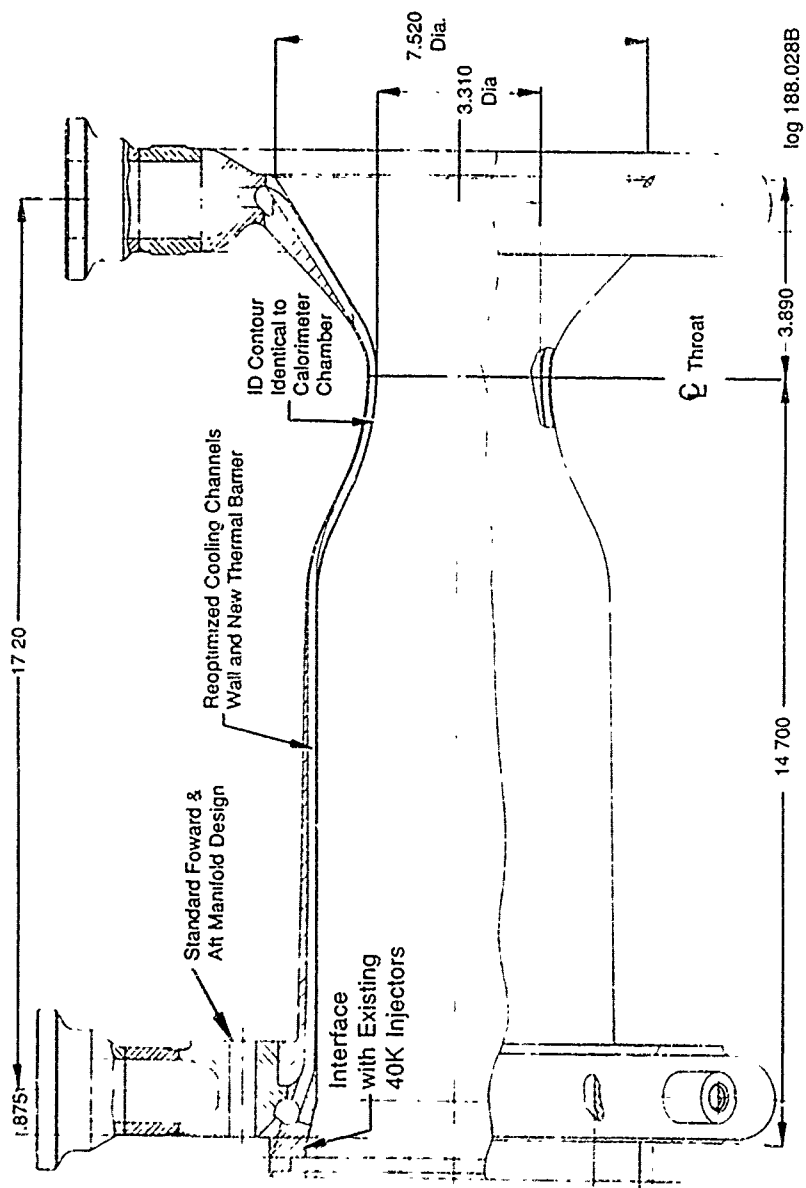


Figure 118. Our 40K Contoured Chamber Will Be Similar to an Existing Design

## 6.0 REFERENCES

1. Roback, R., Szetela, E.J., and Spadaccini, L.J., "Deposit Formation in Hydrocarbon Fuels," NASA CR-165405, August, 1981.
2. Giovanetti, A.J., Spadaccini, L.J., and Szetela, E.J., "Deposit Formation and Heat Transfer in Hydrocarbon Rocket Fuels," NASA CR-168277, October, 1983.
3. Morinoshi, R. and Cook, R.T., "Methane Heat Transfer Investigation," Contract NAS 8-34977.

APPENDIX A  
STATIC TEST LABORATORY  
PROCEDURES

AMPUL TEST  
COPPER-HYDROCARBON COMPATIBILITY  
PROPELLANT PREPARATION

I. Propellants Containing Dissolved Air

1. Using a nitrogen pressurization and purge system, transfer propellant to a sample bottle.
2. In a fume hood, transfer propellant from the sample bottle to an open flask.
3. Bubble air through the propellant in the flask for ~1/2 hour.
4. Make up the required test mixtures by adding the appropriate amounts of contaminants to measured quantities of propellants.
5. Set aside a sample of each mixture for analysis.

II. Propellants Without Dissolved Air

1. Using a nitrogen pressurization and purge system, transfer propellant to a sample bottle.
2. Under a nitrogen atmosphere in the glove box, transfer ~75 ml propellant from the sample bottle to the degassing flask.
3. Close the degassing flask by inserting a tubing section containing a stopcock in the socket at the flask opening.
4. Remove the degassing flask and stopcock assembly from the glove box and install it on the vacuum rack.
5. Pull a vacuum on the contents of the degassing flask for ~1/2 hour.
6. Remove the closed degassing flask and stopcock assembly from the vacuum rack and place it back in the glove box.
7. Set aside a sample of each propellant for analysis.

## AMPUL LOADING

### I. Propellants Containing Dissolved Air

1. Place any required metal specimen in the ampul.
2. In a fume hood, transfer 4.0 ml of the appropriate propellant mixture from the storage container to the ampul using a syringe.
3. Using a torch, seal the ampul 6 in. from the bottom.
4. Place the sealed ampul in a protective sleeve and store the assembly in a freezer until testing begins.

### II. Propellants Without Dissolved Air

1. Place any required metal specimen in the ampul.
2. Place the ampul in the glove box.
3. Using a syringe, transfer 4.0 ml of the appropriate propellant mixture from the storage container to the ampul.
4. Close the ampul by placing the open tygon tube end of a tygon tube/stopcock assembly over the open end of the ampul.
5. Remove the ampul and stopcock assembly from the glove box and install it on the vacuum rack.
6. Partially immerse the ampul in the  $LN_2$  to freeze the propellant.
7. Pull a vacuum on the ampul.
8. Seal the ampul 6 in. from the bottom using a torch.
9. Place the sealed ampul in a protective sleeve and store the assembly in a freezer until testing begins.

## AMPUL UNLOADING

1. Allow the ampul to come to room temperature and remove any moisture that may have condensed on the outer surfaces.
2. Install the ampul in the tygon tube section at the unloading port on the vacuum rack.
3. Pull a vacuum on the manifold up to the sealed ampul.
4. Pressurize the manifold from the manometer to the ampul to approximately 1 atm with  $N_2$  and record the pressure.
5. Close the stopcock at the manifold inlet to the ampul.
6. Break the top of the ampul.
7. Open the stopcock at the manifold inlet slowly. Let the pressure equilibrate and record the equilibrated value.
8. Take gas samples for analysis by CG using the manifold sampling septum.
9. Close the manifold inlet stopcock and the ampul inlet stopcock. Remove the ampul stopcock assembly from the vacuum rack and place it in the glove box.
10. Disconnect the ampul from the tygon tube section.
11. Transfer the propellant from the ampul to a septum sample bottle using a syringe. Submit the propellant sample for chemical analysis.
12. Remove any metal specimen from the ampul and obtain specimen weight, dimensions, 35 mm photographs, and SEM photographs.

## BOMB TEST LOADING

1. Secure a prepared metal specimen on the sample holding rod.
2. Place the specimen/holding rod assembly in the pressure vessel.
3. Put the vessel closure in place and tighten it securely.
4. Calibrate the transducer on the pressure vessel.
5. Fill the pressure vessel with helium and perform a leak check.
6. Connect the pressure vessel to the gas handling system and evaluate the vessel and the handling system.
7. Condense the appropriate quantities of propellants and contaminants into the pressure vessel using P-V-T determinations and vacuum transfer techniques.
8. Bring the vessel to ambient temperature and check the pressure.
9. Place the vessel in the furnace and install insulation over the furnace opening between the instrumentation and the top of the vessel.
10. Allow the vessel to come to the appropriate test temperature. Vessel pressures above the desired test pressure can be adjusted to the appropriate range by venting through a line that exhausts to an area remote from the furnace.

## BOMB TEST UNLOADING

1. Remove the pressure vessel from the furnace.
2. While the vessel is still hot, obtain gas samples for analysis by gas chromatography.
3. Cool the vessel and vent the propellant.
4. Remove the vessel closure and examine the inside of the vessel for evidence of reaction.
5. Remove the specimen/holding rod assembly from the vessel.
6. Take the metal specimen off of the holding rod. Obtain the weight, dimensions, a 35 mm photograph, and SEM photographs of the specimen.

APPENDIX B

DYNAMIC TEST LABORATORY PROCEDURES

**AEROJET TECHSYSTEMS COMPANY  
TEST OPERATIONS**

ATP-TDO	A-CARBOT-1000
ACILITY	CHEM BAY 5
TEST NO.	
UNIT S/N	

CARBOTHERMAL  
METHANE  
TEST

PAGE	1 or 4
PREPARED BY	W.E. Sobieralski 22 Sep 88
APPROVED	<i>[Signature]</i>
APPROVED	N.A.
REFERENCE	

INITIAL		OPERATION
T D	INSP	
		Index and ATP-TDO Change Letters and Revision Dates Verified.
		1.0 Record specimen number _____, specimen size _____, fuel used _____.
		2.0 Zero and calibrate transducers, thermocouples and M.M.
		3.0 Ensure that the CH <sub>4</sub> system is connected to test plumbing and check that the RP-1 system is disconnected.
		4.0 CLOSE all hand and remote valves.
		5.0 Verify 6000 psig in methane cylinders.
		6.0 Set methane regulator outlet to _____ psig.
		7.0 Verify GN <sub>2</sub> supply valve for remote valves is OPEN.
		8.0 Ensure sample bottle is attached to system.
		9.0 Hook vacuum pump to HV-16. OPEN HV-16 and HV-15 and pull vacuum on sample bottle.
		10.0 CLOSE HV-16 and disconnect vacuum pump.
		11.0 OPEN HV-10 and RV-4.
		12.0 Set GN <sub>2</sub> supply regulator to _____ psig.
		13.0 OPEN RV-3 and verify flowmeter working.
		14.0 CLOSE RV-3 and RV-4.
		15.0 Torque channel support bolts 2, 4, 6 and 8 to 140 in-lbs. Torque edge support bolts to 60 in-lbs.

INITIAL		OPERATION
T.D.	INSP.	
		16.0 OPEN RV-3 and pressurize system to 2000 psig and leak check system.
		17.0 CLOSE RV-3.
		18.0 OPEN CH <sub>4</sub> supply valve and RV-2. Pressurize the system to 4000 psig. Leak check.
		19.0 Once leak check is accomplished, vent pressure through HV-17.
		20.0 Torque channel support bolts 2, 4, 6 and 8 to 80 in-lbs.
		21.0 OPEN HV-17.
		22.0 OPEN RV-4.
		23.0 OPEN RV-3 and adjust GN <sub>2</sub> supply regulator to desired flow rate.
		24.0 OPEN main LN <sub>2</sub> valve (at tank), secondary LN <sub>2</sub> valve and bypass LN <sub>2</sub> valve.
		25.0 OPEN cooling water valve HV-19.
		26.0 Give 10 minute warning.
		27.0 OPEN HV-18 GN <sub>2</sub> purge to waste drum and HV-20 GN <sub>2</sub> . Purge to test block.
		28.0 Put cover on box.
		29.0 Turn GN <sub>2</sub> purges on to electrical boxes.
		30.0 Turn overhead blowers ON.
		31.0 Verify heater control box plugged in.
		32.0 Begin data.
		33.0 Turn 440 main breaker ON.
		34.0 Turn heater main switch ON.
		35.0 OPEN HV-11, HV-12, HV-13 and HV-14.
		36.0 CLOSE HV-10 and RV-4.

INITIAL		OPERATION
T.D.	INSP.	
		37.0 Turn control panel heater switch ON and begin adjusting temperature with potentiometer to desired temperature.
		38.0 OPEN methane valve valve at cylinder regulator.
		39.0 Give 5 minute warning
		40.0 CLOSE RV-3 and immediately OPEN RV-2.
		41.0 Use HV-17 to adjust back pressure to 1000 psig and watch for any abnormalities (if filters begin to clog - OPEN RV-4).
		42.0 Run methane for approximately _____ seconds.
		43.0 OPEN RV-5 and take sample of methane at _____ seconds into test.
		44.0 When test duration is completed CLOSE RV-2 and immediately OPEN RV-3.
		45.0 OPEN HV-17 all the way.
		46.0 Turn heaters OFF and begin cool down.
		47.0 Turn bay heater switch OFF on 440 breaker.
		48.0 Clear bay to authorized personnel only.
		49.0 CLOSE methane valve at regulator ,
		50.0 OPEN HV-32, cooling water to block.
		51.0 CLOSE LN <sub>2</sub> bypass valve and secondary LN <sub>2</sub> valve.
		52.0 CLOSE sample bottle valve.
		53.0 Re-restrict the bay to all personnel.
		54.0 CLOSE main LN <sub>2</sub> valve.
		55.0 When the block reaches 500°F, vent remaining methane through RV-2.
		56.0 End data.
		57.0 When the block reaches 200°F, clear bay to all personnel.
		58.0 Turn blowers and GN <sub>2</sub> purges OFF.



APPENDIX C

DYNAMIC TEST DATA REDUCTION PROGRAM  
LISTING AND SAMPLE OUTPUT



```

CLS
PRINT title$; TAB(66); title2$
'LPRINT psetup$
RETURN

```

setrunvars:

```

IF MID$(run$, 1, 1) = "M" OR MID$(run$, 1, 1) = "H" THEN fuel$ = "methane"
IF MID$(run$, 1, 1) = "R" OR MID$(run$, 1, 1) = "P" THEN fuel$ = "RP-1"
IF MID$(run$, 1, 1) = "D" OR MID$(run$, 1, 1) = "P" THEN fuel$ = "propane"
stime = VAL(stime$)
etime = VAL(etime$)
leng = VAL(leng$)
title1$ = ""
title2$ = "Dateded4 vs. " + ver$ + SPACE$(10)
title2$ = title2$ + "channel length = " + leng$
lineno = 1
RETURN

```

getfile:

```

hdrfile$ = "hfile.dat"

'LOCATE 11, 25
'INPUT "Enter Run Number: ", run$
'LOCATE 12, 25
INPUT "Enter Run Date: ", rdate$
LOCATE 13, 25
INPUT "Data file name: ", infile$
LOCATE 14, 25
INPUT "Output written to: ", outfile$
LOCATE 15, 25
INPUT "Start time: ", stime$
'LOCATE 16, 25
'INPUT "Ending time: ", etime$
RETURN

```

fopen:

```

OPEN hdrfile$ FOR INPUT AS #3
RETURN

```

openrunfile:

```

runfile$ = "c:\lang\qb\data\" + run$ + ".PRN"
outfile$ = run$ + ".out"
OPEN outfile$ FOR OUTPUT AS #2
OPEN runfile$ FOR INPUT AS #1
RETURN

```

docalcs:

data starts with channel 41, each seperated by a comma  
 we want to keep channels 46,47,65,66,71,74,75,76,77,81,85.  
 and seperate each field with a comma.

```

LOCATE 16, 25
PRINT "On Run Number: "
LOCATE 17, 25
PRINT "Working on Time: "

```

```

      WHILE NOT EOF(3)
        INPUT #3, run$, roate$, stime$, etime$, leng$
        IF MID$(run$, 1, 1) = " " THEN GOTO skipfile

        LOCATE 16, 52: PRINT run$
        GOSUB openrunfile
        GOSUB setrunvars
        WHILE NOT EOF(1)
          LINE INPUT #1, inline$
          outline$ = ""
          start = 1
          j = 1

          skipchannels = 5: GOSUB fatchannel 46
          skipchannels = 0: GOSUB fatchannel 47
          skipchannels = 17: GOSUB fatchannel 65
          skipchannels = 0: GOSUB fatchannel 66
          skipchannels = 4: GOSUB fatchannel 71
          skipchannels = 2: GOSUB fatchannel 74
          skipchannels = 0: GOSUB fatchannel 75
          skipchannels = 0: GOSUB fatchannel 76
          skipchannels = 0: GOSUB fatchannel 77
          skipchannels = 3: GOSUB fatchannel 81
          skipchannels = 3: GOSUB fatchannel 85
          GOSUB readvars
          LOCATE 17, 52: PRINT USING "####"; time
          GOSUB chektime
          IF tweek = false GOTO skiptime
          GOSUB cpressavg
          GOSUB ctavg
          GOSUB setcoeffs
          GOSUB ccsubp
          GOSUB crho
          GOSUB cvisc
          GOSUB ck
          GOSUB cqfluid
          GOSUB chflux
          GOSUB ctw
          GOSUB cvel
          GOSUB cRe
          GOSUB cPr
          GOSUB chupred
          GOSUB cdP
          GOSUB cff
          GOSUB crough
          GOSUB chfromMu
          GOSUB cMuexp
          GOSUB cMuratio
          GOSUB printline
          PRINT #2, outline$
        skipfile:
        WEND
        CLOSE #1
        CLOSE #2
      skipfile:
      WEND
      RETURN

```

fatchannel:

FOR I = 1 TO skiochannels

```

commaspot = INSTR(start, inline$, comma$)
start = commaspot + 1
NEXT I
length = (INSTR(start, inline$, comma$) - start)
IF length < 0 THEN length = LEN(inline$) - start
IF LEN(outline$) > 1 THEN GOSUB mostchan ELSE GOSUB firstchan
start = INSTR(start, inline$, comma$) + 1
j = j + 1
RETURN

```

mostchan:

```

outline$ = outline$ + "," + MID$(inline$, start, length)
temp$ = MID$(inline$, start, length)
invar(j) = VAL(temp$)
RETURN

```

firstchan:

```

outline$ = MID$(inline$, start, length)
temp$ = MID$(inline$, start, length)
invar(j) = VAL(temp$)
RETURN

```

readvars:

```

time = invar(11)
pressin = invar(1)
pressout = invar(2)
tin = invar(3)
IF (fuel$ <> "RP-1") AND (run$ <> "A207") AND (run$ <> "A208") AND (tin > 0) THEN tin = -tin
IF run$ = "p105" THEN tin = invar(4)
tout = invar(4)
tblock = invar(5)
twall(1) = invar(6)
twall(2) = invar(7)
twall(3) = invar(8)
twall(4) = invar(9)
massflow = invar(10)
FOR I = 1 TO 4
    IF twall(I) > 1500 THEN twall(I) = twall(I) / 10
NEXT I
RETURN

```

chektime:

```

timeok = true
IF time < stime THEN timeok = false
IF time > etime THEN timeok = false
RETURN

```

cpressavg:

```

pressavg = (pressin + pressout) / 2
RETURN

```

ctavg:

```

tavg = (tin + tout) / 2
RETURN

```

setcoeffs:

```
IF fuel$ = "methane" THEN GOSUB methcoef
IF fuel$ = "RP-1" THEN GOSUB rpccoef
IF fuel$ = "propane" THEN GOSUB propcoef
RETURN
```

::

methcoef:

methcp:

```
'c0 - c3 are for heat capacity
IF pressavg > 1500 THEN GOTO methcp2
c0 = .758; c1 = -.00614
c2 = 7.295E-05; c3 = -2.262E-07
GOTO methrho
```

methcp2:

```
IF pressavg > 2900 THEN GOTO methcp3
c0 = 1.039; c1 = -.00211
c2 = -.0000143; c3 = 8.22E-08
GOTO methrho
```

methcp3:

```
c0 = .892; c1 = -.000293
c2 = -.0000054; c3 = 2.53E-08
```

methrho:

```
'r0 - r3 are for rho
IF pressavg > 1500 THEN GOTO methrho2
r0 = 4.182; r1 = -.0655
r2 = .000407; r3 = .000122
GOTO methk
```

methrho2:

```
IF pressavg > 2900 THEN GOTO methrho3
r0 = 10.135; r1 = -.0633
r2 = .000175; r3 = 6.23E-07
GOTO methk
```

methrho3:

```
r0 = 15.586; r1 = -.0473
r2 = .0034; r3 = 1.38E-07
```

methk:

```
k0 - k3 are for therm cond
IF pressavg > 1500 THEN GOTO methk2
k0 = .02002; k1 = -.0001054
k2 = 1.065E-06; k3 = 2.25E-10
GOTO methmu
```

methk2:

```
IF pressavg > 2500 THEN GOTO methk3
k0 = .03431; k1 = -.0001344
k2 = 7.561E-07; k3 = 1.25E-10
GOTO methmu
```

methk3:

```
k0 = .04169; k1 = -.0001321
k2 = 6.612E-07; k3 = -2.5E-11
```

methmu:

```
'v0 - v3 are for viscosity
IF pressavg > 1500 THEN GOTO methmu2
IF tav > -160 AND tav < -60 THEN
v0 = -7.75E-13; v1 = 1.457E-09; v2 = -3.837E-07; v3 = .0000327
ELSEIF tav > -60 AND tav < 40 THEN
v0 = -4.857E-12; v1 = 1.225E-09; v2 = -7.468E-07; v3 = 8.13E-06
```



```

propcp2:
    IF pressavg > 1500 THEN GOTO propcp3
    c0 = .5593; c1 = .0005387
    c2 = 1.68E-06; c3 = 1.693E-08
    GOTO proprho

propcp3:
    IF pressavg > 2500 THEN GOTO propcp4
    c0 = .549; c1 = .0005778
    c2 = .0000011; c3 = 7.167E-10
    GOTO proprho

propcp4:
    c0 = .5417; c1 = .000529
    c2 = 8.6E-07; c3 = -9E-10

proprho:
    'r0 - r3 are for rho
    IF pressavg > 750 THEN GOTO proprho2
    r0 = .555; r1 = -.0002781
    r2 = -6.058E-07; r3 = -4.247E-08
    GOTO propk

proprho2:
    IF pressavg > 1500 THEN GOTO proprho3
    r0 = .5602; r1 = -.0006086
    r2 = -4.834E-07; r3 = -4.619E-09
    GOTO propk

proprho3:
    IF pressavg > 2500 THEN GOTO proprho4
    r0 = .5696; r1 = -.0005832
    r2 = -2.9E-07; r3 = -1.383E-09
    GOTO propk

proprho4:
    r0 = .5774; r1 = -.0005488
    r2 = -1.55E-07; r3 = -6.666E-10

propk:
    'k0 - k3 are for thermal cond
    IF pressavg > 750 THEN GOTO propk2
    k0 = .0671; k1 = -.0001546
    k2 = 2.743E-07; k3 = -3.266E-09
    GOTO propmu

propk2:
    IF pressavg > 1500 THEN GOTO propk3
    k0 = .0689; k1 = -.0001805
    k2 = 3.046E-07; k3 = -4.612E-10
    GOTO propmu

propk3:
    IF pressavg > 2500 THEN GOTO propk4
    k0 = .0717; k1 = -.0001848
    k2 = 3.175E-07; k3 = -1.582E-10
    GOTO propmu

propk4:
    k0 = .0744; k1 = -.0001812
    k2 = 3.629E-07; k3 = -3.743E-10

propmu:
    'v0 - v3 are for viscosity
    IF pressavg > 750 THEN GOTO propmu2
    v0 = .000105; v1 = -5.896E-07
    v2 = 2.315E-09; v3 = -8.895E-12
    GOTO proptn

proptn2:

```

```

                                IF pressavg > 1500 THEN GOTO propou3
                                v0 = .000109; v1 = -6.263E-07
                                v2 = 2.45E-09; v3 = -5.867E-12
                                GOTO propo1n

propou3:
                                IF pressavg > 2500 THEN GOTO propou4
                                v0 = .000118; v1 = -6.682E-07
                                v2 = 2.59E-09; v3 = -5.283E-12
                                GOTO propo1n

propou4:
                                v0 = .000127; v1 = -6.878E-07
                                v2 = 2.75E-09; v3 = -5.767E-12

propo1n:
                                RETURN

%%%%%%%%%%%%%%%%%%%%%%%%%%%%%%%%%%%%%%%%%%%%%%%%%%%%%%%%%%%%%%%%%%%%%%%%

ccsubp:
                                'calc Cp, BTU/lb-F
                                csubp = c0 + c1 * (tavg) + c2 * (tavg ^ 2) + c3 * (tavg ^ 3)
                                RETURN

crho:
                                'calc rho, g/cc
                                rho = (r0 + r1 * (tavg) + r2 * (tavg ^ 2) + r3 * (tavg ^ 3)) / 62.4
                                IF fuel$ = "propane" THEN rho = (r0 + r1 * (tavg) + r2 * (tavg ^ 2) + r3 * (tavg ^ 3))
                                RETURN

cvisc:
                                'calc viscosity, lb/ft-s
                                IF fuel$ = "methane" THEN GOSUB vform1 ELSE GOSUB vform2
                                RETURN

vform1:
                                visc = v0 * ((tavg - t0) ^ 3) + v1 * ((tavg - t0) ^ 2) + v2 * (tavg - t0) + v3
                                RETURN

vform2:
                                visc = v0 + v1 * (tavg) + v2 * (tavg ^ 2) + v3 * (tavg ^ 3)
                                RETURN

ck:
                                'calc thermal conductivity, BTU/ft-hr-F
                                k = k0 + k1 * (tavg) + k2 * (tavg ^ 2) + k3 * (tavg ^ 3)
                                RETURN

cqfluid:
                                ' heat into fluid, kwatts
                                qfluid = massflow * (tout - tin) * csubp * 1.055 / 60
                                RETURN

chflux:
                                ' heat flux based on a wid x wid channel
                                ' BTU/s-in2
                                hflux = qfluid / (3 * wid * leng * 1.055)
                                RETURN

ctw:
                                IF leng < 3' THEN
                                    tw = ((twall(2) + twall(3)) / 2) - (1.852 * hflux)
                                ELSEIF leng >= 3' THEN
                                    tw = ((twall(1) + twall(2) + twall(3) + twall(4)) / 4) - (1.852 * hflux)

```

END IF

```
IF fuel$ = "propane" AND leng < 3! THEN
    tw = ((twall(2) + twall(3)) / 2) - (1.852 * hflux)
ELSEIF fuel$ = "propane" AND leng >= 3! THEN
    tw = ((twall(1) + twall(2) + twall(3)) / 3) - (1.852 * hflux)
END IF
RETURN
```

cvel:

```
' velocity, ft/s
vel = massflow / (60 * (62.4 * rho) * (wid ^ 2 / 144))
RETURN
```

cRe:

```
' Renoylds number.
Re = rho * 62.4 * vel * (wid / 12) / visc
RETURN
```

cPr:

```
' Prandtl number.
Pr = (csubp * visc / k) * 3600
RETURN
```

cNupred:

```
' Nusselt number.
IF (Re < 0) OR (Pr < 0) THEN Nupred = 0: RETURN
IF (tw + 460 < 0) OR (tavg + 460 < 0) THEN Nupred = 0: RETURN
'IF fuel$ = "propane" THEN GOSUB cwallprops: GOSUB setkonst
'IF fuel$ = "propane" THEN Nupred = konst * (1 + 2 * wid / leng) * Re ^ a * Pr ^ c * (rhob / rhow) ^ d * (mub / muw) ^ e * (kb
IF fuel$ = "propane" THEN Nupred = .023 * Re ^ .8 * Pr ^ .4
IF fuel$ = "methane" THEN Nupred = .023 * Re ^ .8 * Pr ^ .4 * ((tw + 460) / (tavg + 460)) ^ .47      1.03 add (tw/tavg) term.
IF fuel$ = "RP-1" THEN Nupred = .005 * Re ^ .95 * Pr ^ .4
RETURN
```

cwallprops:

```
'calc wall properties for propane s Nupred correlation
thold = tavg
phold = pressavg
twallhold = tw

rhob = rho
mub = visc
kb = k
cpb = csubp
p = pressavg

tavg = tw
GOSUB setcoeffs
GOSUB crho: rhow = rho
GOSUB cvisc: muw = visc
GOSUB ck: kw = k
pcrit = 602.7

tavg = thold
pressavg = phold
tw = twallhold
RETURN
```

setkonst:

```
'SET constants for propane s Nupred correlation
konst = .90568
a = .876
c = .4
d = .12
e = .142
```

hflux)

- (i.852 \* hflux.

(44))

nd = 0: RETURN

WJB setkonst

(cpb / 2 \* mid / leng) \* Re ^ a \* Pr ^ c \* (rho\_b / rho\_w) ^ d \* (mu\_b / mu\_w) ^ e \* (k\_b / k\_w) ^ f \* (cp\_b / cp\_w) ^ g \* (D / D\_ref) ^ h

8 \* Pr ^ .4

8 \* Pr ^ .4 \* ((tw + 460) / (tavg + 460)) ^ .47 \* 1.03 add (tw/tavg) term.

1 \* Pr ^ .4

1 correlation

relation

```

g = -.368
h = .254
RETURN

```

```

cdP:
    ' Channel delta P
    tdP = pressin - pressout
    los = (1.5 + 1.2) * (rho * 62.4) * vel ^ 2 / (2 * 32.2 * 144) ' 1.03 added 1.2 term to account for 2 90 degree bends
    dP = tdP - los
    RETURN

cff:
    ' Moody friction factor
    IF (dP <= 0) OR (vel <= 0) OR (rho <= 0) THEN ff = 0: RETURN
    ff = 2 * 32.2 * (wid / 12) * dP * 144 / ((vel ^ 2) * (leng / 12) * (rho * 62.4))
    RETURN

crough:
    ' Roughness of channel based on ff.
    ' units: micro-inches.
    IF (ff <= 0) OR (Re <= 0) THEN rough = 0: RETURN
    rough = 3.7 * (10 ^ (-1 / (2 * SQR(ff)))) - 2.51 / (Re * SQR(ff)) * wid * 1000000
    RETURN

chfromNu:
    ' heat transfer coefficient based on Nusselt number.
    ' units: BTU/s-in2-F
    hfromNu = Nupred * k / (wid / 12) * (1 / 3600) * (1 / 144)
    RETURN

cNuexp:
    ' heat transfer coefficient based on delta T.
    ' units : BTU/s-in2-F
    hfromT = hflux / (tw - tavg)
    Nuexp = (hfromT * wid / k) * 3600 * 12
    RETURN

cMuratio:
    IF Nupred = 0 THEN Muratio = 0: RETURN
    Muratio = Nuexp / Nupred
    RETURN

printline:
    IF lineno > 56 THEN lineno = 1
    IF lineno = 1 THEN GOSUB dopagehead
    IF lineno MOD 10 = 0 THEN GOSUB doseperate
    GOSUB doline
    RETURN

dopagehead:

```

```

GOSUB setpagehead
PRINT #2, CHR$(12): 'LPRINT CHR$(12)
PRINT #2, pline0$: 'LPRINT pline0$
PRINT #2, pline1$: 'LPRINT pline1$
PRINT #2, pline2$: 'LPRINT pline2$
PRINT #2, pline3$: 'LPRINT pline3$
PRINT #2, pline4$: 'LPRINT pline4$
PRINT #2, pline5$: 'LPRINT pline5$
lineno = 6
RETURN

```

doline:

```

PRINT #2, USING mask$: time, pressin, pressout, tin, tout, tblock, twall(1), twall(2), twall(3), twall(4), massflow, pressavg,
'LPRINT USING mask$: time, pressin, pressout, tin, tout, tblock, twall(1), twall(2), twall(3), twa

```

. Nuexp, tw, Muratio

```

lineno = lineno + 1
RETURN

```

doseperate:

```

PRINT #2, alldashes$
'LPRINT alldashes$
lineno = lineno + 1
RETURN

```

setpagehead:

```

pline0$ = "Run No. : " + run$
pline0$ = pline0$ + SPACE$(60)
pline0$ = pline0$ + title2$
pline1$ = "Date : " + rdate$
pline2$ = ""
pline3$ = "Time" + SPACE$(3)
pline3$ = pline3$ + "Pin" + SPACE$(2)
pline3$ = pline3$ + "Pout" + SPACE$(4)
pline3$ = pline3$ + "Tin" + SPACE$(4)
pline3$ = pline3$ + "Tout" + SPACE$(3)
pline3$ = pline3$ + "Tblock" + SPACE$(2)
pline3$ = pline3$ + "Twall1" + SPACE$(2)
pline3$ = pline3$ + "Twall2" + SPACE$(2)
pline3$ = pline3$ + "Twall3" + SPACE$(2)
pline3$ = pline3$ + "Twall4" + SPACE$(3)
pline3$ = pline3$ + "Flow" + SPACE$(2)
pline3$ = pline3$ + "Pavg" + SPACE$(2)
pline3$ = pline3$ + "Tav" + SPACE$(3)
pline3$ = pline3$ + "Cp" + SPACE$(4)
pline3$ = pline3$ + "rho" + SPACE$(5)
pline3$ = pline3$ + "mu" + SPACE$(9)
pline3$ = pline3$ + "k" + SPACE$(8)
pline3$ = pline3$ + "Vel" + SPACE$(3)
pline3$ = pline3$ + "Q" + SPACE$(5)
pline3$ = pline3$ + "q" + SPACE$(6)
pline3$ = pline3$ + "Re" + SPACE$(8)
pline3$ = pline3$ + "Pr" + SPACE$(6)
pline3$ = pline3$ + "Nu" + SPACE$(5)
pline3$ = pline3$ + "fDP" + SPACE$(2)
pline3$ = pline3$ + "los" + SPACE$(3)
pline3$ = pline3$ + "dP" + SPACE$(6)
pline3$ = pline3$ + "fff" + SPACE$(9)
pline3$ = pline3$ + "a" + SPACE$(5)

```

ut, tblock, twall(1), twall(2), twall(3), twall(4), massflow, pressavg, tavg, csubp, rho, visc, k, vel, qfluid, hflux, Re, Pr, Nupred, tdP, los, dP, ff, rough, Nupred, Nuexp, tw, Nuratio  
pressin, pressout, tin, tout, tblock, twall(1), twall(2), twall(3), twall(4), massflow, pressavg, tavg, csubp, rho, visc, k, vel, qfluid, hflux, Re, Pr, Nupred, tdP, los, dP, ff, rough, Nup

```

pline3$ = pline3$ + "Nu" + SPACE$(5)
pline3$ = pline3$ + "twall" + SPACE$(3)
pline3$ = pline3$ + "Nuxp/"
pline4$ = " sec" + SPACE$(3)
pline4$ = pline4$ + "psi" + SPACE$(2)
pline4$ = pline4$ + "psig" + SPACE$(5)
pline4$ = pline4$ + "F" + SPACE$(7)      'tin
pline4$ = pline4$ + "F" + SPACE$(6)
pline4$ = pline4$ + "F" + SPACE$(7)      Tblock
pline4$ = pline4$ + "F" + SPACE$(7)
pline4$ = pline4$ + "F" + SPACE$(7)
pline4$ = pline4$ + "F" + SPACE$(5)
pline4$ = pline4$ + "%/m" + SPACE$(3)
pline4$ = pline4$ + "psi" + SPACE$(3)
pline4$ = pline4$ + "F" + SPACE$(3)
pline4$ = pline4$ + "B/0-F" + SPACE$(9)
pline4$ = pline4$ + "B/f-s" + SPACE$(4)
pline4$ = pline4$ + "B/h-f-F" + SPACE$(5)
pline4$ = pline4$ + "fps" + SPACE$(3)
pline4$ = pline4$ + "kW" + SPACE$(3)
pline4$ = pline4$ + "B/s1" + SPACE$(29)
pline4$ = pline4$ + "psi" + SPACE$(2)
pline4$ = pline4$ + "psi" + SPACE$(3)
pline4$ = pline4$ + "psi" + SPACE$(15)
pline4$ = pline4$ + "uin" + SPACE$(2)
pline4$ = pline4$ + "predict" + SPACE$(3)
pline4$ = pline4$ + "exper" + SPACE$(3)
pline4$ = pline4$ + "(cor)" + SPACE$(3)
pline4$ = pline4$ + "Nupred"
pline5$ = ""
RETURN

```

setmask:

```

mask$ = ""
mask$ = mask$ + "#### "      ' time
mask$ = mask$ + "#### "      ' oin
mask$ = mask$ + "#### "      ' pout
mask$ = mask$ + "####.0 "    ' tin
mask$ = mask$ + "####.0 "    ' tout
mask$ = mask$ + "####.0 "    ' tblock
mask$ = mask$ + "####.0 "    ' twall1
mask$ = mask$ + "####.0 "    ' 2
mask$ = mask$ + "####.0 "    ' 3
mask$ = mask$ + "####.0 "    ' 4
mask$ = mask$ + "0.### "      ' massflow
mask$ = mask$ + "#### "      ' pavg
mask$ = mask$ + "### "       ' tavg
mask$ = mask$ + "0.## "      ' Co
mask$ = mask$ + "0.### "      ' rho
mask$ = mask$ + "0.###~~~~ "  ' mu
mask$ = mask$ + "0.###~~~~ "  ' k
mask$ = mask$ + "### "       ' Vel
mask$ = mask$ + "0.## "      ' Q
mask$ = mask$ + "0.0 "       ' q"
mask$ = mask$ + "0.###~~~~ "  ' Re
mask$ = mask$ + "00.## "     ' Pr
mask$ = mask$ + "##### "    ' Nu
mask$ = mask$ + "##### "    ' TdP
mask$ = mask$ + "##### "    ' los
mask$ = mask$ + "##### "    ' dP
mask$ = mask$ + "0.###~~~~ "  ' ff
mask$ = mask$ + "#### "      ' e
mask$ = mask$ + "#####.0 "   ' Nu (pred)
mask$ = mask$ + "#####.0 "   ' Ni (exo)

```

```
mask$ = mask$ + "####.#"  
mask$ = mask$ + "#.###"  
RETURN
```

```
twall corrected  
Nu(exp)/Nu(pred)
```

```
fclose:
```

```
CLOSE #1, #2, #3  
RETURN
```

```
endit:
```

```
LOCATE 20, 25  
PRINT "ALL DONE"  
'PRINT #2, CHR$(12): 'LPRINT CHR$(12)  
RETURN
```